Open Research Online

The Open University's repository of research publications
and other research outputs

Investigating Inflammatory Pathways as Therapeutic Targets and Biomarkers using Functional Imaging and Pharmacological Interventions in Epilepsy Models.

Thesis

How to cite:

Kostoula, Chrysavgi (2018). Investigating Inflammatory Pathways as Therapeutic Targets and Biomarkers using Functional Imaging and Pharmacological Interventions in Epilepsy Models. PhD thesis The Open University.

For guidance on citations see FAQs.

© 2018 The Author

Version: Version of Record

Copyright and Moral Rights for the articles on this site are retained by the individual authors and/or other copyright owners. For more information on Open Research Online's data policy on reuse of materials please consult the policies page.

oro.open.ac.uk

INVESTIGATING INFLAMMATORY PATHWAYS AS THERAPEUTIC TARGETS AND BIOMARKERS USING FUNCTIONAL IMAGING AND PHARMACOLOGICAL INTERVENTIONS IN EPILEPSY MODELS

Chrysavgi Kostoula

Degree of **Doctor of Philosophy**

The Open University

Discipline of Life and Biomolecular Science

Affiliated Research Centre:

Istituto di Ricerche Farmacologiche Mario Negri IRCCS

Milan, Italy

September 2018

Ό,τι δεν συνέβη ποτέ, είναι ό,τι δεν ποθήσαμε αρκετά.

Νίκος Καζαντζάκης

ACKNOWLEDGEMENTS

I am grateful to **Dr. Annamaria Vezzani** for giving me the opportunity to attend the Open University PhD program, for her support, comments and suggestions during these years and to **Dr. Matthew Walker** who gave me helpful support during all stages of this work.

I would like to thank **Dr. Albert Becker**, **Dr. Susanne Schoch-McGovern** and **Dr. Karen M.J. van Loo** for all the support and our collaboration and for the time spent in Dr.Becker's lab in Bonn.

I am also grateful to **Dr. Mirjana Carli** and **Dr. William Invernizzi** for giving me the opportunity to start a new experience in Italy and for introducing me to this institute and a thank to **Giusy** for her support and our long-lasting conversations even when I was not a member of their lab anymore.

A special thank goes to all my collegues that worked in this lab and shared intense and unforgettable moments with me: **Tere** (thank you for all the support and suggestions), **Silvia** (it took us some time to get to know each other but it was definitely worth it!), **Massimo** (I'll miss your jokes and our conversations), **Vale** (I am grateful for all the work we've done together), **Greta** (my microsurgery teacher), **Gaetano** (our Doc with whom we had endless conversations pretty much about everything!), **Anna** (the smiling girl from the high mountains), **Michele** (our smart and determined student), **Martina** (learn how to make the best out of every difficulty!), **Sara** and **Giulia** (our best students!), my lovely student **Maeve** that shared with me all the work and effort of this last year and finally a thank to all the people that we shared moments with in the lab.

I will always be grateful for meeting some people that are special to me: **Federica** the collegue that became a close friend and we continue sharing lovely moments together, **Katerina** and **Eugenio**, our dear bridesmaid and best man, **Giovanni** and **Paola**, dear friends who are almost like brother and sister to me, **Rosy** our lab diva and close friend, **Federico**,

always ready to find a solution to every problem, **Polina** (my time in Bonn would never have been the same without you, thank you for everything!), **Anne**, **Lia** and **Zakaria**, my multicultural friends that made me feel like home in Germany.

Then some special people that were always close to me even when far away: my dear friends **Anna** and **Georgia** (σας ευχαριστώ για όλα αυτά τα χρόνια φιλίας), then **Federica, Roberta, Nikos, Alicia, Vangelis, Afroditi:** always grateful for your friendship and the moments spent together.

Ευχαριστώ την οικογένειά μου για την αγάπη και την υποστήριξή τους: τον αγαπημένο μου **πατέρα** και την **μητέρα** μου, την αδελφούλα μου **Ειρήνη** και τα αγαπημένα μου αδέλφια **Βασίλη** και **Κώστα** και τέλος την λατρεμένη μου **γιαγιά** που θα έχω πάντα στην καρδιά μου.

Finally, I am grateful to my beloved husband **Ruggiero** that believes in me more than I do myself and chose to be my partner in life no matter what difficulty we may face. Sono fortunata ad averti nella mia vita.

TABLE OF CONTENTS

LIST OF PUBLICATIONS

Ravizza T., **Kostoula C.,** Vezzani A. Immunity activation in brain cells in epilepsy: mechanistic insights and pathological consequences. Neuropediatrics. 2013;44(6):330-335 (Review)

Kostoula C., Pascente R., Ravizza T., McCown T., Schoch S., Vezzani A., Becker AJ., Van Loo KMJ. Development of *in vivo* imaging tools for investigating astrocyte activation in epileptogenesis. Mol Neurobiol. 2017;55(5):4463-4472.

Kostoula C., Iori V., Ravizza T., Cerovic M., Shaker T., Carmant L., Vezzani A. TLR3 activation in astrocytes mediates anti-inflammatory and anti-ictogenic effects: the role of IFN-β and AHR-mediated signaling. *(in preparation)*

COLLABORATIONS

The experiments described in this thesis were carried out in the Laboratory of Experimental Neurology, Department of Neuroscience, Istituto di Ricerche Farmacologiche Mario Negri IRCCS, Milan, Italy and in the laboratory of Dr. A. Becker, Section for Translational Epilepsy Research, Department of Neuropathology, University of Bonn Medical Center, Germany. The development of the viral vectors was done in collaboration with Dr. Thomas McCown, UNC Gene Therapy Center, Chapel Hill, NC 27599, United States.

RT-qPCR measurements described in Chapters 7 and 8 were performed by Dr. Ilaria Craparotta, Translational Genomic Unit, Department of Oncology, Istituto di Ricerche Farmacologiche Mario Negri IRCCS, Milan, Italy.

In vitro electrophysiology experiments were performed by Dr. Milica Cerovic, Department of Neuroscience, Istituto di Ricerche Farmacologiche Mario Negri IRCCS, Milan, Italy and by Dr. Tarek Shaker, CHU Sainte-Justine/Université de Montréal, Montreal, Quebec, Canada.

LIST OF FIGURES AND TABLES

CHAPTER 1 – INTRODUCTION

PART I

CHAPTER 3 – GENERAL MATERIALS AND METHODS

CHAPTER 4 – CHARACTERIZATION OF IL-1β PROMOTER FRAGMENTS AND DEVELOPMENT OF *IN VIVO* BIOLUMINESCENCE IMAGING OF ASTROCYTES

CHAPTER 5 – CHARACTERIZATION OF ASTROCYTE ACTIVATION DURING EPILEPTOGENESIS

PART II

CHAPTER 6 – GENERAL MATERIALS AND METHODS

CHAPTER 7 – EFFECT OF TLR3 PRIMING ON NEURONAL EXCITABILITY AND SEIZURES

CHAPTER 8 – TLR3-MEDIATED MECHANISMS OF NEUROPROTECTION

LIST OF ABBREVIATIONS

ACTH	Adrenocorticotropic hormone
AHR	Aryl hydrocarbon receptor
AMPAR	α-amino-3-hydroxy-5-methyl-4-isoxazolepropionic acid receptor
AMT	Alpha methyl tryptophan
AQP4	Aquaporin 4
ATF-3	Activating transcription factor 3
ATP	Adenosine triphosphate
ASDs	Anti-seizure drugs
BBB	Blood brain barrier
BLI	Bioluminescence imaging
BDNF	Brain derived neurotrophic factor
BSA	Bovine serum albumin
C1q	Complement component 1q
CA	Cornu ammonis
CB	Cannabinoid receptor
CE-MRI	Contrast-enhanced magnetic resonance imaging
COX-2	Cyclooxygenase-2
CNS	Central nervous system
CSF	Cerebrospinal fluid
CCL2	C-C chemokine ligand 2
CCR2	CC receptors subtype 2
C/EBP	CCAAT-enhancer-binding protein
CHIKV	Chikungunya virus
CyP	Cyanobacterial LPS
CX3CL1	Chemokine (C-X3-C motif) ligand 1

CX3CR1	CX3C chemokine receptor 1
DAB	Diaminobenzidine
DAMP	Damage associated molecular pattern
EAE	Experimental autoimmune encephalomyelitis
EEG	Electroencephalographic
eEPSC	Evoked excitatory postsynaptic currents
ERK	Extracellular signal–regulated kinase
FBS	Fetal bovine serum
FCD	Focal cortical displasia
FIRES	Febrile infection-related epilepsy syndrome
FSE	Febrile status epilepticus
GABA	Gamma-aminobutyric acid
GAERS	Genetic absence epilepsy rat from Strasbourg
GAPDH	Glyceraldehyde 3 phosphate dehydrogenase
GAP43	Growth Associated Protein 43
GFAP	Glial fibrillary acidic protein
GLT-1	Glutamate transporter-1
GluR	Glutamate receptor
GNT	Glioneuronal tumors
GSH	Glutathione
HCN	Hyperpolarization-activated cyclic nucleotide-gated potassium channel
HDAC	Histone deacetylase
HMGB1	High mobility group box 1
HSV	Herpes simplex virus infection
ICAM-1	Intercellular Adhesion Molecule 1
ICE/caspase-1	Interleukin-1 converting enzyme
ICV	Intracerebroventricular

IDO	Indoleamine 2,3-dioxygenase
IFN-β	Interferon-β
ILAE	International league against epilepsy
IL-	Interleukin-
IL-1β	Interleukin-1 beta
IL-1Ra	Interleukin-1 receptor antagonist
IRF	Interferon regulatory factor
ITRs	Inverted terminal repeats
JAK	Janus kinase
KA	Kainate
Kir	Inward rectifying potassium channels
LPS	Lipopolysaccharide
LUC	Luciferase
MAGL	Monoacylglycerol lipase
MNPs	Magnetonanoparticles
MAO-B	Monoamine oxidase type B
MAPK	Mitogen activated protein kinase
MCP-1	Monocyte chemoattractant protein-1
MDA-5	Melanoma differentiation-associated gene 5
MRI	Magnetic resonance imaging
MRS	Magnetic resonance spectroscopy
MTS	Mesial temporal sclerosis
mIns	myo-inositol
mGluR	Metabotropic glutamate receptor
miRNA	microRNA
MS	Multiple sclerosis
mTOR	Mammalian target of rapamycin

NF-κB	Nuclear factor-kappa B
NGS	Normal goat serum
NMDA	N-methyl-D-aspartate
PAMP	Pathogen associated molecular pattern
PBS	Phosphate buffered saline
PET	Position emission tomography
PFA	Paraformaldehyde
PHT	Phenytoin
PN	Postnatal
Poly I:C	Polyinisinic:polycytidylic acid
PRRs	Pattern recognition receptors
PS	Population spikes
PTX3	Pentraxin-3
PTZ	Pentylenetetrazol
rAAV	Recombinant adeno-associated viral vector
RAGE	Receptor for advanced glycation end product
RE	Rasmussen encephalitis
RIG-1	Retinoic acid-inducible protein 1
RT-qPCR	Real time polymerase chain reaction
S100β	S100 calcium-binding protein β
SC	Schaffer collaterals
SE	Status epilepticus
S1P	Sphingosine-1-phosphate
S1PR	Sphingosine 1-phosphate receptor
Slm	Stratum lacunosum-moleculare
SPIONs	Superparamagnetic iron oxide nanoparticles
Sr	stratum radiatum

STAT	Signal transducers and activators of transcription
TBI	Traumatic brain injury
TBS	Tris-HCl-buffered saline
TGF-β	Transforming growth factor-β
TICAM-1	TIR-containing adaptor molecule 1
TIR	Toll/Interleukin-1 receptor
TJ	Tight junction
TLE	Temporal lobe epilepsy
TLR	Toll like receptor
TNF-α	Tumor necrosis factor-α
TNFR	Tumor necrosis factor receptor
TSC	Tubero sclerosis complex
TSPO	Translocator protein
TSS	Transcription start site
VCAM-1	Vascular cell adhesion molecule 1
VPA	Valproic acid
WNV	West-Nile Virus
ZO-1	Zonula occludens-1

ABSTRACT

Epilepsy is a neurological disorder that is characterised by spontaneous seizures. After various epileptogenic injuries, astrocytes become dysfunctional and experimental evidence indicates that these cells contribute to seizure mechanisms. The generation of inflammatory molecules in astrocytes appears to play a key pathogenic role in seizures. However, astrocytes may also contribute to repair the hyperexcitable neuronal networks underlying seizures.

We focused our studies on understanding the role of astrocytes in epilepsy by (1) developing a new *in vivo* imaging method to monitor astrocytic cell activation during epileptogenesis and coupled this with their phenotypic characterization; (2) studying the role of Toll-like receptor 3 (TLR3) signaling in seizure mechanisms.

We report that *in vivo* bioluminescence imaging is a powerful tool for monitoring astrocytic activation in diseased conditions. Characterization of astrocytic activation during epileptogenesis showed a rapid cell activation corresponding to their inflammatory phenotype while homeostatic (neuroprotective) mechanisms were activated with a delay. Moreover, we demonstrate that *in vivo* imaging of astrocyte activation allows to study the potential involvement of these cells in the therapeutic effects of anti-inflammatory drugs.

We also show that priming TLR3 activation in astrocytes with the use of a synthetic agonist results in remarkable anti-inflammatory and anti-ictogenic effects. Mechanistic studies revealed that interferon regulatory factor (IRF)-3/Interferon-β mediated cascade is likely responsible for the inhibitory effects of TLR3 priming on seizures and neuronal excitability.

In summary, astroglia activation during the critical epileptogenesis phase provides a potential target for interfering in a timely manner with the inflammatory phenotype of these cells contributing to seizures. Importantly, there are astrocytic cell functions that

mediate decreased neuronal excitability and they should be carefully considered when developing treatments targeting these cells for therapeutic purposes.

CHAPTER 1 - INTRODUCTION

1.1 EPILEPSY

1.1.1 Definition and classification

Epilepsy is one of the most common neurological disorders affecting about 1% of the population worldwide. Epilepsy is characterized by an enduring predisposition to generate epileptic seizures, and by the neurologic, cognitive, psychological, and social consequences of this condition. The definition of epilepsy requires the occurrence of at least two unprovoked or reflex seizures > 24 h apart or one unprovoked or reflex epileptic seizure and a probability of having another seizure similar to the general recurrence risk after two unprovoked seizures (≥ 60%) over the next 10 years, or an epilepsy syndrome (Fisher, 2014). An epileptic seizure is a transient occurrence of signs and/or symptoms due to abnormal excessive or synchronous neuronal activity in the brain (Fisher, 2014). Seizures can be divided in those that have focal onset, involving one hemisphere of the brain, in those that have generalized onset and involve both hemisperes of the brain and those of unknown onset (Figure 1.1.1).

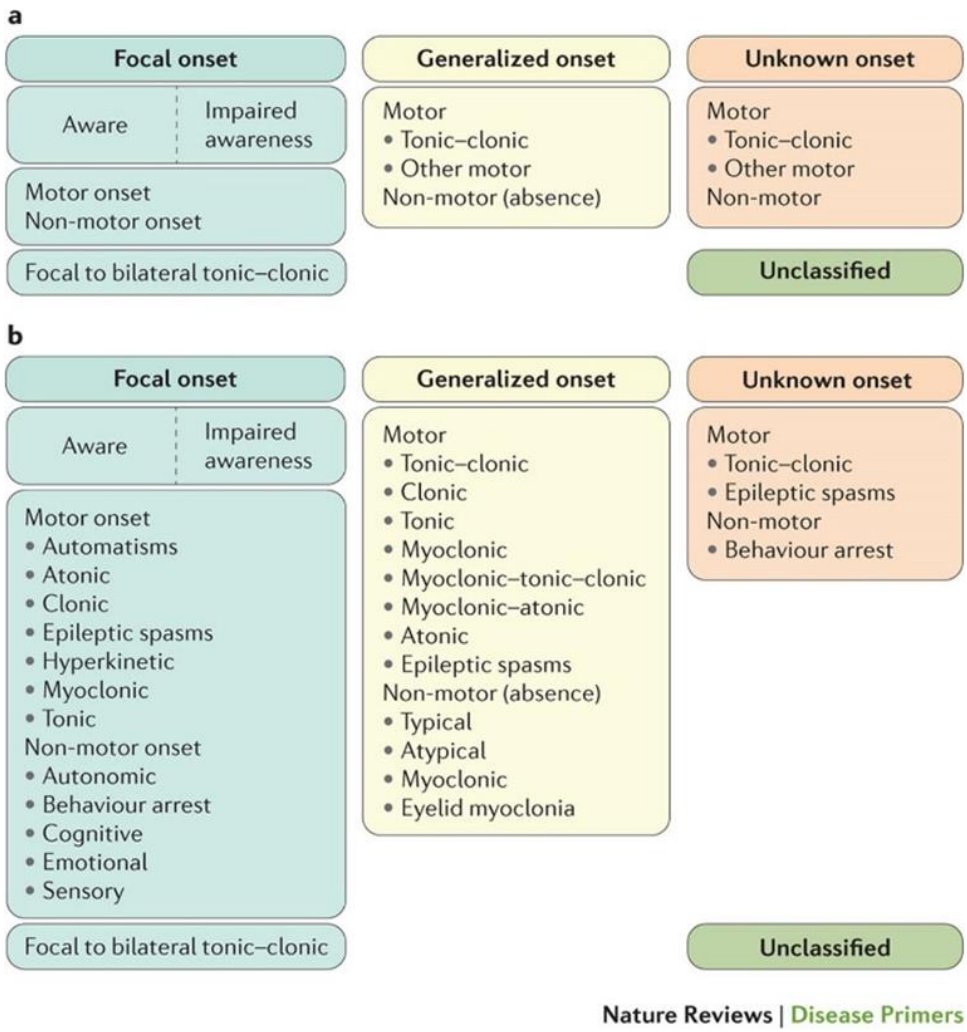

Figure. 1.1.1. Seizure classification *a) Basic seizure classification according to the International League Against Epilepsy 2017. b) Expanded seizure classification where motor and non-motor categories are further divided according to features that might be present during seizures, such as automatisms and myoclonus. Adapted with permission from Fisher, R. S. et al. Operational classification of seizure types by the International League Against Epilepsy: Position Paper of the ILAE Commission for Classification and Terminology. Epilepsia 58, 522–530 (2017)(Devinsky et al., 2018).*

Epilespy is classified as focal, generalized, combined generalized and focal which refers to epilepsy syndromes such as Dravet and Lennox-Gastaut, and finally as unknown when the onset is unknown. Furthermore, epilepsy is divided into six categories based on its etiology. The first category includes structural alterations visualized by imaging, that can increase the risk of being associated with epilepsy (Berg et al., 2010). The second group is genetic

epilepsies that can result from a genetic mutation that leads to seizure manifestation as a core symptom. One of the most common etiologies of epilepsy in less developed countries that can have specific treatment implications is infection (Vezzani et al., 2016). Metabolic etiology involves a known or presumed metabolic disorder that is associated with epilepsy development. Moreover, autoimmune-mediated epilepsies are described in both adults and children (Vezzani et al., 2016). Lastly, epilepsies that do not have a known cause fall into the category of unknown etiology epilepsies. Classification of epilepsies based on the seizure type and etiology is summarized in Figure 1.1.2.

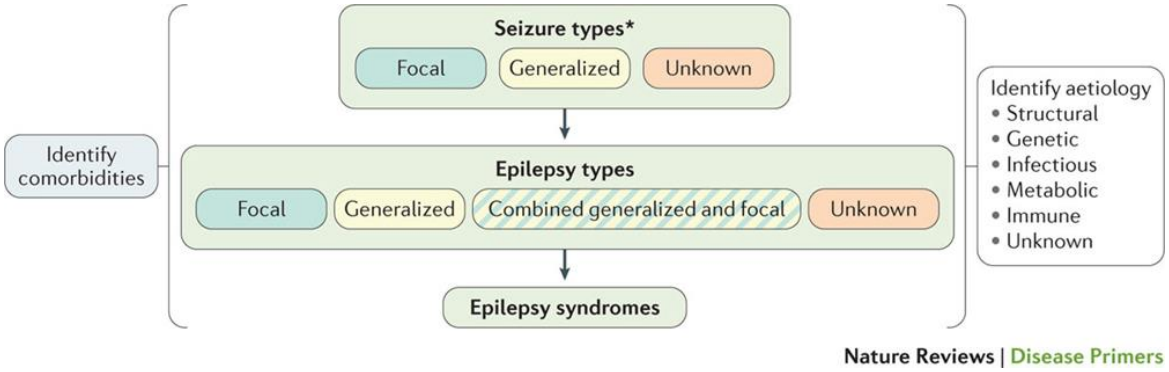

Figure. 1.1.2. Framework for the classification of the epilepsies. *This framework begins with the diagnosis of an epileptic seizure, following which, the diagnosis of an epilepsy type and, if possible, an epilepsy syndrome. After diagnosis of an epileptic seizure, the etiology should be identified where possible. Associated comorbidities should also be considered. *Denotes seizure onset. Adapted with permission from Scheffer, I. E. et al. ILAE classification of the epilepsies: Position paper of the ILAE Commission for Classification and Terminology. Epilepsia 58, 512– 521 (2017)(Devinsky et al., 2018).*

Temporal lobe epilepsy (TLE) is a form of focal epilepsy and is typically resistant to anti-seizure drugs (ASDs). Mesial temporal sclerosis (MTS) is most often associated with TLE (Blair, 2012). Status epilepticus (SE) is one of the causes of TLE and is often induced in animal models to ignite the development of epilepsy.

SE is defined as a clinical situation in which a seizure is manifested continuously for more than 5 minutes, or in which multiple seizures are repeated at very short intervals representing a continuous condition of epileptic activity (Trinka et al., 2015). It is a condition resulting either from the failure of the mechanisms responsible for seizure termination or from the initiation of mechanisms which lead to abnormally prolonged seizures, or both. It is a clinical condition that can result in long-term neurological consequences, including neuronal death and maladaptive neuronal network alterations which contribute to further seizures and neurological deficits (Trinka et al., 2015).

1.1.2 Unmet clinical needs

Despite the availability of a number of ASDs, it is estimated that up to 40% of newly diagnosed epilepsy patients will remain resistant to drug therapy and continue to have seizures (Abraham and Shaju, 2013; Löscher et al., 2013). Drug resistant epilepsy is defined as failure of adequate trials of two tolerated and appropriately chosen and used ASDs schedules (whether as monotherapies or in combination) to achieve sustained seizure freedom (Kwan et al., 2010). This condition impacts negatively on the patients' quality of life and increase the risk of injury and even death. Continuing seizures can also interfere with memory, cognitive functions, educational opportunities and also implicate a socio-economic disadvantage (Abraham and Shaju, 2013; Löscher et al., 2013). Another major unmet clinical need is the lack of treatments for preventing epilepsy in patients at risk of developing seizures after acute brain insults such as traumatic brain injury, stroke and prolonged acute symptomatic seizures such as complex febrile seizures or SE (Löscher et al., 2013). In fact, the available ASDs offer only symptomatic control of seizures without providing preventative or disease-modifying effects. Disease modification applies to

therapeutic strategies which resolve or lessen the pathologic mechanisms underlying epileptogenesis (i.e. the development and extension of tissue capable of generating spontaneous seizures), therefore, preventing or alleviating the development of epilepsy or its progression, or the associated co-morbidities. Thus, the need for more effective therapies remains urgent.

1.2 EPILEPTOGENESIS

1.2.1 Definition

Epileptogenesis is triggered by genetic or acquired causes as shown both in humans and in animal models (Pitkänen et al., 2015). It is a continuous process by which a brain network, previously normal, is altered towards increased excitability, thus showing enhanced propensity to generate seizures. Epileptogenesis encompasses both the period preceding seizure onset as well as disease progression (Dudek and Staley, 2012)(Figure 1.2.1A, B). This is supported by experimental and clinical studies providing evidence of increased frequency of spontaneous seizure over time and development of neurological comorbidities (Pitkänen et al., 2015). Furthermore, the molecular, cellular and functional alterations that precede the occurrence of the first unprovoked seizure, often continue thereafter likely contributing to disease progression (Dudek and Staley, 2012; Pitkänen and Lukasiuk, 2011; Pitkänen and Sutula, 2002; Rakhade and Jensen, 2009). This concept has implications both for therapy and biomarker discovery (Pitkänen and Engel, 2014; Pitkänen et al., 2013).

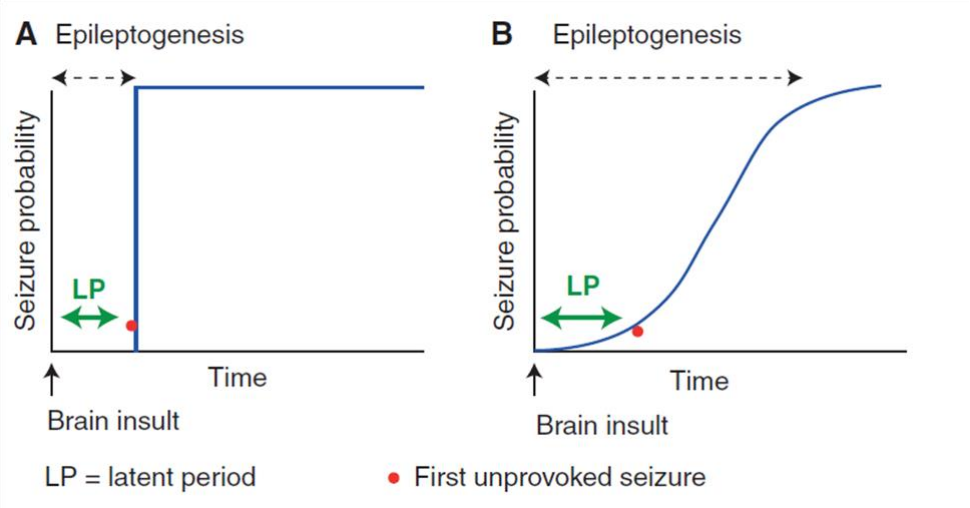

Figure 1.2.1. Definition of epileptogenesis. *(A) Epileptogenesis was considered as the latent period between the precipitating insult and the occurrence of the first unprovoked clinical seizure. (B) Based on experimental and clinical observations, epileptogenesis is now considered to extend beyond the onset of epilepsy (Pitkänen et al., 2015).*

Epileptogenesis is often associated with neurological comorbidities such as anxiety, cognitive deficits and depression (Kanner, 2016; Keezer et al., 2016). It is still unclear whether comorbidities originate from networks overlapping or distinct from those provoking seizures. Notably, animal studies have shown that cognitive deficits may arise before the first manifestation of spontaneous seizures indicating that they may not be a mere consequence of seizures (Hort et al., 2000; Kobow et al., 2012; Pascente et al., 2016; Pitkänen and Kubova, 2004).

Anti-epileptogenesis is defined as a process that counteracts the effects of epileptogenesis, including prevention, seizure modification and cure (Pitkänen et al., 2015). Since the current preclinical and clinical research is focused on developing anti-epileptogenesis or disease modifying drugs, the identification of biomarkers that can reliably predict which patients have a high likelihood of developing epilepsy is essential for clinical studies.

1.2.2 Mechanisms underlying epileptogenesis

The studies in experimental models of epilepsy have provided the main source of current knowledge on the mechanisms underlying the epileptogenic process. Epileptogenesis in these models is induced either by structural brain alterations or by infectious or genetic causes (Table 1.2.1). Most often epileptogenesis is studied in models of SE or neurotrauma (Table 1.2.2) (Pitkänen and Lukasiuk, 2009).

Table 1.2.1. Epileptogenesis models.

ETIOLOGIES	RODENT MODELS
STRUCTURAL	
Neurotrauma*	Fluid percussion; Controlled cortical impact; Cortical undercut
De novo status epilepticus*	Electrical stimulations; Chemoconvulsants; Hyperthermia
Unilateral hippocampal sclerosis*	Intrahippocampal or intracortical kainic acid; Perforant path stimulation
Stroke*	Cortical phototrombosis; Permanent middle cerebral artery occlusion; Intracortical endothelin-1
Blood-brain barrier damage*	Sub-chronic albumin or TGF-β1 intracerebroventricular infusion
Developmental epileptic encephalopathies	Hypoxia-ischemia injury in rats; *Infantile spasms*: Multiple hit rat model; Tetrodotoxin in rats
Cortical dysplasia	*Genetic: Pten*, *Dcx, Otx1* knock-out mice; Knock-in of human *Lis1*; *Arx* mutations in mice *Congenital acquired*: *In utero* rat irradiation or alkylant agents (MAM, BCNU)
Glioblastoma	Neocortical transplantation of human glioma cells in *SCID* mice or glioma cell lines in rat
INFECTIOUS	
Viral encephalitidies	Theiler murine encephalomyelitis virus
Cerebral malaria	Plasmodium berghei ANKA murine model

GENETIC OR PRESUMED GENETIC	
Tuberous sclerosis complex (TSC)	Cell specific-conditional *Tsc1* or *Tsc2* knock-out mice
Spontaneous mutations	*Rat absence epilepsy*: GAERS, WAG/Rij, HVS; *Murine absence epilepsy*: Tottering, Lethargic, Stargazer, Mocha 2j, Slow-wave, Ent, Ducky, Gabrg2 conditional knock-in mutation
Induced monogenic mutations	Mouse knock-out or knock-in mutation of voltage-gated ion channels subunits (Na^+, K^+, Ca^{2+}), neurotransmitter receptor subunits ($GABA_A$, nicotinic) and transporters, accessory synaptic proteins*;* cystatin B *(Cstb)* knock-out
Developmental epileptic encephalopathies	*Dravet syndrome*: *SCN1A, SCN1B*: Knock-in of human mutations in mice; Constitutive or conditional knock-out mice; *Infantile spams*: *ARX:* Knock-in of human mutations in mice; Constitutive or conditional knock-out mice; *Apc:* Conditional knock-out mouse *SCN8A:* Knock-in of human mutations in mice

**Models apply to both rats and mice if not otherwise indicated. Mutiple hit rat model: doxorubicin+lipopolysaccharide±p-chlorophenylalanine.*

Abbreviations: apc, adenomatous polyposis coli; Arx, aristaless related homeobox; BCNU, carmustine 1-3-bis-chloroethyl-nitrosurea; Dcx, doublecortin; GAERS, Genetic absence epilepsy rat from Strasbourg; Gabrg2, GABA-A receptor 2 subunit; HSV, high voltage spike-and-wave spindles; Lis1, lissencephaly 1; MAM, methylazoxymethanol; Otx,1 orthodenticle homeobox 1; Pten, phosphatase and tensin homolog; Scid, severe combined immundeficient; Scn1A,B, sodium voltage-gated channel (Nav1.1α,β subunit); scn8a, sodium voltage-gated channel alpha subunit 8 (Nav1.6); TGF-β1, transforming growth factor-beta1; Tsc1-2, tuberous sclerosis complex 1,2; WAG/Rij, Wistar Albino Glaxo from Rijswijk.

Table 1.2.2. Epileptogenesis models induced by acute brain injury *(modified by Pitkanen and Lukasiuk, 2009)**.***

TYPE	MODEL	REFERENCES
Immature brain		
SE	Kainic acid (PN14)	(Stafstrom et al., 1992)
	Li-Pilocarpine (PN12 or PN21)	(Kubova et al., 2004; Marcon et al., 2009; Roch et al., 2002)
	Prolonged febrile seizures (PN10)	(Dube et al., 2006)
Mature brain		
SE	Kainic acid	(Ben-Ari and Lagowska, 1978; Mouri et al., 2008)
	Pilocarpine	(Turski et al., 1983)
	Li-pilocarpine	(Jope et al., 1986)
	Perforant pathway stimulation	(Mazarati et al., 1998)
	Intrahippocampal stimulation	(Lothman et al., 1989)
	Amygdala stimulation	(Mazzuferi et al., 2013; Nissinen et al., 2000)
Trauma	Lateral fluid percussion	(D'Ambrosio et al., 2004; Kharatishvili et al., 2006a)
	Controlled Cortical Impact	(Bolkvadze et al., 2009; Clausen et al., 2009)
	Cortical or icv albumin	(Seiffert et al., 2004)
Stroke	Cortical photothrombosis	(Karhunen et al., 2007; Kelly et al., 2001)
	Cortical endothelin	(Karhunen et al., 2006)
	Cortical albumin	(Seiffert et al., 2004)

The molecular and cellular alterations along with their pathological outcomes have been best characterized in the hippocampus although the epileptogenic process may involve also other limbic and extralimbic areas (Jutila et al., 2002). The hippocampus has a well known neuronal circuitry and plays a key role in network hyperexcitability in various models of acquired epilepsy (Pitkänen and Lukasiuk, 2009). Figure 1.2.2. summarizes the cellular and molecular alterations identified in the hippocampus during epileptogenesis.

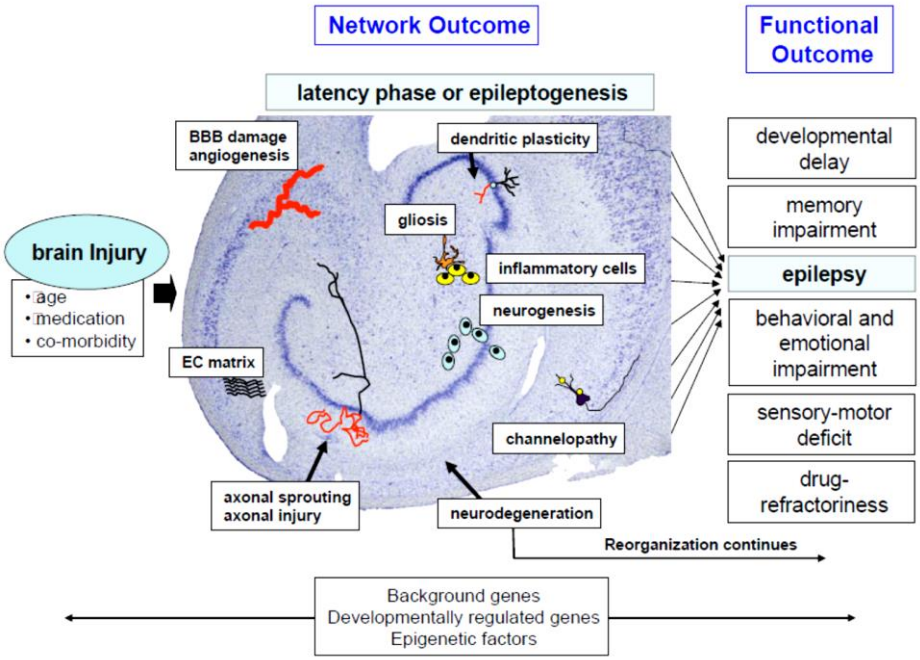

Figure 1.2.2. Cellular and molecular alterations occurring during epileptogenesis. *Acute brain insults, such as SE, TBI or stroke trigger molecular, cellular and functional alterations in the hippocampus, a brain area implicated in epileptogenesis in experimental models and in humans. These alterations include neurodegeneration, neurogenesis, inflammation and gliosis, blood brain barrier (BBB) damage, extracellular matrix reorganization, axonal sprouting and injury, dendritic plasticity and alteration in voltage- and ligand-gated ion channels (channelopathy). They may determine the generation of seizures and neurological deficits and are modulated by epigenetic mechanisms and the genetic background (Pitkänen and Lukasiuk, 2009).*

Neurodegeneration. Neuronal cell loss may occur in the brain after an acute epileptogenic insult. After SE, the two areas of the hippocampus mostly affected by neuronal cell loss are the hilus of the dentate gyrus, where inhibitory interneurons have a key role in controlling the excitability of the granule cells, and the CA1 pyramidal cell layer of the cornu ammonis. Damage often also involves CA3 pyramidal cells. The amygdala and parahippocampal cortices as well as the thalamus may be also affected. Neuroprotection (i.e. rescue of neuronal cells) does not prevent epilepsy development (Brandt et al., 2003; Nehlig, 2007) but it may be associated with improvement of behavioral dysfunctions (Brandt et al., 2006).

Hippocampal neurogenesis. This is a phenomenon observed in both healthy and epileptic animals. In healthy animals newly born neurons correctly migrate to the subgranular cell layer of the dentate gyrus and they integrate into the functional neuronal circuitry (van Praag et al., 2002; Toni et al., 2008). However, in epileptic animals increased neurogenesis is detected within a few days from SE onset and some of these cells aberrantly migrate into the hilus (i.e., ectopic neurogenesis) which results in enhanced dentate excitability (Parent, 2007; Parent et al., 1997; Scharfman et al., 2000). This altered neurogenesis is associated with several comorbidities such as learning and memory impairment and depression and might contribute to epileptogenesis (Cho et al., 2015; Jakubs et al., 2006).

Reactive gliosis. Gliosis and neuroinflammation are two of the most pronounced phenomena induced in the brain by an epileptogenic insult. They are common hallmarks of epilepsy foci (Aronica and Crino, 2011; Vezzani et al., 2011a). A more detailed description of this phenomenon is given in Section 1.3.

Blood brain barrier (BBB) alterations. BBB dysfunction is a common finding described after epileptogenic insults such as SE, TBI and stroke (Friedman and Heinemann, 2012). When BBB permeability is massively altered, serum proteins such as albumin can extravasate into the brain parenchyma and activate transforming growth factor (TGFβ) receptors in perivascular astrocytes. This activation induces modifications in astrocyte phenotype and functions such as (1) reduced expression of potassium inward rectifying channels (Kir4.1) and water channels (aquaporin 4, AQP4), (2) reduced gap junctions, (3) reduced glutamine synthase and changes in its intracellular distribution, (4) impaired glutamate reuptake and (5) increased transcription of inflammatory genes generating mediators with ictogenic properties such as IL-1β, tumor necrosis factor (TNF)-α and HMGB1. Recently, astrocytic release of extracellular matrix proteins such as thrombospondin has been shown to

mediate excitatory synaptogenesis (Weissberg et al., 2015). These functional modifications in concert increase neuronal network excitability thus contributing to establish an epileptic network (Devinsky et al., 2013; Robel et al., 2015; Vargas-Sánchez et al., 2018). Blocking of TGF-β signaling, effectively prevents the development of spontaneous seizures in animal models of BBB dysfunction while mimicking BBB dysfunction is sufficient to induce epilepsy in animals (Bar-Klein et al., 2016; Weissberg et al., 2015). In addition, BBB damage is associated with increased adhesion molecules on endothelial cells which promote the interaction of circulating leukocytes (Fabene et al., 2008). Brain-infiltrating monocytes were identified as a myeloid-cell subclass that contributes to neuroinflammation and morbidity after SE, and preventing monocyte recruitment accelerated weight regain, reduced BBB degradation, and attenuated neuronal damage (Varvel et al., 2016).

Acquired channelopathies. Both voltage-gated and receptor-gated ion channels are functionally altered by brain insults such as SE (Bernard et al., 2004; Chen et al., 2001; Su et al., 2002). This phenomenon, called acquired channelopathy, has been described in the dendritic, somatic, and axonal channels. For example, dendritic HCN channels in hippocampal pyramidal cells are dysregulated after prolonged febrile seizures as well as pilocarpine-induced SE in rodents (Brennan et al., 2016; Brewster et al., 2002; Jung et al., 2011). Acquired channelopathies in epileptogenesis are not restricted to HCN but affect a number of different ion channel subtypes including A-type potassium and sodium (Na_Vs1.2, 1.6) channels and voltage-gated pore-forming Ca^{2+}-subunit Ca_V3.2 (Becker et al., 2008; Su et al., 2002). Increase of Ca_V3.2 mRNA and protein levels as well as up-regulation of the T-Type current after SE increases intrinsic burst firing in CA1 pyramidal neurons (Becker et al., 2008). Notably, neuroinflammation can independently trigger an acquired HCN1 channelopathy in CA1 pyramidal cell dendrites that alters their integrative properties

(Frigerio et al., 2018). Some of the functional changes persist after the brain injury thus contributing to lower seizure threshold (Su et al., 2002).

Mossy fibre sprouting. Axonal and dendritic plasticity in the dentate gyrus include granule cell axon sprouting (mossy fibre sprouting) which establishes excitatory connections with somata and dendrites of both normal or ectopic granule cells (Buckmaster, 2012). Mossy fibre sprouting is often associated with degeneration of excitatory mossy cells and loss of inhibitory γ-aminobutyric acid (GABA)-ergic and neuropeptidergic hilar interneurons (Buckmaster, 2012). The aberrant mossy fibres might either establish excitatory feedback loops with the somata and dendrites of normal and ectopic granule cells in the inner molecular layer and hilar region or innervate inhibitory basket cells located in the granule cell layer and reduce neuronal excitability (the so-called "dormant basket cells hypothesis"; (Buckmaster, 2012; Sloviter et al., 2006). Moreover, several factors released by granule cells can promote this aberrant sprouting such as neuromodulin/GAP43 brain derived neurotrophic factor (BDNF), extracellular matrix proteins and induction of mTOR pathway (Heck et al., 2004; Hester and Danzer, 2014).

Transcriptomic and epigenetic mechanisms. Various genes are differentially expressed during epileptogenesis and microarray analysis of epileptogenic tissue in animal models has revealed common molecular pathways, such as alterations in voltage-gated and receptor-operated ion channels, neuropeptides, neurotrophins, and immune-related molecules (Dingledine et al., 2017; Pitkänen et al., 2015). DNA methylation, histone modification and changes microRNA (miRNAs) biosynthesis are some of the epigenetic mechanisms described in epileptogenesis (Henshall and Kobow, 2015; Henshall et al., 2016). For instance, DNA hypomethylation (leading to gene activation) and DNA hypermethylation (gene silencing) were described in seizure-generating areas in epilepsy

models and in patients with TLE (Henshall and Kobow, 2015). Reduction in seizure-like activity in rodent brain slices and attenuation of seizure progression *in vivo* were induced by DNA methylation inhibitors and adenosine-induced DNA hypomethylation (Machnes et al., 2013; Williams-Karnesky et al., 2013). Histone acetylation and phosphorylation also affect the expression of genes that have a potential role in epileptogenesis through mechanisms that involve neuroprotection and reduction of aberrant neurogenesis (Henshall and Kobow, 2015). Several studies identified changes in more than 100 miRNAs in rodents and human TLE tissue. These miRNAs target dendritic spines, neurotransmitter receptors, transcriptional regulators and inflammatory signalings (Henshall et al., 2016; Iori et al., 2017). Their role in epileptogenesis was identified with the application of either small-molecule inhibitors of miRNA (such as antagomir) or with oligonucleotides that mimic the action of miRNA in animal models. It has been shown for example that targeting miR146a, which controls the activation of the neuroinflammatory IL-1 receptor/Toll-like receptor 4 pathway or miR134, which negatively regulates dendritic spine volume both resulted in strong inhibition of epileptogenesis (Iori et al., 2017; Reschke et al., 2017). miRNAs control broad epileptogenic pathways and their exact role *in vivo* remains to be better identified.

1.3 NEUROINFLAMMATION IN EPILEPSY

1.3.1 Definition and role in epilepsy

Inflammation is a defensive response of the host tissue against infections, sterile injuries or immune cell activation, for example in the context on autoimmunity. It consists of the generation of a cascade of inflammatory mediators, as well as anti-inflammatory molecules and lipid mediators that are induced to resolve the inflammatory response. Inflammation

is characterized by the production of an array of cytokines, chemokines and related effector molecules released from tissue-resident cells and circulating immunocompetent cells, and involves the activation of innate and adaptive immunity (Vezzani et al., 2011a). Both arms of the immune system have been implicated in epilepsy. In the brain, microglia, astrocytes, neurons and endothelial cells of the BBB chiefly contribute to the innate immunity response that generates neuroinflammation by producing and releasing pro-inflammatory cytokines, chemokines and inducing adhesion molecules on endothelial cells of the BBB (Aronica et al., 2012; Vezzani et al., 2011a). In healthy brain tissue, the activation of the immune system acts to eliminate the injurious event, and astrocytes and microglia act in concert to promote tissue repair (Stoll et al., 2000). However, under pathological conditions, the resolution of inflammation is compromised, leading to proliferation of microglia and astrocytes with cytotoxic functions (Walker and Sills, 2012). Changes occurring during epileptogenesis likely comprise both pathogenic and homeostatic functions of glia that depend on the timing of cell activation after the brain insult and the concomitant events occurring in the tissue microenvironment.

Neuroinflammation is a common event in various epileptogenesis models of brain injury such as SE, stroke, neurotrauma, and in structural and genetic human epilepsies (Vezzani et al., 2011a). Importantly, the inflammatory mediators measured in epilepsy brain specimens also act as “neuromodulators” (Vezzani et al., 2011a). In fact, they activate their cognate receptors expressed by neurons, thus directly affecting neuronal functions and excitability (Vezzani et al., 2011b; Viviani et al., 2007). Specific inflammatory mediators significantly contribute to the mechanisms of seizure generation and to pharmacoresistence in experimental models and neuroinflammation is perpetuated by

neuronal damage and recurrent seizures (Dupuis and Auvin, 2015; Vezzani et al., 2011c; van Vliet et al., 2010).

1.3.2 Astrocytes

Astrocytes provide trophic support to neurons, they contribute to synaptic transmission and control BBB function (Lundgaard et al., 2014; Verkhratsky et al., 2013). In the hippocampus, two distinct astrocytic cell populations have been described: 1. astrocytes expressing glutamate transporter are enriched in glial fibrillary acidic protein (GFAP, a cytoskeletal protein), they have irregular cell bodies and branched processes and are involved in glutamate reuptake and gap-junction coupling. 2. astrocytes expressing functional α-amino-3-hydroxy-5-methyl-4-isoxazolepropionic acid (AMPA)-type glutamate receptors (GluRs) but lacking glutamate reuptake are characterized by relatively low GFAP expression and no gap-junction coupling (Matthias et al., 2003). Neuroinflammation promotes the phenotypic switch of astrocytes to AMPAR-expressing cells thereby promoting extracellular glutamate accumulation and hyperexcitability. Indeed, astrocytes form a large intercellular network that regulates extracellular glutamate (Wetherington et al., 2008), ion homehostasis through expression of Kir4.1 channels and AQP4 and dissipation of metabolites that could be detrimental if they accumulate in the extracellular space (Devinsky et al., 2013; Farina et al., 2007; Pekny and Nilsson, 2005). Astrocytes modulate synaptic transmission by releasing gliotransmitters such as D-serine, ATP, glutamate and GABA that act on their cognate neuronal receptors. Gliotransmission is promoted by increased intracellular Ca^{2+} oscillations in astrocytes in response to neuronal stimulation (Devinsky et al., 2013; Farina et al., 2007). For example, glutamate released by neurons activates metabotropic glutamate receptor subtypes (mGluR5 and mGluR3) in

reactive astrocytes thus modulating the release of gliotransmitters and cytokines (Aronica et al., 2005). Together with the pre- and post-synaptic terminals of neurons, astrocytes are part of the tripartite synapse indicating a bidirectional communication between neurons and astrocytes (Wetherington et al., 2008).

Astrocytes are key regulators of BBB integrity since their endfeet wrap around the endothelial cells and by releasing chemical signals they help to form and maintain tight junctions between endothelial cells. Astrocytes also regulate the movement of water and molecules between the blood and brain parenchyma (Devinsky et al., 2013). Pro-inflammatory chemokines and cytokines released by astrocytes activate their cognate receptors in brain microvessels thus affecting BBB permeability at multiple levels and contributing to its dysfunction in epilepsy (Morin-Brureau et al., 2011).

Reactive astrogliosis is a typical feature of many CNS disorders, such as neurotrauma, focal brain ischemia, CNS infections and epilepsy (Pekny and Pekna, 2014). Upregulation of GFAP is most commonly used as a hallmark of reactive astrocytes (Eng et al., 2000). Astrogliosis and scar formation have been often regarded as a tissue-harmful response but it became apparent that they may exert beneficial functions including wound healing, neuronal cell protection, BBB repair and resolution of CNS inflammation (Kang and Hébert, 2011; Pekny and Nilsson, 2005; Sofroniew, 2014).

Reactive astrocytes can be either neurotoxic or neuroprotective depending on their phenotype (Anderson et al., 2016; Benner et al., 2013; Faulkner et al., 2004; Fitch and Silver, 2008; Rodríguez-Arellano et al., 2016). Zamanian et al. (2012) reported that neuroinflammation induced by ischemia and by systemic injection of lipopolysaccharide (LPS), an agonist of TLR4 receptors expressed on microglia and other immune cells, induces two different types of reactive astrocytes, termed ‘‘A1’’ and ‘‘A2,’’ respectively. In this

study, gene transcriptome analysis revealed that many genes involved in synaptic degeneration were upregulated in A1 neuroinflammatory reactive astrocytes induced by LPS, suggesting that A1 may have ‘’harmful’’ function (Zamanian et al., 2012). On the contrary, A2 reactive astrocytes induced by ischemia, upregulated neurotrophic factors, which promote neuronal survival and growth and synapse repair suggesting a ‘’repairing’’ function of A2 reactive astrocytes (Zamanian et al., 2012). Tarassishin et al. (2011) reported that overexpression of transcription factor interferon regulatory factor (IRF)-3 in primary human astrocytes induced shifting of cytokine production profile from A1 to A2 phenotype and was associated with neuroprotection through suppression of the proinflammatory miR-155 (Tarassishin et al., 2011a).

The mechanism of A1 phenotype induction is thought to be mediated by secretion of IL-1alpha, TNF-α, and C1q by activated microglia (Liddelow et al., 2017). A1 astrocytes lose their ability to promote neuronal survival and axonal outgrowth, to promote synapse formation and function, while they secrete neurotoxins that induce neuronal death (Liddelow et al., 2017). In fact, A1 astrocytes are abundant in neurodegenerative diseases, where their presence contributes to neurodegeneration and help to drive disease progression. Under specific circumstances, astrogliosis has the potential to lead to harmful effects, such as contributing to persistent neuroinflammation or to excitotoxicity (Silver and Miller, 2004; Sofroniew, 2014, 2015; Sofroniew and Vinters, 2010). In contrast, the activation of A2 astrocytes is suggested to be mediated by the JAK-STAT3 pathway which is implicated in scar-forming astrocyte reactivity after acute injury (Anderson et al., 2016; Ceyzériat et al., 2016; Herrmann et al., 2008). This pathway regulates multiple cell functions, including cell proliferation, differentiation and growth, and some anti-inflammatory functions (Ceyzériat et al., 2016).

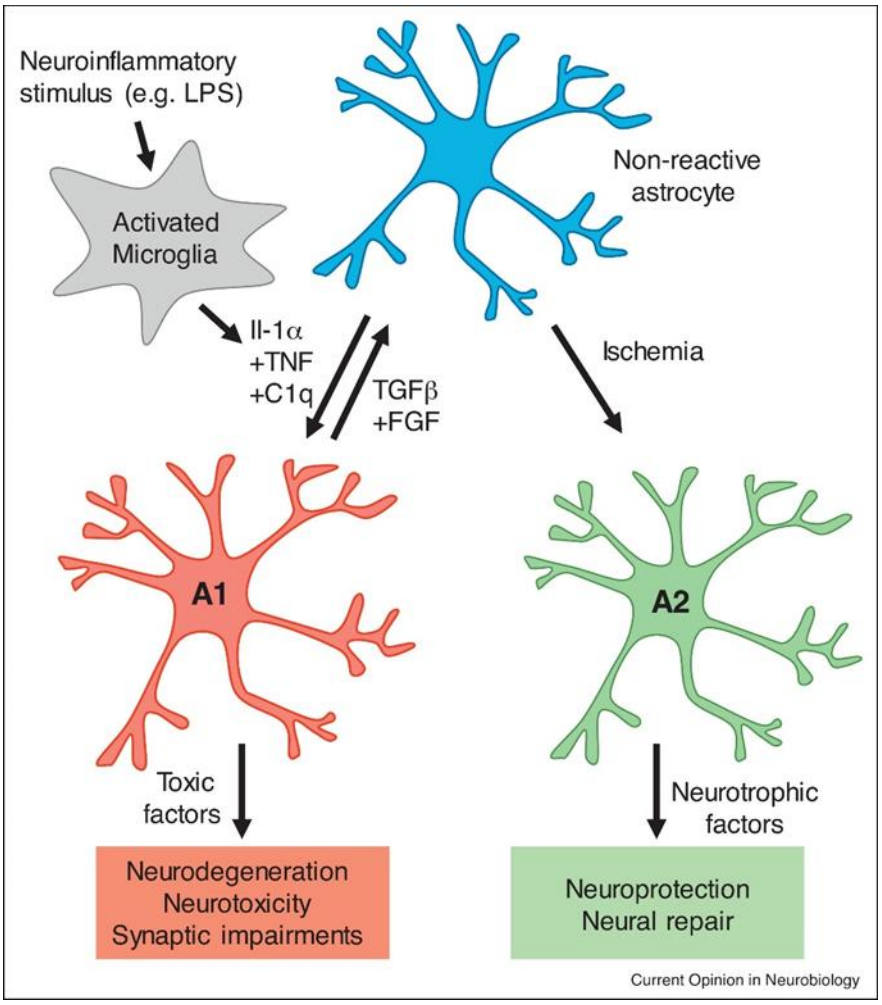

Figure 1.3.1. Heterogeneity of reactive astrocytes. *Following tissue injury, astrocytes become reactive assuming either an A1 neurotoxic phenotype or an A2 neuroprotective phenotype. Neuroinflammatory stimuli such as LPS activate microglia that secretes the inflammatory cytokines IL-1a and IL-1ß, TNF-α, and C1q which yield A1 reactive astrocytes that promote neurodegeneration and neurotoxicity, and are not synaptogenic. In vitro application of TGF-b1 reverts this neurotoxic A1 type to a non-reactive state. Ischemia induces the formation of A2 reactive astrocytes that secrete neurotrophic factors (Baldwin and Eroglu, 2017).*

In several human CNS diseases, including epilepsy, astrocytes can initiate, regulate, and amplify immune-mediated mechanisms that are involved in these pathologies (Farina et al., 2007; Seifert et al., 2010). Both in experimental and in human epilepsy brain tissue, astrocytes produce a wide range of immunologically relevant cytokines and chemokines such as HMGB1, IL-1β, IL-6, TNF-α, TGF-β and monocyte chemoattractant protein-1 (MCP-1; chemokine, C-C motif, ligand 2; CCL2) (Aronica and Crino, 2011; Vezzani et al., 2008).

1.3.3 Microglia

Microglia are the CNS-resident immune cell population (Kreutzberg, 1996). In the adult healthy brain, microglia have a ramified morphology with a small soma and fine cellular processes that are highly mobile in order to patrol the microenvironment (Garden and Möller, 2006; Kettenmann et al., 2011). Several molecules and conditions can induce the transition of microglia from a resting-like to an activated or reactive state (Hanisch and Kettenmann, 2007). Microglial responsiveness can be influenced by factors such as microbial molecules, genomic material, cytokines, ATP and protein aggregates (Block et al., 2007; Hanisch and Kettenmann, 2007; Nakamura, 2002; van Rossum and Hanisch, 2004). Microglia can sense even minor changes in the microenvironment that provoke their rapid morphological changes. Activated microglia assume an amoeboid appearance by retracting their processes (Hanisch and Kettenmann, 2007; Kettenmann et al., 2011) although different reactive phenotypes are described depending on the type and modality of applied stimuli and the microenvironment (Figure 1.3.2).

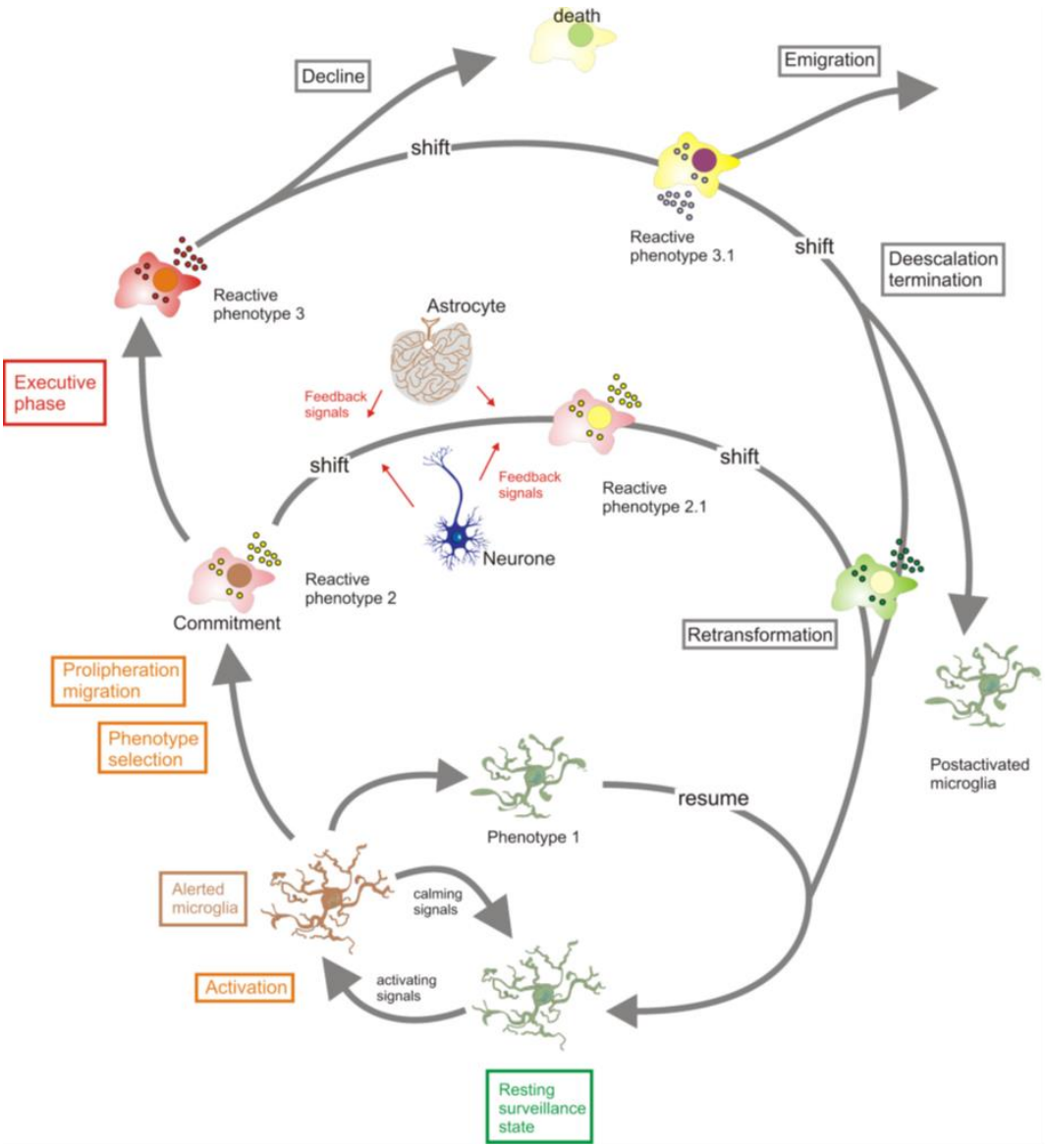

Figure 1.3.2. Microglial activity states. *Microglia at a resting-surveillance state is in a lookout for changes in the microenvironment that can disturb the homeostasis of the neuronal and glial-vascular networks. Appearance of activating signals or loss of inhibitory signals can trigger transitions to alerted and activated state endowed of distinct reactive phenotypes depending on the nature of the stimuli. These phenotypes can be further influenced neurons and astrocytes as well as invading immune cells from the periphery. Microglia may be ''primed'' suggesting that preconditioning with a first stimulus prepares the cell for an enhanced and efficient response to a second stimulus (Kettenmann et al., 2011).*

Microglial cells express a variety of receptors on their cell membrane. Purinergic receptors of both ionotropic and metabotropic receptor subtypes mediate the effect of ATP released from damaged cells after brain injuries (Garden and Möller, 2006; Kettenmann et al., 2011).

Activation of these receptors in microglia mediates the release of superoxide that induces neurotoxicity, cytokine release and autophagy (Brough et al., 2002; Inoue, 2006; Parvathenani et al., 2003; Takenouchi et al., 2009). Purinergic signaling is known to be activated in epilepsy. The P2X7 receptors are sensitive to low concentrations of ATP and an increase in their expression in microglial cells is found in rodent epilepsy models (Avignone et al., 2008; Rappold et al., 2006). Moreover, these receptors are involved in neurodegeneration and neuroinflammation after SE and in seizure recurrence in epileptic mice (Engel et al., 2012; Henshall and Engel, 2015; Jimenez-Pacheco et al., 2013; Takenouchi et al., 2009). P2X4, P2Y6 and P2Y12 receptor expression is also upregulated in microglial cells in rodent hippocampus during seizures (Avignone et al., 2008; Ulmann et al., 2013). Interestingly, microglial P2Y12 receptors were shown to have an anti-epileptogenic effect when upregulated following SE (Eyo et al., 2016).

Microglia express neurotransmitter receptors for glutamate, GABA, monoamines and CB1 and CB2 cannabinoid receptors (Kettenmann et al., 2011). Activation of mGluR2-3 receptors has been associated with microglial activation and neurotoxicity mediated by TNF-α release (Taylor et al., 2005). On the other hand, activation of cannabinoid receptors has been shown to increase microglia proliferation and may reduce microglia-mediated neurotoxicity (Carrier et al., 2004; Stella, 2009).

Receptors for cytokines (IL-1β), chemokines, danger signals and trophic factors are expressed by microglia and play a role in communication between microglia and the surrounding cells as well as in the initiation and regulation of the immune response (Garden and Möller, 2006). Fractalkine (CX3CL1) is one of the molecules mediating the communication between neurons and microglia (Paolicelli et al., 2014; Wolf et al., 2013). CX3CL1 is a chemokine expressed principally by neurons and binds to the CX3CR1 receptor,

which is uniquely expressed in the brain by microglia (Ransohoff and Perry, 2009). Neuronal CX3CL1 acts as an inhibitory signal reducing the activation of CX3CR1-expressing microglia and genetic deletion of CX3CR1 enhanced microglia-mediated neurotoxicity (Cardona et al., 2006; Kettenmann et al., 2011). However, blocking this pathway by administering the anti-CX3CR1 antibody reduced microglial activation induced by SE, neurodegeneration and neuroblast formation in the adult rat hippocampus suggesting a more complex role of this chemokine in microglial activation (Ali et al., 2015).

Toll-like receptors are widely expressed in microglia and directly control their activation (Garden and Möller, 2006; Kettenmann et al., 2011). Activation of TLR4 by LPS exacerbated pilocarpine-induced neurogenesis whereas TLR9 activation following kainic acid seizures reduced aberrant neurogenesis (Matsuda et al., 2015; Yang et al., 2010). Moreover, activation of TLR3 in microglia by its agonist polyinisinic:polycytidylic acid (Poly I:C) or TLR4 by LPS mediates proinflammatory effects *in vitro* (Olson and Miller, 2004) and TLR4 deficiency or pharmacological blockade reduced spontaneous recurrent seizures in epileptic mice (Maroso et al., 2010a).

Microglia rapidly respond to seizures and release proinflammatory cytokines, that lead to neuronal hyperexcitability and neurodegeneration contributing to the development of spontaneous seizures and cognitive decline in epilepsy models (Brewster et al., 2013; Heo et al., 2006; Kwon et al., 2013; Nishimura et al., 2006; van Vliet et al., 2016; Yilmaz et al., 2006; Zeng et al., 2009). However, there is a morphologically heterologous population of microglia in the hippocampus that can potentially promote neuroprotection (Wyatt-Johnson et al., 2017).

1.3.4 Blood-brain barrier

The BBB comprises a monolayer of brain capillary with endothelial cells distinguished by the presence of tight junctions that form an impermeable wall to xenobiotics and other circulating molecules and cells in physiological conditions. Endothelial cells are interconnected with basement membrane, pericytes, astrocytes, microglia (Correale and Villa, 2009; Pardridge, 1999; Persidsky et al., 2006). The BBB is both a physical and metabolic barrier that regulates the blood-to-brain exchange of nutrients, xenobiotics, blood components, and cellular elements by passive diffusion or catalyzed transport of large and/or polar molecules (Pardridge, 1999). BBB maintains brain tissue homeostasis necessary for physiologic neuronal function. BBB dysfunction has been proposed as a causal pathogenic factor in many CNS pathologies including epilepsy (Dallasta et al., 1999; Marchi et al., 2011a; Neuwelt et al., 2011; Ryu and McLarnon, 2009; Tomkins et al., 2011; van Vliet et al., 2007; Weis et al., 1996). Experimental and clinical studies suggest that BBB dysfunction leads to increased propensity for seizure generation in epilepsy (Aronica et al., 2008; Friedman et al., 2009; Frigerio et al., 2012; Marchi et al., 2007; Marcon et al., 2009; Raabe et al., 2012; Seiffert et al., 2004; Shlosberg et al., 2010; Tomkins et al., 2001; van Vliet et al., 2007). BBB dysfunction is a common feature among patients with pharmacoresistant epilepsy (Michalak et al., 2013; Rigau et al., 2007).

Mechanisms responsible for BBB dysfunction include inflammation (Fabene et al., 2008; Librizzi et al., 2012; Vezzani and Friedman, 2011), endothelial apoptosis and dysfunctional perivascular glia, loss of tight junction (TJ) proteins (Abbott et al., 2010; Neuwelt et al., 2011) and altered expression of multidrug transporters such as the ABC efflux transporters that influence the uptake of a variety of xenobiotics, including many ASDs (Abbott et al., 2006; Eugenin et al., 2011; Golden and Pollack, 2003; Wolburg et al., 2003). Loss or

dissociation of proteins responsible for the organization of the TJ such as Zonula occludens-1 (ZO-1), or enhanced transcytosis is associated with increased barrier permeability (Abbott et al., 2010; Bednarczyk and Lukasiuk, 2011). The brain extravasation of serum proteins and in particular of albumin, is one of the consequences of BBB dysfunction following SE. Albumin extravasated in the brain parenchyma can be uptaken by neurons and glia (van Vliet et al., 2015). The presence of albumin in the human epilepsy tissue and in experimental models may contribute to lower seizure threshold through different mechanisms (Cacheaux et al., 2009; Ravizza et al., 2008a; Rigau et al., 2007; van Vliet et al., 2007). In particular, albumin activates transforming growth factor β receptors (TGFβRs) signaling in astrocytes which leads to down regulation of inward rectifying potassium (Kir 4.1) channels and the water channel aquaporin-4 (AQP4) that in turn accounts for the reduced extracellular buffering of potassium and water thus promoting hyperexcitability and epileptiform activity (Ivens et al., 2007). Furthermore, albumin induces transcriptional activation of inflammatory genes via TGFβ signaling (Cacheaux et al., 2009; Ralay Ranaivo and Wainwright, 2010; Ralay Ranaivo et al., 2010) and induces formation of new excitatory synapses by inducing the astrocytic release of trombospondin and other extracellular matrix components (Weissberg et al., 2015). Since albumin binds some ASDs, its presence in brain parenchyma may reduce free ASDs concentrations thereby reducing their effectiveness (Kwan et al., 2011; Neels et al., 2004).

Autoantibodies against neuronal receptors and channels can be transported into the brain tissue through a leaky BBB thus providing another mechanism for alterating neuronal function (Bien and Scheffer, 2011; Rigau et al., 2007; van Vliet et al., 2007) (Figure 1.3.3).

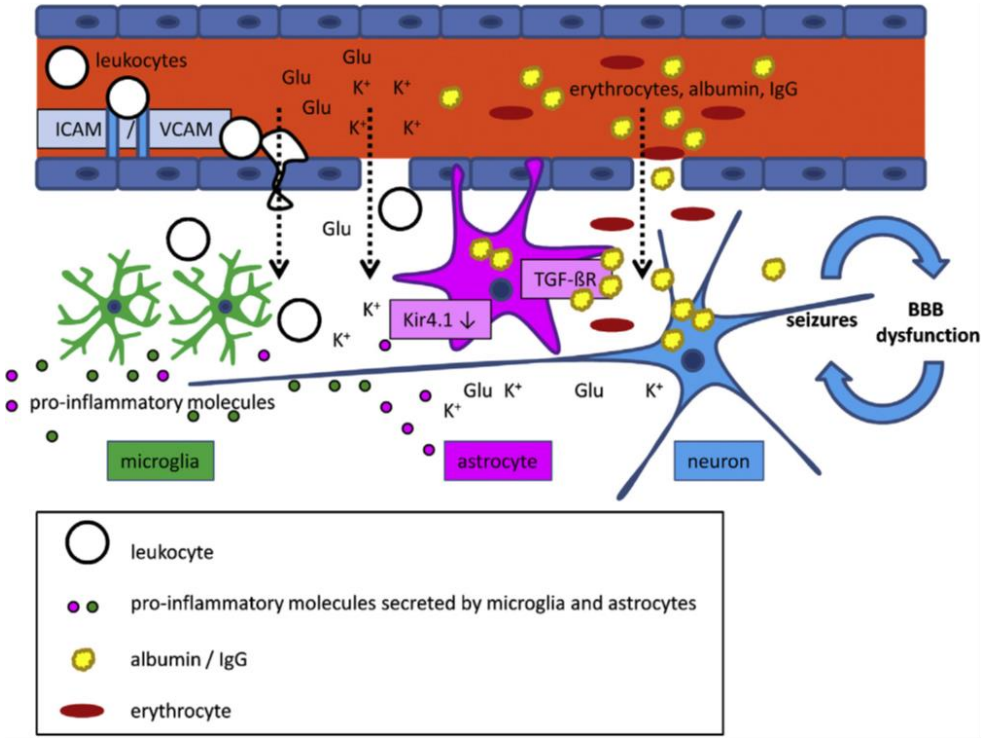

Figure 1.3.3. Schematic representation of processes involved in blood–brain barrier dysfunction. *Leukocytes enter the brain via a dysfunctional BBB or via upregulated adhesion molecule, such as ICAM-1 and VCAM-1, thus contributing to brain inflammatory responses. Increased extracellular K^+ and glutamate due to inflammatory activated astrocytes may also modify neuronal excitability and physiological functions. These changes ultimately may lead to epilepsy (van Vliet et al., 2015).*

1.3.5 Neuroinflammatory ictogenic pathways

The IL-1 receptor/toll-like receptor superfamily (IL-1R/TLR) has been shown to be involved in the generation of neuroinflammation in epilepsy and in seizure mechanisms (Aronica and Crino, 2011; Maroso et al., 2011a; Vezzani et al., 2008, 2010, 2011b). The IL-1R/TLR superfamily is part of the cell surface pattern recognition receptors (PRRs) sharing a conserved intracellular region termed the Toll/IL-1R (TIR) domain (O'Neill, 2008; O'Neill and Dinarello, 2000). TLRs are expressed in immunocompetent cells and several TLRs such as TLR2, TLR3, and TLR4 have been measured in glia, neuronal cells and endothelium in the CNS (Farina et al., 2007). In resting astrocytes, IL-1R1 or TLRs are expressed at low levels but they are upregulated in reactive astrocytes and microglia under different pathological

CNS conditions, including epilepsy (Maroso et al., 2010, 2011a; Ravizza et al., 2006a, 2008a; Vezzani et al., 2011b; Zurolo et al., 2011). TLRs have a key role in pathogen recognition (Kawai and Akira, 2007) but in the absence of pathogens, TLRs can be activated by endogenous molecules, named damage-associated molecular patterns (DAMPs), released from injured or activated cells (sterile inflammation). One of these molecules is the high mobility group box 1 (HMGB1) (Bianchi and Manfredi, 2009), a ubiquitous chromatin binding protein that is actively secreted by immuno-competent cells in response to immune challenges (Muller et al., 2004). Both *in vitro* and *in vivo* findings showed that astrocytes are a source of extracellular HMGB1 (Maroso et al., 2010a; Zurolo et al., 2011). HMGB1 release has been shown to be induced in both rat (Hayakawa et al., 2010) and human astrocytes in culture (Zurolo et al., 2011) in response to the proinflammatory cytokine IL-1β, and nuclear to cytoplasmic translocation, a step required for extracellular release, has been observed in human and experimental epilepsy tissue (Maroso et al., 2010a).

Activation of IL-1R1-mediated signaling by IL-1β induces, via an NF-kB-dependent mechanism, the transcription of other genes encoding downstream mediators of inflammation, including IL-6, TNF-α, cyclooxygenase-2 (COX-2), (Andjelkovic et al., 2000; Dinarello, 2004). IL-1β, by acting on IL-1R type 1, can inhibit the astrocytic reuptake of glutamate (Hu et al., 2000; Ye and Sontheimer, 1996) and increases its glial release likely via induction of TNF-α (Bezzi et al., 2001). TNF-α is a cytokine released from activated astrocytes and microglia, and tightly associated with IL-1β, since the two molecules reciprocally induce their respective release from glia and mutually activate their gene transcription. TNF-α has been shown to increase the mean frequency of AMPA-dependent miniature excitatory postsynaptic currents in hippocampal neurons and to decrease $GABA_A$-mediated inhibitory synaptic strength. These effects are mediated by the

recruitment of AMPA receptors lacking the GluR2 subunit at neuronal membranes (thus in a molecular conformation which favors Ca^{2+} influx into neurons) and by endocytosis of $GABA_A$ receptors respectively (Beattie et al., 2002; Stellwagen et al., 2005). IL-1β can also increase neuronal glutamate release via the activation of inducible nitric oxide synthase in glial cells (Casamenti et al., 1999; Hewett et al., 1994). Activation of NF-kB signaling pathway and induction of a large array of inflammatory mediators in astrocytes in experimental and human TLE suggest that these cells are pivotal for generating and sustaining neuroinflammation (Desjardins et al., 2003; Holtman et al., 2009; Ravizza et al., 2008a; Wu et al., 2008).

TLR4, one of the first Toll-like receptors identified in mammals, has a particular role in epilepsy. It shares its cytosolic domain with IL-1R1 and detects the major component of the gram-negative bacteria lipopolysaccharide LPS. TLR4 signals through both MyD88-dependent and TRIF-dependent pathways in order to induce pro-inflammatory genes through NF-κB and/or MAPK pathways or type I interferons through TRIF/IRF3 axis (Liu and Ji, 2014; O'Neill and Bowie, 2007; Yamamoto et al., 2003). This receptor is rapidly up-regulated in neurons and astrocytes both after seizure onset and during the chronic epileptic phase insults in rodent epileptogenic brain areas (Maroso et al., 2010). Interestingly, knock-out mice lacking this receptor exhibit low seizure susceptibility (Maroso et al., 2010). Its activation by LPS or HMGB1 results in a decreased seizure threshold and is linked to increased hippocampal excitability (Galic et al., 2008; Li et al., 2015a; Rodgers et al., 2009; Sayyah et al., 2003). Moreover, IL-1R1/TLR4 activation leads to a rapid increase in Ca^{2+} influx through phoshorylation of the NR2B subunit of NMDA receptors (Balosso et al., 2008, 2014; Viviani et al., 2003). Activation of the IL-1β and IL-1R1 axis and HMGB1-TLR4 axis in brain tissue from TLE patients is associated with BBB leakage

and albumin extravasation (Aronica et al., 2007; Maroso et al., 2010a; Ravizza et al., 2008b; Rigau et al., 2007; van Vliet et al., 2007). Activating transcriptional factor 3 (ATF-3), a negative regulator of TLR4, has lower expression in patients with frequent seizures whereas TLR4 expression positively correlates with seizure frequency (Pernhorst et al., 2013).

Among the epigenetic modulators studied in animal models of epilepsy and in human brain tissue (Dębski et al., 2016; Sweatt, 2013), miRNA146a is of particular relevance for neuroinflammation since it is tightly linked to the feedback inhibition of IL-1R1/TLR4 signaling (Iyer et al., 2012; van Scheppingen et al., 2016) and is up-regulated in astrocytes and neurons in TLE and focal cortical dysplasia (FCD) and ganglioglioma patients (Aronica et al., 2010; Omran et al., 2012; Quinn and O'Neill, 2011; van Scheppingen et al., 2016). miRNA profiling studies revealed brain region and temporal specific changes in miRNA146a expression in various animal models of epilepsy (Gorter et al., 2014; Roncon et al., 2015). This miRNA downregulates the levels of IL-1R/TLR downstream signaling molecules thus reducing the activation of this pathway (Taganov et al., 2006). Recently, Iori et al.(2017), using a synthetic mimic of miRNA146a injected in an animal model of acquired epilepsy, reported a dramatic reduction in neuronal excitability and chronic seizure recurrence and this treatment prevented disease progression (Iori et al., 2017).

TLR3 has been also implicated in epilepsy. Its stimulation activates NF-kB and the transcription factor interferon regulatory factor (IRF)-3, thereby inducing the production of type I interferon (IFN)-responsive genes (Kawai and Akira, 2010). Differently from TLR4, TLR3 is primarily expressed intracellularly where it acts as a sensor for double-stranded RNA, a product of viral replication.The activation of TLR3 by the synthetic double-stranded RNA polyinosinic-polycytidylic acid (Poly I:C) mimics the effects of viral infection and leads to the production of type I IFNs, IFNα and IFNβ via activation of IRF-3 and IRF-7

(Cunningham et al., 2007). Experimental evidence indicates that the activation of TLR3 by Poly I:C induces the transcription and biosynthesis of cytokines and chemokines (Kirschman et al., 2011; Michalovicz and Konat, 2014). The pro-inflammatory action of Poly I:C in immature rats, is associated with long-lasting hippocampal hyperexcitability and enhanced seizure susceptibility as assessed in adult animals (Galic et al., 2009). Activation of TLR3 may also alter glutamatergic transmission, contributes to epileptogenesis and to the impairment of working and contextual memory in rodents (Costello and Lynch, 2013; Gross et al., 2017; Galic et al., 2009; Okun et al., 2010). However, neuroprotective effects have been also reported specifically mediated by TLR3 activation in astrocytes therefore suggesting that this receptor may have a dual role possibly mediated by different cell types (Bsibsi et al., 2006; Tarassishin et al., 2011b).

1.3.6 Clinical evidence of brain inflammation in human epilepsy

Brain tissue analysis from patients with different forms of epilepsy such as TLE, Rasmussen's encephalitis, FCD and tuberous sclerosis complex (TSC), has revealed inflammatory markers and the presence of activated innate and adaptive immune cells (Boer et al., 2006; Iyer et al., 2010; Maroso et al., 2010; Ravizza and Vezzani, 2006; Ravizza et al., 2006a, 2008a; Vezzani et al., 2011b).

In hippocampal tissue from TLE patients, glial cells display an inflammatory phenotype with overexpression for example of NF-kB, activation of IL-1/TLR4 axis and of the complement system and cytoplasnatic translocation of HMGB1 (Aronica et al., 2007; Crespel et al., 2002; Ravizza et al., 2008a; van Vliet et al., 2007). Despite a common astroglia and microglia activation in human epilepsy specimens, peripheral immune system contribution depends on the epilepsy type. For example, leukocytes are not prominent in TLE specimens except

for the presence of macrophages (Ravizza et al., 2008a). Differently, in patients affected by Rasmussen encephalitis there is an increased expression of inflammatory genes (IL-1β, TNF-α) and the presence of cytotoxic lymphocytes (Baranzini et al., 2002). Interestingly, a marked increase in the expression of TLR3 and TLR9, in the brain tissues of Rasmussen's encephalitis patients was associated with severe brain atrophy suggesting a key role of TLR-related pathway in this rare pediatric disorder (Wang et al., 2017).

Epilepsy is the most common neurologic symptom in patients (70-80%) affected by TSC. TSC is an autosomal dominant and multisystem disorder that results from a mutation in *Tsc1* and *Tsc2* genes that encode for two proteins that act as a negative regulator for the mTOR pathway. This pathway is involved in cell metabolism, growth, proliferation and death as well as synaptic plasticity, neurogenesis, dendritic morphology and axonal sprouting (Ostendorf and Wong, 2015). Cortical tubers, subependymal nodules and giant cell tumors are characteristics of this disorder (DiMario, 2004; Mizuguchi and Takashima, 2001) along with the presence of macrophages, TNF-α and NF-kB expression alterations and activation of the complement system and IL-1β pathway (Boer et al., 2008; Maldonado et al., 2003). Lymphocytes with a T-cytotoxic phenotype and evidence of BBB dysfunction were also observed in the perivascular zone and adjacent brain parenchyma (Boer et al., 2008; Wong, 2008).

FCD represents cytoarchitectural malformations of the cerebral cortex which are among the causes of refractory epilepsy in young individuals (Blumcke, 2009). Specimens from type II FCDs were shown to express the complement system and activation of the IL-1β and TLR pathways, induction of the chemokine CCL2, microglial and astroglial cell reactivity, BBB breakdown, and the presence of cytotoxic T-lymphocytes (Iyer et al., 2010; Zurolo et al., 2011).

Pro-inflammatory mediators were measured in biological fluids such as CSF and plasma from patients with epilepsy of various etiologies (Gallentine et al., 2017; Lehtimaki et al., 2004). In children with febrile SE, the IL-6 cytokine was found elevated in plasma (Gallentine et al., 2017). Moreover, in the same study IL-1RA/IL-6 ratio as a potential biomarker of acute hippocampal injury following febrile status epilepticus (FSE) was identified representing a potential serologic biomarker which offers rapid identification of patients at risk for ultimately developing mesial temporal lobe epilepsy.

Immunomodulatory drugs provide further evidence that inflammation has an important role in epilepsy. Glucocorticoids such as dexamethasone, and adrenocorticotropic hormone (ACTH) can reduce seizure burden in some forms of drug-resistant epilepsies (Marchi et al., 2011b; Vezzani and Granata, 2005). Anti-inflammatory drugs that act on the IL-1β pathway such as VX765 (an ICE/Caspase-1 inhibitor) and Anakinra (IL-1R1 antagonist) have shown therapeutic effects in experimental models and reduced seizures in patients (Bialer et al., 2013; DeSena et al., 2018; Jyonouchi, 2016; Kenney-Jung et al., 2016). The efficacy of VX765 has been tested in a phase II clinical trial where it has shown a positive effect in patients with treatment-resistant partial epilepsy (Bialer et al., 2013). Anakinra induced a reduction on seizure activity and improved cognitive skills in patients with febrile infection-related epilepsy syndrome (FIRES) (Jyonouchi, 2016; Kenney-Jung et al., 2016). Adalimumab (a monoclonal anti-TNF-α antibody) was evaluated in a pilot clinical study in patients with Rasmussen's encephalitis and showed seizure improvement along with functional deficit stabilization in half of the patients recruited (Lagarde et al., 2016). In an open-label trial, patients with severe drug-resistant epilepsy were treated with cannabidiol and motor seizure frequency reduction was reported (Devinsky et al., 2016). In another study, 6 out of 7 patients with FIRES demonstrated improved seizure frequency and

duration after cannabidiol treatment; an anti-inflammatory effect of this drug may in part mediate its therapeutic effects since cannabinoid receptors are found also in cells of the immune system. Furthermore, minocycline, a tetracycline family antibiotic with known inhibitory effects on microglia activation and proinflammatory cytokine release, has been shown to reduce significantly seizure frequency in a patient with severe symptomatic epilepsy (Nowak et al., 2012). In a patient with multiple sclerosis (MS) that manifested tonic-clonic generalized seizures at disease onset, natalizumab (an anti-alpha4 integrin antibody) improved MS condition and reduced seizures (Sotgiu et al., 2010).

1.3.7 Effect of anti-inflammatory treatments in experimental models of ictogenesis and epileptogenesis

Experimental and clinical evidence suggest the involvement of several inflammatory mediators in the generation of seizures and their recurrence. Interestingly, some ASDs, such as valproic acid (VPA) and phenytoin (PHT) have anti-inflammatory properties. VPA inhibits activation of NF-kB and production of TNF-α and IL-6 whereas PHT decreases T- cell activity (Hashiba et al., 2011; Ichiyama et al., 2000).

Some key inflammatory pathways activated in epilepsy along with the effect of anti-inflammatory treatments in experimental studies are discussed below (see also Tables 1.3.1 and 1.3.2).

Interleukin-1 receptor/Toll-like receptor (IL-1R/TLR) signaling

Studies in experimental models have proven that the IL-1R1/TLR4 axis is rapidly activated in brain areas involved in seizure generation and propagation during epileptogenesis (Pauletti et al., 2017; Ravizza et al., 2008a). Activation of this signaling by brain application of endogenous agonists is ictogenic (Balosso et al., 2013; Maroso et al., 2011a; Vezzani et

al., 2011b). Pharmacological blockade and genetic interference with this signaling showed its contribution to seizure mechanisms. Inhibitors of this signaling such a IL-1Ra, caspase-1 inhibitors, TLR4 antagonists, anti-HMGB1 monoclonal antibodies and specific microRNAs (e.g., miR-146a) mediate anti-seizure effects often associated with reduction of the BBB dysfunction and neuroprotection (Balosso et al., 2014; Fu et al., 2017; Maroso et al., 2010, 2011b; Ravizza et al., 2006b; Vezzani et al., 2000; Wang et al., 2018; Zhao et al., 2017). Moreover, this signaling is activated in clinical specimens from patients with pharmacoresistant epilepsies such as low-grade epilepsy-associated glioneuronal tumors (GNT), FCD, TLE and RE (Fuso et al., 2016; Luan et al., 2016; Maroso et al., 2010; Pernhorst et al., 2013; Prabowo et al., 2013; Ravizza et al., 2006a, 2008a; Roseti et al., 2015; Zhang et al., 2018; Zurolo et al., 2011).

Simultaneous targeting of IL-1R1 and TLR4 signaling after SE induction in mice or at disease onset, mediated significant reduction in chronic seizure recurrence and prevented disease progression after treatment withdrawal (Iori et al., 2017; Walker, 2017). In a similar way, inhibition of HMGB1 by a monoclonal antibody reduced seizure frequency and improved cognitive deficits (Zhao et al., 2017). In an experimental model of TBI, treatment with IL-1Ra resulted in a rise in seizure threshold to pentylenetetrazol (PTZ) accompanied by improvement in spatial memory (Semple et al., 2017). Further support for the involvement of this pathway in epilepsy comes from studies in transgenic mice with defective IL-1R1-TLR4 signaling that show reduction in acute seizure susceptibility and in spontaneous seizures evoked by SE (Iori et al., 2013; Maroso et al., 2010; Ravizza et al., 2006b; Vezzani et al., 2000).

Tumor necrosis factor-alpha (TNF-α)

TNF-α is a cytokine with a dual role in seizures. During seizures TNF-α is expressed by glia and endothelial cells in rodents (De Simoni et al., 2000; Dhote et al., 2007; Lehtimaki et al., 2003; Turrin and Rivest, 2004). TNF-α receptor type 2 (TNFR2) levels are reduced in neurons and TNFR1 is increased in neurons and astrocytes (Balosso et al., 2013; Weinberg et al., 2013). TNF-α and its receptors undergo similar changes in TLE and in TSC patients (Balosso et al., 2013; Maldonado et al., 2003).

Activation of TNFR2 in the mouse hippocampus after injection of recombinant TNF-α resulted in reduction of seizures whereas activation of TNFR1 promoted seizure generation (Balosso et al., 2005). The same finding was observed also in two models of amygdala stimulation (Weinberg et al., 2013). Transgenic mice with low or moderate overexpression of TNF-α were less susceptible to develop seizures while mice with high TNF-α expression are more prone to developing seizures (Akassoglou et al., 1997; Balosso et al., 2005). These data support the concept that this cytokine exerts its actions depending on its concentration and the receptor subtype activated.

Arachidonic acid-related pathways

Cyclooxygenase-2 (COX-2), the enzyme responsible for the biosynthesis of prostanoids is expressed in physiological conditions in neurons (Hurley et al., 2002; Yamagata et al., 1993). COX-2 is upregulated in neurons early after SE and in astrocytes at later time points and during chronic seizures (Holtman et al., 2009; Kulkarni and Dhir, 2009; Lee et al., 2007). In TLE patients, COX-2 is expressed in neurons and it is found in astrocytes only in patients with HS (Desjardins et al., 2003).

Increased neuronal expression of COX-2 in transgenic mice induced higher seizure susceptibility whereas COX-2 deficient mice or in mice treated with the COX-2 inhibitor

nimesulide showed reduced seizure susceptibility suggesting thus a proconvulsive role of this enzyme (Kelley et al., 1999; Takemiya et al., 2003). However, studies employing selective COX-2 inhibitors such as celecoxib, parecoxib, indomethacin and SC58236 have highlighted a dual role of this enzyme in epileptogenesis (Aronica et al., 2017; Kulkarni and Dhir, 2009). In particular, COX-2 inhibition before SE induction with pilocarpine or kainate (KA) had procolvusive effect whereas inhibition after SE and during epileptogenesis resulted either in neuroprotection and reduction of spontaneous seizure severity or no effects, or even seizure exacerbation (Holtman et al., 2009; Jung et al., 2006; Kunz and Oliw, 2001a). These differential effects suggest that the timing of COX-2 blockade may determine the suppressive or aggravating outcome on seizures.

These dichotomous results in SE models prompted to target downstream effector molecules of the COX-2 signaling pathway such as the prostanglandin EP1 and EP2 receptors (Jiang et al., 2015; Kawada et al., 2012). The EP1 receptor antagonist SC-51089 had only a moderate effect on seizure severity but antagonizing the EP2 receptors led to reduction of neuronal injury, inflammation, BBB opening and induced neuroprotection (Fischborn et al., 2010; Jiang et al., 2012, 2013). A combined treatment with the COX-2 inhibitor CAY10404 and anakinra resulted in reduction of spontaneous seizure development after SE and limited the extend of CA1 injury and mossy fiber sprouting (Kwon et al., 2013).

Recently, Terrone et al. (2018) showed that Monoacyl-Glycerol-Lipase (MAGL), the enzyme responsible for the brain synthesis of arachidonic acid, is a potential target for the treatment of drug-resistant SE. They reported that administration of a MAGL inhibitor (CPD-4645) early during SE reduced significantly severity and duration of SE as well as neuronal loss and cognitive deficit in mice (Terrone et al., 2018).

Until now no clinical trials using specific COX-2 inhibitors have been conducted in epilepsy patients due to the side effects of such drugs (Radu et al., 2017). Despite that, non-selective COX inhibitors were studied in epilepsy patients (Ma et al., 2012; Xu et al., 2013). Ibuprofen treatment in children with febrile seizures failed to show significant effects (van Stuijvenberg et al., 1998). On the other hand, patients with Sturge-Weber syndrome or focal onset epilepsy showed reduction in seizure frequency although such results should be further validated (Bay et al., 2011; Godfred et al., 2013; Lance et al., 2013; Udani et al., 2007).

Transforming growth factor-beta (TGF-β) signaling

Extravasation of serum albumin into the brain parenchyma after BBB breakdown activates transforming growth factor β (TGF-β) signaling in astrocytes that results in neuronal hyperexcitability and decreased seizure threshold through many mechanisms as discussed before (see sections 1.2.2 and 1.3.4). Transient treatment with losartan, an angiotensin II type 1 receptor antagonist which blocks TGF-β signaling, reduced neuronal loss, BBB dysfunction, neuroinflammation and incidence as well as severity of epilepsy in animal models of vascular injury and SE (Bar-Klein et al., 2014; Tchekalarova et al., 2014). Moreover, losartan delayed seizure onset, showed neuroptotection and alleviated seizure frequency and duration after discontinuation of the treatment in SE-exposed rats (Tchekalarova et al., 2016). In a TBI mouse model, other two angiotensin II type 1 receptor antagonists, candesartan and telmisartan were tested and were shown to reduce glia activation, enchancement of cognitive and motor function along with reduction of lesion volume (Villapol et al., 2015).

Complement system

The complement system consists of more than 30 proteins that interact in order to protect the organism against invading pathogens and from deposition of immune complexes in healthy tissue (Xiong et al., 2003). Both neurons and glia express complement proteins in normal conditions but in animal models of epilepsy and TLE patients several of these protein were overexpressed (Aronica et al., 2007; Becker et al., 2003; Gorter et al., 2006; Jamali et al., 2006; Yu et al., 2002). A number of animal studies has identified a role of the complement system in epilepsy. Mice deficient for C3 demonstrated a lower number of behavioral seizures after Theiler's virus infection compared to wild-type mice and rats deficient for C6 had a delayed kindling development (Holtman et al., 2011; Libbey et al., 2010). Intrahippocampal infusion in rats of C5b6, C7, C8 and C9 (complement proteins that form the membrane attack complex) induced seizures and neuronal cell loss (Xiong et al., 2003). PMX53, a C5ar1 antagonist with short half-life, had anticonvulsant effects in both acute and chronic seizure models (Benson et al., 2015). The same antagonist or C5ar1 genetic deletion resulted in reduced seizures and SE associated mortality along with neuroprotection in the hippocampus (Benson et al., 2015).

Chemokines

Apart from their classic role of chemotactic molecules, they can modulate voltage-gated ion channels and neurotransmitter release. Various chemokines and their receptors were found to be upregulated in human and experimental epilepsy brain tissue (Cerri et al., 2016; Fabene et al., 2010; Guyon and Nahon, 2007; Roseti et al., 2013; Rostène et al., 2007). In particular, CCL2 and its receptor CCR2 (CC receptor subtype 2), are upregulated in both human and experimental epilepsy and a CCL2 polymorphism causing elevated levels of CCL2 is associated with higher susceptibility to drug-resistant epilepsy (Cerri et al., 2016;

He et al., 2013). In a chronic epilepsy mouse model, three modulators of the CCL2/CCR2 pathway, a CCL2 transcription inhibitor (bindarit), a selective antagonist of the CCR2 receptor (RS102895), or an anti-CCL2 antibody prevented spontaneous seizure exacerbation caused by systemic challenge with LPS (Cerri et al., 2016).

Sphingosine 1-Phosphate Receptors

Sphingosine 1-phosphate receptors (S1PRs) are a family of 7 helix transmebrane G protein-coupled receptors that bind extracellular sphingosine 1-phosphate (S1P) and are expressed by many cell types, including immune cells, glia and neurons (Bryan and Del Poeta, 2018). Fingolimod (FTY720) is an analogue of sphingosine and when phosphorylated *in vivo* by sphingosine kinases, binds S1PR1, 3, 4, and 5 (Albert et al., 2005). Its main mechanism of action is sequestration of lymphocytes into lymph nodes which is mediated by S1PR1 that leads to a functional antagonism once the receptor has been internalised and degraded (Brinkmann et al., 2002; Mandala et al., 2002; Oo et al., 2007). Fingolimod crosses the BBB and binds S1P receptors (S1P1, -3, -5) (Foster et al., 2007). It is clinically approved for oral treatment of relapsing forms of multiple sclerosis (Brinkmann, 2007). Apart from its immunomodulatory effects in periphery, fingolimod has shown neuroprotective and anti-inflammatory effects in the brain (Rothhammer et al., 2017; Soliven et al., 2011) acting on astrocytes and extracellular-signal regulated kinase (ERK) phosphorylation through S1P1 receptors (Osinde et al., 2007). *In vitro* data demonstrate that fingolimod can reduce transmigration of peripheral blood mononuclear cells through the BBB (Spampinato et al., 2015). Gao et al. (2012), demonstrated that fingolimod exerts both anti-inflammatory and antiepileptogenic effects in a lithium-pilocarpine rat model of epilepsy (Gao et al., 2012). Fingolimod also inhibited pathological mossy fiber sprouting and activation of microglia and reduced the increased expression of IL-1β and TNF-α in the hippocampus (Gao et al., 2012).

Furthermore, the incidence, duration, frequency, and severity of spontaneous seizures was significantly decreased in fingolimod-treated animals. In a more recent study, fingolimod treatment alleviated overexpression of hippocampal P-glycoprotein (P-gp), an important mediator of ASDs efflux that is implicated in drug-resistant epilepsy, and reduced NF-kB activity and TNF-α and COX-2 expression in the same model (Gao et al., 2018). Interestingly, fingolimod was recently used in an animal model of TLE showing that although it had no effect on SE itself, animals developed less seizures associated with attenuation of gliosis, neuronal cell loss and immune cell infiltrates (Pitsch et al., 2018).

Fingolimod also binds and inhibits histone deacetylases (HDACs) (Hait et al., 2014). Moreover, it can interact with lipids and inhibits the cannabinoid receptor CB1 and the activity of phospholipase A2 in mast cells (Brunkhorst et al., 2014).

S1PR modulation represents therefore a potential therapeutic target for epilepsy (Huwiler and Zangemeister-Wittke, 2018; Pitsch et al., 2018).

Table 1.3.1. Effects of anti-inflammatory treatments on seizures and epileptogenesis *(van Vliet et al., 2018).*

Seizure susceptibility/recurrence			
Drug	**Convulsant stimulus/ Experimental model**	**Effects**	**Reference**
IL-1R/TLR signaling			
IL-1ra (IL-1 receptor antagonist)	acute symptomatic seizures (KA) in rats; (Bic) in mice	↓ total time in seizures delay in seizure onset; ↓ seizure total duration	(Vezzani et al., 1999, 2000)
VX-765 (IL-1β synthesis inhibitor)	acute symptomatic seizures (KA) in rats; (KA) in mice	delay in seizure onset; ↓ seizure number and total duration	(Ravizza et al., 2006b; Vezzani et al., 2010)

VX-765	SRS in mice; GAERS rat	↓ total time in SRS ↓ number and duration of spike-and-waves	(Akin et al., 2011; Maroso et al., 2011b)
BoxA (TLR4 antagonist)	acute symptomatic seizures (KA and Bic) in mice; SRS in mice	delay in seizure onset; ↓ seizure number and total duration ↓ SRS number and total duration	(Maroso et al., 2010)
LPS-Rs (TLR4 antagonist)	acute symptomatic seizures (KA and Bic) in mice; SRS in mice	delay in seizure onset; ↓ seizure number and total duration ↓ SRS number and total duration	(Maroso et al., 2010)
Ifenprodil (NR2B antagonist)	SRS in mice	↓ SRS number and total duration	(Maroso et al., 2010)
HMGB1 monoclonal antibody	MES in mice; PTZ in mice	↑ threshold; ↓ time in tonic-clonic seizures; ↓ death delay onset of generalised seizures; ↓ seizure stage; ↓ incidence of tonic seizures	(Zhao et al., 2017)
A438079 (P2X7 antagonist)	Intra-amygdala KA-induced SE in mice	↓ SE duration	(Engel et al., 2012)
COX-2 signaling			
Celexocib	PTZ in rats	delay in seizure onset; ↓ seizure duration	(Oliveira et al., 2008)
Celexocib	acute symptomatic seizures (KA) in mice; (KA) in rats	↑seizure severity and mortality	(Baik et al., 1999; Gobbo and O'Mara, 2004; Kim

			et al., 2008)
Rofecoxib	PTZ in mice	delay in seizure onset; ↓ seizure duration	(Dhir et al., 2006)
Rofexocib	PTZ in mice	↑seizure threshold	(Akula et al., 2008)
Rofexocib	PTZ in mice	No effects on acute seizures	(Claycomb et al., 2011)
Nimesulide	PTZ in mice	delay in seizure onset; ↓ seizure duration	(Dhir et al., 2006)
Nimesulide	acute symptomatic seizures (KA) in mice; (KA) in rats	↑seizure severity ↑seizure severity and mortality when administered before KA	(Kim et al., 2008; Kunz and Oliw, 2001b)
NS-398	acute symptomatic seizures (KA) in mice	↑seizure severity and mortality	(Baik et al., 1999)
Complement			
PMX53 (C5ar1 antagonist)	6 Hz and corneal kindling model in mice; Pilocarpine-induced SE in mice; Intra amydgala KA-induced SE in mice	↓ seizure severity ↑ seizure threshold ↓ mortality, 30% fewer mice experienced SE when treated after SE ↓ number SRS and time spent in seizures	(Benson et al., 2015)
Chemokines			
Bindarit (CCL2 transcription inhibitor)	SRS in mice	↓ inflammation-induced SRS worsening	(Cerri et al., 2016)

RS102895 (CCR2 antagonist)	SRS in mice	↓ inflammation-induced SRS worsening	(Cerri et al., 2016)
CCL2 antibody	SRS in mice	↓ inflammation-induced SRS worsening	(Cerri et al., 2016)
RNA interference against CCR5	KA-induced SE in rats	delay in SE onset; ↓ SE severity; ↓ recovery time	(Louboutin et al., 2011)
Epileptogenesis			
Drug	**Experimental model**	**Effects**	**Reference**
IL-1R/TLR signaling			
VX-765	Electrical rapid kindling in rats	No kindling development	(Ravizza et al., 2008b)
VX-765+IL1ra	Electrically-induced SE in rats	No effects on SRS; neuroprotection	(Noe et al., 2013)
VX-765+CyP	Intra amygdala KA-induced SE in mice	Blockade of SRS progression; ↓ number SRS	(Iori et al., 2017)
IL-1ra+BoxA +Ifenprodil	Electrically-induced SE in rats	Blockade of SRS progression; ↓ number SRS; neuroprotection	(Walker, 2017)
Synthetic miR-146a	Intra amygdala KA-induced SE in mice	Blockade of SRS progression; ↓ number SRS	(Iori et al., 2017)
HMGB1 monoclonal antibody	Electrical rapid kindling in mice	↓ severity of seizures	(Zhao et al., 2017)
HMGB1 monoclonal antibody	KA-induced SE in mice	↓ number SRS; improvement of cognitive deficits	(Zhao et al., 2017)
JNJ-47965567 (P2X7 antagonist)	Intra amygdala KA-induced SE in mice	↓ number SRS	(Jimenez-Pacheco et al., 2016)
COX-2 signaling			
Rofexocib	PTZ kindling in mice	No effects on kindling	(Claycomb et al., 2011)

Nimesulide	PTZ kindling in mice; Electrical rapid kindling in mice; Electrical rapid kindling in rats	↓ kindling development	(Dhir et al., 2007; Takemiya et al., 2003; Tu and Bazan, 2003)
Celecoxib	Pilocarpine-induced SE in rats	↓ number and duration SRS	(Jung et al., 2006)
Celecoxib or NS-398	Electrical kindling in mice	No effects on kindling	(Fischborn et al., 2010)
Parecoxib	Pilocarpine-induced SE in rats	↓ severity SRS	(Polascheck et al., 2010)
SC-58236	Electrically-induced SE in rats	No effects on SRS	(Holtman et al., 2009)
SC-58236	Electrically-induced SE in rats	↑ mortality	(Holtman et al., 2010)
SC-58236	Electrically-induced SE in rats	↑ number SRS in 50% of the rats	(Holtman et al., 2010)
SC-51089 (EP1 antagonist)	Electrical kindling in mice	↓ seizure severity	(Fischborn et al., 2010)

Bic= bicuculline, GAERS= Genetic Absence Epilepsy Rat from Strasbourg, KA= kainic acid, MES=maximal electroshock, PTZ=pentylenetetrazol, SE= status epilepticus, SRS= spontaneous recurrent seizures. KA= kainic acid, PTZ=pentylenetetrazol, SE= status epilepticus, SRS= spontaneous recurrent seizures.

Table 1.3.2. Clinical studies using anti-inflammatory treatments *(van Vliet et al., 2018).*

Drug	Patients	Effects	Reference
IL-1R/TLR signaling			
VX09-765-401 (IL-1β synthesis inhibitor)	Phase IIa randomized double blind placebo controlled study in drug-resistant focal onset epilepsy	Delayed beneficial effects (subject with ≥50% reduction in seizure frequency) that persist after drug discontinuation	(Bialer et al., 2013)
Kineret (IL-1 receptor antagonist)	Case report: super refractory SE secondary to FIRES	Drastic improvement of seizure control	(Kenney-Jung et al., 2016)
Kineret	4 case reports: drug resistant epilepsy	Drastic improvement of seizure control and cognitive skills	(Jyonouchi, 2016)
COX-2 signaling			
Ibuprofen	Randomized placebo controlled studies in children with febrile seizures (n=230)	Failure of preventive effects on the number of seizure recurrences in children at increased risk	(van Stuijvenberg et al., 1998)
Aspirin	Sturge-Weber (n=9)	8 of 9 patients were seizure-free for 1 year or more	(Udani et al., 2007)
Aspirin	Sturge-Weber (n=58)	Improvement of seizure control in 91% of the patients	(Lance et al., 2013)
Aspirin	Sturge-Weber (n=34)	Improvement of self-reported seizure control and reduction of stroke-like events	(Bay et al., 2011)
Aspirin	Focal onset epilepsy (n=46)	Improvement of seizure control	(Godfred et al., 2013)
TNF-α			
Adalimumab **(**anti-TNF-α monoclonal antibody	Rasmussen's	Seizure improvement in 5 out of 11 patients, associated in 3 of these 5 patients with stabilization of functional deficit	(Lagarde et al., 2016)

1.3.8 Biomarkers of epileptogenesis

The lack of sensitive and specific biomarkers to identify people at risk of developing epilepsy is a major obstacle for developing novel therapeutic interventions to treat, cure or prevent epilepsy (Engel et al., 2013). The ILAE task force's report identifies a biomarker "an objectively measured characteristic of a normal or pathological biological process" (Engel et al., 2013). Biomarkers of epileptogenesis could (1) predict the development of an epilepsy condition, (2) identify the presence and severity of tissue capable of generating spontaneous seizures, (3) measure progression after the condition is established, (4) be used to create animal models for more cost-effective screening of potential anti-epileptogenic and anti-seizure drugs and devices, and (5) reduce the cost of clinical trials of potential antiepileptogenic interventions by enriching the patients population at high risk for developing epilepsy."

Ideally, a biomarker should be sensitive, specific, non invasive, of low cost and easily accessible. Different types of biomarkers are being characterized and validated in both preclinical and clinical studies and these include circulating molecules, genetic markers, electrophysiological and imaging biomarkers as well as behavioral biomarkers. Due to the complex and vast mechanisms implicated in epileptogenesis a single biomarker is assumed to be insufficient for predicting epileptogenesis. Thus, a combined approach may be necessary in order to identify suitable biomarkers at different stages of the disease (Loscher et al., 2013). To this end, the time-dependent evolution of cellular and molecular alterations occurring in the tissue during disease development has to be better understood.

1.4 *IN VIVO* IMAGING OF NEUROINFLAMMATION

Brain imaging has become fundamental for helping the diagnosis of epilepsy and as a tool for identifying surgical candidates. However, a recent application of molecular neuroimaging is to detect alterations within brain networks which may be predictive of epilepsy development or disease severity and could act as early biomarkers of therapeutic effects of interventions (Obenaus, 2013). In this respect, imaging of activated glial cells in epilepsy has attracted much attention and research efforts.

1.4.1 *In vivo* bioluminescence imaging

Non-invasive bioluminescence imaging (BLI) is based on the ability of several organisms to produce light by luciferase-catalyzed reaction of the substrate luciferin in the presence of oxygen and ATP. When used for imaging purposes, a "luciferase" gene (bacterial lux, firefly luc or Renilla Rluc) is inserted into the genome of cells under the control of a specific promoter. Whenever the promoter is active, luciferase is expressed, resulting in the emission of light when its substrate luciferin is administered. This technique can be used to visualize gene expression, to study protein–protein interactions, and to track cells non-invasively (Contag, 2007; Welsh and Kay, 2005).

A number of studies have reported the use of BLI to track neuroinflammation in several CNS disorders. In particular, transgenic mice bearing the GFAP promoter upstream of the luciferase gene have been used. In an experimental autoimmune encephalomyelitis (EAE) model, GFAP-luc mice showed increased signal after immunization and this signal preceded the onset of clinical symptoms, correlated with clinical score, weight loss and histological markers of activated astrocytes (GFAP) and microglia (Luo et al., 2007, 2008). Zhu et al, using the same transgenic mouse detected reactive astrogliosis at 24 h and 48 h after

intracranial injection of kainic acid and this result correlated with endogenous GFAP and luciferase RNA levels as well as with hippocampal cell death (Zhu et al., 2004). Another study, proposed the use of a dual transgenic reporter mouse for monitoring glial activation. Firefly luciferase was under the control of the GFAP promoter and Renilla luciferase under the control of glyceraldehyde 3 phosphate dehydrogenase (GAPDH) promoter providing thus a normalized GFAP signal under inflammatory conditions (Cho et al., 2009). In the same study it was shown that changes in GFAP/GAPDH ratio preceded those in total GFAP protein assessed *ex vivo* after kanic acid-induced seizures (Cho et al., 2009). GFAP-luc mice were used successfully to study astrocytic activation in response to peripheral immune activation elicited by LPS or Poly I:C and in a model of mild TBI (Biesmans et al., 2015; Luo et al., 2014).

Another approach for studying inflammation using BLI is to develop transgenic mice that express luciferase downstream the promoter for a specific inflammatory gene. Accordingly, transgenic mouse models were developed for monitoring immune activation in synucleinopathies, amyotrophic lateral sclerosis and ischemia (Breid et al., 2017; Keller et al., 2009; Lalancette-Hébert et al., 2009, 2017). Transcription factor CCAAT enhancer binding protein (C/EBP) and nestin, regulate inflammation through transcriptional activation of inflammatory genes and differentiation of astrocytes and microglia under neuroinflammatory conditions from nestin-positive cells (Krishnasamy et al., 2017; Lopez de Heredia et al., 2011). They both have been used for transgenic mouse generation in order to provide information on the cellular mechanisms underlying inflammation and their utility for noninvasive pre-clinical evaluation of therapeutic agents targeting inflammatory diseases or as context-dependent biomarkers of the inflammatory response has been suggested (Krishnasamy et al., 2017; Lopez de Heredia et al., 2011). Interestingly, IL-1β

gene promoter was also used for the generation of a transgenic mouse line that expressed luciferase (Li et al., 2008). In this study, LPS-induced sepsis and zymosan-induced arthritis were used as models of inflammatory diseases and increased luciferase activity was correlated with an increase of endogenous IL-1β mRNA and pro-IL-1β protein levels which was suppressed in both models by application of the anti-inflammatory drug dexamethasone (Li et al., 2008).

BLI offers several advantages such as high sensitivity, use of non-ionizing radiation and requirement for relatively inexpensive and simple instrumentation. One of the main limitations is the relatively low spatial resolution due to light scattering (~1 mm) that decreases with the depth of the luminescent source. However, the penetration depth is sufficient to image most tissue is rodents (Ntziachristos, 2006). This technique is based on the insertion of reporter luciferase genes into the organism thus restricting its use only to experimental models. Nevertheless, BLI does not require a light source for illumination limiting this way the background signal due to auto-luminescence and achieving high signal-to-background ratios (Troy et al., 2004).

1.4.2 Magnetic Resonance Spectroscopy

^{1}H-MRS spectroscopy is used in epilepsy models and in the clinic to reveal specific metabolic changes in the brain tissue that cannot be identified by MRI. Several metabolites implicated in epileptogenesis can be measured by this quantitative technique. In particular, glutathione (GSH) and myo-inositol (mIns) are strictly associated with astrogliosis. GSH is an antioxidant peptide synthesized mainly in astrocytes (Dringen et al., 1999). It exerts major antioxidant activity and may have antagonistic action at NMDA receptors (Janaky et al., 1999). Myo-inositol is a metabolic marker of astrocytes and is elevated during

epileptogenesis (Filibian et al., 2012; Lee et al., 2012). Filibian et al. (2012), suggested that GSH and mIns in the hippocampus are biomarkers of epileptogenesis (Filibian et al., 2012). Moreover, GSH hippocampal levels were negatively correlated with seizure frequency and mIns levels were negatively correlated with neuronal loss (Filibian et al., 2012). Additionally, in a pilocarpine status epilepticus model, where only a subpopulation of animals develops epilepsy, mIns levels were found elevated before the onset of the disease and could predict which animals developed epilepsy (Pascente et al., 2016).

An increase in mIns levels was found in patients with TSC, TLE and Rasmussen's encephalitis and was associated with astrogliosis (Doelken et al., 2008; Mizuno et al., 2000; Turkdogan-Sozuer et al., 2000)

1.4.3 Positron Emission Tomography

Several PET ligands have been developed to target specific molecules expressed by immune cells in the brain tissue (Amhaoul et al., 2014) such as the translocator protein (TSPO). TSPO is a 18kDa protein located in the outer membrane of the mitochondria and has a role in physiological processes such as the translocation of cholesterol into the mitochondria (Casellas et al., 2002; Papadopoulos et al., 2006; Rupprecht et al., 2010). In healthy brain this protein is expressed at low levels but under inflammatory conditions it is upregulated both in animal models of epilepsy and in human tissue (Altar and Baudry, 1990; Amhaoul et al., 2015; Guilarte et al., 1995; Johnson et al., 1992; Kumlien et al., 1992; Sauvageau et al., 2002). Microglia is thought to be the primary cell population expressing this protein since TSPO was found to co-localize with markers of microglia (Amhaoul et al., 2015; Cosenza-Nashat et al., 2009; Dedeurwaerdere et al., 2012; Ji et al., 2008; Martín et al., 2010). Higher uptake of the TSPO tracer ^{18}F-DPA-714 has been shown in both epilepsy and

stroke models and this uptake was correlated histologically to activated microglia/macrophages (Harhausen et al., 2013). Furthermore, in a KA-induced SE rat model, [^{18}F]-PBR111 ligand uptake was higher during early epileptogenesis phase in different epileptogenic regions including the hippocampus and the amygdala and was associated with activated microglia after *post-mortem* autoradiography (Dedeurwaerdere et al., 2012). The same study demonstrated that there is a correlation between SE severity and the extent of brain inflammation since animals that had a less severe SE displayed a lower TSPO overexpression (Dedeurwaerdere et al., 2012).

Similarly, TSPO was upregulated in specific brain regions during epileptogenesis in the lithium-pilocarpine rat model of TLE (Brackhan et al., 2016; Yankam Njiwa et al., 2017). Interestingly, in a self-sustained SE rat model the higher uptake of the TSPO ligand ^{11}C-PK11195 was associated with drug resistance although the higher uptake might be related to higher seizure frequency of the non-responder to phenobarbital animals (Bogdanovic et al., 2014). TSPO imaging was sensitive enough to detect the anti-inflammatory effect of minocycline in a stroke model and of fingolimod in an experimental autoimmune encephalitis model implying its role as a biomarker of drug response (Airas et al., 2015; Martín et al., 2011).

However, experimental and clinical data provide evidence that TSPO is also increased in astrocytes (Chen et al., 2004; Cosenza-Nashat et al., 2009; Dickens et al., 2014; Ji et al., 2008; Lavisse et al., 2012; Nguyen et al., 2018). In particular, a longitudinal PET imaging study in an intra-hippocampal KA mouse model using the TSPO ligand ^{18}F-DPA-714 has revealed a time dependent switch of glia cells expressing TSPO. At 7 days the signal reached a peak and microglia was the cell population mainly involved in the TSPO PET uptake while at 6 months this uptake derived mostly from reactive hypertrophic astrocytes (Nguyen et

al., 2018). In the same model, quantitative longitudinal [^{18}F]GE180 PET imaging revealed microglia activation early after SE in the KA-injected hippocampus and to a lesser extent in the contralateral homotipic area, indicating a neuroinflammatory response also in areas of seizure propagation as in humans (Amhaoul et al., 2015; Bogdanovic et al., 2014; Brackhan et al., 2018; Gershen et al., 2015). PET imaging of TSPO is therefore a sensitive and useful tool for identifying neuroinflammation during epileptogenesis (Amhaoul et al., 2015; Brackhan et al., 2016; Dedeurwaerdere et al., 2012; Russmann et al., 2017).

Since elevated TSPO levels were found in various cell types (microglia, macrophages and astrocytes) and its distribution was disease, time and region dependent, combined histological evaluation should be performed in order to determine specific cell expression of TSPO.

TSPO PET imaging has already been performed in clinic in order to identify the epileptogenic zone or determine the underlying pathology (Banati et al., 1999; Butler et al., 2013; Goerres et al., 2001; Kumar et al., 2008). Importantly, TSPO has been detected in post-surgical tissue from patients with epilepsy: TSPO gene expression was increased in patients with HS and a correlation between higher TSPO binding and density of glial cells has been shown (Johnson et al., 1992; Kumlien et al., 1992; Sauvageau et al., 2002). An increased TSPO binding has been shown both ipsilaterally and contralaterally to the seizure focus in TLE patients (Gershen et al., 2015; Hirvonen et al., 2012). Moreover, activated microglia was identified by [^{18}F]-PBR111 uptake in tissue from Rasmussen's encephalitis and FCD patients (Banati et al., 1999; Butler et al., 2011). In a recent case report, seizure focus with no visible MRI correlate was successfully identified using TSPO PET imaging during a seizure-free period (Butler et al., 2016). Importantly, post-seizure imaging revealed increased inflammation spreading further from the clinically-defined seizure focus

and highlighted that post-seizure evaluation of inflammation may lead to less precise localization of the seizure focus (Butler et al., 2016).

Other molecules are potential targets for developing imaging markers of microglia/macrophage activation such as CB2 receptors (Hosoya et al., 2017; Tolón et al., 2009). In specimens from patients with FCD and cortical tubers, CB2 receptor was upregulated in balloon and giant cells and co-localized with astrocytes, microglia and macrophages (Zurolo et al., 2010). Some newly synthesised probes such as CB2 tracer [^{11}C]NE40 have been shown to be useful for monitoring microglia activation early after stoke induction in rats (Hosoya et al., 2017). Another CB2-specific tracer, [^{11}C]A-836339 failed to monitor changes in CB2 expression in rat models of neuroinflammation whereas Moldovan et al. (2016) developed a CB2 ligand with high affinity over CB1 receptors that showed a high brain uptake in a mouse model of acute neuroinflammation induced by LPS (Moldovan et al., 2016, 2017; Pottier et al., 2017).

Methionine can be also used to monitor microglia activation (by the PET tracer 11C-methionine). Higher methionine uptake in epileptic foci of Rasmussen's encephalitis and FCD patients was reported and might be related to microglia activation and proliferation (Madakasira et al., 2002; Maeda et al., 2003; Sasaki et al., 1998). Tryptophan can be related to neuroinflammation since its catabolism by indoleamine 2,3-dioxygenase (IDO) is induced by cytokines during inflammatory processes (Chugani and Chugani, 2005; Chugani and Muzik, 2000; Haber et al., 1993; Taylor and Feng, 1991; Yamazaki et al., 1985). α-[^{11}C]methyl-L-tryptophan ([^{11}C]AMT) was used in TSC patients to image epileptogenic tubers and provide information on the presence and localization of the tubers (Asano et al., 2000; Chugani et al., 1998, 2013; Kagawa et al., 2005; Rubí et al., 2013). Recently, P2X7

receptors were proposed as a novel molecular target for neuroinflammation imaging (Territo et al., 2017).

Monoamine oxidase type B (MAO-B) is an enzyme abundantly present in activated astrocytes (Eddleston and Mucke, 1993; Ekblom et al., 1993, 1994; Gulyás et al., 2011; Saura et al., 1994). MAO-B is the main target for imaging astrocytes with PET and [^{11}C]L-deprenyl was used both in experimental and in clinical studies (Carter et al., 2012; Santillo et al., 2011). In TLE patients, imaging with [^{11}C]-deuterium-deprenyl revealed epileptogenic regions with the presence of reactive astrocytes (Kumlien et al., 1995, 2001). Interestingly, recent studies have identified [^{18}F]-fluorodeoxyglucose (FDG) as a possible marker for astrogliosis. In particular, in the rat lithium-pilocarpine model of epilepsy, [^{18}F]-FDG-microPET imaging showed hippocampal glucose hypometabolism during epileptogenesis correlating with neuronal loss, but a partial recovery of glucose uptake in the chronic phase associated with GFAP-positive astrocytes (Zhang et al., 2015a). In support, Zimmer et al. (2017) demonstrated that astroglial glutamate transport via GLT1 can trigger glucose uptake suggesting a re-evaluation of [^{18}F]FDG imaging data in different CNS disorders (Zimmer et al., 2017).

Non-invasive PET imaging of inflammation still needs to be improved in order to increase cell-specificity and affinity of radioligands.

1.4.4 Magnetic Resonance Imaging

Magnetic resonance imaging has been used widely as a tool for anatomic imaging since it provides strong spatial resolution in soft tissues such as the brain. Several studies have tried to employ this imaging technique for visualising neuroinflammation.

BBB dysfunction can be monitored using contrast-enhanced MRI (CE-MRI) and contrast agents such as Gd-diethylenetriaminepentaacetate (Gd-DTPA) or gadobutrol that leak out of the blood vessels and accumulate in the brain parenchyma after BBB disruption in rat models of epilepsy (van Vliet et al., 2014, 2016). In an immature rodent model of febrile status epilepticus, MRI changes (reduction of T2 relaxation time) in the hippocampus and amygdala correlated with energy-demanding intracellular translocation of HMGB1 (Choy et al., 2014). VCAM-1, known to mediate extravasation of leukocytes across the vascular endothelium is another target molecule for MRI imaging of inflammation. Duffy et al. (2012) using an iron oxide labelled VCAM-1 antibody, reported marked focal signal in the hippocampus and cortex after SE in rats (Duffy et al., 2012). Other studies have exploited nanoparticles for MRI imaging of neuroinflammation. Small and ultrasmall particles of iron oxide were used to visualize inflammation in experimental models of encephalomyelitis and stroke as well as in patients with multiple sclerosis and stroke (Stoll and Bendszus, 2009). Non-radioactive alpha methyl tryptophan (AMT) attached to magnetonanoparticles (MNPs) composed of iron oxide and dextran helped visualize epileptogenic regions with inflammation and correlated with the occurrence of spontaneous seizures in rodent model of TLE (Akhtari et al., 2008). Recently, fluorescent and magnetite-labeled nanoparticles were injected intravenously to rats with lithium-pilocarpine-induced chronic epilepsy (Portnoy et al., 2016). In this study, *ex vivo* MRI nanoparticle signal was detected in macrophages and microglia in areas of seizure origin (Portnoy et al., 2016). VCAM-1 expression was visualized *in vivo* in a mouse model of acute neuroinflammation with the use of paramagnetic gadolinium (Gd)-loaded targeted micelles (Garello et al., 2017). Interestingly, IL-1β was the molecule targeted in another study employing superparamagnetic iron oxide nanoparticles (SPIONs). Functionalized SPIONs with anti-IL-

1β monoclonal antibody attached, were used to simultaneously visualise and target IL-1β overexpressed in the brain of an acute rat model of TLE (Fu et al., 2016). The nanoparticles were administered intravenously and after crossing the BBB they concentrated in astrocytes and neurons of the hippocampus rendering this area visible on MRI and delivering neutralizing anti-IL-1β antibody to the epileptic focus (Fu et al., 2016). Indirect approaches for visualization of inflammatory mediators were applied in clinic using fluid-attenuated inversion recovery (FLAIR)-MRI that enhances the visualization of lesions. A positive correlation between FLAIR-MRI and expression of nitric oxide and IL-1β was found in post-surgical specimens of TLE patients (Varella et al., 2011).

CHAPTER 2 - AIMS OF THE THESIS

In the past two decades various ASDs have been developed but treatment efficacy on pharmacoresistant epilepsies has not been improved significantly. ASDs affect mainly neuronal functions and alleviate symptoms rather than targeting the mechanisms underlying the disease. Increasing evidence has shown that astrocytes assume a reactive functional state in response to epileptogenic insults and they may be major contributors to epilepsy development. Thus, shifting the focus of therapeutic targets from neurons to astrocytes might improve the development of therapeutic interventions for treating patients not responsive to the currently available ASDs and for developing anti-epileptogenic drugs.

Based on this premise, the main scope of this research project is to improve our understanding of the role of astrocytes in epilepsy. Two principal studies were developed as follows:

1. To develop a new *in vivo* imaging method to investigate the dynamics of astroglia activation during epileptogenesis. By coupling this method with *post-hoc* immunohistochemistry, we aimed at characterizing the inflammatory vs anti-inflammatory phenotype of these cells vis-à-vis with their functional activation state. Moreover, we wished to determine whether drugs with anti-epileptogenic effects could modulate the dynamics of astrocyte activation and/or their phenotype in the early aftermath of a brain insult.

2. To uncover pathogenic vs homeostatic mechanisms related to astrocyte activation during seizures by focusing on Toll-like receptor (TLR)-mediated signaling. While the role of TLR4 in epilepsy has been deeply investigated, limited evidence is available on the role

of TLR3 and results have been reported on their pathogenic vs neuroprotective functions, the later possibly mediated by astrocytes.

The two studies relied upon the use of *in vivo* models of either epileptogenesis (1) or acute seizures (2) in mice focusing our analyses in the hippocampus since this is a key area involved in seizure generation in these models and in human temporal lobe epilepsy.

PART I

CHAPTER 3 – GENERAL MATERIALS AND METHODS

3.1 CLONING

3.1.1 IL-1β promoter

DNA sequence of IL-1β gene from the Ensembl Genome Browser (gene code: ENSG00000125538) was analysed and compared to the previously described human IL-1β promoter/enhancer fragment (H-IL-1β) (Shirakawa et al., 1993). H-IL-1β fragments were cloned by polymerase chain reaction (PCR) using human genomic DNA as template. Phusion High-Fidelity DNA Polymerase (Thermo Scientific) was used to amplify the human IL-1β promoter/enhancer DNA. The thermocycling conditions used were: initial denaturation for 1 min at 98°C, denaturation for 10 sec at 98°C, annealing for 40 sec at 70°C, extension for 200 sec at 72°C for 35 cycles, final extention for 15 min at 72°C and hold at 4°C. The samples obtained from the PCR reaction were loaded in an 1% agarose-TBE gel and bands at the correct size were excised and DNA was recovered using Zymoclean Gel DNA Recovery Kit (Zymo Research). Each sample was digested with BglII and EcoRI (both from Thermo Scientific) at 37°C for 2h. Digestion product was then purified using DNA Clean and Concentrator-5 Kit (Zymo Research). For construction of the rAAV luciferase (LUC) reporter plasmids, pAAV-Ca_v3.2-LUC (Kulbida et al., 2015) harboring the AAV2 inverted terminal repeats was modified. pAAV-Ca_v3.2-LUC was digested with BamHI and EcoRI to excise the Ca_v3.2 promoter from the pAAV-backbone and the digested plasmid was loaded in an agarose gel. The pAAV-backbone was excised and purified from the gel using Zymoclean Gel DNA Recovery Kit (Zymo Research). The quantity and quality of the plasmids were assessed using a nanodrop by light absorption at 260/280 nm ratio. All plasmids were dissolved in nuclease free water. Fifty ng of H-IL-1β template were ligated, at room temperature overnight, to the pAAV-backbone using T4 DNA Ligase (5 U/μL, Thermo Scientific). Stbl2 bacteria (Invitrogen) were used for transformation and bacterial cultures

to minimize recombination events. All clones were confirmed by sequencing analysis. Plasmid DNA for viral production was prepared using the Qiagen Maxiprep kit, according to the manufacturer's protocol.

3.1.2 GFAP promoter

AAV2-GFAP-GFP-WPRE plasmid, which was kindly provided by Prof. Thomas McCown (UNC Gene Therapy Center, NC, USA), was digested with BamHI and EcoRI to excise the GFP reporter gene. The luciferase-coding sequence (pGL3-basic; Promega) was amplified and digested as for the H-IL-1β promoter/enhancer and then ligated into the backbone plasmid to form pAAV-GFAP-LUC-WPRE. All clones were confirmed by sequencing analysis. Plasmid DNA for viral production was prepared using the Qiagen Maxiprep kit, according to the manufacturer's protocol. The quantity and quality of the plasmids were assessed using a nanodrop by light absorption at 260/280 nm ratio. All plasmids were dissolved in nuclease free water.

3.2 CELL CULTURES

3.2.1 Transfection

Raw 264.7 cells were maintained at 37°C and 5% CO_2 in Dulbecco's Modified Eagle's Medium (DMEM, Life Technologies) supplemented with 10% (v/v) heat inactivated Fetal Calf Serum (FCS) and 100 units/ml penicillin/streptomycin. Viability, which was assayed using trypan blue dye exclusion, was typically greater than 95%. Cultures were maintained until passage 20 and then discarded.

Transfection was performed in 24-well tissue culture plates (80% confluency) using Lipofectamine™ 2000 (Invitrogen, USA) following the manufacturer's protocol. 0.8 µg of IL-1β luciferase reporter plasmid with firefly luciferase, 0.2 µg of control pRL-TK vector with the Renilla luciferase gene (Promega) were mixed with 50 µl Opti-MEM® I reduced serum media (Invitrogen, USA). The mixture was incubated for 20 min at room temperature and then added to the appropriate wells. Cells were grown in complete culture medium at 37°C and 5% CO_2.

3.2.2 Luciferase assays

The luciferase assays were performed using the Dual Luciferase Reporter Assay System (Promega) and Glomax Luminometer (Promega) was used for measuring Renilla and firefly luciferase activities. The results are given as firefly/Renilla relative luciferase activity and fold-induction compared to the basal activity for each construct.

3.3 RECOMBINANT ADENO-ASSOCIATED VIRUSES (rAAVs)

3.3.1 rAAV serotype 8 production

For transfection HEK293T cells were seeded at a density of $1.5x10^6$ cells/15 cm dish and allowed to reach 50-60% confluency. Three to four hours prior to transfection the DMEM medium (Thermo Scientific) (with 10% Fetal Calf Serum, 1% Penicillin/Streptomycin) was exchanged with IMDM medium (Thermo Scientific), supplemented with 5% FCS. To the transfection mixture containing water, $CaCl_2$ and DNA, 2X HeBS (50 mM HEPES, 280 mM NaCl, 1.5 mM Na_2HPO_4, pH 7.05) buffer was added under vortexing drop-wise fashion and further incubated for 2 minutes, to allow complexes formation (Table 3.1). For transfection, p5E18-VD2/8 (AAV2 rep and AAV8 cap), pFdelta6 and the AAV plasmid were used.

Table 3.1. rAAV8 production method.

Components	*Serotype 8 (15 cm dish)*
dH_2O	2.4 ml
$CaCl_2$ (2.5 M)	330 µl
AAV plasmid	5 µg
pFdelta6- *helper virus*	10 µg
p5E18-VD2/8	5 µg
2x HEBS - added under vortexing	2.6 ml

3.3.2 rAAV serotype 8 purification

After 48 h, cells were harvested in 1 ml DMEM medium and centrifuged at 1.200rpm/20min. The pellet was resuspended in 10 ml lysis buffer (150 mM NaCl, 50 mM Tris-HCl, pH 8.5) and three cycles of freezing-thawing were performed. In order to get rid of nucleic acids, 20 µl benzonase (50 U/ml suspension) was added to the lysate and incubated for 30 min at 37°C. After the incubation, the suspension was centrifuged at 4.000rpm/30min/4°C and the clear suspension was collected. The purification of the virus was performed using four layer discontinuous iodixanol gradients (Zolotukhin et al., 2002). The gradients were layered (Table 3.2) in ultracentrifuge tubes (Sorvall) using a peristaltic pump (P-1).

Table 3.2. Iodixanol gradients.

Components	*15% Iodixanol*	*25% Iodixanol*	*40% Iodixanol*	*54% Iodixanol*
PBS 10x	5 ml	5 ml	5 ml	5 ml
Iodixanol	12.5 ml	20 ml	33.3 ml	45 ml
NaCl 5M	10 ml	-	-	-
KCl 2.5M	50 µl	50 µl	50 µl	50 µl
$MgCl_2$ 1M	50 µl	50 µl	50 µl	50 µl
0.5% Phenol red	75 µl	75 µl	-	75 µl
H_2O	22.3 ml	24.9 ml	11.6 ml	-
Volume used for one gradient				
	8-9 ml	5-6 ml	5 ml	2-4 ml

The cellular suspension (8-9 ml) was layered on top of the iodixanol gradients; the tubes were sealed, and centrifuged at 60.000rpm/2h/4°C (fixed angle rotor T865, Thermo Scientific). rAAV particles were recovered from the 40% iodixanol layer and iodixanol was removed by several rounds of washing with PBS, using Amicon centrifugal filters (Thermo Scientific). The purity of the virus was determined by SDS-PAGE and Coomassie staining. rAAV8 particles for GFAP-promoter-GFP plasmid were produced by triple transfection of HEK293T cells and purified by column chromatography at the UCN Vector Core (Chapel Hill, NC, USA).

3.4 INTRAHIPPOCAMPAL ADMINISTRATION OF rAAVs

Animals were anaesthetised with isoflurane 1.5% and head fixed to the stereotaxic device. For each injection one µl of viral suspension containing ~10^8 transducing units of the rAAVs: rAAV8-H-IL-1β(-2987/+570)-GFP, rAAV8-GFAP-GFP-WPRE, rAAV8-GFAP-LUC-WPRE or rAAV1/2-synI-dtTomato was used and was infused (100 nl/min) into both the dorsal (from bregma, AP: -1.8, L: ±1.5, V: -2) and ventral (AP:-3, L: ±3, V: -3.3) poles of the hippocampus, bilaterally, using a 10 µl Hamilton syringe and a microprocessor controlled mini-pump (World Precision Instruments). After injection, the needle was left in place for 5 min before the incision was closed. Animals were allowed to recover on a heating pad and injected subcutaneously daily for 3 days with Ketoprofen (Gabrilen, 5.0 mg/kg,), Enrofloxacin (Baytril, 5.0 mg/kg) and twice/day with Buprenorphin (Buprenovet 0.05 mg/kg). Mice were daily observed for one week for their general health status.

3.5 CELL SORTING

Mice were anaesthetised with 6 mg/kg xylazine (Rompun; Bayer, Germany) and 90-120 mg/kg ketamine (Ketavet; Pfizer, Germany) intraperitoneally and decapitated. Hippocampi were isolated on ice and transferred into ice-cold HBSS. After 3 washing steps, 200 µl trypsin (dissolved in 1.8 ml HBSS) was added for 20 min at 37°C. The cell pellet was washed three times with Hank's Balanced Salt Solution (HBSS, Life technologies) and then DNase (0.1 mg/ml; Roche) was added. Cells were dissociated using a 1 ml pipette tip and stored on ice until sorted. The fluorescent samples were sorted on a BD FACS Aria III instrument using a 100 µm diameter nozzle (University of Bonn, Medical School FACS Core Facility). Digital data collection was performed using BD FACS DIVA software (BD Diagnostics, Baltimore, MD, USA).

3.6 BIOCHEMICAL ANALYSIS

3.6.1 RNA isolation and real-time quantitative polymerase chain reaction

Mice were deeply anaesthetised with 6 mg/kg xylazine (Rompun; Bayer, Germany) and 90–120 mg/kg ketamine (Ketavet; Pfizer, Germany) intraperitoneally and then decapitated. Four-hundred µm slices were cut on a vibratome in pre-chilled PBS. Hippocampi were microdissected under the microscope and subsequently homogenized in 100 µl lysis buffer with a tissue mincer (Dynabeads® mRNA DIRECT Micro Kit). Both mRNA from tissue lysates and FACS-sorted neurons were isolated using the Dynabeads® mRNA DIRECT Micro Kit, according to the manufacturer's protocol (Life Technologies). mRNA was retranscribed into cDNA using the RevertAid H Minus First Strand cDNA Synthesis Kit (ThermoScientific). Transcript quantification was performed in triplicates by real-time reverse transcription–PCR (RT-qPCR) according to the ΔΔCt method. A final reaction volume of 6.25 µl/well was

used containing 1.25 µl of cDNA, 0.1875 µl of forward and reverse primer (100 pM stock) and 3.125 µl 2x Master mix (Maxima SyBr green/ROX qPCR; Thermo Scientific).

Primer sets were:

- IL-1β*:* forward: 5'-TTGACGGACCCCAAAAGATG-3'

  reverse: 5'-CAGCTTCTCCACAGCCACAA-3'
- β-actin: forward: 5'-ACCGTGAAAAGATGACCCAGA-3'

  reverse: 5'-ATGGGCACAGTGTGGGTGA-3'

Quantitative PCR was performed in an ABI Prism 7900HT apparatus (PE Applied Biosystems, Foster City, CA, USA) with the following conditions: 50°C for 2 min, 94°C for 1 min, 40 cycles of 94°C for 20 s, 59°C for 30 s, 72°C for 40 s, 95°C for 15s and a final step of 60°C for 15 s. The signal threshold was set within the exponential phase of the amplification to determine the Ct values. β-actin, an endogenous non cell-specific gene, was used as a reference gene to normalize candidate gene expression.

3.6.2 Western blot

Hippocampi from mice deeply anaesthetised with ketamine (75 mg/kg) and medetomidine (0.5 mg/kg) were dissected out at 4°C and quickly frozen into liquid nitrogen. Tris-HCl 20 mM buffer (pH 7.4) containing 1 mM EDTA, 5 mM EGTA, 1 mM Na-vanadate, 2 µg/µl aprotinin, 1 µg/µl pepstatin, and 2 µg/µl leupeptin was used for homogenization. Total proteins (20 µg) assessed with BCA Protein Assay Kit (ThermoScientific) were separated using SDS-polyacrylamide gel electrophoresis (PAGE) 10% acrylamide, for 40-50 min at 200V. Each sample was run in duplicate. Then, proteins were transferred via electroblotting to Hybond nitrocellulose membranes overnight at 30mA at 4°C.

Non-specific binding sites were blocked by incubating the membranes in milk 10% and TBS-Tween for 60 min at room temperature. For immunoblotting, an overnight incubation with blocking buffer (TBS-Tween and milk 3%) and GFAP (1:15000, Merck, Germany; # MAB3402) or anti-rabbit GLT-1 (1:1000, Abcam, USA; #ab178401) or anti-rabbit Kir4.1 (1:2000, Alomone Labs, Israel; #APC-035) was carried out at 4°C. The following day the membranes were washed, incubated with secondary antibody anti-mouse or anti-rabbit HRP (1:10000, Sigma Aldrich) for 90 min at room temperature in blocking buffer, and then washed. GFAP, GLT-1 or Kir4.1 bands were visualized with ECL Luminata solution (Luminata forte, Western HRP substrate, Millipore, MA, USA) and a ChemiDoc Imaging system (Biorad). Images of GFAP, GLT-1 or Kir4.1 and the marker lane bands were captured and merged together. Afterwards, membranes were washed and incubated with β-actin (1:5000, Immunological Sciences, Italy; #MAB24007) in blocking buffer for 2 h at room temperature. β-actin was used since it represents an internal control with which to compare GFAP protein levels. The membranes were washed, incubated in secondary antibody, and protein bands visualized as above.

Quantification was performed using Image Lab software (Biorad) in which a ROI was drawn around the protein bands to determine the optical density and thus the amount of protein present, for GFAP, GLT-1 or Kir4.1 and β-actin. Optical density values in each sample were normalized using the corresponding amount of β-actin and GFAP.

3.7 EXPERIMENTAL ANIMALS

Adult C57BL/6N male mice (~50 days, 20-25 g) were obtained from Charles River (Germany and Italy). Mice were housed at a constant room temperature (23°C) and relative humidity (60 ± 5%) with free access to standard food pellet and water, and with a fixed 12 h light/dark

cycle. Adult animals were housed two or four per cage and environmental enrichment was used.

3.8 ANIMAL CARE

Procedures involving animals were conducted at the University of Bonn and Istituto di Ricerche Farmacologiche "Mario Negri" IRCCS which both adhere to the principles set out in the following laws, regulations, and policies governing the care and use of laboratory animals: guidelines of the University of Bonn Medical Centre Animal-Care-Committee, Italian Governing Law (D.lgs 26/2014; Authorization n.19/2008-A issued March 6, 2008 by Ministry of Health); Mario Negri Institutional Regulations and Policies providing internal authorization for persons conducting animal experiments (Quality Management System Certificate - UNI EN ISO 9001:2008 - Reg. No. 6121); the NIH Guide for the Care and Use of Laboratory Animals (2011 edition) and EU directives and guidelines (EEC Council Directive 2010/63/UE). The Statement of Compliance (Assurance) with the Public Health Service (PHS) Policy on Human Care and Use of Laboratory Animals has been recently reviewed (9/9/2014) and will expire on September 30, 2019 (Animal Welfare Assurance #A5023-01).

3.9 *IN VIVO* MODELS OF EPILEPTOGENESIS

3.9.1 Intra-amygdala kainic acid in mice

Mice were injected under general gas anesthesia (1-3% isoflurane in O_2) and stereotaxic guidance. A needle was unilaterally lowered into the brain tissue for the intra-amygdala injection of kainic acid (from bregma, mm: nose bar 0; anteroposterior -1.06, lateral -3.3, ventral -4) (Franklin and Paxinos, 2008). Kainic acid (0.3 μg in 0.2 μl) was unilaterally injected in the basolateral amygdala. The needle was left in place for 5 min post-injection

before closing the incision with sutures. Mice recovered from anesthesia within a few minutes and SE was developed after approximately 10 min from kainic acid injection. Animals were observed for motor convulsions in order to assess the ictal activity since in this model ictal activity was always associated with generalized motor convulsions. After 40 min from SE onset, mice received diazepam (10 mg/kg, intraperitoneally, i.p.) to improve their survival rate. Mice were sacrificed at different time points after SE for subsequent biochemical or immunohistochemical analysis according to the experimental protocol (for details regarding experimental groups, see Chapter 5). Control mice were animals subjected to surgery and injected with saline into the basolateral nucleus of the amygdala thus they were not exposed to SE (referred to as Saline or Control). No mice from the Saline/Control group showed any behavioural convulsions and were used for brain histological and biochemical analysis.

This is an epileptogenesis model were epilepsy develops in 100% of mice exposed to at least 1.5 h of SE and is a model extensively described and used (Diviney et al., 2015; Iori et al., 2017; Jimenez-Mateos et al., 2012; Mouri et al., 2008). Spontaneous generalized motor seizures occur after a short latent period that is of 5.4 ± 0.5 days after the induction of SE (Iori et al., 2017). The number of seizures per day is stable for the first 60 days after the epilepsy onset and then seizure score increases in 80% of the mice by about 3-fold after 2 months and remains stable thereafter (Iori et al., 2017). This model recapitulates the major co-morbidities found in epilepsy patients showing cognitive deficits and anxiety-like behaviours (Liu et al., 2013). Moreover, neuronal cell loss occurs progressively and mostly at the unilateral side to the injected amygdala (Mouri et al., 2008).

This model was used to characterize the glia activation during the epileptogenesis phase and to study the effects of anti-inflammatory treatment during epileptogenesis using the *in vivo* imaging tool developed (see data in Chapter 5).

3.9.2 Intra-cortical kainic acid in mice

Animals were anaesthetised with 6 mg/kg xylazine (Rompun; Bayer, Germany) and 90–120 mg/kg ketamine (Ketavet; Pfizer, Germany) intraperitoneally, and head fixed to the stereotaxic device. Kainic acid (70 nl of 20 mM solution) was infused unilaterally in the cortex above the left dorsal hippocampus (coordinates from bregma, anteroposterior -2, lateral -2, ventral -1.3) using a microprocessor controlled mini-pump at a rate of 35 nl/min in order to induce status epilepticus. Animals recovered from anesthesia about 90 min later and were visually observed for the occurrence of behavioural motor seizures characterized by rearing and forelimb clonus which persisted for about 12 h and resulted in epilepsy development as previously described (Jefferys et al., 2016).

The latent period in this model is 5 ± 2.9 days and is not free of ictal activity (Jefferys et al., 2016). In this model 93% of the mice exposed to SE develop spontaneous recurrent seizures associated with motor seizures which vary significantly between animals ranging from 1 to 20 seizures per day (Jefferys et al., 2016). Sponteaneous seizure frequency increases with time reaching a 4-fold increase 7-9 months after SE and does not correlate with the duration of SE or the length of the latent period (Jefferys et al., 2016). Neuronal loss is seen in the CA1, CA3 and hilus of the ispilateral hippocampus already at 2 days after KA injection and pyramidal cell degeneration induced by seizure activity along with reactive gliosis increases throughout a 9-month period after SE (Jefferys et al., 2016). This a model that mirrors the

morphological and functional alterations seen in human TLE patients thus making it suitable for drug testing.

This model was used for production of the data reported in Chapter 4 where we developed an *in vivo* bioluminescence imaging tool.

3.10 IMMUNOHISTOCHEMISTRY

3.10.1 Immunohistochemical studies from *in vivo* preparations

Mice used in Chapter 4 were anaesthetised with 6 mg/kg xylazine (Rompun; Bayer, Germany) and 90–120 mg/kg ketamine (Ketavet; Pfizer, Germany) intraperitoneally and perfused via the ascending aorta with 50 mM cold phosphate buffered saline (PBS, pH 7.4) followed by chilled 4% paraformaldehyde (PFA) in PBS. Brains were removed and fixed in PFA over-night. Forty µm coronal sections were cut using a vibratome (Thermo Scientific) throughout the septal-temporal extension of the mouse hippocampus (-0.94 to -3.64 mm from bregma; Franklin and Paxinos, 2008) and slices were used for GFP staining and co-localization with the neuronal marker NeuN and the astrocytic marker GFAP. Two slices per animal were used for IL-1β staining and co-localization with GFP were processed as described in section 3.10.2. Slices from animals used to localize the GFP signal deriving from AAV8-GFAP-GFP-WPRE vector were not stained further for GFP since signal was strong enough to co-localize with GFAP and NeuN markers (see details below).

Mice used in Chapter 5 were deeply anaesthetised with ketamine (75 mg/kg) and medetomidine (0.5 mg/kg) and perfused via the ascending aorta with 50mM cold PBS, pH 7.4 and then with 4% paraformaldehyde (Merck, Darmstadt, Germany) in PBS. Brains were removed and post-fixed for 90 min at 4°C and then transferred to glucose solution 20% in PBS for 24 h at 4°C. Then brains were frozen by immersion in isopentane at -45°C for 3 min

and stored at -80°C until assayed. Using a cryostat serial coronal sections (40 µm) were cut and collected from -0.94 to -2.80 mm from bregma (Franklin and Paxinos, 2008). Two series of 30 sections each were prepared and in each series the first slice was used for staining for GFAP, the second for CD11b, the third for S100β, the forth for HMGB1, the fifth for TNF-α and the sixth for PTX3. Three slices per animal were used for each marker.

In order to stain astrocytes and microglia (Chapter 5), sections were incudated for 1h at RT with 10% normal goat serum, 1% Triton X-100 in Tris-buffered saline 0.1 m, pH 7.4, then overnight at 4°C with the following primary antibodies: mouse anti-GFAP (1:3500, Chemicon, Temecula, CA, USA; #MAB3402) and anti-rabbit S100β antibody (1:3000, Abcam, UK; #Ab52642) markers of astrocytes, or rat anti-CD11b (1:1000, MAC-1, Serotec; Cat# MCA719, Clone 5C6), a marker of microglia followed by visualization with the Vectastain ABC kit (Vector Laboratories), with diaminobenzidine (DAB; Sigma, #D8001 or nickel-intensified DAB for IL-1β) as chromogen.

Slices from different animals and experimental groups were matched at comparable anteroposterior and dorsoventral levels.

3.10.2 Green fluorescent protein (GFP)

Slices (see Chapter 4 data) were blocked for 2 h at 37°C in blocking buffer (0.1% Triton-X100, 0.1%Tween20, 2% BSA in PBS; Invitrogen) and then incubated with primary antibody against GFP (1:1000; Abcam, Cambridge, UK; #ab290) overnight at 4°C. After washing with PBS, slices were incubated with secondary antibody Alexa Fluor 488 donkey-anti-rabbit 1:200 (Jackson Immunoresearch Laboratories, Inc., USA) for 2 h at room temperature and then mounted on slides with fluorescein mounting medium after a final wash (Vectashield,

Vector laboratories, USA). Slices were evaluated for fluorescent signal using Nikon Eclipse Ti confocal microscope (Nikon Instruments, Germany).

3.10.3 TNF-α, HMGB1 and PTX3

Slices were incubated at 4°C for 10 min in 70% methanol and 2% H_2O_2 in Tris-HCl-buffered saline (TBS, pH 7.4), followed by 30 min incubation in 10% fetal bovine serum (FBS), 1-10% bovine serum albumin (BSA) in 1% Triton X-100 in TBS. Overnight incubation was performed with goat anti-mouse primary antibody against TNF-α (1:1000, Peprotech, NJ, USA; #500-P64G) at 4°C in 10% FBS, 1-10% BSA in 1% Triton X-100 in TBS.

For HMGB1 immunostaining sections were incubated at 4°C for 60 min in 10% normal goat serum (NGS) in 0.1% Triton X-100 in PBS (Ravizza and Vezzani, 2006). Then the slices were incubated with the primary rabbit polyclonal antibody against HMGB1 (1:1000, Abcam, Cambridge, UK; #AB18256) overnight at 4°C in 4% NGS in 0.1% Triton X-100 in PBS.

PTX3 immunostaining was done as follows: slices were incubated with Triton X-100 0.3%, PBS, and normal goat serum (NGS) 2% for 60 min before overnight incubation at 4°C with the primary antibody against PTX3 (1:250, rabbit polyclonal anti-hPTX3 1mg/ml purified, kindly provided by C. Garlanda, Istituto Clinico Humanitas–IRCCS, Rozzano, Italy) in blocking buffer (PBS and NGS 1%).

For HMGB1 and PTX3 immunostainings, after 1 h incubation with anti-rabbit biotinylated secondary antibodies (1:200, Vector Labs), immunoreactivity for HMGB1 and PTX3 was assessed using the avidin-biotin-peroxidase technique (Vectastain ABC kit, Vector Labs): PBS, avidin 1%, and biotin 1% were applied to the slices for 60 min, before reacting the slices and visualising the signal with 3',3'-diaminobenzidine (DAB, 5mg) (Sigma, Munich, Germany), TBS (Tris-HCl-buffered saline, pH 7.4, 10ml), and H_2O_2 (3 µl). For TNF-α, after

incubation for 1 h with anti-goat biotinylated secondary antibody (1:200, Vector Labs), the avidin-biotin-peroxidase technique was used and signal was further amplified with addition of nickel ammonium into the DAB solution.

Then sections were washed twice in TBS and once in saline and mounted on gelatin-coated slides and allowed to dry at room temperature overnight. The following day, slices were dehydrated using a series of ethanol concentrations (70%, 95%, and 100%) and xylene before covering with DPX mountant for histology (Sigma, Germany) and a coverslip.

No immunostaining was observed in control slices when incubating with the primary antibody preabsorbed with the corresponding peptides (1 µM, 24 h at 4°C), or without the primary antibodies (Ravizza and Vezzani, 2006; Vezzani et al., 1999).

Quantitative analysis of S100β, HMGB1 and TNF-α staining in DAB coloured sections was done by counting automatically the total number of positive cells marked using Fiji software. Three slices per mouse were used for quantification of the signal in the whole hippocampus captured at 20X using a BX61 microscope equipped with motorised and digitised platform (Virtual Slider Microscope, Olympus, Germany) and one field representing the CA1 area was captured for representation. GFAP-, CD11b-, S100β-, TNF-α- and PTX3-positive total area (μm^2) occupied by the staining was quantified with the same tool. Data obtained in each slice/mouse were averaged, providing a single value per mouse, and this value was used for the statistical analysis.

3.10.4 Double and triple immunostaining

Two slices from 4 mice perfused at 24 h after SE were used in order to identify the cell type marked by the H-IL-1β(-2987/+570)-GFP construct (Chapter 4). After incubation with the GFP primary and secondary antibody slices were incubated with primary antibody mouse

anti-GFAP (1:2500, Chemicon, Temecula, CA, USA; #MAB3402) or mouse anti-NeuN (1:1000, Chemicon; #MAB377) followed by the corresponding secondary antibodies (1:400, Alexa Fluor 488 and Alexa Fluor 568, Jackson Immunoresearch Laboratories, Inc., USA).

Two slices from 3 animals were used in order to identify whether the cells expressing endogenous IL-1β are the same as the ones marked by the H-IL-1β(-2987/+570)-GFP construct (data reported in Chapter 4). Briefly, after GFP staining, slices were incubated at 4°C for 10 min in 70% methanol and 2% H_2O_2 in Tris-HCl-buffered saline (TBS, pH 7.4), followed by 30 min incubation in 10% fetal bovine serum (FBS), 10% bovine serum albumin (BSA) in 1% Triton X-100 in TBS. Overnight incubation was performed with the goat polyclonal primary antibody against IL-1β (1:200, Santa Cruz Bio., CA, USA; #sc-1252) and followed by incubation with secondary biotylinated anti-goat antibody (1:500, Vector Labs) and streptavidin–horseradish peroxidase with amplification of the signal with tyramide conjugated to Fluorescein using TSA amplification kit (NEN Life Science Products, Boston, MA, USA). Identification of the cell type expressing the endogenous IL-1β was done in the same slices after IL-1β and incubation with primary antibody mouse anti-GFAP.

Two slices from 3 randomly chosen animals and adjacent to those used for single immunohistochemistry were used for double or triple immunostaining to identify the cells expressing HMGB1, TNF-α and PTX3 (Chapter 5). After incubation with the primary antibodies to HMGB1, TNF-α and PTX3, the slices stained for HMGB1 and PTX3 were incubated with anti-goat (for TNF-α) or anti-rabbit (for HMGB1 and PTX3) secondary antibody conjugated with Alexa488 (1:500; Molecular Probes, Leiden, The Netherlands) while sections stained for TNF-α were incubated with streptavidin–HRP and the signal was revealed with tyramide conjugated to Fluorescein using TSA amplification kit (SAT-701001EA; NEN Life Science Products, Boston, MA, USA). Sections for all stainings were

subsequently incubated with primary antibodies against GFAP, CD11b and NeuN. Fluorescence was detected using secondary antibodies conjugated with Alexa546 (1:500, Molecular Probes, Leiden, Netherlands). Cells expressing S100β were co-localised with GFAP using the same method. For HMGB1-stained sections, an additional incubation of 15 min in DAPI (1:500; Molecular Probes) was done in order to visualize the cell nucleus. Slide-mounted sections were examined with an Olympus Fluoview laser scanning microscope (microscope BX61 and confocal system FV500) using excitations of 488 nm (Ar laser), 546 nm (He-Ne green laser) and 350 nm (ultraviolet) for fluorescein, Alexa546 and DAPI, respectively. The emission of fluorescent probes was collected on separate detectors. To eliminate the possibility of bleed-through between channels, the sections were scanned in a sequential mode.

3.11 *IN VIVO* BIOLUMINESCENCE IMAGING

Two weeks after intrahippocampal injection with the AAV8-GFAP-LUC virus, mice were randomly divided into the experimental groups and were injected intraperitoneally with D-Luciferin (150mg/kg; Cayman, USA) and then anaesthetised with 2% isoflurane and placed in an IVIS-Spectrum Optical In Vivo Imaging System (PerkinElmer) for baseline bioluminescent signal measurement. The head of each mouse was shaved with clippers and a depilatory cream before imaging in order to increase the signal detected by the ultrasensitive charged coupled device (CCD) camera. At each time point, a sequence of images was acquired every 2 minutes for 14 minutes (exposure time: 2 min, binning: medium, f/stop: 1) to ensure that the peak luciferase activity was captured. Twenty-four hours after baseline measurement, KA was injected into the cortex as described previously and the bioluminescent signal was recorded at 24 h and 3 d post-SE (Chapter 4). For data

reported in Chapter 5, mice were injected intraperitoneally with saline or with FTY720 (6mg/kg) 1 h after intra-amygdala injection of KA and then daily, once per day for 7 consequitive days and monitored at 2 h, 24 h, 3 d and 7 d post-SE (Chapter 5). Control group were mice injected in the cortex (Chapter 4) or amygdala (Chapter 5) with PBS or saline and treated with saline with the same protocol described above. Images were analysed using Living Image 4.5.5 software (PerkinElmer) and regions of interest (ROI) contouring the area of bioluminescent signal were drawn in order to quantify the surface radiance in photons per second per square centimeter per steradian (photons/s/cm^2/sr).

3.12 STATISTICS

Quantification of each experiment was done blindly. Sample size was determined a priori based on previous experience with the respective models and statistical tests were prospectively selected. All efforts were made to reduce the number of animals used to minimum. GraphPad Prism 6 (GraphPad Software, USA) for Windows was used for statistical analysis using absolute values. Data are presented as mean ± S.E.M. (n indicates the number of individual samples). For each variable, differences between the groups were assessed using Mann–Whitney U test for two independent groups and one-way ANOVA followed by Tukey or Dunnet's *post-hoc* test or Kruskal-Wallis followed by Dunn's *post-hoc* test for more than two independent groups (details are reported in the figure legends). Differences were considered significant with a $p<0.05$.

CHAPTER 4 – CHARACTERIZATION OF IL-1β PROMOTER FRAGMENTS AND DEVELOPMENT OF *IN VIVO* BIOLUMINESCENCE IMAGING OF ASTROCYTES

4.1 INTRODUCTION

Astrocytes are among the principal cells involved in the expression and release of this cytokine during epileptogenesis and they are pivotal for sustaining the inflammatory brain response (Aronica et al., 2012; Maroso et al., 2011a; Vezzani et al., 2011a). Reactive astrocytes with an inflammatory phenotype express high levels of glial fibrillary acidic protein (GFAP), a member of the cytoskeleton protein, essential for the process of astrogliosis (Eng et al., 2000). Astrocytes become dysfunctional cells during epileptogenesis and they contribute to seizure generation by various mechanisms. Pivotal for their involvement in epileptogensis is their abilty to release IL-1β and other ictogenic cytokines such as HMGB1 and TNF-α as well as promoting an hyperexcitable microenvinronment due to their impaired capacity of buffering extracellular glutamate and K^+ ions (Devinsky et al., 2013; Friedman et al., 2009). Thus, one therapeutic option to interfere with epileptogenesis is to modulate astrocytic activation and restore their physiological functions, however, this intervention requires a better understanding of the extent and timing of the astroglia activation after epileptogenic injuries. Since dysfunctional astrocytes express high levels of both IL-1β and GFAP, we focused on these two genes and developed an experimental design to monitor the dynamics and extent of cell activation during epileptogenesis based on *in vivo* bioluminescence signal of gene promoter activation by viral vector gene delivery.

Gene promoter activation. The IL-1β gene promoter is well characterised since various regions of the gene's promoter and enhancer have been identified (Kominato et al., 1995; Shirakawa et al., 1993; Toda et al., 2002). The transcription of the IL-1β gene requires the interaction between the promoter sequence (from −131 to +12) that contains the TATA box and the far upstream enhancer known as upstream inducible sequence (UIS) located at −3134 to− 2179 (Adamik et al., 2013; Figure 4.1). Gene transcription depends on the

lineage-specific Spi-1/PU.1 (Spi1) transcription factor. Spi1 acts as an anchor for induction-dependent interaction with two TLR-activated transcription factors, C/EBPβ and NF-kB, in order to induce transcription, likely in the context of a specific chromatin architecture (Figure 4.1; Adamik et al., 2013).

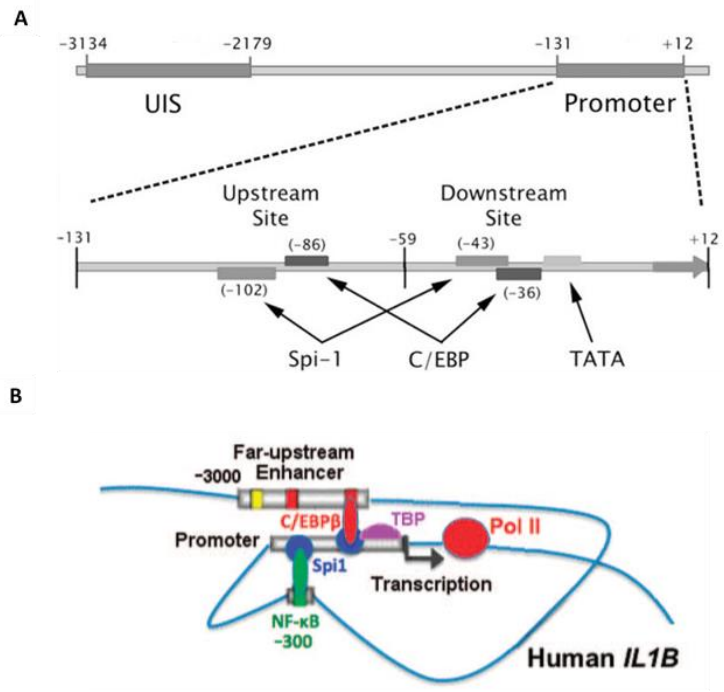

Figure 4.1. Schematic depiction of IL-1β gene promoter regulatory region. *(A) The upstream induction sequence (UIS) is located at −3134 to− 2179 whereas the promoter sequence at −131 to +12. The relative Spi-1, C/EBP and TATA sites are noted. (B) Model for chromatin looping during activation of IL-1β (adapted from Adamik et al., 2013).*

The GFAP (gfa2) promoter has been thoroughly studied (Brenner et al., 1994; Lee et al., 2006, 2008; de Leeuw et al., 2006; Yeo et al., 2013). A shorter 681 bp GFAP promoter fragment, gfaABC1D, has the same expression pattern of the 2210 bp gfa2 promoter and about two-fold greater activity, thus recommending it for gene targeting applications such

as insertion in a recombinant adeno-associated viral vector (rAAV) system where the size of the construct is a limiting factor (Lee et al., 2008; Figure 4.2).

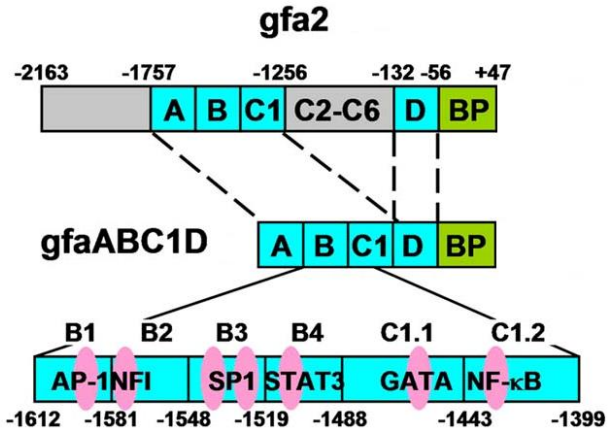

Figure 4.2. Schematic depiction of GFAP (gfa2) gene promoter and of the shorter gfaABC1D fragment. *Coordinates for the 4 B subregions and the approximate position of the transcription factor (TF) binding sites are shown. Three subregions were identified as important contributors to activity in addition to the basal promoter (BP), regions A (bp −1757 to −1613), B (−1612 to −1489), and D (−132 to −56). The C1 (bp −1488 to – 1256) segment contains sequences required for astrocytes to express in certain brain regions, and for suppression of* GFAP *expression in neurons. The 681 bp gfaABC1D promoter drives expression of transgenes with the same developmental, spatial, and cell specificity properties as the 2.2 kb gfa2 promoter (Lee et al., 2008). (adapted from Yeo et al., 2013).*

Expression system. rAAVs are the most commonly used vectors for gene delivery and expression in the CNS. They contain a single stranded DNA and their serotype is important for targeting specific cell types. AAV hybrid serotypes or pseudo-serotypes have been created by viral engineering, and are constructed with integrated genome containing (cis-acting) inverted terminal repeats (ITR) derived from AAV2 and capsid genes of other serotypes (Figure 4.3). This strategy increased viral cell specificity and transduction (Choi et al., 2005). In particular, AAV8-based vectors show selective expression in astrocytes of the spinal cord, hippocampus, striatum and substantia nigra of adult rats and were previously used to drive transgene expression of the human GFAP promoter (Lawlor et al.,

2009; Li et al., 2014). An important limitation is the restrained construct size that can be accommodated in the rAAV genome (about 4.7-5.0 kb).

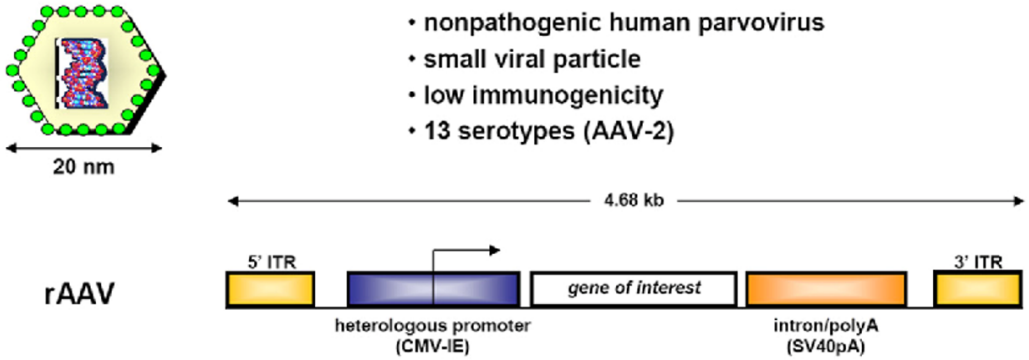

Figure 4.3. Structure and characteristics of recombinant adeno-associated viral vectors (rAAVs). *The gene of interest is inserted between the inverted terminal repeats (ITRs) that contain cis-elements required for replication and packaging resulting in a vector genome of approximately 4.7 kb flanked by the viral ITRs. The late SV40 poly A sequence (Simian virus 40 PolyA, also called PolyA) possesses the activity of transcription termination and can add PolyA tail to mRNA (adapted from Cucchiarini et al., 2015).*

In this study we focused on the generation of rAAV expressing reporter genes (GFP or luciferase) under the control of either the IL-1β or the GFAP promoters. In order to identify the minimal IL-1β promoter fragment with full activity to be accommodated into the AAV vector backbone, we first analysed the activity of various promoter fragments in Raw 246.7 cells exposed to lipopolysaccharide (LPS). For GFAP, we choose the well characterised 681bp promoter fragment suitable for rAAV (Lee et al., 2008). Both promoters were tested *in vivo* in a mouse model of status epilepticus (SE)-induced epileptogenesis, and their cell-specific expression was analysed by *post-mortem* immunohistochemistry and compared with the expression of either IL-1β or GFAP proteins. Finally, we studied the induction of the GFAP promoter by *in vivo* bioluminescence imaging at different time points after SE.

4.2 SPECIFIC MATERIALS AND METHODS

Cloning

Human IL-1β promoter/enhancer fragment and several shorter promoter fragments were cloned as previously described in the General materials and methods, Section 3.1.1. Briefly, the human IL-1β promoter/enhancer fragment H-IL-1β(-3757/+570), 4327bp, was cloned by polymerase chain reaction (PCR) using human genomic DNA as template. Several shorter promoter fragments [H-IL-1β(-3757/+12), 3769bp; H-IL-1β(-3132/+570), 3702bp; H-IL-1β(-3132/+1), 3131bp; H-IL-1β(-2987/+570), 3557bp; H-IL-1β(-2987/+1), 2987bp] were subsequently cloned using the H-IL-1β(-3757/+570) sequence as template with the following primer sets (Table 4.1; Figure 4.4). Construction of the AAV-GFAP-LUC-WPRE plasmid was done as previously described in the General materials and methods, Section 3.1.2.

Cell cultures

Raw 264.7 cells were transfected as described in the General materials and methods, Section 3.2.1 and luciferase assays were performed as described in Section 3.2.2. For IL-1β promoter induction, Escherichia coli 055:B5 LPS (Sigma, St. Louis, MO, USA) was suspended in sterile water and added to the cell culture to obtain the desired concentrations. Luciferase assays were performed in four different experiments where Raw 264.7 cells were treated 24 h after transfection with LPS (100 ng/ml; Sigma) for 18 h prior to harvesting (Figure 4.4).

Adeno-associated viral vectors

rAAV8 were produced and purified are reported in the General materials and methods, Sections 3.3.1 and 3.3.2.

Mouse model of epileptogenesis

SE was induced by intracortical injection of KA as described in Section 3.9.2 of General materials and methods. Mice (n=28) were not implanted with electrodes to minimise tissue damage and do not interfere with the bioluminescence signal, thus SE was visually monitored for behavioural motor seizures occurrence. Mice injected in the cortex with PBS served as controls for immunohistochemistry (n=3), cell sorting (n=5) and bioluminescence imaging (n=6).

Immunohistochemistry

A group of mice (n=4) was injected with KA to measure IL-1β promoter induction 24 h post-SE (3.9.2 of General materials and methods). Mice were injected 2 weeks before SE induction with AAV8-H-IL-1β(-2987/+570)-GFP and GFP expression was assessed by immunohistochemistry (n=4; Figure 4.5; General materials and methods, sections 3.4 and 3.10.2). Histological evaluation of IL-1β protein levels and its co-localization with GFP and GFAP was done in a separate group of mice (n=3) 24 h after SE induction (Figure 4.6; General materials and methods, sections 3.4, 3.10.1, 3.10.2 and 3.10.4). AAV8-GFAP-GFP-WPRE tissue spread and cell specificity were evaluated by immunohistochemistry in 3 mice injected with the rAAV and sacrificed 2 weeks later (Figure 4.8 and 4.9; see sections 3.4 and 3.10.1 from General materials and methods). GFP staining was strong enough to be detected directly by confocal microscopy withouth using a secondary antibody.

Cell sorting

rAAV1/2-synI-dtTomato that is specifically expressed by neurons was kindly provided by Dr. A. Becker. Five mice were injected in the hippocampus with rAAV1/2-synI-dtTomato 2 weeks before performing neuronal cell sorting (Figure 4.7; sections 3.4 and 3.5 of General

materials and methods). A laser (561 nm) was used to excite tdTomato and a 582/15 filter was used to detect the tdTomato signal.

RT-qPCR analysis

Five animals injected with KA were sacrificed 24 h later and their hippocampi were rapidly removed (3.9.2 of General materials and methods). Dissected hippocampi (as well as sorted neurons, see above) were used to measure IL-1β mRNA levels as described in section 3.6.1 of General materials and methods (Figure 4.7). β-actin was used as a reference gene to normalize IL-1β mRNA levels.

In vivo bioluminescence imaging

Mice (n=6-11/group) were injected with AAV8-GFAP-LUC (section 3.4 of General materials and methods). SE was induced 2 weeks later as described in section 3.9.2 of General materials and methods. Mice were behaviourally monitored by two investigators before SE induction and then at 24 h and 3 days after KA injection using *in vivo* bioluminescence imaging (Figure 4.10; General materials and methods, section 3.11).

4.3 RESULTS

4.3.1 *In vitro* characterization of IL-1β promoter fragments

To identify the minimal H-IL-1β promoter region eligible for *in vivo* bioluminescence imaging, we cloned six H-IL-1β promoter fragments (Table 4.1; Figure 4.4) and we tested them for their luciferase activity in RAW 264.7 cells. The three fragments harbouring the 570 nucleotides downstream of the transcription start site (TSS) (-3757/+570, -3132/+570 and -2987/+570) showed stronger basal expression compared to the fragments lacking these downstream nucleotides (-3757/+12, -3132/+1 and -2987/+1) (Figure 4.4B). This indicates that the 570 nucleotides downstream of the TSS are necessary for efficient basal

H-IL-1β promoter activity. Next, we tested if stimulation with the pro-inflammatory agent LPS (100 ng/ml for 18 h) activates the various promoter fragments transfected in RAW 264.7 by analysing their luciferase activity. We found that all fragments showed a significant activation after stimulation with LPS, with the -3757/+570, 3757/+12 and -3132/+570 fragments having the strongest activation (12-fold increase, $p<0.01$). Among the shorter fragments, the one including the -2987/+570 region of the promoter showed a significant activation up to 8-fold ($p<0.01$) compared to the basal activity (Figure 4.4C).

Table 4.1. Primers used for H-IL-1β promoter cloning and the respective restriction enzymes.

Fragment	PCR primers	Restriction enzymes
H-IL-1β(-3757/+570)	For:5´-GCGAGATCTTCTAGACCAGGGAGGAGAATGGAATG-3´	*BglII/ EcoRI*
	Rev:5´-GCGGAATTCAGACACCTGTGTAAAAAGGAGAAAATGAGTG-3´	
H-IL-1β(-3757/+12)	For:5´-GCGAGATCTTCTAGACCAGGGAGGAGAATGGAATG-3´	*BglII/ EcoRI*
	Rev:5´- GCGGAATTCTCGAAGAGGTTTGGTATCTGCCAGTTTC-3´	
H-IL-1β(-3132/+570)	For:5´-GCGAGATCTCAGCTGAGAAAGGCTTTAGTGACTCAA-3´	*BglII/ EcoRI*
	Rev:5´-GCGGAATTCAGACACCTGTGTAAAAAGGAGAAAATGAGTG-3´	
H-IL-1β(-3132/+1)	For:5´-GCGAGATCTCAGCTGAGAAAGGCTTTAGTGACTCAA-3´	*BglII/ EcoRI*
	Rev:5´-GCGGAATTCTGTTTTTATGGCTTTCAAAAGCAGAAGTAGGAG-3´	
H-IL-1β(-2987/+570)	For:5´-GCGAGATCTTCCCTTAGTGCCAACTATGTTTATAGCG-3´	*BglII/ EcoRI*
	Rev:5´-GCGGAATTCAGACACCTGTGTAAAAAGGAGAAAATGAGTG-3´	
H-IL-1β(-2987/+1)	For:5´-GCGAGATCTTCCCTTAGTGCCAACTATGTTTATAGCG-3´	*BglII/ EcoRI*
	Rev:5´-GCGGAATTCTGTTTTTATGGCTTTCAAAAGCAGAAGTAGGAG-3´	

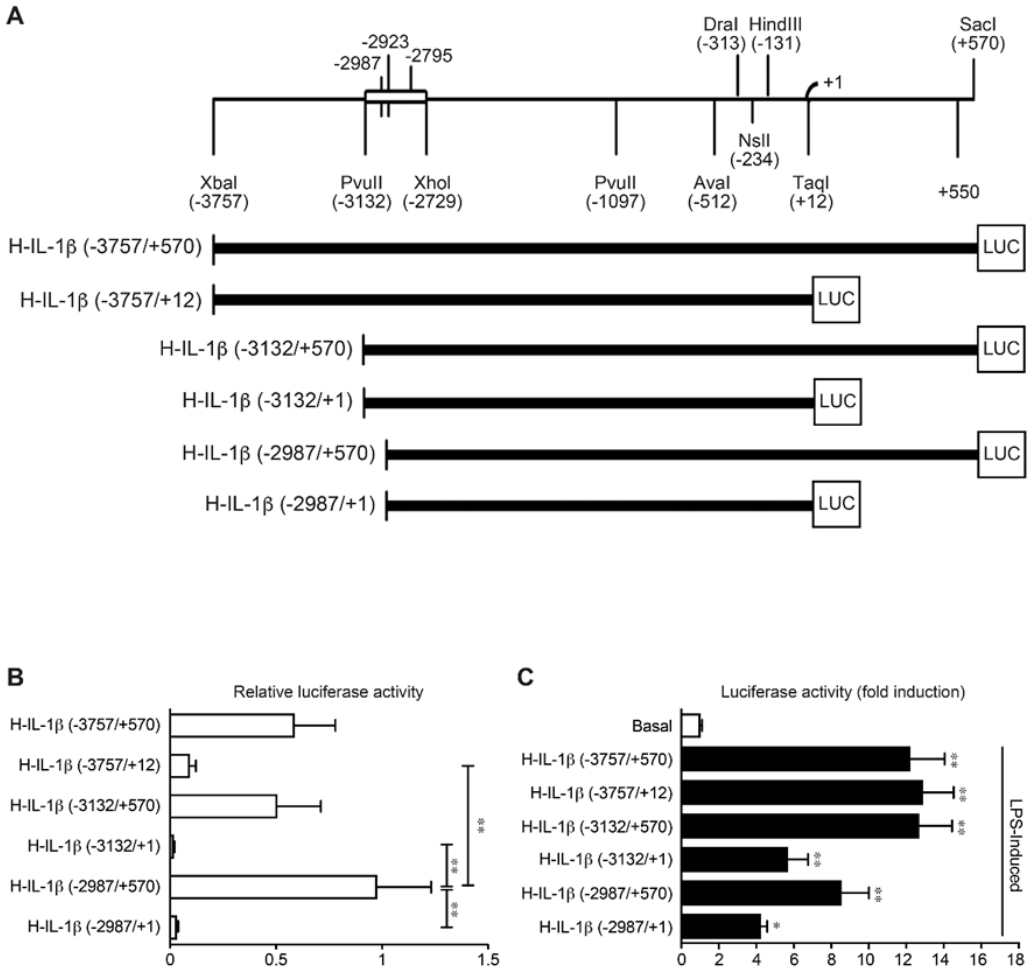

Figure 4.4. Schematic representation of the human IL-1β promoter fragments and the corresponding luciferase activity. *(A) The full-length H-IL-1β promoter (upper fragment: -3757/+570) and five deletion fragments based on Shirakawa et al., 1993 and the Ensembl Genome Browser. Restriction enzyme sites are numbered relative to the transcription start site (TSS)(+1). (B, C) Luciferase activity in RAW 264.7 cells in basal conditions (B) and 18 h after stimulation with 100 ng/ml LPS (C). Data (mean ± SEM for duplicate samples from four independent experiments) were calculated as fold induction relative to the respective basal expression. *p<0.05; **p<0.01 by one-way ANOVA followed by Tukey's and Dunnett's multiple comparison tests.*

4.3.2 *In vivo* characterization of IL-1β promoter fragments

Next, we examined if the H-IL-1β(-2987/+570) promoter fragment, showing high basal activity and strong LPS-induced activation was suitable for *in vivo* monitoring of the IL-1β gene transcriptional activation. We first developed a rAAV8 vector containing GFP under control of the H-IL-1β(-2987/+570) promoter fragment. In order to induce a detectable

promoter activation, we induced SE in mice (n=4) injected 2 weeks before with the AAV8-H-IL-1β(-2987/+570)-GFP viral particles. Indeed, 24 h after KA injection, strong GFP fluorescence signal was observed in the hippocampal region (Figure 4.5). However, a prominent activation of the promoter fragment was observed in neurons (Figure 4.5, panels a-c) whereas astrocytes accounted only for about 15% of the total cells expressing GFP (Figure 4.5A, panels d-f; Figure 4.5B).

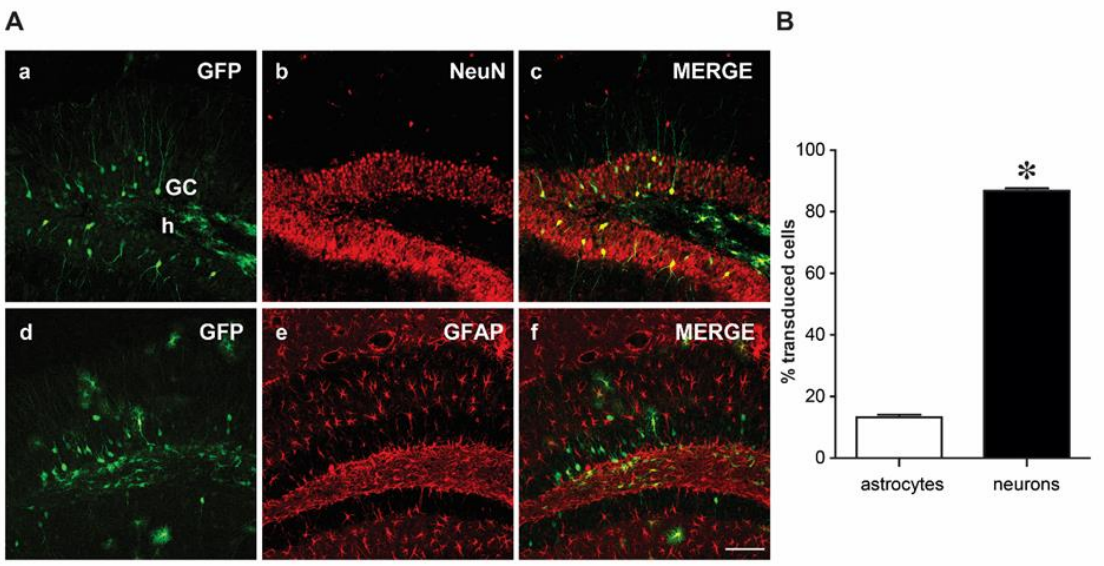

Figure 4.5. Ectopic neuronal induction of H-IL-1β promoter fragment in neurons after KA-induced status epilepticus (SE). *(A) Representative photomicrographs of AAV8-H-IL-1β(-2987/+570)-GFP transduction in neurons but not in astrocytes 2 weeks after intrahippocampal vector injection. Mouse brains were analyzed 24 h after KA-induced SE. GC, granule cells, h, hilus. Scale bar, 100 µm. (B) Percent of cell type (mean ± SEM, n=4 mice) expressing the GFP reporter gene under control of the H-IL-1β(-2987/+570) promoter fragment. *p<0.05 compared to astrocytes by Mann-Whitney.*

Subsequent immunohistochemistry in the hippocampus of SE-exposed and AAV8-H-IL-1β(-2987/+570)-GFP-injected mice (n=3) demonstrated that the GFP reporter gene did not co-

localize with the endogenous IL-1β expression (Figure 4.6A) since endogenous IL-1β was expressed in activated GFAP-positive astrocytes (Figure 4.6B).

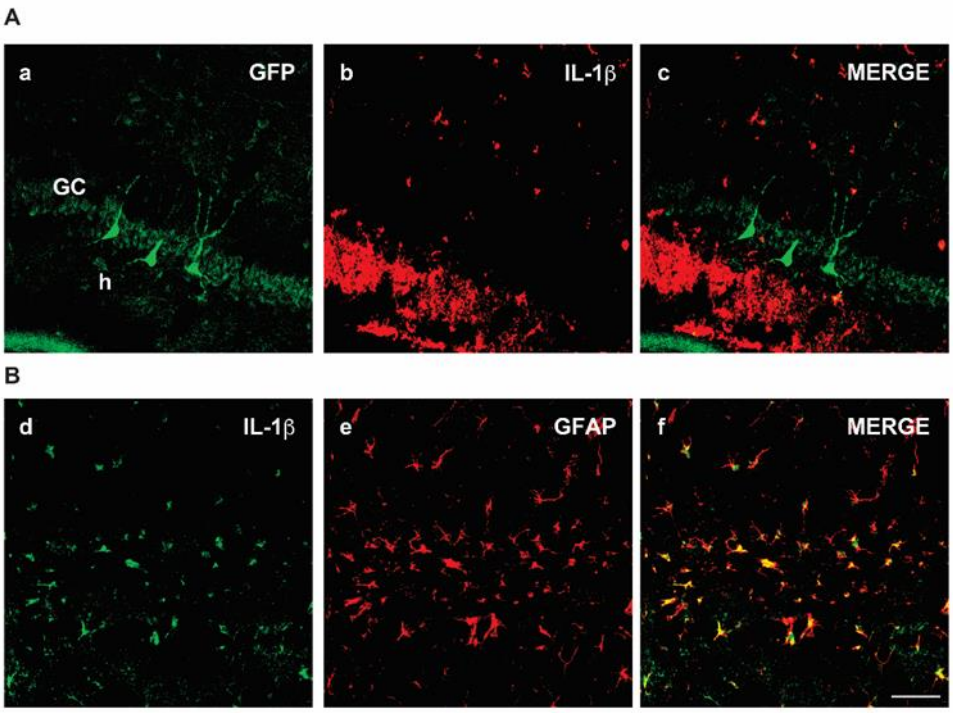

Figure 4.6. H-IL-1β promoter activation and endogenous IL-1β protein expression after KA-induced SE. *(A) Representative images of IL-1β protein expression in the hippocampus 2 weeks after injection of AAV8-H-IL-1β(-2987/+570)-GFP in mice (n=3) killed 24 h after KA-induced SE. The GFP signal does not co-localize with endogenous IL-1β expression. (B) Localization of endogenous IL-1β protein in GFAP-positive astrocytes in mice killed 24 h after KA. GC, granule cells, h, hilus. Scale bar 50µm.*

Since this result was in contrast with the astrocytic induction of this cytokine after SE, we further investigated if the endogenous IL-1β promoter was activated in neurons after SE. To this end, we injected mice (n=5) with rAAV1/2-synI-dtTomato which labels neurons and 2 weeks later mice were exposed to SE and killed 24 h later. RT-qPCR analysis on total hippocampal homogenates revealed a massive (up to 500-fold, $p<0.05$) of IL-1β mRNA induction after SE (Figure 4.7A). Subsequent RT-qPCR analysis on Tomato-expressing FACS-sorted hippocampal neurons showed that IL-1β mRNA was not up-regulated in neurons (Figure 4.7B).

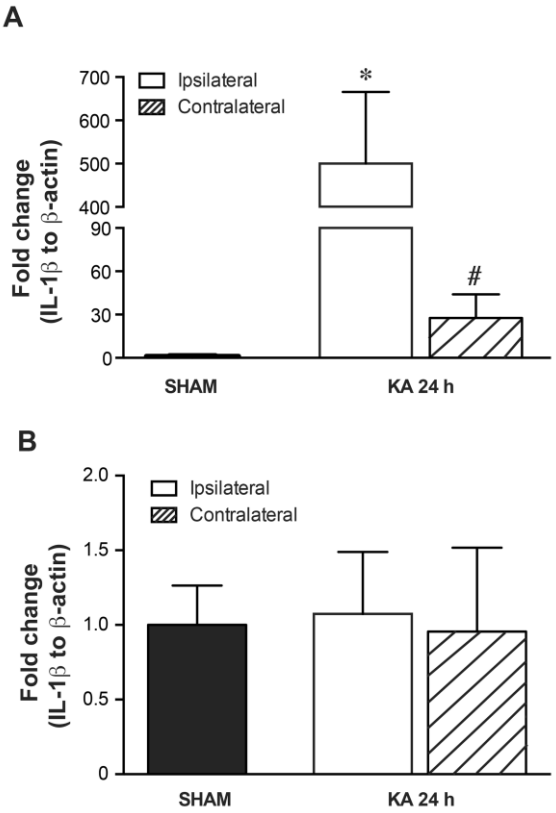

Figure 4.7. Endogenous IL-1β expression after KA-induced SE. *IL-1β mRNA expression levels measured by RT-qPCR in hippocampal homogenates (A) and in FACS-sorted neurons (B) from mice killed 24 h after KA-induced SE. Data (mean ± SEM, n=5 mice each group) represent the fold-increase in mRNA expression levels relative to basal expression measured in vehicle-injected mice (SHAM). Bargrams report measures in the hippocampi ipsilateral and contralateral to the injected cortex. *p<0.05 compared to SHAM; #p<0.05 compared to ipsilateral by one-way ANOVA followed by Tukey's multiple comparison tests.*

4.3.3 *In vivo* characterization of GFAP promoter

We evaluated the cell specificity and transduction efficiency of the AAV8-GFAP-GFP-WPRE vector containing the 681bp GFAP promoter fragment injected in the hippocampus of naive mice (n=3). Mice were sacrificed 2 weeks after the injection and the viral spread (Figure 4.8) and cellular expression (Figure 4.9) of the GFP reported gene were determined. The anteroposterior spread of the virus around the injection sites was ~ 3 mm (from -1.25 mm to -3.98 mm relative to bregma) while the medio-lateral spread was ~ 1 mm. The signal was

mainly restricted to the dentate gyrus including the molecular and polymorphic layers as well as in the stratum radiatum of the CA3 region (Figure 4.8). Notably, the GFP signal co-localized with GFAP-positive astrocytes (Figure 4.9, panels a-c) but not with NeuN-positive neurons (Figure 4.9, panels d-f).

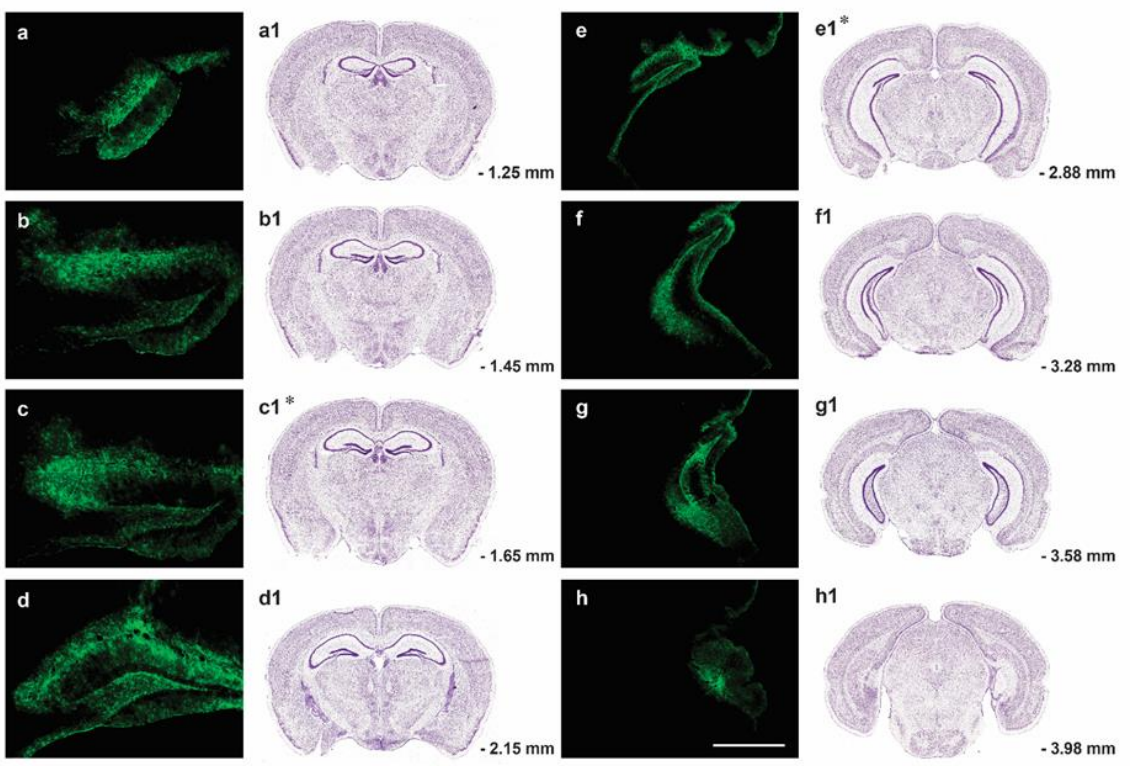

Figure 4.8. Antero-posterior spread of the GFP reporter gene in the hippocampus of rAAV8-GFAP-GFP-WPRE-injected mice. *Representative fluorescence pictures depicting the hippocampal spread (~ 3 mm) of the GFP reporter gene under the control of the GFAP promoter fragment (panels a-h). The GFP signal was mainly localised in the molecular and polymorphic layers of the dentate gyrus and stratum radiatum of the CA3 region. Slices close to the injection site are depicted by asterisks (c1, e1). Nissl-stained photomicrographs (panels a1-h1) depict the levels of antero-posterior slice analysis (Allen Mouse Brain Atlas; http://mouse.brain-map.org). Scale bar 100 µm.*

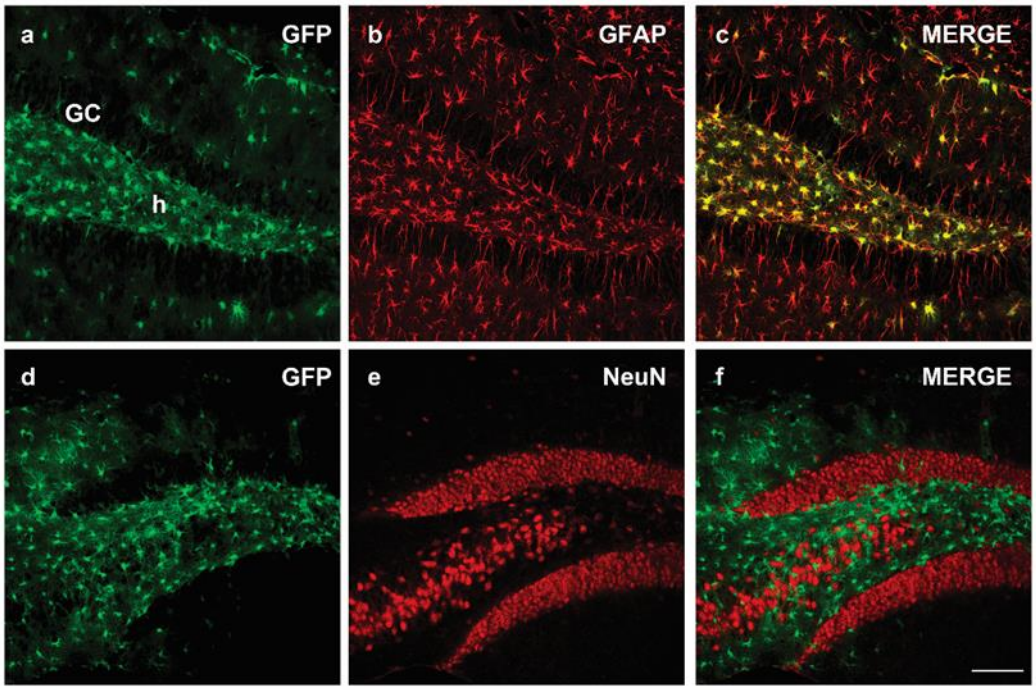

Figure 4.9. Induction of the GFAP promoter fragment in astrocytes after KA-induced SE. *Representative photomicrographs of rAAV8-GFAP-GFP-WPRE-transduced mice (n=3) 24 h after SE. GFP reporter gene transduction was observed in astrocytes (a-c) but not in neurons (d-f). GC, granule cells, h, hilus. Scale bar, 100 µm.*

4.3.4 *In vivo* bioluminescence imaging of GFAP promoter

To determine whether the 681bp GFAP promoter fragment could be used for *in vivo* bioluminescence imaging, rAAV8 vector particles harbouring a luciferase gene under control of the GFAP promoter fragment were bilaterally infused in the mouse hippocampus. Two weeks later, mice (n=6-11) were injected with KA in order to evoke SE. Twenty-four hours after SE induction, we detected a 3-fold ($p<0.05$) increase in bioluminescence signal bilaterally in the hippocampus compared to the respective basal signal in the same mice (Figure 4.10A, B). A further up-regulation (up to 7-fold, $p<0.01$) was observed 3 days after KA injection (Figure 4.10A, B).

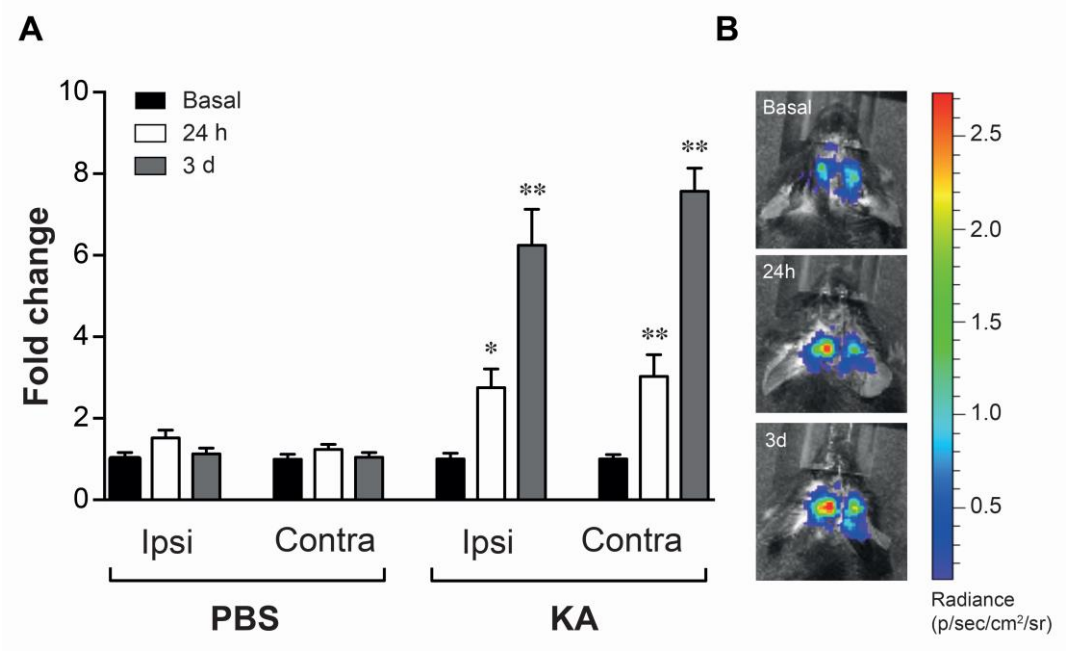

Figure 4.10. In vivo imaging of rAAV8-GFAP-LUC-injected mice. *Mice were monitored longitudinally 24 h and 3 days after KA-induced SE. (A) Data (mean ± SEM, n=6-11 mice) represent the fold-induction of bioluminescence activity in the hippocampus relative to the respective basal signal in each group. Basal signal did not differ inPBS-injected mice. *p<0.05, **p<0.01 compared to the respective basal signal by one-way ANOVA followed by Tukey's multiple comparison tests. Ipsi, ipsilateral to KA injection, Contra, contralateral to KA injection referred to the injected cortex. (B) Representative images of mice monitored before KA injection and 24 h and 3 days later.*

4.4 DISCUSSION

Astrocytic activation and induction of IL-1β are two processes which occur concomitantly during epileptogenesis (Maroso et al., 2011b; Vezzani et al., 2011b). So far, these phenomena have been investigated *post-mortem* in cross-sectional studies in animal models and they have been validated in epileptic foci surgically resected from pharmacoresistant human epilepsies (Aronica and Crino, 2011; Vezzani et al., 2011b). *In vivo* bioluminescence imaging is a powerful tool for performing longitudinal studies in animals since it allows to follow up the dynamics of these changes during epileptogenesis. Moreover, this approach permits to correlate the bioluminescence changes with disease

outcomes, and potentially with the therapeutic response to drugs. To this end, we developed an *in vivo* approach for long-term monitoring of the astrocyte activation and the related inflammatory response to an epileptogenic stimulus.

We provide evidence that the IL-1β promoter sequence upstream of the start ATG contains important elements for promoter activation in Raw 246.7 cells following inflammatory stimuli. Indeed, our *in vitro* results showed that the three fragments harbouring the 570 nucleotides downstream the TSS showed sufficient basal activity and were significantly activated by LPS. This may be due to the presence of binding sites for transcriptional factors that control IL-1β gene induction by LPS in this cell line. However, we observed that the 3557 kb promoter fragment, which responds to LPS stimulation *in vitro*, does not reflect the endogenous promoter cell-specific expression following SE since the promoter expression was observed in hippocampal neurons rather than in astrocytes. Likely, this promoter fragment lacks some regulatory elements that are required for the cell-specific IL-1β expression upon its transcriptional gene activation and that are instrumental for repressing IL-1β gene activation in neurons *in vivo*.

We conclude that for *in vivo* imaging of the IL-1β promoter, the full-length IL-1β should be used instead of smaller core-promoter fragments. However, due to the limited packaging capacity of rAAVs (maximum of 5.000 basepairs), we could not analyze the full-length IL-1β promoter *in vivo* (Dong et al., 1996; Hermonat et al., 1997). Other types of vectors should be considered, such as the lentiviral systems hosting larger sequences of foreign DNA. The use of these systems, however, requires a higher level of safety procedures; moreover, these vectors are mostly neurotropic although modifications of the capsid serotype may help to improve transfection in other cells types (Fassler et al., 2013). The development of transgenic mice harboring the luciferase gene under the control of the full H-IL-1β

promoter provides another possibility to study the whole body induction of this cytokine (Li et al., 2008).

As an alternative strategy, we studied the GFAP promoter fragment since it has been extensively characterized before (Lee et al., 2008). This fragment exhibits high specificity for astrocytes and shows prominent activation after SE, as shown by *in vivo* imaging. We used rAAV8 vectors containing the GFAP promoter fragment for delivering the transgene expressing luciferase into the hippocampus. Using this approach, we detected a significant increase in bioluminescence in astrocytes that expressed IL-1β at representative time points of epileptogenesis.

In conclusion, we developed an efficient *in vivo* imaging tool for monitoring activated astrocytes expressing an inflammatory phenotype after SE. This tool represents a powerful approach to monitor the dynamics of glial cell activation during epileptogenesis as well as after various acute and chronic CNS injuries associated with an inflammatory component.

CHAPTER 5 - CHARACTERIZATION OF ASTROCYTE ACTIVATION DURING EPILEPTOGENESIS

5.1 INTRODUCTION

Astrocyte activation in epilepsy importantly contributes to neuroinflammation, neuronal network hyperexcitability and hypersynchrony thus promoting the generation and recurrence of seizures (Devinsky et al., 2013). Similar to microglia astrocytes have been identified to assume either a pro-inflammatory phenotype named A1 or an A2 anti-inflammatory phenotype (Baldwin and Eroglu, 2017; Liddelow et al., 2017; Zamanian et al., 2012). Reactive A1-type astrocytes release toxic compounds and pro-inflammatory molecules which may lead to tissue damage and neuronal cell death (Devinsky et al., 2013; Liddelow et al., 2017). On the other hand, A2 astrocytes upregulate neurotrophic factors which promote neuronal survival and synapse repair, thus suggesting a ''helpful'' and homeostatic functions (Zamanian et al., 2012). These two types of astrocyte can be distinguished based on specific molecular traits. Pentraxin-3 (PTX3), for example, is an anti-inflammatory protein expressed by A2-type astrocytes and is neuroprotective (Ravizza et al., 2001). TNF-α instead is upregulated in activated A1-type astroglia and contributes to increase neuronal excitability (Balosso et al., 2013). Similarly, to TNF-α other molecules potentially neurotoxic are expressed by A1-type astrocytes such as HMGB1 (Maroso et al., 2010; Pedrazzi et al., 2007). Collectively, this evidence indicates the importance of monitoring astrocytic cell activation and determine their phenotype during epileptogenesis in order to understand when and how these cells contribute to epileptogenesis.

In this study, we investigated the dynamics of phenotypic changes in astrocytes during epileptogenesis by combining immunohistochemistry, western blot and *in vivo* bioluminescence imaging approaches.

Moreover, we also analysed whether drugs that have anti-epileptogenesis effects, as previously demonstrated in SE models, such as fingolimod (FTY720), modulate astrocyte

activation. We choose this drug since its inhibitory effects on inflammatory A1-type astrocytes appear to mediate the therapeutic action in animal models of epilepsy (Gao et al., 2012; Pitsch et al., 2018).

FTY720 is a sphingosine-1-phosphate (S1P) analog that is phosphorylated by sphingosine kinase 2 to FTY720-P, the active metabolite and a ligand for S1P 1, 3, 4 and 5 receptors receptors (S1PRs) (Spiegel and Milstien, 2011). Microglia and astrocytes both express S1PRs mRNA. Loss of S1P1 through functional antagonism by FTY720-P is considered to be the primary mechanism of action of the drug in astrocytes (Choi et al., 2011). FTY720 removes S1PRs from the cell surface through irreversible internalisation, vesicular storage and degradation (Choi et al., 2011; Oo et al., 2007). This accounts for the amelioration of experimental autoimmune encephalomyelitis (EAE) by both genetic S1P1 deletion and exposure to FTY720 (Choi et al., 2011; Mandala et al., 2002). Interestingly, after the S1P receptors are internalised and plasma membrane-dependent signaling responses to FTY720 or S1P are reduced, the signaling activated by internalised S1P1Rs persists for hours (Mullershausen et al., 2009; Wu et al., 2013).

FTY720 was found to reduce astrocytic activation and the expression of pro-inflammatory cytokines and to mediate an increase in anti-inflammatory cytokines and neuroprotective mediators (Choi et al., 2011; Hoffmann et al., 2015; Rothhammer et al., 2017). In epilepsy models, FTY720 reduced astroglia activation and TNF-α expression, and decreased the frequency and duration of seizures in pilocarpine- and kainate-induced SE in rodents (Gao et al., 2012; Pitsch et al., 2018). In our study, we explored whether FTY720 modulates the extent of activation and the A1 vs A2 phenotype of astrocytes during epileptogenesis using *in vivo* bioluminescence imaging of astrocytes, *post-mortem* immunohistochemistry and western blot analyses in a mouse model of epilepsy.

5.2 SPECIFIC MATERIALS AND METHODS

Induction of status epilepticus (SE)

Kainic acid (0.3 μg in 0.2 μl) was unilaterally injected in the basolateral amygdala to induce SE (Section 3.9.1 of General materials and methods). Control mice were injected with saline under the same conditions but were not exposed to SE. Mice were not implanted with electrodes in order not to interfere with bioluminescence signal. Thus, SE was monitored visually by two independent investigators who observed the occurrence of behavioural motor seizures for at least 3 hours from KA injection, a condition required for developing spontaneous seizures after 7 days on average. Mice injected with KA but displaying SE shorter then 3 h were excluded from further analysis.

Immunohistochemistry

Mice (n= 5 each group) were exposed to SE and sacrificed at 2 h, 24 h, 3 and 7 days later by transcardial perfusion and their brains were collected for immunohistochemical evaluation of astrocytes (Figures 5.2 and 5.3), microglia (Figure 5.5) and expression of HMGB1, TNF-α and PTX3 (Figures 5.6, 5.7 and 5.8; section 3.10 of General materials and methods for details). The cell type expressing HMGB1, TNF-α and PTX3 was identified by co-localization with GFAP, CD11b or NeuN (section 3.10.4 of General materials and methods).

In vivo bioluminescence imaging

Mice (n=9-12) were injected with AAV8-GFAP-LUC (section 3.4 of General materials and methods) 2 weeks before SE induction (Section 3.9.1 of General materials and methods). Mice injected with saline but not exposed to SE served as controls. Mice were monitored using *in vivo* bioluminescence imaging before SE induction for baseline measurement, then longitudinally at 2 h, 24 h, 3 and 7 days post-SE (Figure 5.4; General materials and methods, section 3.11).

Pharmacological treatment

Mice were injected with AAV8-GFAP-LUC 2 weeks before being exposed to SE. One hour after SE onset mice were randomly assigned to treatment or saline groups (n=6-12 each group). FTY720 (6 mg/kg, i.p.) was injected according to a treatment schedule previously shown to exert anti-inflammatory and anti-epileptogenic effects: i.e., for seven consecutive days starting 1 h after SE onset (Figure 5.1). Mice were monitored by *in vivo* bioluminescence analysis and at the end of the last imaging session, they were sacrificed for *post-mortem* immunohistochemistry (Figures 5.9, 5.10, 5.11, 5.12 and 5.13; section 3.10 of General materials and methods). One additional group of mice was treated with FTY720 or saline (n=5 each group) and killed after the last imaging session (7 days post-SE). The hippocampi ipsilateral to the injected amygdala were dissected out and used for Western blot analysis of GFAP, GLT-1 and Kir4.1 (Figure 5.14; Section 3.6.2 of General materials and methods).

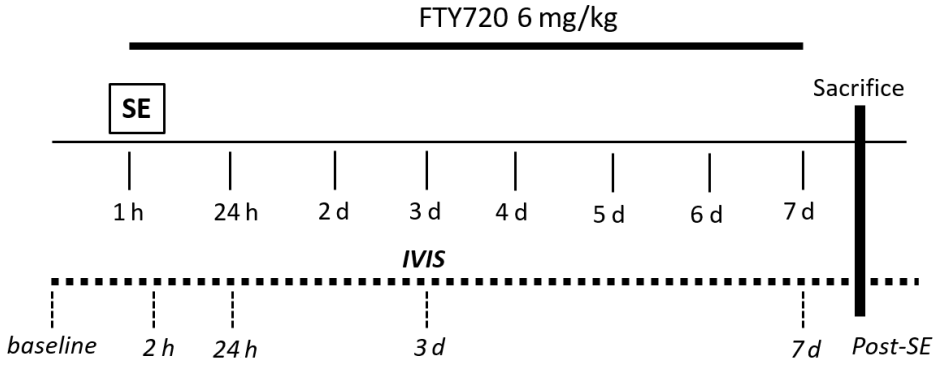

Figure 5.1. Experimental design in SE-exposed mice treated with FTY720 and monitored by in vivo bioluminescence imaging (IVIS). *Baseline in vivo bioluminescence imaging measurement was done in each mouse 1 day before SE induction (baseline) and imaging sessions were repeated in the same animal at 2 h, 24 h, 3 and 7 days post-SE. Mice were sacrificed at the end of the experiment (7 days after SE) for either immunohistochemical or western blot analysis of GFAP. Data related to this protocol are reported in Figures 5.9, 5.10, 5.11, 5.12, 5.13 and 5.14).*

Western blot

At the end of the last bioluminescence imaging session (7 days post-SE), mice exposed to SE and treated with saline or FTY720 and control mice (not exposed to SE) (n=5/group) were perfused via the ascending aorta with 50 mM cold PBS, pH 7.4 for 1 min, then the hippocampi ipsilateral to the injected amygdala were dissected and homogenised for immunoblotting (Figure 5.14; section 3.6.2 of General materials and methods). Anti-mouse GFAP (1:15000), anti-rabbit GLT-1 (1:1000) and anti-rabbit Kir4.1 (1:2000) were used and immunoreactivity was visualised with ECL Luminata solution (Luminata forte, Western HRP substrate, Millipore, MA, USA) using peroxydase-conjugated anti-mouse IgG or anti-rabbit IgG (1:10000; Sigma, St Louis, MO, USA) as secondary antibodies (section 3.6.2 of General materials and methods).

5.3 RESULTS

5.3.1 Astrocyte activation

In order to characterise the dynamics and extent of astrocyte activation during epileptogenesis, we assessed GFAP immunostaining in hippocampal slices of SE-exposed mice and their saline-injected controls (n=5 each group). In the hippocampus ispilateral to KA-injected amygdala, the GFAP-positive area was increased up to 2-fold ($p<0.01$) between 2 h and 7 days post-SE (Figure 5.2; $p<0.01$) compared to time-matched controls. A delayed increase was observed 3 and 7 days post-SE in the homotypic contralateral area ($p<0.05$ and $p<0.01$).

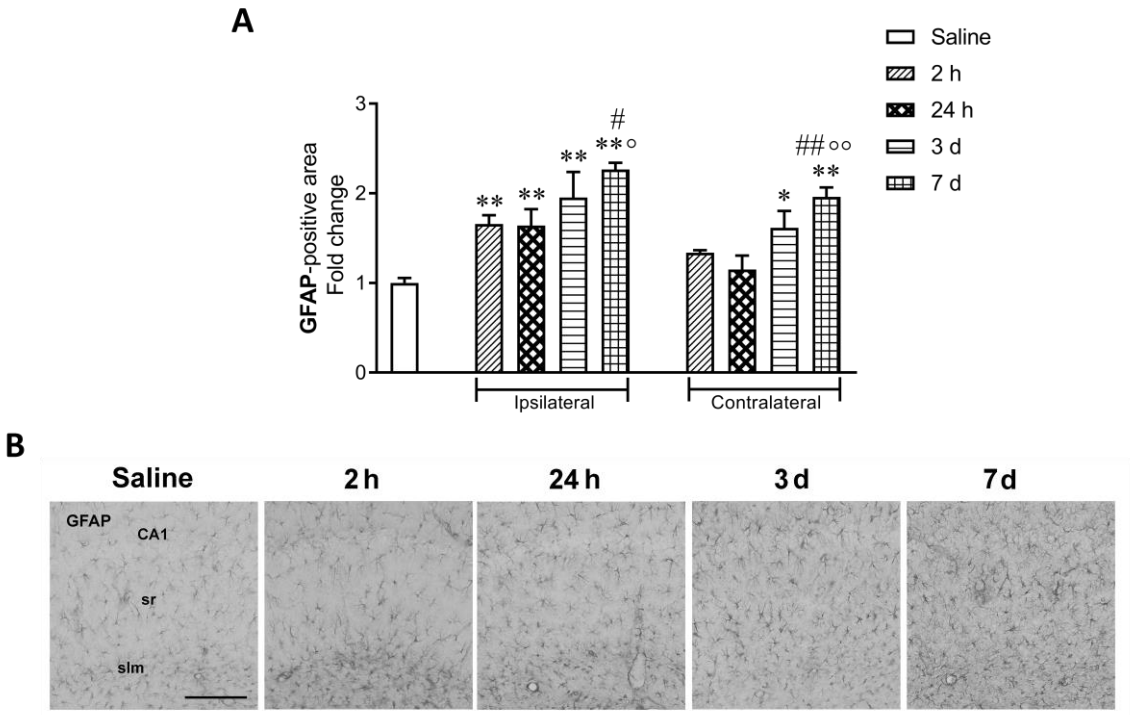

Figure 5.2. GFAP immunohistochemical signal in the hippocampus during epileptogenesis. *(A) GFAP-positive area in ipsilateral and contralateral dorsal hippocampus of mice sacrificed at 2 h, 24 h, 3 and 7 days post-SE. (B) Representative photomicrographs of corresponding hippocampal slices (CA1 area) stained for GFAP. Data (mean ± SEM, n=5 mice each group) *p<0.05; **p<0.01 compared to saline; #p<0.05; ##p<0.01 compared to 2 h and °p<0.05; °°p<0.01 compared to 24 h by one-way ANOVA followed by Tukey's multiple comparison tests. sr, stratum radiatum; slm, stratum lacunosum-moleculare. Scale bar, 50 µm.*

S100β-labeled astrocytes (high percentage of co-localization with GFAP) were also increased 3 and 7 days post-SE as shown by counting the number of postive cells and the area occupied by the specific signal ($p<0.01$) in both the ipsilateral and contralateral hippocampi (Figure 5.3).

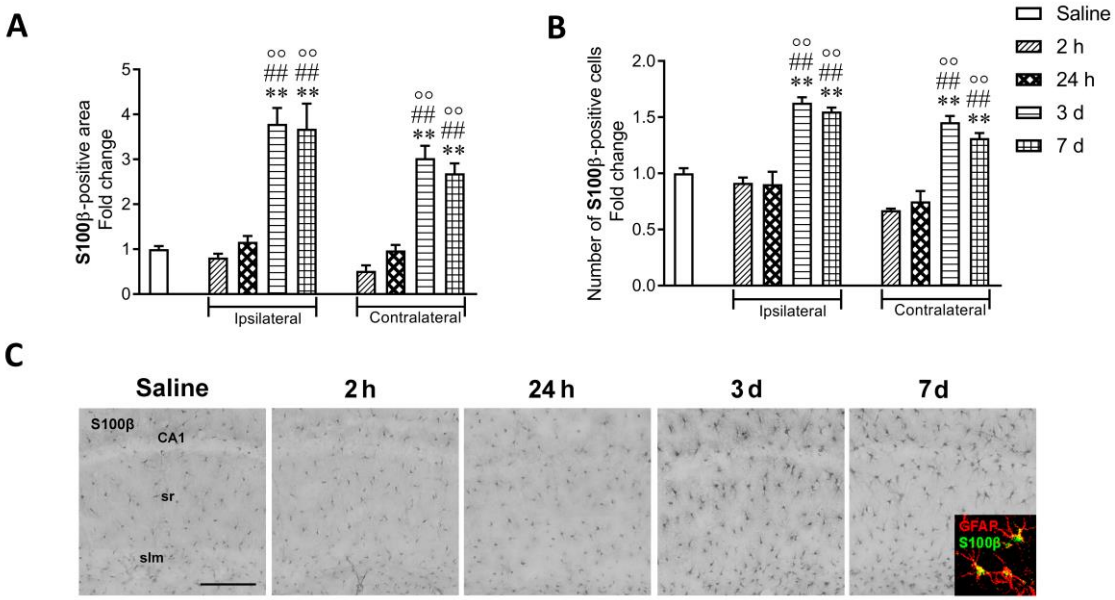

Figure 5.3. S100β-positive astrocytes in the hippocampus during epileptogenesis. *(A) S100β-positive area and (B) number of cells in the hippocampus of mice sacrificed at 2 h, 24 h, 3 days and 7 days post-SE. (C) Representative photomicrographs of corresponding hippocampal slices (CA1 area). Cells expressing S100β (green) were identified as GFAP-positive astrocytes (red). Co-localization signal is depicted in yellow (insert). Data (mean ± SEM, n=5 mice each group) **p<0.01 compared to saline; ##p<0.01 compared to 2 h and °°p<0.001 compared to 24 h by one-way ANOVA followed by Tukey's multiple comparison tests. sr, stratum radiatum; slm, stratum lacunosum-moleculare. Scale bar, 50 µm.*

Next, *in vivo* bioluminescence imaging was used in order to monitor longitudinally the astrocytic cell activation at the same time points analysed by immunohistochemistry. The bioluminescence signal was stable over time in the control group (saline-injected mice not exposed to SE; n=9). In mice exposed to SE, the GFAP promoter was significantly induced during epileptogenesis (n=12) already 2 h post-SE (1.8-fold, $p<0.05$) and was further

increased at 24 h (4-fold, p<0.01) then declining at 3 days (2.8-fold, p<0.01) and returning to basal level at 7 days post-SE (Figure 5.4).

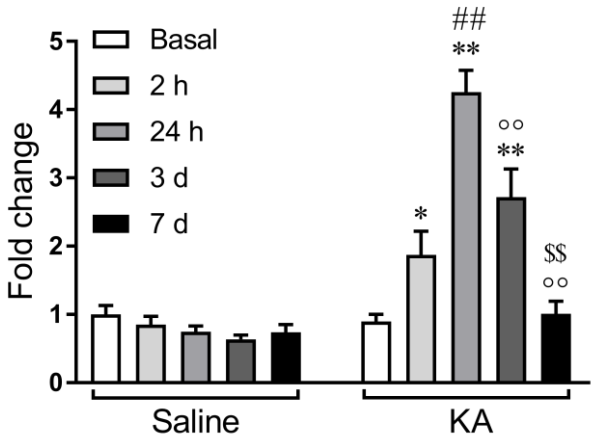

Figure 5.4. In vivo bioluminescence imaging of activated astrocytes in the hippocampus during the epileptogenesis. *Mice were injected with AAV8-GFAP-LUC and monitored longitudinally 2 h, 24 h, 3 and 7 days after SE onset. Data (mean ± SEM, n=9-12 mice) represent fold-increase of reporter gene relative to the respective basal signal (before SE) in each group. Basal signal did not differ from control mice (saline-injected mice not exposed to SE). *p<0.05; **p<0.01 compared to respective basal signal; ##p<0.01 compared to 2 h; °°p<0.01 compared to 24 h; $$p<0.01 compared to 3 d by one-way ANOVA followed by Tukey's multiple comparison tests.*

5.3.2 Microglia activation

We also evaluated the microglia activation during epileptogenesis in order to compare with the astrocytic cell response. Microglia was activated as astrocytes from 2 h post-SE until 7 days (18-fold on average, p<0.01) in the ipsilateral hippocampus (Figure 5.5), and a similar pattern of activation, although less pronounced, was detected in the contralateral side.

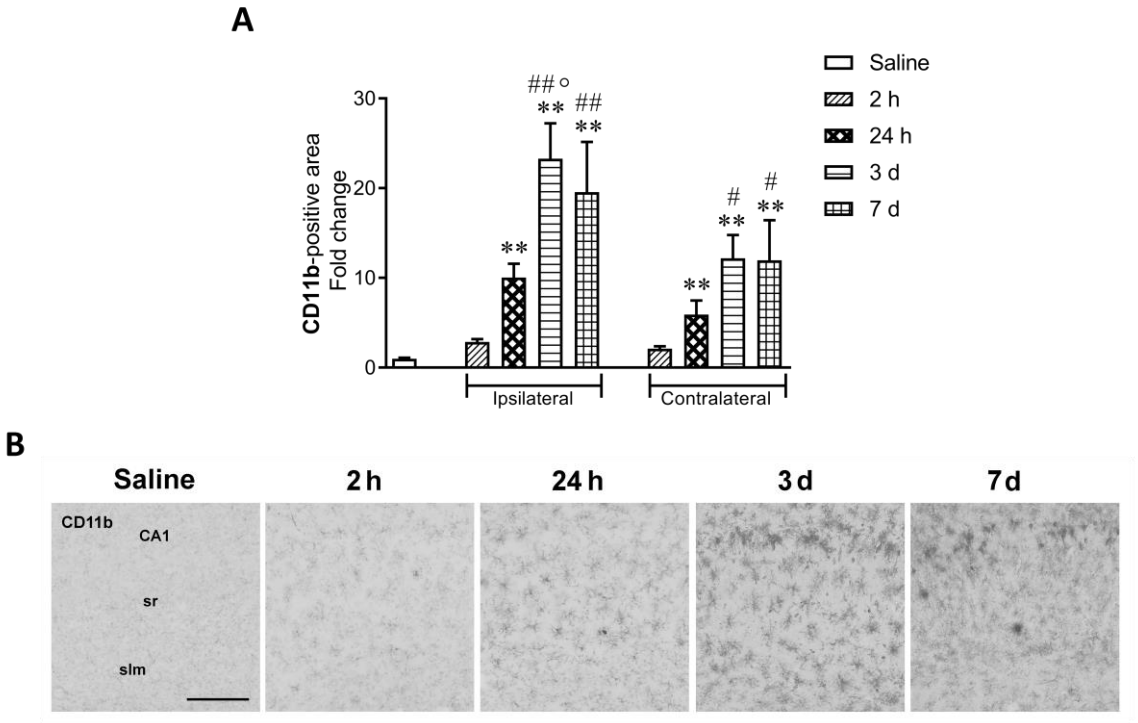

Figure 5.5. CD11b-positive cell activation in the hippocampus during epileptogenesis. *(A) CD11b-positive area in the ipsilateral and contralateral dorsal hippocampus of mice sacrificed at 2 h, 24 h, 3 days and 7 days post-SE. (B) Representative photomicrographs of corresponding hippocampal slices stained for CD11b. Data (mean ± SEM, n=5 mice each group) **p<0.01 compared to saline; #p<0.05; ##p<0.01 compared to 2 h and °p<0.05 compared to 24 h by one-way ANOVA followed by Tukey's multiple comparison tests. sr, stratum radiatum; slm, stratum lacunosum-moleculare. Scale bar, 50 µm.*

5.3.3 HMGB1, TNF-α and PTX3 expression in glial cells

Next, we characterised the phenotype of the astrocytes during epileptogenesis to determine their A1- vs A2- phenotype. Thus, we stained hippocampal slices from the same mice as above (n=5) for detecting proinflammatory, ictogenic and neurotoxic molecules such as HMGB1 and TNF-α (markers of A1 reactive astrocytes) and PTX3, a marker of A2 anti-inflammatory and neuroprotective astrocytes.

We found an increased number of HMGB1-positive cells 3 and 7 days post-SE but not at earlier time points in both hippocampi. This signal was localized in the nuclei of neurons and astrocytes but not in microglia (Figure 5.6).

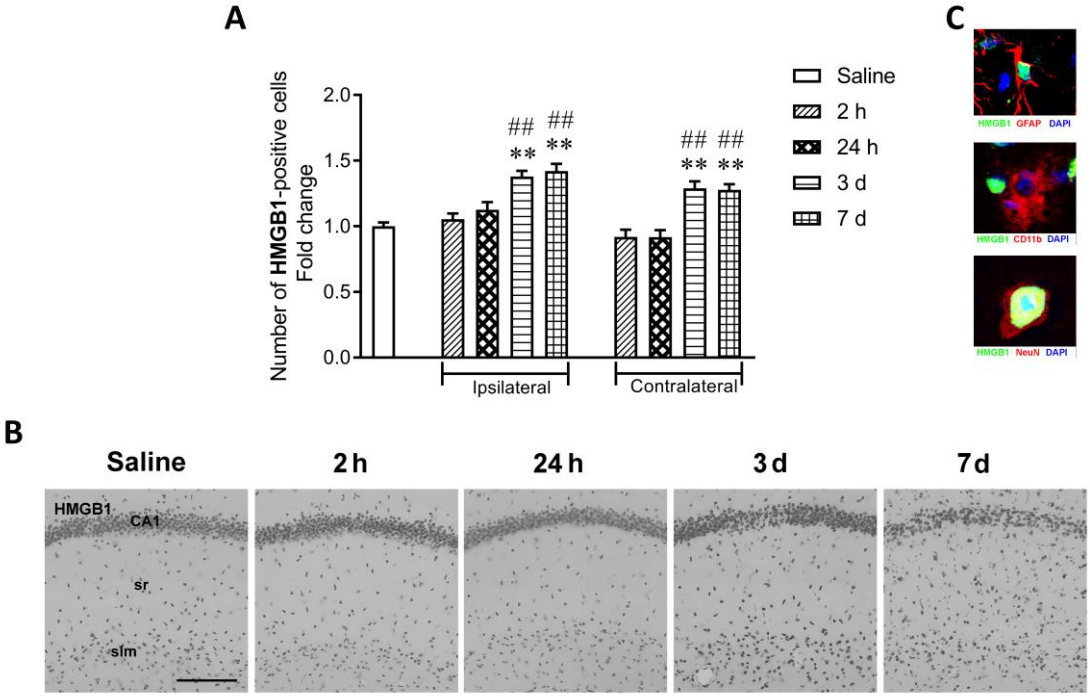

Figure 5.6. HMGB1 expression in hippocampal astrocytes and neurons during epileptogenesis. *(A) HMGB1-positive cells in the ipsilateral and contralateral dorsal hippocampus of mice sacrificed at 2 h, 24 h, 3 days and 7 days post-SE. (B) Photomicrographs of corresponding hippocampal slices stained for HMGB1. (C) HMGB1 nuclear signal (green) co-localises with the astrocytic marker GFAP (red) and the neuronal marker NeuN (red) but not with the microglial marker CD11b (red). Co-localization signal is depicted in yellow. DAPI-positive nuclei are shown in blue. Data (mean ± SEM, n=5 mice each group) **p<0.01 compared to saline; ##p<0.01 compared to 2 h by one-way ANOVA followed by Tukey's multiple comparison tests. sr, stratum radiatum; slm, stratum lacunosum-moleculare. Scale bar, 50 µm.*

While TNF-α staining was virtually absent in control slices, the TNF-α-positive area increased from 24 h (8330 ± 833 µm^2) until 7 days (53805 ± 8195 µm^2) post-SE (Figure 5.7). TNF-α-positive cells were detected in both hippocampi from 24 h (1245 ± 167, ipsilateral side) until 3-7 days post-SE (1764 ± 310).

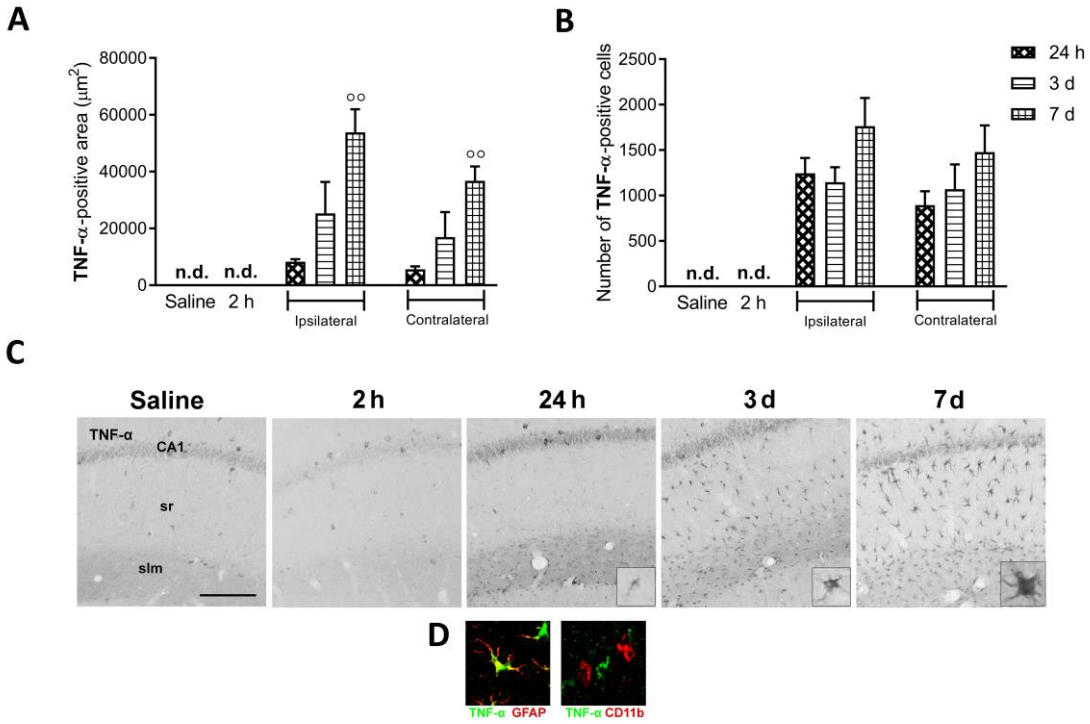

Figure 5.7. TNF-α expression in hippocampal astrocytes during epileptogenesis. *(A) Area occupied by the TNF-α signal and (B) the number of cells in the ipsilateral and contralateral dorsal hippocampus of mice sacrificed at 2 h, 24 h, 3 days and 7 days post-SE. (C) Photomicrographs of corresponding hippocampal slices depicting TNF-α-positive cells. (D) TNF-α (green) co-localises with the astrocytic marker GFAP (red) but not with microglia cells marked by CD11b (red). Co-localization signal is depicted in yellow. Data (mean ± SEM, n=5 mice each group) °°p<0.01 compared to 24 h by one-way ANOVA followed by Tukey's multiple comparison tests. sr, stratum radiatum; slm, stratum lacunosum-moleculare. Scale bar, 50 µm.*

PTX3 was not detected in control slices until 24 h post-SE (Figure 5.8). However, 3 days post-SE, a strong signal was detected in both hippocampi (183212 ± 55095 µm^2, ipsilateral side) and this signal further increased at 7 days post-SE (698829 ± 64316 µm^2, ipsilateral hippocampus). PTX3 was co-expressed with the astrocytic marker GFAP at all time points (Figure 5.8, insert).

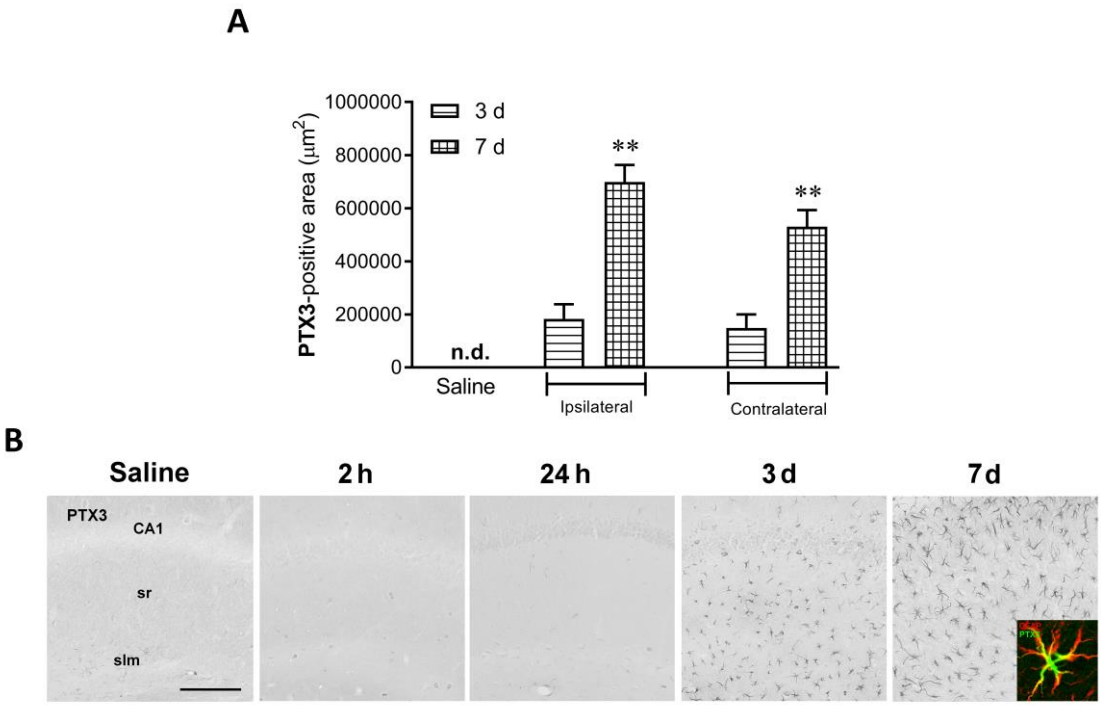

Figure 5.8. PTX3 expression in hippocampal astrocytes during epileptogenesis. *(A) Area occupied by the PTX3 signal and (B) PTX3 expression in cells with glial morphology at the different time points during epileptogenesis. Cells expressing PTX3 (green) were identified as GFAP-positive astrocytes (red). Co-localization signal is depicted in yellow (insert). Data (mean ± SEM, n=5 mice each group) **p<0.01 compared to 3 days by Mann-Whitney. sr, stratum radiatum; slm, stratum lacunosum-moleculare. Scale bar, 50 µm.*

5.3.4 Effect of FTY72 treatment on astrocyte activation

The effect of FTY720 (6 mg/kg i.p., 7-day treatment; protocol in Figure 5.1) on astrocyte activation during epileptogenesis was assessed first by *in vivo* bioluminescence imaging reflecting GFAP promoter activation (n=9-12). FTY720-treated mice showed a significantly higher increase in GFAP promoter activity from 24 h until 7 days post-SE ($p<0.01$) compared to SE-exposed mice injected with saline. At 2 h the promoter activity in FTY720-treated mice did not differ significantly from saline controls ($p=0.08$) whereas it was significantly enhanced in SE-exposed mice ($p<0.05$) (Figure 5.9).

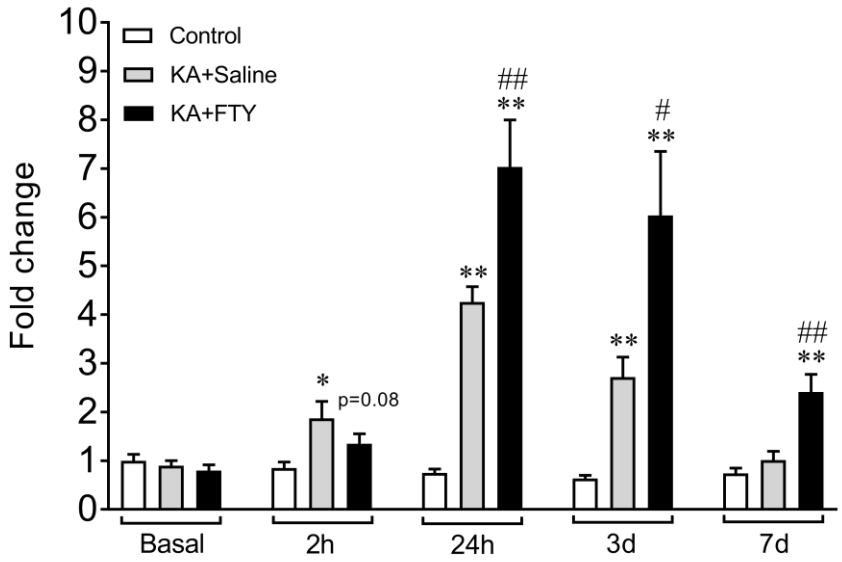

Figure 5.9. FTY720 effect on GFAP promoter activity in the hippocampus during epileptogenesis assessed by in vivo bioluminescence imaging. *AAV8-GFAP-LUC-injected mice were monitored longitudinally 2 h, 24 h, and 7 days after SE onset and treated either with saline (KA) or FTY720 (KA+FTY; 6 mg/kg; i.p. for 7 days). Control mice (n=9) were injected with saline but not exposed to SE. Data (mean ± SEM, n=9-12 mice) represent fold-induction of the reporter gene relative to the respective basal signal of each group (before SE). *p<0.05 **p<0.01 compared to control group and $^{\#}$p<0.05 $^{\#\#}$p<0.01 compared to KA+Saline group by one-way ANOVA followed by Tukey's multiple comparison tests.*

Next, we analyzed the effect of FTY720 on astrocytes activation and their phenotype by immunohistochemical analysis of mouse hippocampi after 7-day treatment. Three groups of mice were studied: control mice not exposed to SE and injected with saline (n=6), SE-exposed mice treated with either saline (n=9) or FTY720 (n=6). GFAP-postitive area was higher in SE-exposed mice ($p<0.01$) and FTY720 further increased the activated GFAP-positive area compared to the SE-exposed mice ($p<0.01$; Figure 5.10). FTY720 did not modify the S100β-positive area (ipsilateral hippocampus; Saline: 51364 ± 3424 μm^2; KA: 189134 ± 28531 μm^2; KA+FTY720: 179365 ± 18644 μm^2; Figure 5.11A) or the number of S100β-positive cells (ipsilateral hippocampus; Saline: 1852 ± 84; KA: 2873 ± 64; KA+FTY720: 2927 ± 77; Figure 5.11B).

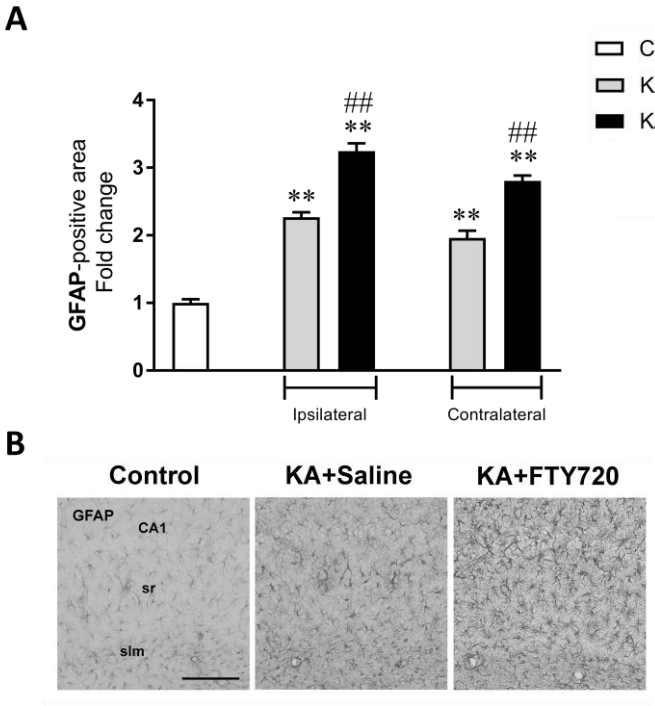

Figure 5.10. FTY720 effect on GFAP-positive astrocytes. *(A) GFAP-activated area in mice exposed to SE and treated with saline or FTY720 (6 mg/kg; i.p. for 7 days). (B) Representative photomicrographs of hippocampal slices from control mice (injected with saline but not exposed to SE) and SE-exposed mice treated with either saline or FTY720. Ipsilateral hippocampus (CA1 area) is depicted. Data (mean ± SEM, n=6-9 mice each group) **p<0.01 compared to control and ##p<0.01 compared to KA+Saline by one-way ANOVA followed by Tukey's multiple comparison tests. sr, stratum radiatum; slm, stratum lacunosum-moleculare. Scale bar, 50 µm.*

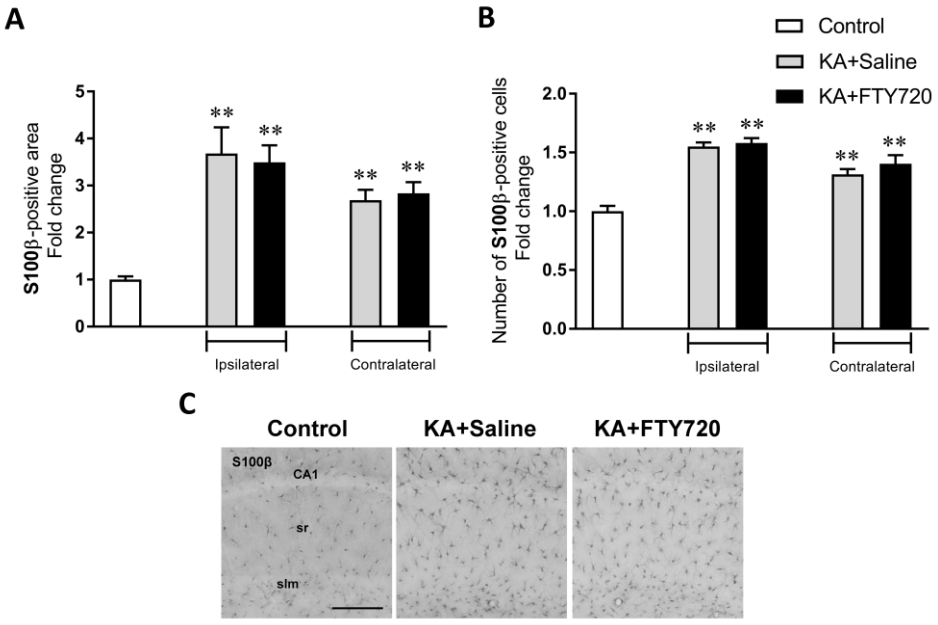

Figure 5.11. FTY720 effect on S100β-positive astrocytes. *(A) S100β-activated area and number of positive cells in mice exposed to SE and treated with saline or FTY720 (6 mg/kg; i.p. for 7 days). (B) Representative photomicrographs of hippocampal slices from control mice (injected with saline but*

*not exposed to SE) and SE-exposed mice treated with either saline or FTY720. Ipsilateral hippocampus (CA1 area) is depicted. Data (mean ± SEM, n=6-9 mice each group) **p<0.01 compared to control by one-way ANOVA followed by Tukey's multiple comparison tests. sr, stratum radiatum; slm, stratum lacunosum-moleculare. Scale bar, 50 µm.*

Similarly, no effects of FTY720 were detected on TNF-α-positive area (ipsilateral hippocampus; Saline: 53805 ± 8195 µm^2; KA+FTY720: 56890 ± 6790 µm^2; Figure 5.12A) or the number of TNF-α-positive cells (ipsilateral hippocampus; Saline: 1764 ± 310; KA+FTY720: 1672 ± 147; Figure 5.12B) and on PTX3 expression (ipsilateral hippocampus; Saline: 698829 ± 64316 µm^2; KA+FTY720: 698435 ± 102019 µm^2; Figure 5.13).

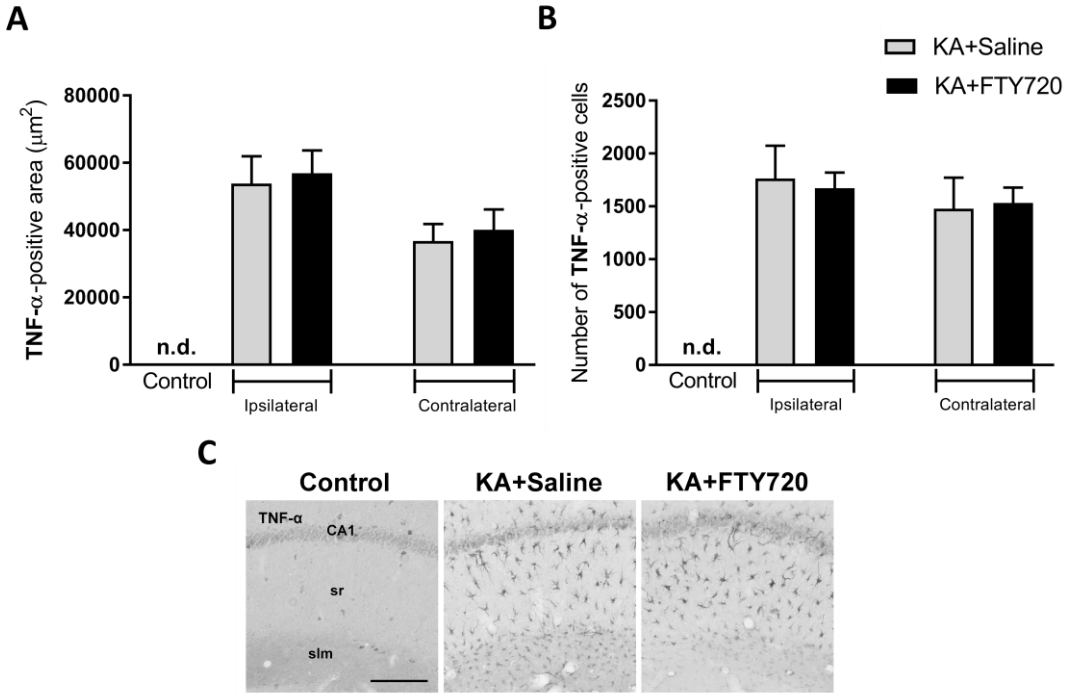

Figure 5.12. FTY720 effect on astrocitic TNF-α expression. *(A) TNF-α-positive area and number of TNF-α-positive astrocytes in SE-exposed mice treated with either FTY720 (6 mg/kg; i.p.) or saline. Controls are mice injected with saline but not exposed to SE. (B) Representative photomicrographs of corresponding hippocampal slices depicting TNF-α-positive astrocytes. Ipsilateral hippocampus (CA1 area) is depicted. Data (mean ± SEM, n=6-9 mice each group). sr, stratum radiatum; slm, stratum lacunosum-moleculare. Scale bar, 50 µm.*

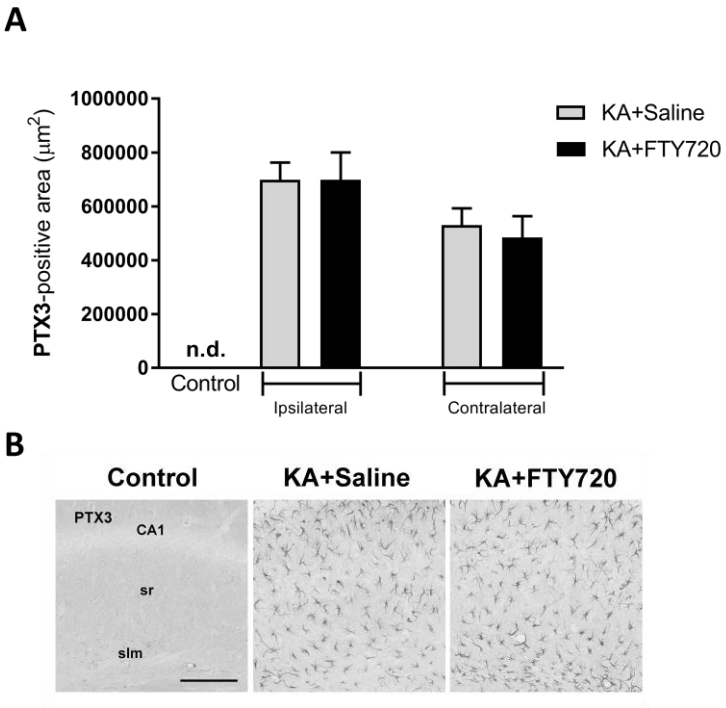

Figure 5.13. FTY720 effect on A2-type astrocytes. *(A) PTX3-positive area and (B) representative photomicrographs of hippocampla slices (CA1 area) from control mice and SE-exposed mice treated with either saline or FTY720 (6 mg/kg; i.p for 7 days). Ipsilateral hippocampus (CA1 area) is depicted. Data (mean ± SEM, n=6-9 mice each group). sr, stratum radiatum; slm, stratum lacunosum-moleculare. Scale bar, 50 μm.*

In line with the bioluminescence and immunohistochemical analysis, GFAP levels measured by western blot in the hippocampus (n=5) showed a 2-fold increase in protein levels ($p<0.01$) in SE-exposed mice which was higher in mice treated with FTY720 for 7 days ($p<0.05$) (Figure 5.14A). We also measured the protein levels of the GLT-1 glutamate transporter and Kir4.1 channel in the same brain homogenates used above to determine whether FTY720 treatment may enhance the buffering capacity of astrocytes which is compromized during epileptogenesis. We found a 50% decrease ($p<0.05$) in both proteins in SE-exposed mice as previously shown (Hubbard et al., 2016; Ueda et al., 2001; Zurolo et al., 2012) as compared to control mice (saline-injected but not exposed to SE) but FTY720 did not rescue this decrease (Figure 5.14B,C).

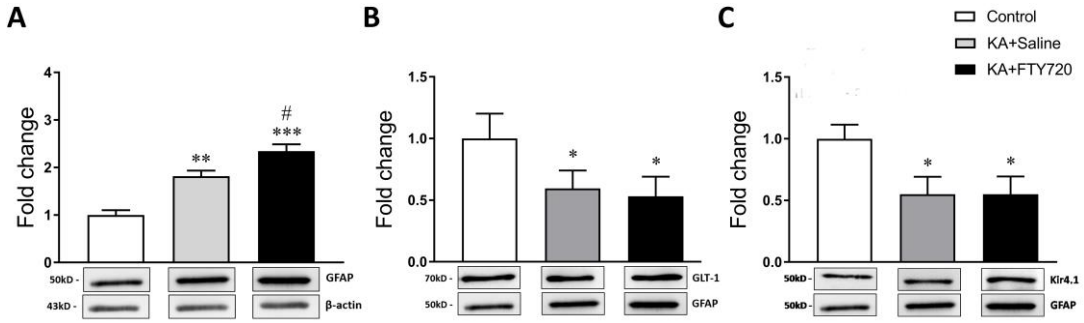

Figure 5.14. GFAP, GLT-1 and Kir4.1 levels in the hippocampus during epileptogenesis in mice treated with FTY720 or saline. *(A) GFAP (B) GLT-1 and (C) Kir4.1 protein levels 7 days post-SE in mice treated with FTY720 (6 mg/kg; i.p.) or saline. Representative bands corresponding to GFAP levels in the hippocampus ipsilateral to KA-injected amygdala. Controls are mice treated with saline but not exposed to SE. GFAP protein (50 kD), GLT-1 protein (70 kD), Kir4.1 protein (50 kD) and β-actin (43 kD). FTY720 (6 mg/kg; i.p.) or saline was administered for 7 days during epileptogenesis Data (mean ± SEM, n=5 mice each group) are optical density values of the relevant bands normalized to the corresponding β-actin or GFAP values. *p<0.05; **p<0.01 compared to control and $^{\#}$p<0.05 compared to KA by one-way ANOVA followed by Tukey multiple comparison tests.*

5.4 DISCUSSION

Astrocytes have a key role in the innate immune response to epileptogenic insults and they are also pivotal cells for maintaining brain homeostasis through regulation of ions, metabolites and neurotransmitters (Aronica and Crino, 2011; Danbolt, 2001; Olsen et al., 2015). During epileptogenesis, numerous pathologic changes occur in astrocyte functions. These alterations include increased expression of GFAP denoting their activation state and reduced expression of proteins involved in the regulation of extracellular potassium ($[K^+]_o$) and glutamate. These changes lead to altered tissue homeostasis that results in increased neuronal excitability and promote seizure generation (Seifert et al., 2010; Steinhäuser and Seifert, 2012). However, there is also evidence of compensatory mechanisms activated in astrocytes in order to balance the deleterious alterations occurring during the disease course. These include, secretion of growth factors that mediate neuronal survival,

generation of anti-inflammatory and proresolving lipids and proteins and PTX3 expression that may confer neuroprotection (Borges et al., 2003; Fellin, 2009; Nagao et al., 2013; Pan et al., 2018; Ravizza et al., 2001). Thus, understanding how astrocytes respond to epileptogenic insults that lead to seizures and the dynamics of these detrimental or compensatory responses is important to understand their role in the disease mechanisms, hence for the development of drugs that specifically target the pathologic phenotype of astrocytes.

The GFAP protein staining rapidly and progressively increases during epileptogenesis indicating that astrocytic activation precedes the onset of the spontaneous seizures. Microglia activation also occurs in parallel with GFAP-positive astrocytes showing a rapid increase that progresses over time and persists for at least one week post-SE.

S100β was also induced in astrocytes but with a delay of days compared to GFAP possibly revealing the late activation of a specific set of astrocytes. In accord, these two astrocytic markers were previously reported to follow a different patter of induction in the hippocampus after KA, a phenomenon linked to distinct regulatory mechanisms of the respective gene expression (Bendotti et al., 2000). S100β is a calcium-binding protein (Donato, 2001; Heizmann, 2002) and its upregulation in the late epileptogenesis phase may reflect the activation of a population of astrocytes attempting to buffer the intracellular calcium increase which induces gliotransmitters release such as glutamate and D-serine (Araque et al., 2014; Bazargani and Attwell, 2016; Yang et al., 2003) or ATP and TNF-α (Agulhon et al., 2008, 2012). These gliotransmitters contribute to neuronal network synchronization and to neuroinflammation thus promoting seizure generation (Devinsky et al., 2013; Robel and Sontheimer, 2016). Notably, S100β can be also released extracellularly by astrocytes and relatively high concentrations (μM) exert excitatory and neurotoxic

effects (Nishiyama et al., 2002; Rothermundt et al., 2003; Sakatani et al., 2008); moreover, its hippocampal levels correlate with the severity of epilepsy in animal models (Filibian et al., 2012; Pascente et al., 2016). Neurotrophic and gliotrophic effects of relatively low S100β concentrations (nM) have also been reported (Rothermundt et al., 2003).

Overall, the early vs late activation of GFAP- and S100β-positive astrocytes, respectively supports the heterogeneity of the glial cell populations (Höft et al., 2014; Matthias et al., 2003; Schitine et al., 2015) which may subserve different functions during epileptogenesis. It would be important to selectively interfere with these two cell populations to better understand their roles. In this respect, the induction of GFAP-positive astrocytes *per se* induces hippocampal hyperexcitability and spontaneous seizures (Ortinski et al., 2010; Robel et al., 2015) thus supporting that these cells contribute to the disease and their pathologic phenotype during epileptogenesis overcomes their homeostatic functions. When interpreting our results, we should also consider that S100β labels the soma and large astrocytic processes while GFAP is visible also in fine processes, therefore the GFAP staining may represent a more sensitive marker for slight morphological modifications of astrocytes which cannot be detected by assessing S100β.

In vivo bioluminescence imaging of astrocyte activation supports the immunohistochemical evidence. The GFAP promoter induction follows the temporal pattern observed by measuring GFAP in histological specimens. However, promoter induction elapses between 3 and 7 days post-SE while the GFAP protein is still upregulated at 7 days. This result is compatible with the slow turnover rate of GFAP which levels outlast the gene promoter activity (Chiu and Goldman, 1984; DeArmond et al., 1986; Morrison et al., 1985; Price et al., 2010).

The *in vivo* monitoring of the GFAP promoter activation provides therefore a longitudinal information on the timing of morphological activation of astrocytes although it does not directly inform on the A1 or A2 phenotype of these cells or the molecules they might release upon cell activation.

Our cross-sectional study addressed the astrocytic phenotype during epileptogenesis by comparing the expression of both A1 and A2 markers. Among the A1 markers we found an upregulation in nuclear HMGB1 indicating increased gene transcription of this ictogenic and neurotoxic mediator at late time points (3 and 7 days post-SE) matching the timing of activation of the S100β-positive cells. The ictogenic cytokine TNF-α also showed a relatively late induction (from 24 h post-SE) in astrocytes. PTX3 expression (A2-phenotype marker) was detectable at 3 and 7 days post-SE. The PTX3 promoter displays a NF-κB-sensitive element which responds to both TNF-α and IL-1β (Basile et al., 1997; Goodman et al., 1996). Indeed, we showed that PTX3 induction in astrocytes follows that of TNF-α. We observed therefore a mixed induction of pathologic (HMGB1 and TNF-α) and homeostatic (PTX3) molecules at overlapping time points during epiletogenesis. In accord, both the A1- and A2-phenotype markers were detected 24 h (TNF-α) and 3 days (HMGB1 and PTX3) but not earlier. This late induction (3 and 7 days post-SE) by matching the activation of S100β-positive astrocytes suggests that it occurs predominantly in these cells although we were not able to co-localize S100β with A1- and A2-phenotype markers due to incompatibility of the primary antibodies. Although S100β signal highly co-localized with GFAP in astrocytes as all A2 and A1 markers, GFAP-positive, but not S100β-positive, astrocytes are rapidly activated within 2 h after SE. It would be very informative to determine which are the early markers of activated GFAP-positive astrocytes within hours of SE onset by analysing gene transcription in cell sorted cells (experiments are in progress).

In the second part of our study, we assessed the effect of FTY720 on astrocyte activation and their phenotype since this drug provided significant anti-epileptogenesis and neuroprotective effects in different animal models which were in part attributed to anti-inflammatory actions on activated astrocytes (Gao et al., 2012; Pitsch et al., 2018). Our *in vivo* and *ex vivo* results showed lack of effect of FTY720 on both astrocyte activation and proliferation following a treatment schedule that provided anti-epileptogenic effects. Similarly, FTY720 did not modify the pro-inflammatory phenotype of astrocytes neither boosted the neuroprotective PTX3 expression. On the contrary, FTY720 further increased the astrocyte's promoter induction as shown by *in vivo* bioluminescence analysis reflecting activation of pre-existing cells rather than proliferation of new cells since FTY720 treatment increased the GFAP-positive area but not the number of positive cells (see also Wu et al., 2013). However, cell activation was not accompanied by a concomitant induction of GLT-1 or Kir4.1 therefore indicating the persistence of dysfunctional astrocytes. In accordance with our results, FTY720 did not change the mRNA or protein levels of GLT-1 in astrocyte cell culture after a pro-inflammatory stimulus (Lee et al., 2017). However, in a murine EAE model FTY720 treatment restored the reduced expression of GLT-1 presumably via anti-inflammatory mechanisms (Lee et al., 2017). The lack of effect of FTY720 on GLT-1 protein levels in our model is therefore compatible with the lack of anti-inflammatory effects.

FTY720 may activate astrocytes primarily through S1P3 and S1P5 receptors whereas S1P1 signaling appears to inhibit astrogliosis in organotypic cerebellar slice cultures modeling MS possibly by inducing the release of factors that modulate the astrocytic cell response (Miron et al., 2010). Indeed, S1Ps receptor engagement on astrocytes can induce growth factor production which in turn results in increased S1P5 levels (Furukawa et al., 2007; Healy et al., 2013; Miron et al., 2010; Sato et al., 1999). These mechanisms may be

operative also in our experimetal conditions. Release of growth factors from activated astrocytes even in an inflamed environment can afford neuroprotection as suggested by evidence in a demyelination model (Janssen et al., 2015).

The increased GFAP promoter activation and protein levels induced by FTY720 may be caused also by epigenetic alterations mediated by the drug. Histone acetylation controls GFAP expression (Asano et al., 2009; Hsieh et al., 2004; Zhou et al., 2011). The acetylation state of histone proteins is regulated by histone acetylase and histone deacetylase (HDAC) enzymes. Inhibition of HDACs results in increased histone acetylation. Indeed, treatment with the HDAC inhibitor valproic acid increased histone H3 acetylation at the STAT3-binding site leading to enhanced STAT3 binding to the GFAP promoter resulting in gene activation (Asano et al., 2009; Cheng et al., 2011; Nakashima and Taga, 2002; Sauvageot and Stiles, 2002; Taga and Fukuda, 2005). Similarly, nuclear FTY720-P binds to the active site of HDACs and inhibits their activity (Gardner et al., 2016; Hait et al., 2014). Moreover, both S1P receptor and FTY720-P inhibit HDAC activity and increase histone acetylation at H3K9, H4K8, H3K18, and H3K23 (Ebenezer et al., 2016, 2017; Gardner et al., 2016; Hait et al., 2009, 2015).

Overall, our study does not support that the anti-epileptogenic effects of FTY720 shown in *in vivo* models are mediated by drug's inhibition of GFAP- and S100 β-positive astrocytes or rescue of their proinflammatory phenotype. Although this mechanism appears to mediate the reduction of spontaneous seizure frequency when FTY720 is administered in the chronic epilepsy phase (Pitsch et al., 2018), it is unlikely to be involved in the epileptogenesis phase preceding the onset of the disease.

PART II

CHAPTER 6 – GENERAL MATERIALS AND METHODS

6.1 EXPERIMENTAL ANIMALS

Adult C57BL/6N male mice (~50 days, 20-25 g) were obtained from Charles River (Italy) and Sprague–Dawley male rats were purchased from Charles River Laboratories (St. Constant, Quebec, Canada). Animals were housed at a constant room temperature (23°C) and relative humidity (60 ± 5%) with free access to standard food pellet and water, and with a fixed 12 h light/dark cycle. Adult animals were housed two or four per cage and environmental enrichment was used. TICAM knock-out mice were provided by Dr. Cecilia Garlanda (Istituto Clinico Humanitas –IRCCS, Rozzano, Italy) and were housed at the same conditions described above.

6.2 ANIMAL CARE

Procedures involving animals were conducted at Istituto di Ricerche Farmacologiche Mario Negri IRCCS which adheres to the guidelines of the Italian Governing Law (D.lgs 26/2014; Authorization n.19/2008-A issued March 6, 2008 by Ministry of Health); Mario Negri Institutional Regulations and Policies providing internal authorization for persons conducting animal experiments (Quality Management System Certificate - UNI EN ISO 9001:2008 - Reg. No. 6121); the NIH Guide for the Care and Use of Laboratory Animals (2011 edition); EU directives and guidelines (EEC Council Directive 2010/63/UE) and the institutional policies and guidelines of Sainte-Justine Hospital Research Centre and Université de Montréal (Montreal, QC, Canada). The Statement of Compliance (Assurance) with the Public Health Service (PHS) Policy on Human Care and Use of Laboratory Animals has been recently reviewed (9/9/2014) and will expire on September 30, 2019 (Animal Welfare Assurance #A5023-01).

6.3 *IN VIVO* MODEL OF ICTOGENESIS

6.3.1 Intrahippocampal kainic acid in mice

Adult male mice were surgically implanted under general gas anesthesia (1-3% isoflurane in O_2) and stereotaxic guidance. Two nichrome-insulated bipolar depth electrodes (60 µm OD) were implanted bilaterally into the dorsal hippocampus (from bregma, mm: nose bar 0; anteroposterior –1.8, lateral 1.5 and 2.0 below dura mater; Franklin and Paxinos, 2008). A 23-gauge cannula was unilaterally positioned on top of the dura mater and glued to one of the depth electrodes for the intrahippocampal injection of kainic acid (KA; see later). Two screw electrodes were positioned over the nasal sinus and the cerebellum, and used as ground and reference electrodes, respectively. The electrodes were connected to a multipin socket and, together with the injection cannula secured to the skull by acrylic dental cement. The correct position of the electrodes and injection needle in each mouse was evaluated by *post-hoc* histological analysis of brain tissue at the end of the experiments.

Intrahippocampal injection of KA in freely moving mice was done 7 days after surgery as previously described (Balosso et al., 2008; Iori et al., 2017; Maroso et al., 2010). Briefly, KA (7 ng/0.5 µl; Sigma, Saint Louis, MI, USA) was dissolved in 0.1 M phosphate-buffered saline (PBS, pH 7.4) and injected unilaterally in the dorsal hippocampus by using a needle protruding 2.0 mm from the bottom of the guide cannula. The needle was left in place for one additional minute to avoid backflow through the guide cannula and then was removed. Mice were freely moving for the rest of the experiment.

This dose of KA induces EEG ictal episodes in the hippocampus in 100% of mice without mortality (Balosso et al., 2008; Maroso et al., 2010). Selective cell loss in CA3 region of the injected hippocampus is observed 7 days after KA injection (Balosso et al., 2005, 2008;

Ravizza et al., 2006b). Previous experiments demonstrated that this dose of KA provokes seizures in rodents that could be either inhibited or exacerbated by pharmacological or genetic interventions (Balosso et al., 2005, 2008; Maroso et al., 2010, 2011b; Vezzani et al., 2000). Thus, this model is suitable, and sensitive enough, to detect changes in seizure activity determined by specific target manipulation.

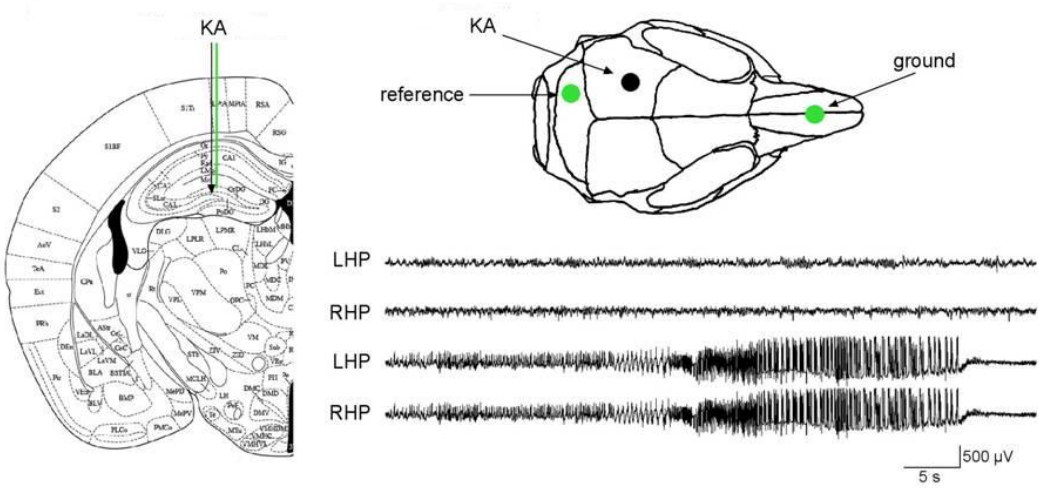

Figure 6.1. Experimental model of acute seizures and related injection protocol. *Brain atlas plate depicting kainic acid (KA, 7 ng/0.5 µl) unilateral injection site (black arrow) and the depth bipolar recording electrode that was placed in the hippocampus (green line) bilaterally. Schematic skull reproduction shows surface electrode placement (green circles) and the position of the guide cannula for intrahippocampal injection of KA (black circle). Representative EEG tracings depicting baseline recordings (top) and ictal activity after KA injection (bottom) simultaneously occurring in the left (LHP) and right (RHP) hippocampus in freely moving mice.*

6.3.2 Seizure assessment and quantification

EEG seizures induced by intrahippocampal injection of KA in freely-moving mice have been extensively described before (Balosso et al., 2005, 2008; Ravizza et al., 2006b). A minimum of 30 min recording was done before KA injection to assess the basal EEG activity, and then recording continued for 180 min after KA injection. At least a 30 min recording similar to baseline was required before ending the experiment. Ictal episodes are characterized by high-frequency (7-10 Hz) and/or multispike complexes and/or high-voltage (700 µV-1.0

mV) synchronized spikes simultaneously occurring in the injected and contralateral hippocampi (Figure 8.1). Spiking activity may occur between seizures and after seizures subside. Quantification of seizure activity was done by measuring the time elapsed from KA injection to the occurrence of the first EEG seizure (onset), the number of seizures and the total duration of seizures (sum of the duration of every ictal episode during the EEG recording period). Seizures occur with an average latency of 10 min from KA injection, then recurred for about 90 min from their onset, and were associated with motor arrest of the mice.

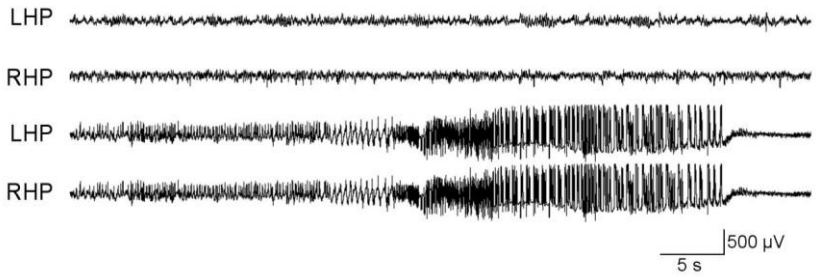

Figure 6.2. EEG tracings in KA-induced acute seizures. *Representative EEG tracings depicting baseline recordings (top) and ictal activity after unilateral intrahippocampal KA injection (bottom) simultaneously occurring in the left (LHP) and right (RHP) hippocampus in freely moving mice (Iori et al., 2013).*

6.4 INTRACEREBROVENTRICULAR ADMINISTRATION OF DRUGS

Mice were surgically implanted under general gas anesthesia (1-3% isoflurane in O_2) and stereotaxic guidance (Iori et al., 2013; Maroso et al., 2010) with a guide cannula positioned on top of the dura mater (from bregma, mm: nose bar 0; anteroposterior +0.3, lateral 0.9) (Franklin and Paxinos, 2008) ipsilateral to the intrahippocampal injection of KA one week before treatments. Poly I:C (tlrl-pic, Invivogen) was dissolved in sterile PBS (10 mg/1.5 ml) and injected at doses of 33 µg/5 µl, 10 µg/1.5 µl, 1 µg/1.5 µl and 0.1 µg/1.5 µl, intracerebroventricularly (i.c.v., 0.5 µl/min) in freely moving mice using a 30-gauge injection needle protruding 2.3 mm from the bottom of the guide cannula connected to a

10 µl Hamilton microsyringe via PE20 tubing, according to convection-enhanced delivery method (Gasior et al., 2007). At the end of infusion, the needle was left in place for one additional minute to avoid backflow through the guide cannula, then gently removed.

6.5 INTRAHIPPOCAMPAL ADMINISTRATION OF DRUGS

Mice were surgically implanted under general gas anesthesia as described above (Section 6.4) with a guide cannula positioned on top of the dura mater at the same position as for intrahippocampal injection of KA (from bregma, mm: nose bar 0; anteroposterior –1.8, lateral 1.5) (Franklin and Paxinos, 2008) one week before treatments. Recombinant mouse-IFNβ (8234-MB, R&D Systems) was dissolved at 100ug/ml in sterile PBS containing 0.1% BSA and injected at 50 IU, 500 IU or 5000 IU intra-hippocampally (i.h., 0.5 µl/min, 0.5 µl in total) in freely moving mice over 1 min using a 30-gauge injection needle protruding 2.0 mm from the bottom of the guide cannula connected to a 10 µl Hamilton microsyringe via PE20 tubing, as described above (Section 6.4).

6.6 IMMUNOHISTOCHEMISTRY

6.6.1 Immunohistochemical studies from *in vivo* preparations

Mice were deeply anaesthetised with ketamine (75 mg/kg) and medetomidine (0.5 mg/kg) and perfused via the ascending aorta with 50mM cold PBS, pH 7.4 and then with 4% paraformaldehyde (Merck, Darmstadt, Germany) in PBS. Brains were removed and post-fixed for 90 min at 4°C and then transferred to glucose solution 20% in PBS for 24 h at 4°C. Then brains were frozen by immersion in isopentane at -45°C for 3 min and stored at -80°C until assayed. Using a cryostat serial coronal sections (40 µm) were cut and collected from -0.94 to -2.80 mm from bregma (Franklin and Paxinos, 2008). Two series of 30 sections each

were prepared and three slices per animal were used for GFAP and CD11b staining. Briefly, sections were incudated for 1h at RT with 10% normal goat serum, 1% Triton X-100 in Tris-buffered saline 0.1 m, pH 7.4, then overnight at 4°C with the mouse anti-GFAP (MAB3402, Merck, Germany; 1:3500) to mark astrocytes, or rat anti-CD11b (1:1000, MAC-1, Serotec; MCA719, Clone 5C6) to mark microglia. Visualization of the signal was done with the Vectastain ABC kit (Vector Laboratories), with diaminobenzidine (DAB; or nickel-intensified DAB for IL-1β) as chromogen. Matching slices at comparable levels from control mice and mice injected with Poly I:C were compared in order to evaluate glia activation.

Tissue preparation for TLR3 staining differ, since TLR3 antibody does not react with the specific antigen in PFA-fixed slices. Therefore, mice were perfused for 1 min via the ascending aorta with 50mM cold PBS in order to remove blood from brain capillaries and their brains were carefully removed from the skull and rapidly frozen in −50 °C isopentane for 3 min. Serial coronal sections of 14 µm were cut on a cryostat throughout the septal extension of the hippocampus (−1.22 to −2.54 mm from bregma; Franklin and Paxinos, 2008), collected on lysine-coated slides, fixed in acetone for 10 min and kept at −20 °C until use.

Signal in the hippocampus was captured at 20X using a BX61 microscope equipped with motorized and digitized platform (Virtual Slider Microscope, Olympus, Germany) and one field representing the CA1 area was used for representation.

6.6.2 TLR3

Slides were incubated at room temperature for 10 min with 0.03% H_2O_2. After 3 washes in PBS slides were incubated with 10% fetal bovine serum (FBS) and 4% BSA in PBS. Then, slides were incubated at 4°C overnight in the same solution with rabbit polyclonal anti-TLR3

antibody (1:75, IMGENEX, San Diego, CA, USA; IMG-516). Immunoreactivity was tested by the avidin–biotin–peroxidase technique (Vector Labs, Burlingame, USA) using DAB as chromogen. Sections were dried, dehydrated in graded alcohols, and coverslipped.

Two additional slides from 5 randomly chosen animals were used for double immunostaining to identify the cells expressing TLR3 (Chapter 7). After incubation with the primary antibody against TLR3, slices were incubated for 1 h with anti-rabbit secondary antibody conjugated with Alexa488 (1:500; Molecular Probes, Leiden, The Netherlands) and then overnight with primary antibody against GFAP (1:3500, Chemicon, Temecula, CA, USA; #MAB3402) and fluorescence was detected using secondary antibody conjugated with Alexa546 (1:500, Molecular Probes, Leiden, The Netherlands). Slide-mounted sections were examined with an Olympus Fluoview laser scanning microscope (microscope BX61 and confocal system FV500) using excitations of 488 nm (Ar laser), 546 nm (He-Ne green laser) for fluorescein and Alexa546 respectively.

6.7 RNA ISOLATION AND REAL-TIME QUANTITATIVE POLYMERASE CHAIN REACTION

For RNA isolation, frozen hippocampi dissected from mice perfused via the ascending aorta with 50mM cold PBS for 1 min, were homogenized in Qiazol Lysis Reagent (Qiagen Benelux, Venlo, The Netherlands). The total RNA including the miRNA fraction was isolated using the miRNeasy Mini kit (Qiagen Benelux, Venlo, the Netherlands) according to manufacturer's instructions. The concentration and purity of RNA were determined at 260/280 nm using a high-speed microfluidic UV/VIS spectrophotometer QIAxpert (Qiagen, Milano, Italy) and the integrity and quality of RNA was evaluated by 4200 Tapestation (Agilent Technologies, Santa Clara, CA, USA).

cDNA was synthesized from 1000 ng RNA using the high capacity cDNA reverse transcription kit (Applied Biosystems, California, USA) following the manufacturer's protocol (Applied Biosystems, California, USA). RT-qPCR experiments were run in triplicate for each case to assess technical variability using 384-well reaction plates using an automatic liquid handling station (epMotion 5075LH, Eppendorf, Hamburg, Germany), on an Applied Biosystems 7900HT System (Applied Biosystems, California, USA). cDNA was analyzed using Applied Biosystems TaqMan gene expression assays (IL-1β, NF-kB, HMGB1, TLR3, IRF3, IFNAR1, IFN-β, AHR, CYP1B1 and SOCS2) according to protocol's instructions.

CT values were obtained using manual threshold and baseline, analyzed using the 2-ΔΔCt method and normalized using geometric mean of 3 independent house-keeping genes (hprt1, pdg1, sv2b).

RT-qPCR measurements were performed by Dr. Ilaria Craparotta, Translational Genomic Unit, Department of Oncology, IRCCS - Istituto di Ricerche Farmacologiche Mario Negri, Milan, Italy.

6.8 ELECTROPHYSIOLOGY

6.8.1 Acute hippocampal slices

Mice were killed by cervical dislocation and brains quickly removed and placed in ice-cold modified artificial cerebrospinal fluid (aCSF) containing the following (in mM): 87 NaCl, 2.5 KCl, 1 NaH_2PO4, 75 sucrose, 7 $MgCl_2$, 24 $NaHCO_3$, 11 D-glucose, and 0.5 $CaCl_2$ and bubbled with 95% O_2 and 5% CO_2. Coronal brain slices (350 um thick) were cut with vibrating-blade microtome VT1000s (Leica Microsystems GmbH). Slices were then transferred into an incubating chamber and submerged in aCSF containing (in mM): 130 NaCl, 3.5 KCl, 1.2 NaH_2PO_4, 1.3 $MgCl_2$, 25 $NaHCO_3$, 11 D-glucose, 2 $CaCl_2$ and constantly bubbled with 95% O_2

and 5% CO_2 at room temperature. Slices were incubated in this condition for at least 1 h, then transferred in a submerged recording chamber, perfused with oxygenated aCSF at a rate of 2 ml/min and a constant temperature of 28-30°C. Extracellular recordings of population spikes (PS) were obtained in CA1 pyramidal layer using glass micropipettes filled with 3 M NaCl. Stimulation of Schaffer collaterals was delivered by a Constant Voltage Isolated Stimulator (Digitimer Ltd., Welwyn Garden City, UK) through bipolar twisted Ni/Cr stimulating electrode. PS amplitude was measured as the amplitude of the first negative deflection overriding the field EPSP waveform. The input-output curves were plotted as the relationship of PS amplitude versus stimulus intensity (2V steps). Four consecutive PS were averaged for each stimulus intensity. Data were amplified and filtered (low filter 10 Hz, high filter 3 kHz) by a DAM 80 AC Differential Amplifier (World Precision Instruments, Sarasota, FL, USA), and digitized at 10 kHz by a Digidata 1322 (Molecular Devices, Foster City, CA, USA).

Electrophysiological measurements were performed by Dr. Milica Cerovic, Laboratory of Biology of Neurodegenerative Disorders, Department of Neuroscience, IRCCS - Istituto di Ricerche Farmacologiche Mario Negri, Milan, Italy.

6.8.2 Organotypic hippocampal slices

Male rats at postnatal day 10 (P10) were decapitated, and the brains were quickly removed and placed in ice-cold buffer solution optimised for organotypic slice preparation (slicing solution), which contained the following: 1x GIBCO Hanks' Balanced Salt Solution (HBSS) supplemented with calcium and magnesium (ThermoScientific), 30 mM glucose, and 0.5 mM kynurenic acid; the pH was adjusted to 7.3-7.4, and osmolarity to 310-315 mOsm/L. Under sterile conditions, brains were hemisected and embedded in low melting point

TopVision agarose (ThermoScientific) dissolved in 37ºC pre-warmed slicing solution (2% weight/volume). After the agarose was allowed to solidify in an ice-bath, the brain-containing agarose block was mounted on a slicing stage with superglue, and coronal brain slices perpendicular to the longitudinal axis of the dorsal hippocampus were cut with vibrating-blade microtome VT-1000-S (Leica Microsystems GmbH) at a thickness of 350 µm. Dorsal hippocampal slices were then transferred into a Petri dish containing slicing solution and incubated at 4°C for at least 1 hour. Then, individual slices were placed on 12 mm, PTFE, 0.4 µm Millicell membrane inserts (Millipore, MA, USA) at an interface with culture medium in 24-well culture plates and placed in a 5% CO_2 incubator at 34ºC. Fresh medium was added after 48 hours, and thereafter the medium was replaced every 2-3 days throughout the course of the experiment. The composition of the culture medium was the following: 50% minimum essential medium with 25 mM HEPES, 20% heat inactivated horse serum, 25% HBSS supplemented with calcium and magnesium, 1 mM GlutaMAX, 0.5 mM L-ascorbic acid, 55 mM glucose, 50-100 U/mL Penicillin-Streptomycin; pH 7.3-7.4; 310-315 mOsm/L. All culture medium components were purchased from ThermoScientific. No anti-mitotics were used in these experiments.

Whole-cell patch-clamp electrophysiological recordings were conducted between 7 and 11 days *in vitro* (DIV). To investigate the effects of Poly I:C and IFN-β on synaptic excitability of brain slices, on the day of the recording, 5 µl of Poly I:C (tlrl-pic, Invivogen) or IFN-β (8234-MB, R&D Systems) were added directly to the media at the doses and incubation times indicated in the results section. Following drug incubation, individual slices were transferred into a recording chamber, and continuously perfused with an artificial cerebrospinal fluid (aCSF), at a rate of 2-3 ml/min, constantly bubbled with 95% O_2 and 5% CO_2, and at a constant temperature of 32-34°C. The composition of aCSF was the following

(in mM): 124 NaCl, 3 KCl, 1.3 $MgSO_4$-H_2O, 1.4 NaH_2PO_4, 10 D-glucose, 26 $NaHCO_3$ and 2.5 $CaCl_2$; pH 7.3-7.4; 320–325 mOsm/L. CA1 hippocampal pyramidal cells were visually identified based on cell morphology and the presence of a large apical dendrite with an upright microscope (Olympus) mounted on a differential interference contrast optics and infrared video camera (Hitachi Kokusai Electric). Recording pipettes pulled from borosilicate glass (World Precision Instruments) with a PP-83 two-stage puller (Narishige) to a resistance of 5–7 MΩ were filled with intracellular solution containing (in mM): 130 K-gluconate, 10 HEPES, 5 KCl, 2.5 $MgCl_2$, 1 EGTA, 0.5 $CaCl_2$, 3 Tris-ATP, 0.4 GTP-Li, 5 phosphocreatine and 2.5 QX314-Cl; pH 7.20-7.25; 300-305 mOsm/L. To establish the whole-cell configuration, the membrane of pyramidal cell bodies was ruptured using negative pressure after a tight seal (>1 GΩ) is formed between the recording pipette and the cell membrane. Then, neurons were held at -60 mV for 5 mins in voltage-clamp before experimental recordings. Stimulation of Schaffer collaterals (SC) was achieved by a Constant Voltage Isolated Stimulator (World Precision Instruments) through a tungsten concentric bipolar stimulating electrode (World Precision Instruments) placed ~100 µm from the recording pipette, where 15 µS biphasic pulses were delivered to afferent SC fibers with successive incremental intensities of 25 µA ranging in amplitude from 25 µA to a maximum of 275 µA. Before placing the stimulating electrode, a cut was made at the CA3-CA1 junction to prevent anti-dromical evoked stimulation in the CA3 to propagate through the SC to recorded cells in the CA1. During SC stimulation, cells were held at -60 mV in voltage-clamp in order to eliminate the inhibitory component of evoked responses, mainly $GABA_A$ receptor-mediated currents. Recordings were repeated three times for each stimulus intensity and average values of evoked currents were used to generate input-output graphs when plotted against each stimulus intensity. Data was amplified and low-

pass filtered at 1 kHz using Axopatch 200B amplifier (Molecular Devices), digitized at a sampling rate of 10 kHz with a Digidata 1440A analog-digital converter (Molecular Devices), and signals were acquired using the pCLAMP software 10.4 (Molecular Devices).

Data was analyzed using Clampfit 10.4 (Molecular Devices). Only one neuron per slice per animal was included in the analysis. Current outputs (I) were normalized relative to the maximal current (Imax), where Imax was considered the amplitude of currents evoked in response to the maximal stimulation intensity at 275 µA, and results are shown as a ratio of Imax, i.e. I/Imax. A sigmoidal curve was fitted to the input-output data using Boltzmann equation in order to calculate the stimulation intensity required to evoke half-maximal current amplitude.

Electrophysiological measurements were performed by Dr. Tarek Shaker, Division of Neurology, Department of Pediatrics and Neurosciences, CHU Sainte-Justine, University of Montreal, Montreal, Quebec, Canada.

6.9 STATISTICS

Quantification of each experiment was done blindly and sample size was determined a priori based on previous experience with the respective models and statistical tests were prospectively selected. All efforts were made to reduce the number of animals used to minimum. GraphPad Prism 6 (GraphPad Software, USA) for Windows was used for statistical analysis using absolute values. Data are presented as mean ± S.E.M. (n indicates the number of individual samples). For each variable, differences between the groups were assessed using Mann–Whitney U test for two independent groups and one-way ANOVA followed by Tukey *post-hoc* test or Kruskal-Wallis followed by Dunn's *post-hoc* test or by

two-way ANOVA for repeated measures followed by Bonferroni *post-hoc* test (details are reported in the figure legends). Differences were considered significant with a $p<0.05$.

CHAPTER 7 - EFFECT OF TLR3 PRIMING ON NEURONAL EXCITABILITY AND SEIZURES

7.1 INTRODUCTION

TLR3 is a dsRNA-sensing TLR, known as a regulator of both anti-viral responses and injury repair processes since it also detects host-derived RNA. Different from other TLR family members, TLR3 does not activate MyD88-dependent signalling but signals through the Toll/IL-1 receptor (TIR) domain-containing adaptor TRIF, also known as TIR-containing adaptor molecule 1, (TICAM-1) pathway (Takeda and Akira, 2004). TRIF signalling activates NF-kB and the nuclear translocation of the transcription factor interferon regulatory factor (IRF)-3 that mediate the production of type I interferon (IFN), IFN-inducible products, and other inflammatory mediators (Kawai and Akira, 2010).

TLR3 is primarily expressed intracellularly, in the endosomes, where it acts as a sensor for double-stranded RNA, an intermediate product of replicating viruses. In the CNS, TLR3 is expressed by neurons, microglia and astrocytes (Bsibsi et al., 2002; Carpentier et al., 2005; Farina et al., 2005; Olson and Miller, 2004; Préhaud et al., 2005; Scumpia et al., 2005). In glial cells and in neurons, TLR3 is expressed both in the endosomes and at the cell surface (Bsibsi et al., 2002; Lafon et al., 2008). Adult human astrocytes express TLR3 constitutively and upon TLR3 engagement they regulate immune response following viral infection (Bsibsi et al., 2002; Farina et al., 2005). Stimulation of TLR3 in human astrocytes also induces several neuroprotective and anti-inflammatory molecules implicated in neuroprotection such as brain-derived neurotropic factor, neurotrophin 4, pleiotrophin, TGF-β2 and IL-10 (Bsibsi et al., 2006; Endres et al., 2000; Yeh et al., 1998).

TLR3 stimulation can have a protective or detrimental effect on tissues depending on the type of virus or endogenous activator involved and the cell type mediating the TLR3 response (Verma and Bharti, 2017). In infection models, TLR3 activation may have deleterious effects. For example, TLR3-deficient mice were more resistant to West-Nile

Virus (WNV) encephalitis and Rabies virus infection (Ménager et al., 2009; Wang et al., 2004).

In epilepsy, TLR3 expression was increased in brain tissue of Rasmussen's encephalitis patients and this expression positively correlated with the extent of brain atrophy (Wang et al., 2017). By contrast, other studies showed a protective role of TLR3 stimulation. For instance, TLR3 deficiency leads to enhanced viral replication in the primary cortical neuron cultures and greater WNV burden in CNS neurons (Daffis et al., 2008). Moreover, TLR3 deficiency renders mice susceptible to herpes simplex virus infection (HSV-2) and astrocytes show a defective type I IFN production (Reinert et al., 2012). Interestingly, pretreatment with the TLR3 agonist polyinosinic-polycytidylic acid (Poly I:C), a synthetic double-stranded RNA, protected mice against Chikungunya virus (CHIKV) infection (Priya et al., 2014).

Poly I:C mimics the effect of viral infection and leads to the production of type I IFNs, IFN-α and IFN-β via activation of IRF-3 and IRF-7 (Cunningham et al., 2007; Farina et al., 2005). Furthermore, it induces the transcription and biosynthesis of cytokines and chemokines (Kirschman et al., 2011; Michalovicz and Konat, 2014). In neonatal animals, Poly I:C exerts a pro-inflammatory action associated with increased seizure susceptibility in adulthood suggesting that TLR3 activation during brain development has detrimental effects that increase vulnerability to later insults (Galic et al., 2009). TLR3 activation was shown to modulate hippocampal excitability and alter glutamatergic transmission by IFN-β production (Costello and Lynch, 2013). Another study revealed that TLR3 deficiency reduced spontaneous seizures, microglia activation and proinflammatory cytokine levels indicating a contribution of this pathway to epileptogenesis (Gross et al., 2017). Finally, TLR3 activation was shown to mediate working and contextual memory impairment in

rodents (Galic et al., 2009; Okun et al., 2010). However, neuroprotective effects have been also reported specifically following TLR3 activation in astrocytes due to induction of anti-inflammatory cytokines and neuroprotective factors (Bsibsi et al., 2006; Li et al., 2015b; Pan et al., 2012; Tarassishin et al., 2011b; Zhang et al., 2015b). Therefore, TLR3 may have a dual role possibly mediated by different cell types.

Our main goal was to explore the role of TLR3 activation in acute seizure susceptibility by activating these receptors with Poly I:C. Using a mouse model of acute symptomatic seizures we measured the astrocytic induction of TLR3. Notably, pre-treatment with Poly I:C led to a strong reduction of seizures which was both dose and time dependent. TLR3 specificity was confirmed in TICAM-1 knock-out mice. Finally, hippocampal excitability in brain slices as well as morphological activation of glia and induction of pro-inflammatory genes were measured after Poly I:C injection in mice, and the mechanisms underlying its neuroprotective effects were explored.

7.2 SPECIFIC MATERIALS AND METHODS

Kainic acid model of acute seizures

Mice (n=5-9 mice/group) were implanted with depth electrodes and guide cannula for KA injection and intracerebroventricular administration of different doses of Poly I:C and for the time-course experiments (Figures 7.2, 7.3; Sections 6.3.1 and 6.4 of General materials and methods). TICAM-1 knock-out mice (n=5-6) were implanted as described above and treated with 10 μg Poly I:C 6 h before intrahippocampal KA injection (Figure 7.4). Seizures occurred with an average latency of 10 min from KA injection in all mice and recurred for about 90 min from their onset. Seizure quantification (section 6.3.2 of General materials and methods) was done by measuring the time elapsed from KA injection to the occurrence

of the first EEG seizure (onset) and the number and total duration of seizures (sum of the duration of every ictal episode during the EEG recording period). After the end of the EEG recordings mice were sacrificed and the correct position of the electrodes and injection needle was evaluated by *post-hoc* histological analysis of the brain (see section 6.6 of General materials and methods).

Intracerebroventricular administration of Poly I:C

Mice were implanted with a guide cannula under isoflurane anesthesia (1-3% isoflurane in O_2) above the left ventricle and injected with saline or 10 μg Poly I:C 1 week after recovery from surgery (sections 6.4 of General materials and methods). After 6 h mice (n=16) were sacrificed and hippocampal tissue was prepared for either electrophysiological recordings, immunohistochemistry or RT-qPCR analysis as previously described (Figures 7.5 and 7.8; sections 6.6, 6.7 and 6.8.1 of General materials and methods). Mice (n=16) injected with saline served as controls.

Immunohistochemistry

Mice (n=5) were implanted with depth electrodes and a guide cannula for KA injection and sacrificed 3 h after seizure induction for TLR3 immunohistochemical evaluation (Figure 7.1; sections 6.3.1 and 6.6.2 of General materials and methods). A second group of mice (n=6) was implanted with a guide cannula above the left ventricle for intracerebroventricular administration of 10 μg Poly I:C and sacrificed 6 h later for glia activation assessment by immunohistochemistry (Figure 7.8; sections 6.6.1 of General materials and methods).

RT-qPCR analysis

Five animals injected with Poly I:C were sacrificed 6 h later and their hippocampi were used to measure IL-1β, NFkB1, NFkB2 and HMGB1 mRNA levels as described in section 6.7 of General materials and methods (Figure 7.8). HPRT1, PDG1 and SV2B were used as reference genes to normalize mRNA levels.

Electrophysiology

Mice (n=5/group) were implanted with a guide cannula above the left ventricle and injected with 10 μg Poly I:C or saline and sacrificed 6 h later for *in vitro* electrophysiological recording of acute hippocampal slices as described in section 6.8.1 of General materials and methods (Figure 7.5).

Male rats at postnatal day 10 (n=4-9) were used for preparation of organotypic hippocampal slices. In one group of slices (n=4-7), Poly I:C (tlrl-pic, Invivogen) was added directly to the media at the doses of 1-2 μg, 5-10 μg or 25 μg for 6 h (Figure 7.6). Another group of slices (n=4-7) was used for incubation of 25 μg Poly I:C for 6 h continuously or for 6 h with media replacement overnight or for 24h continuous incubation (Figure 7.7). Whole-cell patch-clamp electrophysiological recordings were performed as described in section 6.8.2 of General materials and methods. Slices (n=9 in total) incubated with sterile water added to the media served as controls (Naïve).

7.3 RESULTS

7.3.1 Effect of TLR3 stimulation on acute seizures

First, we investigated the cell type expressing TLR3 using immunohistochemistry in brain slices of naïve and KA-injected animals (n=5/group). We found that the specific signal was absent in control tissue while the receptor was induced 3 h after seizures onset in GFAP-positive astrocytes (Figure 7.1).

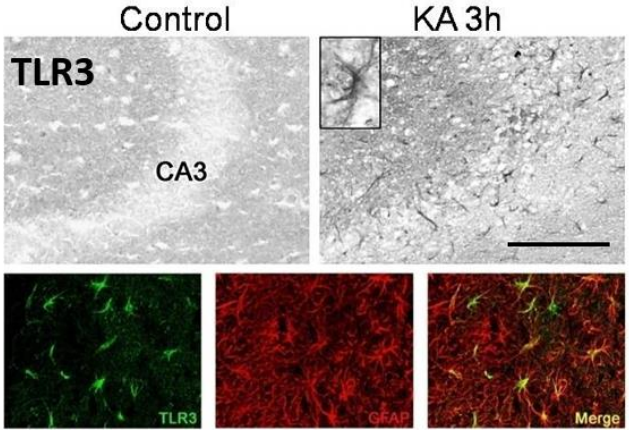

Figure 7.1. TLR3 immunoreactivity in the hippocampus of KA-injected mice. *Representative photomicrographs from control (saline-injected) and 3 h after KA injection (n=5 each group). CA1 pyramidal cell layer is shown. Scale bar: 50 µm.*

Next, mice (n=5-9/group) were injected into the left ventricle with Poly I:C at different doses (0.1, 1, 10 and 33 µg) 6 h before the induction of seizures. This time frame was chosen in order to allow sufficient time for transcriptional gene activation and related protein synthesis. Doses of 10 µg and 33 µg of Poly I:C mediated anti-ictogenic effects since the number ($p<0.05$; $p<0.01$) and the time spent in seizures ($p<0.05$; $p<0.01$) were significantly reduced compared to saline-injected mice (Figure 7.2). Lower doses were ineffective.

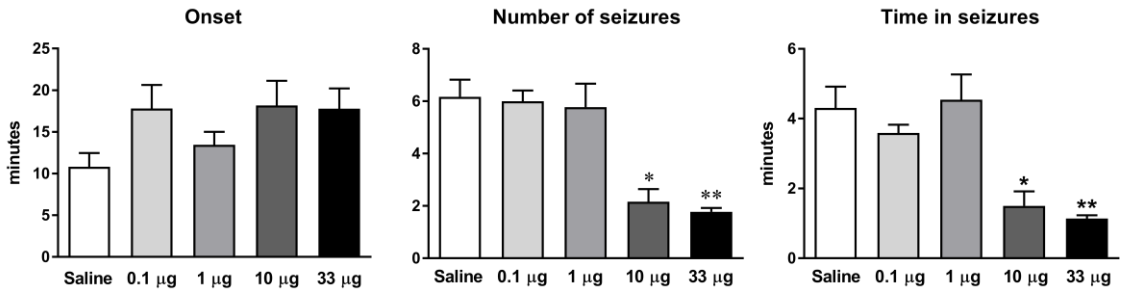

Figure 7.2. Dose-dependent effects of TLR3 stimulation on seizures. *Mice were i.c.v. injected with 0.1, 1, 10 and 33 μg Poly I:C 6 h before the intrahippocampal injection (unilateral to the Poly I:C-injected ventricle) of 7 ng in 0.5 μl KA. Data are the mean ± SEM (n=5-9), *p<0.05, **p<0.01 compared to saline by Kruskal-Wallis followed by Dunn's multiple comparison test.*

In order to study the time course of this anti-ictogenic effect we used 10 μg of Poly I:C, the lower effective dose and we injected KA (n=5-9) at 15 min, 1 h, 6 h and 24 h after Poly I:C administration. Seizures were unaffected by Poly I:C when the TLR3 agonist was administered 15 min, 1 h or 24 h before KA injection (Figure 7.3). However, when Poly I:C was injected 6 h before KA it significantly delayed the onset of seizures ($p<0.05$) and reduced the number of seizures and time spent in seizures ($p<0.01$; Figure 7.3). These data indicate that the anti-ictogenic effect of Poly I:C develops over a specific time window before seizure induction and is transient since it elapses within 24 h.

Figure 7.3. Time-dependent effects of TLR3 stimulation on seizures. *Mice were i.c.v. injected with 10 μg Poly I:C at different time points before seizure induction Data are the mean ± SEM (n=5-9), *p<0.05, **p<0.01 compared to saline by Kruskal-Wallis followed by Dunn's multiple comparison test.*

Cytosolic RNA helicases retinoic acid-inducible protein 1 (RIG-1) and melanoma differentiation-associated gene 5 (MDA-5) are two additional receptors that are activated by Poly I:C. In order to investigate the specific TLR3 involvement in the Poly I:C-mediated effects on seizures, we used knock-out mice (n=5-6) for TICAM-1, the adaptor molecule TRIF essential for TLR3 signalling. These mice were intrinsically less susceptible to KA-induced seizures as shown by the increased latency time to the first seizure ($p<0.05$) and the reduction of both the number ($p<0.05$) and time spent in seizures ($p<0.05$) as compared to wild-type mice. When these mice were injected with 10 µg Poly I:C 6 h before KA, the anti-ictogenic effects observed in wild type mice were precluded (Figure 7.4). Thus, the anti-ictogenic properties of Poly I:C are specifically mediated by TLR3.

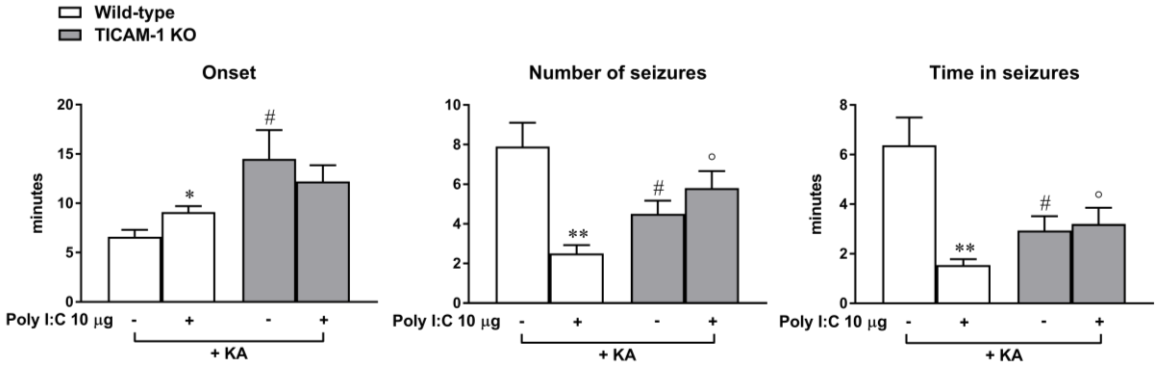

Figure 7.4. Effect of Poly I:C on seizures in TICAM-1 KO mice. *Wild-type (n=10) and TICAM-1 KO (n=5-6) mice were i.c.v. injected with 10 µg Poly I:C (+) or saline (-) 6 h before the intrahippocampal injection of KA. Data are the mean ± SEM, *p<0.05 **p<0.01 compared to respective saline; #p<0.05 and °p<0.01 compared to respective wild-type by Mann-Whitney test.*

7.3.2 Effect of TLR3 stimulation on hippocampal neuronal excitability

We studied the effect of Poly I:C-induced TLR3 stimulation on neuronal excitability in acute hippocampal slices obtained from naïve mice injected 6 h before with either Poly I:C or saline (n=8-15 slices from 5 mice/each group). We performed extracellular recordings of population spikes in CA1 pyramidal cell layer evoked by electrical stimulation of the

Schaffer collateral pathway. The relationship between stimulus intensity and population spike peak amplitude was used to assess neuronal excitability. Neuronal excitability was reduced in slices from Poly I:C-injected mice as shown by a right shift of the input-output curve compared to control slices ($F_{1.500}$= 46.22, p<0.01; Figure 7.5).

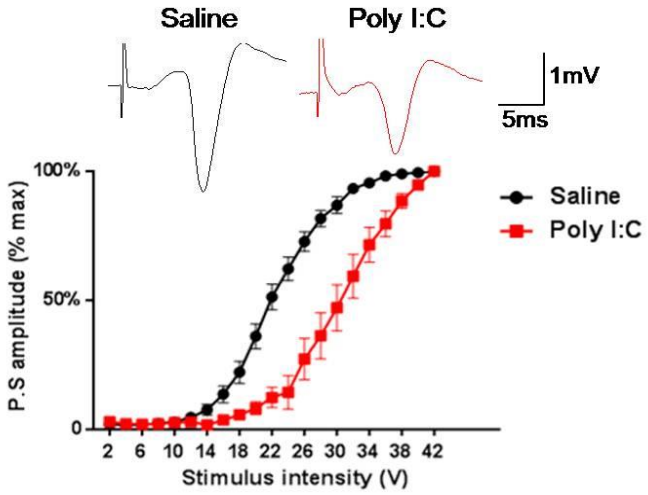

Figure 7.5. Effect of Poly I:C on hippocampal neuronal excitability. *Graph reports population spike (PS) amplitude of CA1 pyramidal neurons in response to increasing stimulation intensities of afferent Schaffer collaterals. Acute hippocampal slices were obtained from naive mice injected i.c.v. with either saline (black) or 10 µg Poly I:C (red), 6 h before in vitro stimulation. Insets are representative traces of PS obtained in response to 30 V stimulation. PS amplitudes are shown as percent of maximal response (mean ± SEM; n=8-15 slices from 5 mice/each group).* $F_{1.500}$*= 46.22, p<0.01 by two-way ANOVA for repeated measures.*

We next evaluated the effects of Poly I:C on excitatory synaptic transmission using whole cell patch recording from organotypic hippocampal slices (n=4-9 slices/group). Evoked excitatory postsynaptic currents (eEPSC) recorded from pyramidal neurons in CA1 region upon stimulation of Schaffer collaterals were reduced after incubation with 25 µg/ml Poly I:C for 6 h as shown by measuring both half-maximal eEPSC amplitude (Naïve: 162 ± 10.5; Poly I:C 25 µg/ml: 204.7 ± 5.3; p<0.01; Figure 7.6A) and maximal eEPSC amplitude (Naïve: -1937 ± 98.3; Poly I:C 25 µg/ml: -973.5 ± 108.5; p<0.01 Figure 7.6B). Lower doses of Poly I:C

were ineffective. These data are in line with the *in vivo* data, since the dose of 25 µg/ml Poly I:C corresponds to the dose of 10 µg Poly I:C used in the *in vivo* experiments.

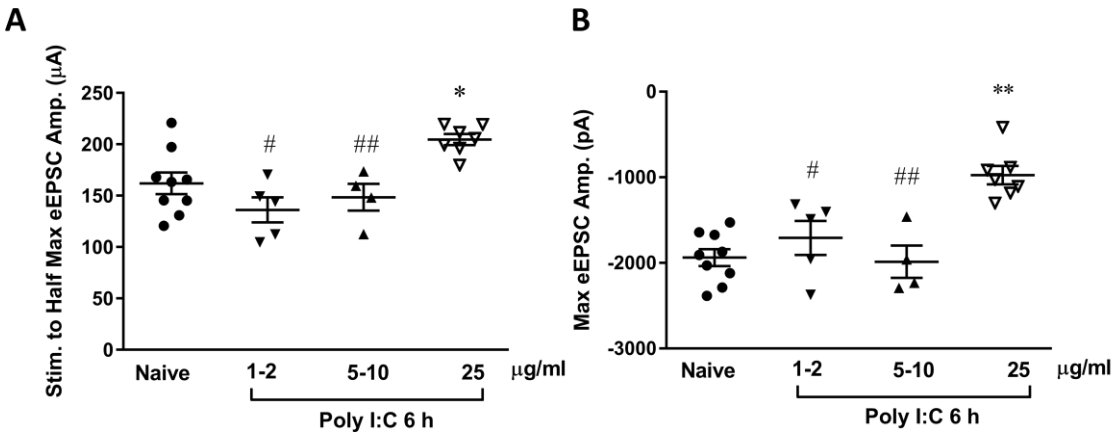

Figure 7.6. Effect of Poly I:C on hippocampal synaptic excitability. *(A) Half-maximal and (B) Maximal eEPSC amplitude recorded from CA1 pyramidal neurons of brain slices incubated with 1-2 µg/ml, 5-10 µg/ml and 25 µg/ml POLY I:C for 6 h. Data are the mean ± SEM (n=4-9), *p<0.05 and **p<0.01 compared to naive; #p<0.05 and ##p<0.01 compared to respective POLY I:C 25 ug/ml by one-way ANOVA followed by Tukey's multiple comparison tests.*

The reduction of excitatory synaptic transmission mediated by continuous incubation for 6 h with 25 µg/ml Poly I:C was partially lost after 24 h of incubation. Only maximal evoked EPSC amplitude remained reduced while the stimulus intensity required to reach half-maximal EPSC in treated and naïve slices was not significantly different (Half-maximal eEPSC amplitude: Naïve: 162 ± 10.5; Poly I:C 24 h: 118 ± 7.7, Maximal eEPSC amplitude: Naïve: -1937 ± 98.3; Poly I:C 24 h: -586.8 ± 80.8; p<0.01; Figure 7.7). Six hours incubation with Poly I:C followed by media replacement overnight gave similar results to 6 h incubation (Half-maximal eEPSC amplitude: Poly I:C 6 h: 204.7 ± 5.3; Poly I:C 6 h + wash: 170.2 ± 14.1, Maximal eEPSC amplitude: Poly I:C 25 µg/ml: -973.5 ± 108.5; Poly I:C 6 h + wash: -961 ± 143.9; Figure 7.7).

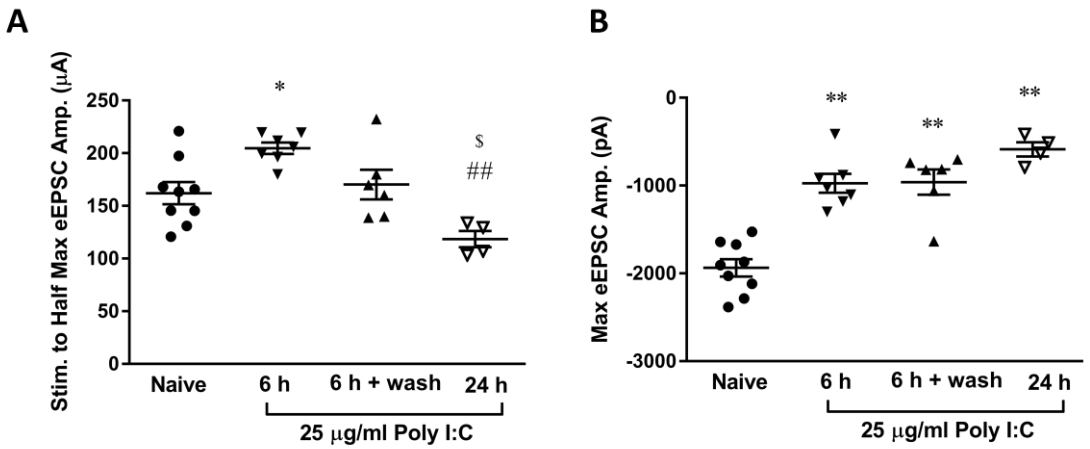

Figure 7.7. Effect of incubation time of Poly I:C on hippocampal synaptic excitability. *(A) Half-maximal and (B) Maximal eEPSC amplitude recorded from CA1 pyramidal neurons of brain slices incubated with 25 μg/ml Poly I:C continuously for 6 h, or for 6 h with media replacement or continuously for 24 h. Data are the mean ± SEM (n=4-9), *p<0.05 and **p<0.01 compared to naive; $^{\#\#}$p<0.01 compare to 6 h group and $^{\$}$p<0.05 compared 6 h+wash group by one-way ANOVA followed by Tukey's multiple comparison tests.*

7.3.3 Effect of TLR3 stimulation on glia activation and their phenotype

Finally, glia activation and induction of pro-inflammatory mediators by Poly I:C were studied by immunohistochemistry and RT-qPCR analysis (n=6 each group), respectively. There was no morphological activation of astrocytes and microglia and IL-1β, NF-kB and HMGB1 mRNA levels were not upregulated in the whole hippocampus by Poly I:C (Figure 7.8).

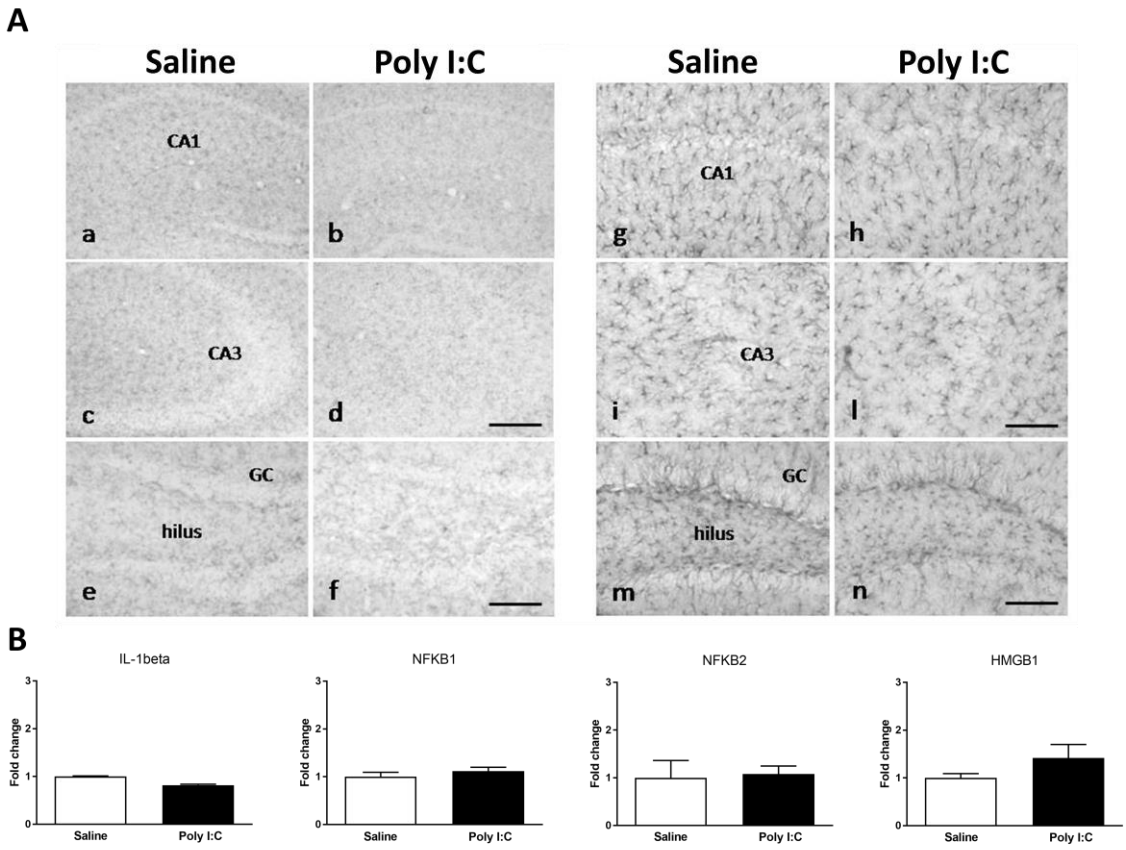

Figure 7.8. Effect of Poly I:C on morphological activation of glia and pro-inflammatory gene transcription. *Mice were i.c.v. injected with saline or 10 µg Poly I:C. After 6 h, hippocampal tissue was prepared for immunohistochemistry or RT-qPCR analysis. (A) Representativephotomicrographs showing CD-11b-immunoreactive microglia (left) and GFAP-immunoreactive astrocytes (right) in saline- (a,c,e,g,l,m) and Poly I:C-injected mice (b,d,f,h,l,n) in CA1 (a,b,g,h), CA3 (c,d,i,l) pyramidal layers and hilus (e,f,m,n).Scale bar: 100 µm (a-d,g-l), 50 µm (e,f,m,n). DG: dentate gyrus. (B) RT-qPCR measurement of IL-1β, NF-kB and HMGB1 mRNA in the hippocampus from saline- and Poly I:C-injected mice. Data are mean ± SEM (n=6 each group).*

7.4 DISCUSSION

The TLR3 pathway has been studied mostly in animal models of viral infections and little is known about its contribution to seizures. The data gathered so far show a dual role of this receptor in the immune system response after a challenge.

We provide novel *in vivo* and *in vitro* evidence of a neuroprotective role of TLR3 possibly mediated by a priming-like effect after Poly I:C activation. Reduced neuronal excitability

and decreased number of seizures were observed when TLR3 stimulation was done hours but not minutes before the ictogenic challenge suggesting that a transcriptional pathway is involved. Moreover, this phenomenon was transient. In our study Poly I:C did not induce pro-inflammatory effects unlike the Poly I:C mediated neuroinflammation and glia activation that contribute to epileptogenesis (Dupuis et al., 2016; Galic et al., 2009; Gross et al., 2017). In accordance with the inhibitory effects on seizures, our *in vivo* paradigm of Poly I:C injection reduced neuronal excitability in hippocampal slices. Our data therefore suggest a novel and protective role of TLR3 stimulation that reduces neuronal excitability. Astrocytes were previously shown to be the cells responsible for the neuroprotective effects of Poly I:C. In fact, activation of the TLR3 axis by Poly I:C in human astrocytes induced expression of anti-inflammatory cytokines and neuroprotective mediators (Bsibsi et al., 2006; Ghaemi et al., 2016; Tarassishin et al., 2011b). Recent studies have reported neuroprotective and anti-inflammatory effects of Poly I:C in cerebral ischemia models through downregulation of pro-inflammatory cytokines and expression of anti-inflammatory cytokines in astrocytes (Li et al., 2015b; Pan et al., 2014; Wang et al., 2014). Poly I:C can promote neuronal survival and reduce cell death by oxygen-glucose deprivation or oxidative stress (Bsibsi et al., 2006; Marsh et al., 2009; Patel and Hackam, 2014).

In our seizure model, TLR3 is induced in astrocytes suggesting that this cell-specific TLR3-mediated pathway may represent a homeostatic attempt to control neuronal hyperexcitability.

CHAPTER 8 - TLR3-MEDIATED MECHANISMS OF NEUROPROTECTION

8.1 INTRODUCTION

IFN-β signalling activation in astrocytes exerts protective effects in experimental autoimmune encephalomyelitis (EAE) animal models mediated by the immunomodulatory transcription factor AHR, its target cytochrome P4501B1 (CYP1B1) and SOCS2 (Rothhammer et al., 2016). In EAE, AHR signalling in astrocytes controls inflammatory pathways involved in the recruitment of monocytes, glia activation and the neurotoxic activities of astrocytes (Rothhammer et al., 2016). IFN-β is used to treat multiple sclerosis (MS) and inflammation in EAE animal models (Khorooshi et al., 2015). Moreover, Poly I:C increases IFN-β expression and has a therapeutic effect in the disease outcome (Khorooshi et al., 2015). In ischemia models, the activation of TLR3 by Poly I:C induces IFN-β and mediates neuroprotective effects. Poly I:C preconditioning reduced cerebral ischemia injury in a TLR3-dependent manner by IFN-β increased expression in astrocytes and inhibition of inflammatory pathways (Gesuete et al., 2012; Kuo et al., 2016; Li et al., 2015b). Furthermore, IFN-β was reported to suppress astrocyte activation and glial scar formation after spinal cord injury (Ito et al., 2009; Nishimura et al., 2013).

Based on this evidence, we have investigated the TLR3-mediated mechanisms of neuroprotection after Poly I:C stimulation in our experimental setting.

8.2 SPECIFIC MATERIALS AND METHODS

Intracerebroventricular administration of Poly I:C

Mice (n=6-12) were implanted with a guide cannula above the left ventricle and injected with saline or 10 μg Poly I:C. After 6 h, hippocampal tissue was prepared for RT-qPCR analysis as previously described (Figure 8.1; sections 6.4 and 6.7 of General materials and methods).

Intrahippocampal administration of drugs

Mice (n=3/group) were implanted with a guide cannula above the left hippocampus and injected with saline or 50, 500, 5000 IU mouse IFN-β 15 min, 1 h, 3h or 6h before intrahippocampal KA (Figure 8.2; sections 6.3.1 and 6.5 of General materials and methods).

Kainic acid model of acute seizures

Mice were implanted with depth electrodes and guide cannula for KA injection and intra-hippocampal administration of mIFN-β as described before (see also sections 6.3.1 and 6.5 of General materials and methods). Groups of 3 mice (n=12-18/group) were used for intra-hippocampal mIFN-β injections at 15 min, 1h, 3h or 6h before KA injection and seizure assessment was done as described before (Figure 8.2; section 6.3.2 of General materials and methods).

RT-qPCR analysis

Five animals injected with Poly I:C were sacrificed 6 h later and their hippocampi were used to measure TLR3, IRF3, IFNB1, IFNAR1, AHR, CYP1B1 and SOCS2 mRNA levels as described in section 6.7 of General materials and methods (Figure 8.1). HPRT1, PDG1 and SV2B were used as reference genes to normalise mRNA levels.

Electrophysiology

Organotypic hippocampal slices were prepared from male rats at postnatal day 10 (n=6-9) as described in section 6.8.2 of General materials and methods. In one group of slices (n=7), Poly I:C was added directly to the media of slices (n=7) at a dose of 25 μg for 6 h (Figure 8.3). Another group of slices (n=6) was incubated with 5 μl of 500 IU IFN-β for 1 h (Figure 8.3). Whole-cell patch-clamp electrophysiological recordings were performed as described in section 6.8.2 of General materials and methods. Slices (n=9) incubated with media and sterile water served as controls (Naïve).

8.3 RESULTS

8.3.1 Effect of TLR3 stimulation on IRF3-mediated pathway activation

Stimulation with Poly I:C (n=6) induced upregulation of TLR3 (2-fold, $p<0.01$), IRF3 (6-fold, $p<0.01$) and IFN-β (2-fold, $p<0.05$) transcripts in the hippocampus 6 h after injection in naive mice (Figure 8.1). To further explore IFN-β downstream pathways, we analyzed the mRNA levels of AHR, and its targets CYP1B1 and SOCS2. AHR mRNA levels did not change but both CYP1B1 and SOCS2 levels were increased 6 h after Poly I:C (CYP1B1: 2-fold. $p<0.01$ and SOCS2: 0.5-fold, $p<0.05$; Figure 8.1). AHR induction might have occurred at earlier time points which may account for the lack of changes in this gene.

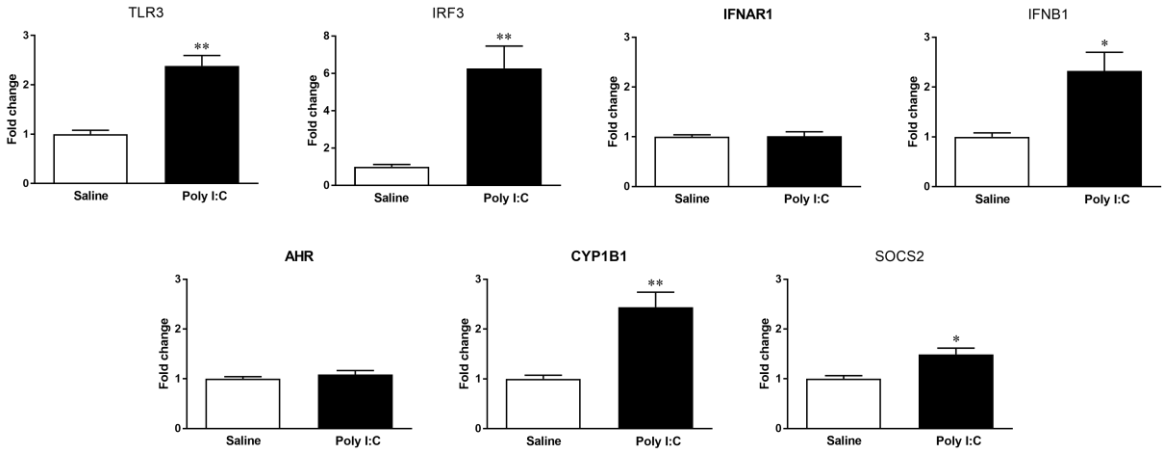

Figure 8.1. Poly I:C promotes the induction of TLR3, IRF3, IFN-β and IFN-β-regulated genes. *Mice were icv injected with saline (n=6) or 10 µg Poly I:C (n=6-12) and hippocampal tissue was collected 6 h later for RT-qPCR analysis. Data are mean ± SEM, *p<0.05 **p<0.01 vs saline by Mann-Whitney test.*

8.3.2 Effect of IFNβ on seizures and synaptic excitability *in vitro*

To test the hypothesis that IFN-β mediated and AHR-dependent cascade may be responsible for the effects of Poly I:C on seizures, we injected various doses of mouse (m)IFN-β into the hippocampus (n=3/group) before inducing seizures in order to mimic the endogenous increase provoked by Poly I:C. We found that the dose of 50 IU mIFN-β given 15 min before kainate increased both the number ($p<0.05$) and time spent in seizures ($p<0.01$; Figure 8.2). The doses of 500 and 5000 IU given either at 15 min, 1 h, 3 h or 6 h before KA had no effect compared to saline treated animals (Figure 8.2). We conclude that intrahippocampal injection of mIFN-β at various doses does not reproduce the TLR3-mediated anti-ictogenic effects of Poly I:C. The lack of evidence for IFN-β involvement may be due to biological barriers encountered by IFN-β when injected *in vivo* which impair the efficient activation of its receptors.

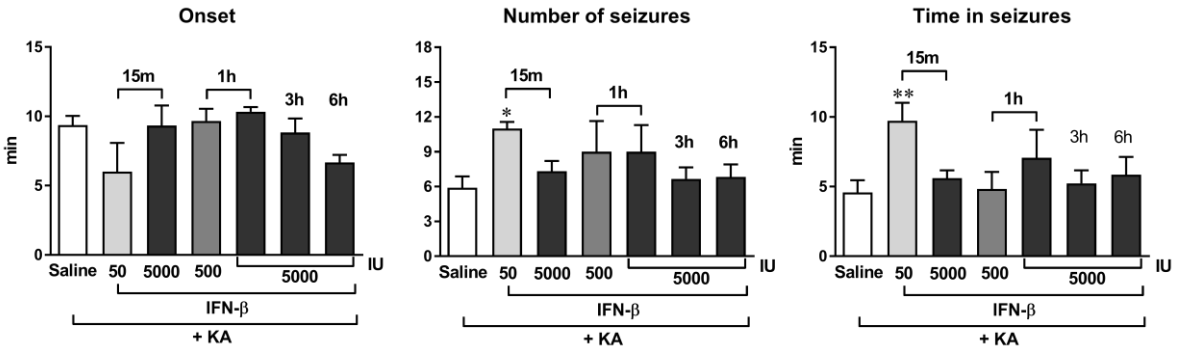

Figure 8.2. Effects of mIFN-β injection on seizures. *Mice were intrahippocampally injected with 50, 500, 5000 IU mouse IFN-β (n=3 each dose) or saline (n=12) 15 min, 1 h, 3h or 6h before intrahippocampal KA. Data are the mean ± SEM, *p<0.05, **p<0.01 compared to saline by by Kruskal-Wallis test multiple comparison tests.*

We tested therefore the effect of IFN-β on synaptic excitability using *in vitro* slices and compared with Poly I:C effects. 500 IU of IFN-β for 1 hour resulted in similar reduction of synaptic excitability as seen with Poly I:C since both half-maximal and maximal eEPSC amplitude values were significantly decreased (Half-maximal eEPSC amplitude: Naive: 162 ± 10.5; Poly I:C 25 μg/ml: 204.7 ± 5.3; 500 IU mIFN-β: 211.6 ± 8.8, $p<0.01$; Maximal eEPSC amplitude: Naive: -1937 ± 98.3; Poly I:C 25 μg/ml: -973.5 ± 108.5; 500 IU mIFN-β: -911.7 ± 82.7, $p<0.01$; Figure 8.3).

These data suggest that IFN-β may mediate the Poly I:C effects on synaptic excitability, hence the anti-ictogenic effects observed *in vivo* after TLR3 stimulation.

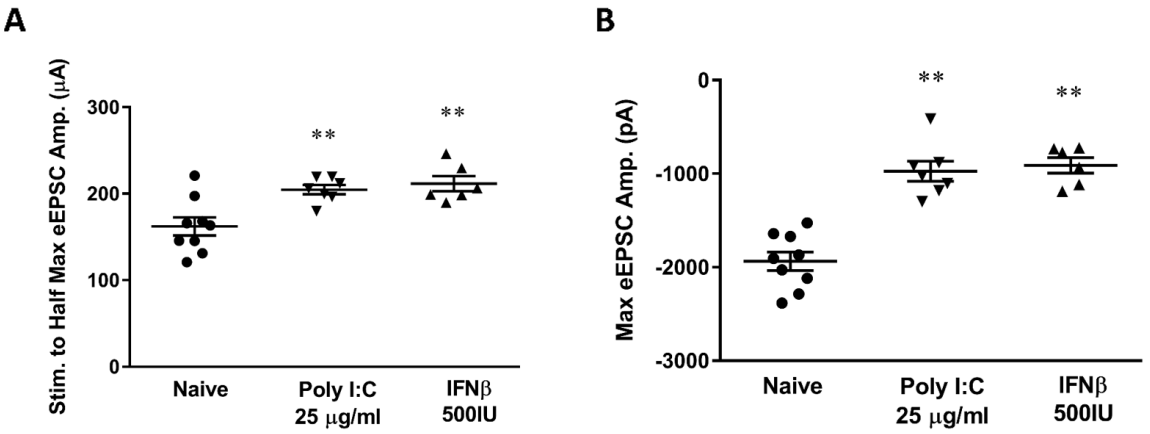

Figure 8.3. Effect of incubation with IFN-β on hippocampal synaptic excitability. *(A) Half-maximal and (B) Maximal eEPSC amplitude recorded from CA1 pyramidal neurons of brain slices incubated with 500 IU IFN-β for 1 h. Data are the mean ± SEM (n=6-9), *p<0.05, **p<0.01 compared to naïve by one-way ANOVA followed by Tukey's multiple comparison tests.*

8.4 DISCUSSION

IFN-β is a first line drug in MS treatment and is effective in the EAE animal model. Poly I:C injection in mice at the initial stages of the disease has therapeutic effects by inducing the expression of type I IFN genes by TLR3 activation (Khorooshi et al., 2015). In our experimental conditions, we found induction of IRF3 and IFN-β genes that may mediate the reduction in neuronal excitability and seizures due to TLR3 stimulation. IRF3 is a key element of the TLR3 pathway and its activation in glia cultures can switch the cytokine expression profile from pro- to anti-inflammatory and mediate neuroprotection (Tarassishin et al., 2011a, 2011c). In particular, IRF3 suppresses the expression of miR-155 and miR155* in astrocytes which are involved in pro-inflammatory gene induction by targeting SOCS1 (Tarassishin et al., 2011a). IFN-β regulates inflammatory responses and provides neuroprotection in models of ischemic stroke (Liu et al., 2002; Marsh et al., 2009; Veldhuis et al., 2003). Our results indicate an activation of IFN-β pathway after Poly I:C challenge. Moreover, we found increased levels of CYP1B1, downstream target of AHR, and

SOCS2 that provide further support to a IRF3/IFN-β-mediated cascade responsible for the inhibitory effects of Poly I:C on seizures and neuronal excitability. In fact, in a model of EAE, IFN-β administered intranasally, resulted in reduced inflammation and improvement of clinical scores that were attributed to astrocytic AHR and SOCS2 signalling (Rothhammer et al., 2016). However, in our study, IFN-β injected directly into the brain failed to reproduce the TLR3-mediated anti-ictogenic effects of Poly I:C. This may be due to the inability of an exogenous application of the cytokine to activate the relevant signalling cascade induced when IFN-β is endogenously increased. Therefore we explored the possibility to reproduce the protective effect of Poly I:C in brain slices by direct incubation with IFN-β and indeed found an inhibitory effect on neuronal excitability similarly to that mediated by Poly I:C. Previous studies associate IFN-β with enhanced synaptic excitability in the hippocampus and other neocortical areas (Beyer et al., 2009; Costello and Lynch, 2013; Hadjilambreva et al., 2005). However, we report a reduction of evoked excitatory postsynaptic currents (eEPSC) within 6 hours indicating an inhibitory effect of IFN-β on neuronal excitability. The apparent discrepancy may be due to differences in the administration route, doses or the need for an additional trigger for enveiling the inhibitory effects.

In conclusion, this study shows a new mechanism of neuroprotection mediated by the TLR3 stimulation and subsequent induction of IFN-β involving astrocytes.

CHAPTER 9 - GENERAL DISCUSSION

Neuroinflammation is a key process for the pathogenesis of seizures as suggested by experimental studies and clinical data. Inflammatory pathways are commonly activated following various epileptogenic insults leading to the overexpression of molecules such as IL-1β, TNF-α and HMGB1 in seizure generating brain areas in both animal models and brain tissue from patients with parmaco-resistant epilepsy. Notably, these molecules possess neuromodulatory functions that contribute to seizure generation and recurrence (Aronica and Crino, 2011; Aronica et al., 2017; Vezzani et al., 2011b, 2011a, 2015).

Glia and in particular astrocytes have been the focus of the research project described in this thesis since these cells are key modulators of brain homeostasis and neuronal function and their dysregulation, which includes an inflammatory phenotype, contributes significantly to experimental epilepsy development. It is crucial, therefore, to develop means to monitor the activation of the inflammatory pathways or the cells generating this response in the brain in order to interfere and possibly revert their detrimental effects in a timely manner. To be able to define the optimal time window for therapeutic interventions at the various stages of the disease may determine the success of disease-modifying or anti-epileptogenic therapies.

One of our attempts was to monitor *in vivo* the activation of IL-1β in astrocytes using an adeno-associated virus. However, manipulation of gene promoter sequences was challenging since it resulted in ectopic gene expression and thus alternative approaches were required. To this end, we developed an *in vivo* imaging tool that allowed to monitor astrocyte activation during the disease and compare the time course of activation with their phenotype in *post-mortem* brain tissue. This comparison is important since astrocyte may have either a pro-inflammatory or an anti-inflammatory phenotype during epileptogenesis which will impact on their pathophysiological effects. Our data show an

activation of their pro-inflammatory phenotype as exemplified by TNF-α and HMGB1 induction. However, we also identified increased PTX3 expression at the later stages of epileptogenesis possibly representing a homeostasic tissue response. These data suggest that pharmacological treatments that inhibit the inflammatory response should be administered promptly after the inciting event and that boosting the anti-inflammatory and neurotrophic phenotype of astrocytes may help to resolve the pro-inflammatory pathways' activation.

Anti-inflammatory drugs clinically available for other indications such as autoinflammatory or autoimmune disorders may offer a facilitated translation to the clinic. Recent studies have provided evidence that FTY720, a drug used for MS therapy, can exert anti-inflammatory and anti-epileptogenic effects in animal models of epilepsy (Gao et al., 2012; Pitsch et al., 2018). Nevertheless, in our study, FTY720 failed to reduce astrocytic activation and proliferation and to alter the expression of both TNF-α and PTX3 during the epileptogenesis phase. Notably, FTY720 further increased the GFAP promoter activity and protein levels during the treatment period. We attribute this effect to additional mechanisms of action of this drug such as HDAC inhibition and activation of other S1P receptors, such as S1P3 and S1P5, that in turn activate astrocytes rather than inhibiting astrogliosis through the S1P1 pathway (Miron et al., 2010). Additionally, FTY720 did not restore the protein levels of GLT-1 and Kir4.1 during epileptogenesis. These data indicate that the anti-epileptogenic effects of previous studies (Gao et al., 2012; Pitsch et al., 2018) are likely mediated by mechanisms of action that do not involve modulation of astrocytic cell phenotype or their activation during the epileptogenesis phase. Our *in vivo* bioluminescence approach can therefore highlight if and how drugs affecting epileptogenesis impact on astrocytes, and could be also exploited for correlating the extent

of astrocytic acivation with the disease outcomes (e.g., seizure frequency, progression of seizures or comorbidities) using models of epileptogenesis where only a cohort of animals develops the disease (Brandt et al., 2003; Dube et al., 2006; Kharatishvili et al., 2006b; Nissinen et al., 2000; Pascente et al., 2016).

The second part of this thesis is focused on the role of astrocytic TLR3 in ictogenesis. Innate immune system activation after pathogen invasion or cell damage is an important mechanism to fight infections or repair tissue by re-establishing homeostasis. TLR3 are amongst the pattern recognition receptors (PRRs) with a fundamental role in igniting innate immune responses to viral infections. There is limited investigation of their role in neuronal excitability. Moreover, the activation of TLR3 in the CNS has been associated with variable outcomes ranging from providing neuroprotection to provoking neuropathology.

Viral infections and specifically viral encephalitis can cause seizures and epilepsy that appear to be dependent on the type of virus and multifactorial mechanisms (Vezzani et al., 2016). Specifically, epilepsy development following viral encephalitis is probably due to neuronal cell loss and persistent neuronal hyperexcitability (Libbey and Fujinami, 2011). Patients with infection-related seizure disorders are often refractory to the available ASDs (Libbey and Fujinami, 2011).

So far, various studies support that TLR3 activation promotes neuronal excitability. In fact, activation of TLR3 receptors in immature brain led to pro-inflammatory cytokine expression that in turn contributes to epileptogenesis and the associated comorbidities in adulthood (Galic et al., 2009; Okun et al., 2010). Moreover, TLR3-deficient adult mice showed a delayed epiletogenesis and less frequent spontaneous seizures than wild-type mice (Gross et al., 2017).

On the other hand, a beneficial outcome of TLR3 stimulation in astrocytes has been suggested both *in vitro* and *in vivo*. TLR3 activation in astrocytes by its synthetic agonist Poly I:C results in the production of neurotrophic factors and type I IFNs that exert neuroprotective effects in animal models of ischemia, and EAE as well as in human organotypic brain slices (Bsibsi et al., 2006; Li et al., 2015b; Pan et al., 2014; Rothhammer et al., 2016; Tarassishin et al., 2011a).

In line with this set of data, we report a reduced neuronal excitability, as shown by reduced seizures evoked in mice by KA, several hours after TLR3 stimulation with Poly I:C. In this seizure model, TLR3 is induced in astrocytes. This reduced neuronal excitability *in vivo* was reinforced by *in vitro* data showing a decrease in hippocampal neuronal excitability in both acute and organotypic brain slices after long lasting application of Poly I:C.

Further evidence attributes this neuroprotective effect of Poly I:C to IRF3 axis activation and IFN-β expression whereas pro-inflammatory pathways involving IL-1β, HMGB1 and NF-kB were not activated in our experimental paradigm. Previous evidence has shown that IFN-β expression in astrocytes mediates neuroprotective effects in CNS disease models (Marsh et al., 2009; Rothhammer et al., 2016; Tarassishin et al., 2011b). We propose therefore that TLR3 priming of astrocytes before a convulsive challenge activates an alternative neuroprotective mechanism which differs from the pathway favoring seizure generation in epilepsy models.

This evidence also underscores that fine tuning of TLR3-activated pathway may be required at the appropriate time of disease development to attain therapeutic effects without interfering with the neuroprotective signalling mediated by astrocytes. Astrocytic TLR3 could therefore represent a target for promoting neuroprotective mediators and anti-inflammatory cytokines. The complexity of the mechanisms involved in epileptogenesis

after viral infections argues for a more careful evaluation of the results obtained in experimental studies since the same TLR may have a dual role depending on the cell type, the timing and persistence of activation in brain tissue.

In conclusion, astrocytes are dynamic cells that react to an epileptogenic insult by rapid and lasting changes in their phenotype which involve both pro- and anti-inflammatory pathways. Dysfunction of astrocytes can contribute to seizure generation and recurrence and targeting this cell population during the critical phase of epileptogenesis may represent a promising avenue for drug development.

BIBLIOGRAPHY

Abbott, N.J., Ronnback, L., and Hansson, E. (2006). Astrocyte-endothelial interactions at the blood-brain barrier. Nat Rev Neurosci *7*, 41–53.

Abbott, N.J., Patabendige, A.A., Dolman, D.E., Yusof, S.R., and Begley, D.J. (2010). Structure and function of the blood-brain barrier. Neurobiol Dis *37*, 13–25.

Abraham, S., and Shaju, M. (2013). Innovations in Epilepsy Management – An Overview. J. Pharm. Pharm. Sci. *16*, 564–576.

Adamik, J., Wang, K.Z.Q., Unlu, S., Su, A.-J.A., Tannahill, G.M., Galson, D.L., O'Neill, L.A., and Auron, P.E. (2013). Distinct Mechanisms for Induction and Tolerance Regulate the Immediate Early Genes Encoding Interleukin 1β and Tumor Necrosis Factor α. PLoS ONE *8*.

Agulhon, C., Petravicz, J., McMullen, A.B., Sweger, E.J., Minton, S.K., Taves, S.R., Casper, K.B., Fiacco, T.A., and McCarthy, K.D. (2008). What Is the Role of Astrocyte Calcium in Neurophysiology? Neuron *59*, 932–946.

Agulhon, C., Sun, M.-Y., Murphy, T., Myers, T., Lauderdale, K., and Fiacco, T.A. (2012). Calcium Signaling and Gliotransmission in Normal vs. Reactive Astrocytes. Front. Pharmacol. *3*.

Airas, L., Dickens, A.M., Elo, P., Marjamaki, P., Johansson, J., Eskola, O., Jones, P.A., Trigg, W., Solin, O., Haaparanta-Solin, M., et al. (2015). In vivo PET imaging demonstrates diminished microglial activation after fingolimod treatment in an animal model of multiple sclerosis. J Nucl Med *56*, 305–310.

Akassoglou, K., Probert, L., Kontogeorgos, G., and Kollias, G. (1997). Astrocyte-specific but not neuron-specific transmembrane TNF triggers inflammation and degeneration in the central nervous system of transgenic mice. J Immunol *158*, 438–445.

Akhtari, M., Bragin, A., Cohen, M., Moats, R., Brenker, F., Lynch, M.D., Vinters, H.V., and Engel Jr, J. (2008). Functionalized magnetonanoparticles for MRI diagnosis and localization in epilepsy. Epilepsia *49*, 1419–1430.

Akin, D., Ravizza, T., Maroso, M., Carcak, N., Eryigit, T., Vanzulli, I., Aker, R.G., Vezzani, A., and Onat, F.Y. (2011). IL-1beta is induced in reactive astrocytes in the somatosensory cortex of rats with genetic absence epilepsy at the onset of spike-and-wave discharges, and contributes to their occurrence. Neurobiol Dis *44*, 259–269.

Akula, K.K., Dhir, A., and Kulkarni, S.K. (2008). Rofecoxib, a selective cyclooxygenase-2 (COX-2) inhibitor increases pentylenetetrazol seizure threshold in mice: possible involvement of adenosinergic mechanism. Epilepsy Res. *78*, 60–70.

Albert, R., Hinterding, K., Brinkmann, V., Guerini, D., Müller-Hartwieg, C., Knecht, H., Simeon, C., Streiff, M., Wagner, T., Welzenbach, K., et al. (2005). Novel immunomodulator FTY720 is phosphorylated in rats and humans to form a single stereoisomer. Identification, chemical proof, and biological characterization of the biologically active species and its enantiomer. J. Med. Chem. *48*, 5373–5377.

Ali, I., Chugh, D., and Ekdahl, C.T. (2015). Role of fractalkine-CX3CR1 pathway in seizure-induced microglial activation, neurodegeneration, and neuroblast production in the adult rat brain. Neurobiol. Dis. *74*, 194–203.

Altar, C.A., and Baudry, M. (1990). Systemic injection of kainic acid: gliosis in olfactory and limbic brain regions quantified with [3H]PK 11195 binding autoradiography. Exp. Neurol. *109*, 333–341.

Amhaoul, H., Staelens, S., and Dedeurwaerdere, S. (2014). Imaging brain inflammation in epilepsy. Neuroscience *279*, 238–252.

Amhaoul, H., Hamaide, J., Bertoglio, D., Reichel, S.N., Verhaeghe, J., Geerts, E., Van Dam, D., De Deyn, P.P., Kumar-Singh, S., Katsifis, A., et al. (2015). Brain inflammation in a chronic epilepsy model: Evolving pattern of the translocator protein during epileptogenesis. Neurobiol. Dis. *82*, 526–539.

Anderson, M.A., Burda, J.E., Ren, Y., Ao, Y., O'Shea, T.M., Kawaguchi, R., Coppola, G., Khakh, B.S., Deming, T.J., and Sofroniew, M.V. (2016). Astrocyte scar formation aids central nervous system axon regeneration. Nature *532*, 195–200.

Andjelkovic, A.V., Kerkovich, D., and Pachter, J.S. (2000). Monocyte:astrocyte interactions regulate MCP-1 expression in both cell types. J. Leukoc. Biol. *68*, 545–552.

Araque, A., Carmignoto, G., Haydon, P.G., Oliet, S.H.R., Robitaille, R., and Volterra, A. (2014). Gliotransmitters travel in time and space. Neuron *81*, 728–739.

Aronica, E., and Crino, P.B. (2011). Inflammation in epilepsy: Clinical observations. Epilepsia *52*, 26–32.

Aronica, E., Gorter, J.A., Rozemuller, A.J., Yankaya, B., and Troost, D. (2005). Activation of metabotropic glutamate receptor 3 enhances interleukin (IL)-1beta-stimulated release of IL-6 in cultured human astrocytes. Neuroscience *130*, 927–933.

Aronica, E., Boer, K., van Vliet, E.A., Redeker, S., Baayen, J.C., Spliet, W.G., van Rijen, P.C., Troost, D., da Silva, F.H., Wadman, W.J., et al. (2007). Complement activation in experimental and human temporal lobe epilepsy. Neurobiol Dis *26*, 497–511.

Aronica, E., Boer, K., Becker, A., Redeker, S., Spliet, W.G., van Rijen, P.C., Wittink, F., Breit, T., Wadman, W.J., Lopes da Silva, F.H., et al. (2008). Gene expression profile analysis of epilepsy-associated gangliogliomas. Neuroscience *151*, 272–292.

Aronica, E., Fluiter, K., Iyer, A., Zurolo, E., Vreijling, J., van Vliet, E.A., Baayen, J.C., and Gorter, J.A. (2010). Expression pattern of miR-146a, an inflammation-associated microRNA, in experimental and human temporal lobe epilepsy. Eur J Neurosci *31*, 1100–1107.

Aronica, E., Ravizza, T., Zurolo, E., and Vezzani, A. (2012). Astrocyte immune responses in epilepsy. Glia *60*, 1258–1268.

Aronica, E., Bauer, S., Bozzi, Y., Caleo, M., Dingledine, R., Gorter, J.A., Henshall, D.C., Kaufer, D., Koh, S., Löscher, W., et al. (2017). Neuroinflammatory targets and treatments for epilepsy validated in experimental models. Epilepsia *58*, 27–38.

Asano, E., Chugani, D.C., Muzik, O., Shen, C., Juhász, C., Janisse, J., Ager, J., Canady, A., Shah, J.R., Shah, A.K., et al. (2000). Multimodality imaging for improved detection of epileptogenic foci in tuberous sclerosis complex. Neurology *54*, 1976–1984.

Asano, H., Aonuma, M., Sanosaka, T., Kohyama, J., Namihira, M., and Nakashima, K. (2009). Astrocyte Differentiation of Neural Precursor Cells is Enhanced by Retinoic Acid Through a Change in Epigenetic Modification. STEM CELLS *27*, 2744–2752.

Avignone, E., Ulmann, L., Levavasseur, F., Rassendren, F., and Audinat, E. (2008). Status epilepticus induces a particular microglial activation state characterized by enhanced purinergic signaling. J. Neurosci. Off. J. Soc. Neurosci. *28*, 9133–9144.

Baik, E.J., Kim, E.J., Lee, S.H., and Moon, C. (1999). Cyclooxygenase-2 selective inhibitors aggravate kainic acid induced seizure and neuronal cell death in the hippocampus. Brain Res *843*, 118–129.

Baldwin, K.T., and Eroglu, C. (2017). Molecular mechanisms of astrocyte-induced synaptogenesis. Curr. Opin. Neurobiol. *45*, 113–120.

Balosso, S., Ravizza, T., Perego, C., Peschon, J., Campbell, I.L., De Simoni, M.G., and Vezzani, A. (2005). Tumor necrosis factor-alpha inhibits seizures in mice via p75 receptors. Ann Neurol *57*, 804–812.

Balosso, S., Maroso, M., Sanchez-Alavez, M., Ravizza, T., Frasca, A., Bartfai, T., and Vezzani, A. (2008). A novel non-transcriptional pathway mediates the proconvulsive effects of interleukin-1beta. Brain *131*, 3256–3265.

Balosso, S., Ravizza, T., Aronica, E., and Vezzani, A. (2013). The dual role of TNF-alpha and its receptors in seizures. Exp Neurol *247C*, 267–271.

Balosso, S., Liu, J., Bianchi, M.E., and Vezzani, A. (2014). Disulfide-containing High Mobility Group Box-1 promotes N-methyl-d-aspartate receptor function and excitotoxicity by activating Toll-like receptor 4-dependent signaling in hippocampal neurons. Antioxid Redox Signal *21*, 1726–1740.

Banati, R.B., Goerres, G.W., Myers, R., Gunn, R.N., Turkheimer, F.E., Kreutzberg, G.W., Brooks, D.J., Jones, T., and Duncan, J.S. (1999). [11C] (R)-PK11195 positron emission tomography imaging of activated microglia in vivo in Rasmussen's encephalitis. Neurology *53*, 2199–2203.

Baranzini, S.E., Laxer, K., Bollen, A., and Oksenberg, J.R. (2002). Gene expression analysis reveals altered brain transcription of glutamate receptors and inflammatory genes in a patient with chronic focal (Rasmussen's) encephalitis. J Neuroimmunol *128*, 9–15.

Bar-Klein, G., Cacheaux, L.P., Kamintsky, L., Prager, O., Weissberg, I., Schoknecht, K., Cheng, P., Kim, S.Y., Wood, L., Heinemann, U., et al. (2014). Losartan prevents acquired epilepsy via TGF-β signaling suppression. Ann. Neurol. *75*, 864–875.

Bar-Klein, G., Klee, R., Brandt, C., Bankstahl, M., Bascuñana, P., Töllner, K., Dalipaj, H., Bankstahl, J.P., Friedman, A., and Löscher, W. (2016). Isoflurane prevents acquired epilepsy in rat models of temporal lobe epilepsy. Ann. Neurol. *80*, 896–908.

Basile, A., Sica, A., d'Aniello, E., Breviario, F., Garrido, G., Castellano, M., Mantovani, A., and Introna, M. (1997). Characterization of the promoter for the human long pentraxin PTX3. Role of NF-kappaB in tumor necrosis factor-alpha and interleukin-1beta regulation. J. Biol. Chem. *272*, 8172–8178.

Bay, M.J., Kossoff, E.H., Lehmann, C.U., Zabel, T.A., and Comi, A.M. (2011). Survey of aspirin use in Sturge-Weber syndrome. J. Child Neurol. *26*, 692–702.

Bazargani, N., and Attwell, D. (2016). Astrocyte calcium signaling: the third wave. Nat. Neurosci. *19*, 182–189.

Beattie, E.C., Stellwagen, D., Morishita, W., Bresnahan, J.C., Ha, B.K., Von Zastrow, M., Beattie, M.S., and Malenka, R.C. (2002). Control of synaptic strength by glial TNFalpha. Science *295*, 2282–2285.

Becker, A.J., Chen, J., Zien, A., Sochivko, D., Normann, S., Schramm, J., Elger, C.E., Wiestler, O.D., and Blumcke, I. (2003). Correlated stage- and subfield-associated hippocampal gene expression patterns in experimental and human temporal lobe epilepsy. Eur J Neurosci *18*, 2792–2802.

Becker, A.J., Pitsch, J., Sochivko, D., Opitz, T., Staniek, M., Chen, C.-C., Campbell, K.P., Schoch, S., Yaari, Y., and Beck, H. (2008). Transcriptional Upregulation of Cav3.2 Mediates Epileptogenesis in the Pilocarpine Model of Epilepsy. J. Neurosci. *28*, 13341–13353.

Bednarczyk, J., and Lukasiuk, K. (2011). Tight junctions in neurological diseases. Acta Neurobiol. Exp. (Warsz.) *71*, 393–408.

Ben-Ari, Y., and Lagowska, J. (1978). [Epileptogenic action of intra-amygdaloid injection of kainic acid]. Comptes Rendus Hebd. Seances Acad. Sci. Ser. Sci. Nat. *287*, 813–816.

Bendotti, C., Guglielmetti, F., Tortarolo, M., Samanin, R., and Hirst, W.D. (2000). Differential Expression of S100β and Glial Fibrillary Acidic Protein in the Hippocampus after Kainic Acid-Induced Lesions and Mossy Fiber Sprouting in Adult Rat. Exp. Neurol. *161*, 317–329.

Benner, E.J., Luciano, D., Jo, R., Abdi, K., Paez-Gonzalez, P., Sheng, H., Warner, D.S., Liu, C., Eroglu, C., and Kuo, C.T. (2013). Protective astrogenesis from the SVZ niche after injury is controlled by Notch modulator Thbs4. Nature *497*, 369–373.

Benson, M.J., Thomas, N.K., Talwar, S., Hodson, M.P., Lynch, J.W., Woodruff, T.M., and Borges, K. (2015). A novel anticonvulsant mechanism via inhibition of complement receptor C5ar1 in murine epilepsy models. Neurobiol Dis *76*, 87–97.

Berg, A.T., Berkovic, S.F., Brodie, M.J., Buchhalter, J., Cross, J.H., van Emde Boas, W., Engel, J., French, J., Glauser, T.A., Mathern, G.W., et al. (2010). Revised terminology and concepts for organization of seizures and epilepsies: report of the ILAE Commission on Classification and Terminology, 2005-2009. Epilepsia *51*, 676–685.

Bernard, C., Anderson, A., Becker, A., Poolos, N.P., Beck, H., and Johnston, D. (2004). Acquired Dendritic Channelopathy in Temporal Lobe Epilepsy. Science *305*, 532–535.

Beyer, S., Raether, G., Stadler, K., Hoffrogge, R., Scharf, C., Rolfs, A., Mix, E., and Strauss, U. (2009). Interferon-beta modulates protein synthesis in the central nervous system. J. Neuroimmunol. *213*, 31–38.

Bezzi, P., Domercq, M., Brambilla, L., Galli, R., Schols, D., De Clercq, E., Vescovi, A., Bagetta, G., Kollias, G., Meldolesi, J., et al. (2001). CXCR4-activated astrocyte glutamate release via TNFalpha: amplification by microglia triggers neurotoxicity. Nat Neurosci *4*, 702–710.

Bialer, M., Johannessen, S.I., Levy, R.H., Perucca, E., Tomson, T., and White, H.S. (2013). Progress report on new antiepileptic drugs: a summary of the Eleventh Eilat Conference (EILAT XI). Epilepsy Res *103*, 2–30.

Bianchi, M.E., and Manfredi, A.A. (2009). Immunology. Dangers in and out. Science *323*, 1683–1684.

Bien, C.G., and Scheffer, I.E. (2011). Autoantibodies and epilepsy. Epilepsia *52 Suppl 3*, 18–22.

Biesmans, S., Acton, P.D., Cotto, C., Langlois, X., Ver Donck, L., Bouwknecht, J.A., Aelvoet, S.-A., Hellings, N., Meert, T.F., and Nuydens, R. (2015). Effect of stress and peripheral immune activation on astrocyte activation in transgenic bioluminescent Gfap-luc mice. Glia *63*, 1126–1137.

Blair, R.D.G. (2012). Temporal Lobe Epilepsy Semiology. Epilepsy Res. Treat. *2012*.

Block, M.L., Zecca, L., and Hong, J.-S. (2007). Microglia-mediated neurotoxicity: uncovering the molecular mechanisms. Nat. Rev. Neurosci. *8*, 57–69.

Blumcke, I. (2009). Neuropathology of focal epilepsies: a critical review. Epilepsy Behav. *15*, 34–39.

Boer, K., Spliet, W.G., van Rijen, P.C., Redeker, S., Troost, D., and Aronica, E. (2006). Evidence of activated microglia in focal cortical dysplasia. J Neuroimmunol *173*, 188–195.

Boer, K., Jansen, F., Nellist, M., Redeker, S., van den Ouweland, A.M., Spliet, W.G., van Nieuwenhuizen, O., Troost, D., Crino, P.B., and Aronica, E. (2008). Inflammatory processes in cortical tubers and subependymal giant cell tumors of tuberous sclerosis complex. Epilepsy Res *78*, 7–21.

Bogdanovic, R.M., Syvanen, S., Michler, C., Russmann, V., Eriksson, J., Windhorst, A.D., Lammertsma, A.A., de Lange, E.C., Voskuyl, R.A., and Potschka, H. (2014). (R)-[11C]PK11195 brain uptake as a biomarker of inflammation and antiepileptic drug resistance: evaluation in a rat epilepsy model. Neuropharmacology *85*, 104–112.

Bolkvadze, T., Nissinen, J., Kharatishvili, I., and Pitkanen, A. (2009). A development of post-traumatic epilepsy in C57BL/6 mice after controlled cortical impact. Soc. Neuotrauma Meet.

Borges, K., Gearing, M., McDermott, D.L., Smith, A.B., Almonte, A.G., Wainer, B.H., and Dingledine, R. (2003). Neuronal and glial pathological changes during epileptogenesis in the mouse pilocarpine model. Exp. Neurol. *182*, 21–34.

Brackhan, M., Bascunana, P., Postema, J.M., Ross, T.L., Bengel, F.M., Bankstahl, M., and Bankstahl, J.P. (2016). Serial quantitative TSPO-targeted PET reveals peak microglial activation up to 2 weeks after an epileptogenic brain insult. J Nucl Med *57*, 1302–1308.

Brackhan, M., Bascuñana, P., Ross, T.L., Bengel, F.M., Bankstahl, J.P., and Bankstahl, M. (2018). [18 F]GE180 positron emission tomographic imaging indicates a potential double-hit insult in the intrahippocampal kainate mouse model of temporal lobe epilepsy. Epilepsia *59*, 617–626.

Brandt, C., Glien, M., Potschka, H., Volk, H., and Löscher, W. (2003). Epileptogenesis and neuropathology after different types of status epilepticus induced by prolonged electrical stimulation of the basolateral amygdala in rats. Epilepsy Res. *55*, 83–103.

Brandt, C., Gastens, A.M., Sun, M.Z., Hausknecht, M., and Löscher, W. (2006). Treatment with valproate after status epilepticus: Effect on neuronal damage, epileptogenesis, and behavioral alterations in rats. Neuropharmacology *51*, 789–804.

Breid, S., Bernis, M.E., Tachu, J.B., Garza, M.C., Wille, H., and Tamgüney, G. (2017). Bioluminescence Imaging of Neuroinflammation in Transgenic Mice After Peripheral Inoculation of Alpha-Synuclein Fibrils. J. Vis. Exp. JoVE.

Brennan, G.P., Baram, T.Z., and Poolos, N.P. (2016). Hyperpolarization-Activated Cyclic Nucleotide-Gated (HCN) Channels in Epilepsy., Hyperpolarization-Activated Cyclic Nucleotide-Gated (HCN) Channels in Epilepsy. Cold Spring Harb. Perspect. Med. Cold Spring Harb. Perspect. Med. *6*, *6*, a022384–a022384.

Brenner, M., Kisseberth, W.C., Su, Y., Besnard, F., and Messing, A. (1994). GFAP promoter directs astrocyte-specific expression in transgenic mice. J. Neurosci. Off. J. Soc. Neurosci. *14*, 1030–1037.

Brewster, A., Bender, R.A., Chen, Y., Dube, C., Eghbal-Ahmadi, M., and Baram, T.Z. (2002). Developmental febrile seizures modulate hippocampal gene expression of hyperpolarization-activated channels in an isoform- and cell-specific manner. J. Neurosci. Off. J. Soc. Neurosci. *22*, 4591–4599.

Brewster, A.L., Lugo, J.N., Patil, V.V., Lee, W.L., Qian, Y., Vanegas, F., and Anderson, A.E. (2013). Rapamycin reverses status epilepticus-induced memory deficits and dendritic damage. PloS One *8*, e57808.

Brinkmann, V. (2007). Sphingosine 1-phosphate receptors in health and disease: Mechanistic insights from gene deletion studies and reverse pharmacology. Pharmacol. Ther. *115*, 84–105.

Brinkmann, V., Davis, M.D., Heise, C.E., Albert, R., Cottens, S., Hof, R., Bruns, C., Prieschl, E., Baumruker, T., Hiestand, P., et al. (2002). The immune modulator FTY720 targets sphingosine 1-phosphate receptors. J. Biol. Chem. *277*, 21453–21457.

Brough, D., Le Feuvre, R.A., Iwakura, Y., and Rothwell, N.J. (2002). Purinergic (P2X7) receptor activation of microglia induces cell death via an interleukin-1-independent mechanism. Mol. Cell. Neurosci. *19*, 272–280.

Brunkhorst, R., Vutukuri, R., and Pfeilschifter, W. (2014). Fingolimod for the treatment of neurological diseases—state of play and future perspectives. Front. Cell. Neurosci. *8*.

Bryan, A.M., and Del Poeta, M. (2018). Sphingosine-1-phosphate receptors and innate immunity. Cell. Microbiol. *20*, e12836.

Bsibsi, M., Ravid, R., Gveric, D., and van Noort, J.M. (2002). Broad Expression of Toll-Like Receptors in the Human Central Nervous System. J. Neuropathol. Exp. Neurol. *61*, 1013–1021.

Bsibsi, M., Persoon-Deen, C., Verwer, R.W.H., Meeuwsen, S., Ravid, R., and Van Noort, J.M. (2006). Toll-like receptor 3 on adult human astrocytes triggers production of neuroprotective mediators. Glia *53*, 688–695.

Buckmaster, P.S. (2012). Mossy Fiber Sprouting in the Dentate Gyrus. In Jasper's Basic Mechanisms of the Epilepsies, J.L. Noebels, M. Avoli, M.A. Rogawski, R.W. Olsen, and A.V. Delgado-Escueta, eds. (Bethesda (MD): National Center for Biotechnology Information (US)), p.

Butler, T., Ichise, M., Teich, A.F., Gerard, E., Osborne, J., French, J., Devinsky, O., Kuzniecky, R., Gilliam, F., Pervez, F., et al. (2011). Imaging Inflammation in a Patient with Epilepsy Due to Focal Cortical Dysplasia. J Neuroimaging *doi: 10.1111/j.1552-6569.2010.00572.x.*

Butler, T., Ichise, M., Teich, A.F., Gerard, E., Osborne, J., French, J., Devinsky, O., Kuzniecky, R., Gilliam, F., Pervez, F., et al. (2013). Imaging Inflammation in a Patient with Epilepsy Due to Focal Cortical Dysplasia. J. Neuroimaging *23*, 129–131.

Butler, T., Li, Y., Tsui, W., Friedman, D., Maoz, A., Wang, X., Harvey, P., Tanzi, E., Morim, S., Kang, Y., et al. (2016). Transient and chronic seizure-induced inflammation in human focal epilepsy. Epilepsia *57*, e191-194.

Cacheaux, L.P., Ivens, S., David, Y., Lakhter, A.J., Bar-Klein, G., Shapira, M., Heinemann, U., Friedman, A., and Kaufer, D. (2009). Transcriptome profiling reveals TGF-beta signaling involvement in epileptogenesis. J Neurosci *29*, 8927–8935.

Cardona, A.E., Pioro, E.P., Sasse, M.E., Kostenko, V., Cardona, S.M., Dijkstra, I.M., Huang, D., Kidd, G., Dombrowski, S., Dutta, R., et al. (2006). Control of microglial neurotoxicity by the fractalkine receptor. Nat. Neurosci. *9*, 917–924.

Carpentier, P.A., Begolka, W.S., Olson, J.K., Elhofy, A., Karpus, W.J., and Miller, S.D. (2005). Differential activation of astrocytes by innate and adaptive immune stimuli. Glia *49*, 360–374.

Carrier, E.J., Kearn, C.S., Barkmeier, A.J., Breese, N.M., Yang, W., Nithipatikom, K., Pfister, S.L., Campbell, W.B., and Hillard, C.J. (2004). Cultured rat microglial cells synthesize the endocannabinoid 2-arachidonylglycerol, which increases proliferation via a CB2 receptor-dependent mechanism. Mol. Pharmacol. *65*, 999–1007.

Carter, S.F., Schöll, M., Almkvist, O., Wall, A., Engler, H., Långström, B., and Nordberg, A. (2012). Evidence for Astrocytosis in Prodromal Alzheimer Disease Provided by 11C-Deuterium-L-Deprenyl: A Multitracer PET Paradigm Combining 11C-Pittsburgh Compound B and 18F-FDG. J. Nucl. Med. *53*, 37–46.

Casamenti, F., Prosperi, C., Scali, C., Giovannelli, L., Colivicchi, M.A., Faussone-Pellegrini, M.S., and Pepeu, G. (1999). Interleukin-1beta activates forebrain glial cells and increases nitric oxide production and cortical glutamate and GABA release in vivo: implications for Alzheimer's disease. Neuroscience *91*, 831–842.

Casellas, P., Galiegue, S., and Basile, A.S. (2002). Peripheral benzodiazepine receptors and mitochondrial function. Neurochem. Int. *40*, 475–486.

Cerri, C., Genovesi, S., Allegra, M., Pistillo, F., Puntener, U., Guglielmotti, A., Perry, V.H., Bozzi, Y., and VCaleo, M. (2016). The Chemokine CCL2 mediates the seizure-enhancing effects of systemic inflammation. J Neurosci *36*, 3777–3788.

Ceyzériat, K., Abjean, L., Carrillo-de Sauvage, M.-A., Ben Haim, L., and Escartin, C. (2016). The complex STATes of astrocyte reactivity: How are they controlled by the JAK-STAT3 pathway? Neuroscience *330*, 205–218.

Chen, K., Aradi, I., Thon, N., Eghbal-Ahmadi, M., Baram, T.Z., and SoltesZ, I. (2001). Persistently modified h-channels after complex febrile seizures convert the seizure-induced enhancement of inhibition to hyperexcitability. Nat. Med. *7*, 331–337.

Chen, M.-K., Baidoo, K., Verina, T., and Guilarte, T.R. (2004). Peripheral benzodiazepine receptor imaging in CNS demyelination: functional implications of anatomical and cellular localization. Brain *127*, 1379–1392.

Cheng, P.-Y., Lin, Y.-P., Chen, Y.-L., Lee, Y.-C., Tai, C.-C., Wang, Y.-T., Chen, Y.-J., Kao, C.-F., and Yu, J. (2011). Interplay between SIN3A and STAT3 mediates chromatin conformational changes and GFAP expression during cellular differentiation. PloS One *6*, e22018.

Chiu, F.C., and Goldman, J.E. (1984). Synthesis and turnover of cytoskeletal proteins in cultured astrocytes. J. Neurochem. *42*, 166–174.

Cho, K.-O., Lybrand, Z.R., Ito, N., Brulet, R., Tafacory, F., Zhang, L., Good, L., Ure, K., Kernie, S.G., Birnbaum, S.G., et al. (2015). Aberrant hippocampal neurogenesis contributes to epilepsy and associated cognitive decline. Nat. Commun. *6*.

Cho, W., Hagemann, T.L., Johnson, D.A., Johnson, J.A., and Messing, A. (2009). Dual transgenic reporter mice as a tool for monitoring expression of glial fibrillary acidic protein. J. Neurochem. *110*, 343–351.

Choi, J.W., Gardell, S.E., Herr, D.R., Rivera, R., Lee, C.-W., Noguchi, K., Teo, S.T., Yung, Y.C., Lu, M., Kennedy, G., et al. (2011). FTY720 (fingolimod) efficacy in an animal model of multiple sclerosis requires astrocyte sphingosine 1-phosphate receptor 1 (S1P1) modulation. Proc. Natl. Acad. Sci. U. S. A. *108*, 751–756.

Choi, V.W., McCarty, D.M., and Samulski, R.J. (2005). AAV hybrid serotypes: improved vectors for gene delivery. Curr. Gene Ther. *5*, 299–310.

Choy, M., Dubé, C.M., Patterson, K., Barnes, S.R., Maras, P., Blood, A.B., Hasso, A.N., Obenaus, A., and Baram, T.Z. (2014). A novel, noninvasive, predictive epilepsy biomarker with clinical potential. J. Neurosci. Off. J. Soc. Neurosci. *34*, 8672–8684.

Chugani, D.C., and Muzik, O. (2000). α[C-11]Methyl-l-Tryptophan PET Maps Brain Serotonin Synthesis and Kynurenine Pathway Metabolism. J. Cereb. Blood Flow Metab. *20*, 2–9.

Chugani, H.T., and Chugani, D.C. (2005). Imaging of Serotonin Mechanisms in Epilepsy. Epilepsy Curr. *5*, 201–206.

Chugani, D.C., Chugani, H.T., Muzik, O., Shah, J.R., Shah, A.K., Canady, A., Mangner, T.J., and Chakraborty, P.K. (1998). Imaging epileptogenic tubers in children with tuberous sclerosis complex using alpha-[11C]methyl-L-tryptophan positron emission tomography. Ann. Neurol. *44*, 858–866.

Chugani, H.T., Luat, A.F., Kumar, A., Govindan, R., Pawlik, K., and Asano, E. (2013). α-[11C]-Methyl-l-tryptophan–PET in 191 patients with tuberous sclerosis complex. Neurology *81*, 674–680.

Clausen, F., Hanell, A., Bjork, M., Hillered, L., Mir, A.K., Gram, H., and Marklund, N. (2009). Neutralization of interleukin-1beta modifies the inflammatory response and improves histological and cognitive outcome following traumatic brain injury in mice. Eur J Neurosci *30*, 385–396.

Claycomb, R.J., Hewett, S.J., and Hewett, J.A. (2011). Prophylactic, prandial rofecoxib treatment lacks efficacy against acute PTZ-induced seizure generation and kindling acquisition. Epilepsia *52*, 273–283.

Contag, C.H. (2007). In Vivo Pathology: Seeing with Molecular Specificity and Cellular Resolution in the Living Body. Annu. Rev. Pathol. Mech. Dis. *2*, 277–305.

Correale, J., and Villa, A. (2009). Cellular elements of the blood-brain barrier. Neurochem. Res. *34*, 2067–2077.

Cosenza-Nashat, M., Zhao, M.L., Suh, H.S., Morgan, J., Natividad, R., Morgello, S., and Lee, S.C. (2009). Expression of the translocator protein of 18 kDa by microglia, macrophages and astrocytes based on immunohistochemical localization in abnormal human brain. Neuropathol Appl Neurobiol *35*, 306–328.

Costello, D.A., and Lynch, M.A. (2013). Toll-like receptor 3 activation modulates hippocampal network excitability, via glial production of interferon-β. Hippocampus *23*, 696–707.

Crespel, A., Coubes, P., Rousset, M.C., Brana, C., Rougier, A., Rondouin, G., Bockaert, J., Baldy-Moulinier, M., and Lerner-Natoli, M. (2002). Inflammatory reactions in human medial temporal lobe epilepsy with hippocampal sclerosis. Brain Res *952*, 159–169.

Cucchiarini, M., Henrionnet, C., Mainard, D., Pinzano, A., and Madry, H. (2015). New trends in articular cartilage repair. J. Exp. Orthop. *2*.

Cunningham, C., Campion, S., Teeling, J., Felton, L., and Perry, V.H. (2007). The sickness behaviour and CNS inflammatory mediator profile induced by systemic challenge of mice with synthetic double-stranded RNA (poly I:C). Brain. Behav. Immun. *21*, 490–502.

Daffis, S., Samuel, M.A., Suthar, M.S., Keller, B.C., Gale, M., and Diamond, M.S. (2008). Interferon regulatory factor IRF-7 induces the antiviral alpha interferon response and protects against lethal West Nile virus infection. J. Virol. *82*, 8465–8475.

Dallasta, L.M., Pisarov, L.A., Esplen, J.E., Werley, J.V., Moses, A.V., Nelson, J.A., and Achim, C.L. (1999). Blood-brain barrier tight junction disruption in human immunodeficiency virus-1 encephalitis. Am. J. Pathol. *155*, 1915–1927.

D'Ambrosio, R., Fairbanks, J.P., Fender, J.S., Born, D.E., Doyle, D.L., and Miller, J.W. (2004). Post-traumatic epilepsy following fluid percussion injury in the rat. Brain J. Neurol. *127*, 304–314.

Danbolt, N.C. (2001). Glutamate uptake. Prog. Neurobiol. *65*, 1–105.

De Simoni, M.G., Perego, C., Ravizza, T., Moneta, D., Conti, M., Marchesi, F., De Luigi, A., Garattini, S., and Vezzani, A. (2000). Inflammatory cytokines and related genes are induced in the rat hippocampus by limbic status epilepticus. Eur J Neurosci *12*, 2623–2633.

DeArmond, S.J., Lee, Y.L., Kretzschmar, H.A., and Eng, L.F. (1986). Turnover of glial filaments in mouse spinal cord. J. Neurochem. *47*, 1749–1753.

Dębski, K.J., Pitkanen, A., Puhakka, N., Bot, A.M., Khurana, I., Harikrishnan, K.N., Ziemann, M., Kaspi, A., El-Osta, A., Lukasiuk, K., et al. (2016). Etiology matters - Genomic DNA Methylation Patterns in Three Rat Models of Acquired Epilepsy. Sci. Rep. *6*, 25668.

Dedeurwaerdere, S., Callaghan, P.D., Pham, T., Rahardjo, G.L., Amhaoul, H., Berghofer, P., Quinlivan, M., Mattner, F., Loc'h, C., Katsifis, A., et al. (2012). PET imaging of brain inflammation during early epileptogenesis in a rat model of temporal lobe epilepsy. EJNMMI Res *2*, 60.

DeSena, A.D., Do, T., and Schulert, G.S. (2018). Systemic autoinflammation with intractable epilepsy managed with interleukin-1 blockade. J. Neuroinflammation *15*, 38.

Desjardins, P., Sauvageau, A., Bouthillier, A., Navarro, D., Hazell, A.S., Rose, C., and Butterworth, R.F. (2003). Induction of astrocytic cyclooxygenase-2 in epileptic patients with hippocampal sclerosis. Neurochem Int *42*, 299–303.

Devinsky, O., Vezzani, A., Najjar, S., De Lanerolle, N.C., and Rogawski, M.A. (2013). Glia and epilepsy: excitability and inflammation. Trends Neurosci. *36*, 174–184.

Devinsky, O., Marsh, E., Friedman, D., Thiele, E., Laux, L., Sullivan, J., Miller, I., Flamini, R., Wilfong, A., Filloux, F., et al. (2016). Cannabidiol in patients with treatment-resistant epilepsy: an open-label interventional trial. Lancet Neurol. *15*, 270–278.

Devinsky, O., Vezzani, A., O'Brien, T.J., Jette, N., Scheffer, I.E., de Curtis, M., and Perucca, P. (2018). Epilepsy. Nat. Rev. Dis. Primer *4*, 18024.

Dhir, A., Naidu, P.S., and Kulkarni, S.K. (2006). Effect of cyclooxygenase inhibitors on pentylenetetrazol (PTZ)-induced convulsions: Possible mechanism of action. Prog. Neuropsychopharmacol. Biol. Psychiatry *30*, 1478–1485.

Dhir, A., Naidu, P.S., and Kulkarni, S.K. (2007). Neuroprotective effect of nimesulide, a preferential COX-2 inhibitor, against pentylenetetrazol (PTZ)-induced chemical kindling and associated biochemical parameters in mice. Seizure *16*, 691–697.

Dhote, F., Peinnequin, A., Carpentier, P., Baille, V., Delacour, C., Foquin, A., Lallement, G., and Dorandeu, F. (2007). Prolonged inflammatory gene response following soman-induced seizures in mice. Toxicology *238*, 166–176.

Dickens, A.M., Vainio, S., Marjamäki, P., Johansson, J., Lehtiniemi, P., Rokka, J., Rinne, J., Solin, O., Haaparanta-Solin, M., Jones, P.A., et al. (2014). Detection of Microglial Activation in an Acute Model of Neuroinflammation Using PET and Radiotracers 11C-(R)-PK11195 and 18F-GE-180. J. Nucl. Med. *55*, 466–472.

DiMario, F.J. (2004). Brain abnormalities in tuberous sclerosis complex. J. Child Neurol. *19*, 650–657.

Dinarello, C.A. (2004). Infection, fever, and exogenous and endogenous pyrogens: some concepts have changed. J Endotoxin Res *10*, 201–222.

Dingledine, R., Coulter, D.A., Fritsch, B., Gorter, J.A., Lelutiu, N., McNamara, J., Nadler, J.V., Pitkänen, A., Rogawski, M.A., Skene, P., et al. (2017). Transcriptional profile of hippocampal dentate granule cells in four rat epilepsy models. Sci. Data *4*.

Diviney, M., Reynolds, J.P., and Henshall, D.C. (2015). Comparison of short-term effects of midazolam and lorazepam in the intra-amygdala kainic acid model of status epilepticus in mice. Epilepsy Behav *51*, 191–198.

Doelken, M.T., Stefan, H., Pauli, E., Stadlbauer, A., Struffert, T., Engelhorn, T., Richter, G., Ganslandt, O., Doerfler, A., and Hammen, T. (2008). (1)H-MRS profile in MRI positive- versus MRI negative patients with temporal lobe epilepsy. Seizure *17*, 490–497.

Donato, R. (2001). S100: a multigenic family of calcium-modulated proteins of the EF-hand type with intracellular and extracellular functional roles. Int. J. Biochem. Cell Biol. *33*, 637–668.

Dong, J.Y., Fan, P.D., and Frizzell, R.A. (1996). Quantitative analysis of the packaging capacity of recombinant adeno-associated virus. Hum. Gene Ther. *7*, 2101–2112.

Dringen, R., Pfeiffer, B., and Hamprecht, B. (1999). Synthesis of the antioxidant glutathione in neurons: supply by astrocytes of CysGly as precursor for neuronal glutathione. J Neurosci *19*, 562–569.

Dube, C., Richichi, C., Bender, R.A., Chung, G., Litt, B., and Baram, T.Z. (2006). Temporal lobe epilepsy after experimental prolonged febrile seizures: prospective analysis. Brain *129*, 911–922.

Dudek, F.E., and Staley, K.J. (2012). The Time Course and Circuit Mechanisms of Acquired Epileptogenesis. In Jasper's Basic Mechanisms of the Epilepsies, J. Noebels, M. Avoli, M. Rogawski, R. Olsen, and A. Delgado-Escueta, eds. (Oxford University Press), pp. 405–415.

Duffy, B.A., Choy, M., Riegler, J., Wells, J.A., Anthony, D.C., Scott, R.C., and Lythgoe, M.F. (2012). Imaging seizure-induced inflammation using an antibody targeted iron oxide contrast agent. Neuroimage *60*, 1149–1155.

Dupuis, N., and Auvin, S. (2015). Inflammation and Epilepsy in the Developing Brain: Clinical and Experimental Evidence. CNS Neurosci. Ther. *21*, 141–151.

Dupuis, N., Mazarati, A., Desnous, B., Chhor, V., Fleiss, B., Le Charpentier, T., Lebon, S., Csaba, Z., Gressens, P., Dournaud, P., et al. (2016). Pro-epileptogenic effects of viral-like inflammation in both mature and immature brains. J. Neuroinflammation *13*.

Ebenezer, D.L., Fu, P., and Natarajan, V. (2016). Targeting Sphingosine-1-Phosphate Signaling in Lung Diseases. Pharmacol. Ther. *168*, 143–157.

Ebenezer, D.L., Fu, P., Suryadevara, V., Zhao, Y., and Natarajan, V. (2017). Epigenetic regulation of pro-inflammatory cytokine secretion by sphingosine 1-phosphate (S1P) in acute lung injury: Role of S1P Lyase. Adv. Biol. Regul. *63*, 156–166.

Eddleston, M., and Mucke, L. (1993). Molecular profile of reactive astrocytes-Implications for their role in neurologic disease. Neuroscience *54*, 15–36.

Ekblom, J., Jossan, S.S., Bergström, M., Oreland, L., Walum, E., and Aquilonius, S.-M. (1993). Monoamine oxidase-B in astrocytes. Glia *8*, 122–132.

Ekblom, J., Jossan, S.S., Oreland, L., Walum, E., and Aquilonius, S.-M. (1994). Reactive gliosis and monoamine oxidase B. In Amine Oxidases: Function and Dysfunction, K.F. Tipton, M.B.H. Youdim, C.J. Barwell, B.A. Callingham, and G.A. Lyles, eds. (Springer Vienna), pp. 253–258.

Endres, M., Fan, G., Hirt, L., Fujii, M., Matsushita, K., Liu, X., Jaenisch, R., and Moskowitz, M.A. (2000). Ischemic brain damage in mice after selectively modifying BDNF or NT4 gene expression. J. Cereb. Blood Flow Metab. Off. J. Int. Soc. Cereb. Blood Flow Metab. *20*, 139–144.

Eng, L.F., Ghirnikar, R.S., and Lee, Y.L. (2000). Glial fibrillary acidic protein: GFAP-thirty-one years (1969-2000). Neurochem. Res. *25*, 1439–1451.

Engel, J., Pitkänen, A., Loeb, J.A., Dudek, F.E., Bertram, E.H., Cole, A.J., Moshé, S.L., Wiebe, S., Fureman, B.E., Jensen, F.E., et al. (2013). EPILEPSY BIOMARKERS. Epilepsia *54*, 61–69.

Engel, T., Gomez-Villafuertes, R., Tanaka, K., Mesuret, G., Sanz-Rodriguez, A., Garcia-Huerta, P., Miras-Portugal, M.T., Henshall, D.C., and Diaz-Hernandez, M. (2012). Seizure suppression and neuroprotection by targeting the purinergic P2X7 receptor during status epilepticus in mice. FASEB J. Off. Publ. Fed. Am. Soc. Exp. Biol. *26*, 1616–1628.

Eugenin, E.A., Clements, J.E., Zink, M.C., and Berman, J.W. (2011). Human immunodeficiency virus infection of human astrocytes disrupts blood-brain barrier integrity by a gap junction-dependent mechanism. J. Neurosci. Off. J. Soc. Neurosci. *31*, 9456–9465.

Eyo, U.B., Peng, J., Murugan, M., Mo, M., Lalani, A., Xie, P., Xu, P., Margolis, D.J., and Wu, L.-J. (2016). Regulation of Physical Microglia-Neuron Interactions by Fractalkine Signaling after Status Epilepticus. ENeuro *3*.

Fabene, P.F., Mora, G.N., Martinello, M., Rossi, B., Merigo, F., Ottoboni, L., Bach, S., Angiari, S., Benati, D., Chakir, A., et al. (2008). A role for leukocyte-endothelial adhesion mechanisms in epilepsy. Nat. Med. *14*, 1377–1383.

Fabene, P.F., Bramanti, P., and Constantin, G. (2010). The emerging role for chemokines in epilepsy. J Neuroimmunol.

Farina, C., Krumbholz, M., Giese, T., Hartmann, G., Aloisi, F., and Meinl, E. (2005). Preferential expression and function of Toll-like receptor 3 in human astrocytes. J. Neuroimmunol. *159*, 12–19.

Farina, C., Aloisi, F., and Meinl, E. (2007). Astrocytes are active players in cerebral innate immunity. Trends Immunol. *28*, 138–145.

Fassler, M., Weissberg, I., Levy, N., Diaz-Griffero, F., Monsonego, A., Friedman, A., and Taube, R. (2013). Preferential lentiviral targeting of astrocytes in the central nervous system. PloS One *8*, e76092.

Faulkner, J.R., Herrmann, J.E., Woo, M.J., Tansey, K.E., Doan, N.B., and Sofroniew, M.V. (2004). Reactive astrocytes protect tissue and preserve function after spinal cord injury. J. Neurosci. Off. J. Soc. Neurosci. *24*, 2143–2155.

Fellin, T. (2009). Communication between neurons and astrocytes: relevance to the modulation of synaptic and network activity. J. Neurochem. *108*, 533–544.

Filibian, M., Frasca, A., Maggioni, D., Micotti, E., Vezzani, A., and Ravizza, T. (2012). In vivo imaging of glia activation using 1H-magnetic resonance spectroscopy to detect putative biomarkers of tissue epileptogenicity. Epilepsia *53*, 1907–1916.

Fischborn, S.V., Soerensen, J., and Potschka, H. (2010). Targeting the prostaglandin E2 EP1 receptor and cyclooxygenase-2 in the amygdala kindling model in mice. Epilepsy Res. *91*, 57–65.

Fisher, R.S. (2014). Final comments on the process: ILAE definition of epilepsy. Epilepsia *55*, 492–493.

Fitch, M.T., and Silver, J. (2008). CNS Injury, Glial Scars, and Inflammation. Exp. Neurol. *209*, 294–301.

Foster, C.A., Howard, L.M., Schweitzer, A., Persohn, E., Hiestand, P.C., Balatoni, B., Reuschel, R., Beerli, C., Schwartz, M., and Billich, A. (2007). Brain Penetration of the Oral Immunomodulatory Drug FTY720 and Its Phosphorylation in the Central Nervous System during Experimental Autoimmune Encephalomyelitis: Consequences for Mode of Action in Multiple Sclerosis. J. Pharmacol. Exp. Ther. *323*, 469–475.

Franklin, K.B.J., and Paxinos, G. (2008). The mouse brain in stereotaxic coordinates. Acad. Press San Diego.

Friedman, A., and Heinemann, U. (2012). Role of Blood-Brain Barrier Dysfunction in Epileptogenesis. In Jasper's Basic Mechanisms of the Epilepsies, J.L. Noebels, M. Avoli, M.A. Rogawski, R.W. Olsen, and A.V. Delgado-Escueta, eds. (Bethesda (MD): National Center for Biotechnology Information (US)), p.

Friedman, A., Kaufer, D., and Heinemann, U. (2009). Blood–brain barrier breakdown-inducing astrocytic transformation: Novel targets for the prevention of epilepsy. Epilepsy Res. *85*, 142–149.

Frigerio, F., Frasca, A., Weissberg, I., Parrella, S., Friedman, A., Vezzani, A., and Noe', F.M. (2012). Long-lasting pro-ictogenic effects induced in vivo by rat brain exposure to serum albumin in the absence of concomitant pathology. Epilepsia *53*, 1887–1897.

Frigerio, F., Flynn, C., Han, Y., Lyman, K., Lugo, J.N., Ravizza, T., Ghestem, A., Pitsch, J., Becker, A., Anderson, A.E., et al. (2018). Neuroinflammation Alters Integrative Properties of Rat Hippocampal Pyramidal Cells. Mol. Neurobiol. 1–12.

Fu, L., Liu, K., Wake, H., Teshigawara, K., Yoshino, T., Takahashi, H., Mori, S., and Nishibori, M. (2017). Therapeutic effects of anti-HMGB1 monoclonal antibody on pilocarpine-induced status epilepticus in mice. Sci. Rep. *7*, 1179.

Fu, T., Kong, Q., Sheng, H., and Gao, L. (2016). Value of Functionalized Superparamagnetic Iron Oxide Nanoparticles in the Diagnosis and Treatment of Acute Temporal Lobe Epilepsy on MRI. Neural Plast. *2016*, 1–12.

Furukawa, A., Kita, K., Toyomoto, M., Fujii, S., Inoue, S., Hayashi, K., and Ikeda, K. (2007). Production of nerve growth factor enhanced in cultured mouse astrocytes by glycerophospholipids, sphingolipids, and their related compounds. Mol. Cell. Biochem. *305*, 27–34.

Fuso, A., Iyer, A.M., van Scheppingen, J., Maccarrone, M., Scholl, T., Hainfellner, J.A., Feucht, M., Jansen, F.E., Spliet, W.G., Krsek, P., et al. (2016). Promoter-Specific Hypomethylation Correlates with IL-1β Overexpression in Tuberous Sclerosis Complex (TSC). J. Mol. Neurosci. *59*, 464–470.

Galic, M.A., Riazi, K., Heida, J.G., Mouihate, A., Fournier, N.M., Spencer, S.J., Kalynchuk, L.E., Teskey, G.C., and Pittman, Q.J. (2008). Postnatal inflammation increases seizure susceptibility in adult rats. J Neurosci *28*, 6904–6913.

Galic, M.A., Riazi, K., Henderson, A.K., Tsutsui, S., and Pittman, Q.J. (2009). Viral-like brain inflammation during development causes increased seizure susceptibility in adult rats. Neurobiol Dis *36*, 343–351.

Gallentine, W.B., Shinnar, S., Hesdorffer, D.C., Epstein, L., Nordli, D.R., Lewis, D.V., Frank, L.M., Seinfeld, S., Shinnar, R.C., Cornett, K., et al. (2017). Plasma cytokines associated with febrile status epilepticus in children: A potential biomarker for acute hippocampal injury. Epilepsia *58*, 1102–1111.

Gao, F., Liu, Y., Li, X., Wang, Y., Wei, D., and Jiang, W. (2012). Fingolimod (FTY720) inhibits neuroinflammation and attenuates spontaneous convulsions in lithium-pilocarpine induced status epilepticus in rat model. Pharmacol. Biochem. Behav. *103*, 187–196.

Gao, F., Gao, Y., Meng, F., Yang, C., Fu, J., and Li, Y. (2018). The Sphingosine 1-Phosphate Analogue FTY720 Alleviates Seizure-induced Overexpression of P-Glycoprotein in Rat Hippocampus. Basic Clin. Pharmacol. Toxicol. *123*, 14–20.

Garden, G.A., and Möller, T. (2006). Microglia Biology in Health and Disease. J. Neuroimmune Pharmacol. *1*, 127–137.

Gardner, N.M., Riley, R.T., Showker, J.L., Voss, K.A., Sachs, A.J., Maddox, J.R., and Gelineau-van Waes, J.B. (2016). Elevated Nuclear and Cytoplasmic FTY720-Phosphate in Mouse Embryonic Fibroblasts Suggests the Potential for Multiple Mechanisms in FTY720-Induced Neural Tube Defects. Toxicol. Sci. *150*, 161–168.

Garello, F., Pagoto, A., Arena, F., Buffo, A., Blasi, F., Alberti, D., and Terreno, E. (2017). MRI visualization of neuroinflammation using VCAM-1 targeted paramagnetic micelles. Nanomedicine Nanotechnol. Biol. Med.

Gasior, M., White, N.A., and Rogawski, M.A. (2007). Prolonged attenuation of amygdala-kindled seizure measures in rats by convection-enhanced delivery of the N-type calcium channel antagonists omega-conotoxin GVIA and omega-conotoxin MVIIA. J Pharmacol Exp Ther *323*, 458–468.

Gershen, L.D., Zanotti-Fregonara, P., Dustin, I.H., Liow, J.S., Hirvonen, J., Kreisl, W.C., Jenko, K.J., Inati, S.K., Fujita, M., Morse, C.L., et al. (2015). Neuroinflammation in Temporal Lobe Epilepsy Measured Using Positron Emission Tomographic Imaging of Translocator Protein. JAMA Neurol *72*, 882–888.

Gesuete, R., Packard, A.E.B., Vartanian, K.B., Conrad, V.K., Stevens, S.L., Bahjat, F.R., Yang, T., and Stenzel-Poore, M.P. (2012). Poly-ICLC preconditioning protects the blood-brain barrier against ischemic injury in vitro through type I interferon signaling. J. Neurochem. *123 Suppl 2*, 75–85.

Ghaemi, A., Sajadian, A., Khodaie, B., Lotfinia, A.A., Lotfinia, M., Aghabarari, A., Khaleghi Ghadiri, M., Meuth, S., and Gorji, A. (2016). Immunomodulatory Effect of Toll-Like Receptor-3 Ligand Poly I:C on Cortical Spreading Depression. Mol. Neurobiol. *53*, 143–154.

Gobbo, O.L., and O'Mara, S.M. (2004). Post-treatment, but not pre-treatment, with the selective cyclooxygenase-2 inhibitor celecoxib markedly enhances functional recovery from kainic acid-induced neurodegeneration. Neuroscience *125*, 317–327.

Godfred, R.M., Parikh, M.S., Haltiner, A.M., Caylor, L.M., Sepkuty, J.P., and Doherty, M.J. (2013). Does aspirin use make it harder to collect seizures during elective video-EEG telemetry? Epilepsy Behav. EB *27*, 115–117.

Goerres, G.W., Revesz, T., Duncan, J., and Banati, R.B. (2001). Imaging Cerebral Vasculitis in Refractory Epilepsy Using [11C] (R)-PK11195 Positron Emission Tomography. Am. J. Roentgenol. *176*, 1016–1018.

Golden, P.L., and Pollack, G.M. (2003). Blood-brain barrier efflux transport. J. Pharm. Sci. *92*, 1739–1753.

Goodman, A.R., Cardozo, T., Abagyan, R., Altmeyer, A., Wisniewski, H.G., and Vilcek, J. (1996). Long pentraxins: an emerging group of proteins with diverse functions. Cytokine Growth Factor Rev. *7*, 191–202.

Gorter, J.A., van Vliet, E.A., Aronica, E., Breit, T., Rauwerda, H., Lopes da Silva, F.H., and Wadman, W.J. (2006). Potential new antiepileptogenic targets indicated by microarray analysis in a rat model for temporal lobe epilepsy. J Neurosci *26*, 11083–11110.

Gorter, J.A., Iyer, A., White, I., Colzi, A., van Vliet, E.A., Sisodiya, S., and Aronica, E. (2014). Hippocampal subregion-specific microRNA expression during epileptogenesis in experimental temporal lobe epilepsy. Neurobiol Dis *62*, 508–520.

Gross, A., Benninger, F., Madar, R., Illouz, T., Griffioen, K., Steiner, I., Offen, D., and Okun, E. (2017). Toll-like receptor 3 deficiency decreases epileptogenesis in a pilocarpine model of SE-induced epilepsy in mice. Epilepsia *58*, 586–596.

Guilarte, T.R., Kuhlmann, A.C., O'Callaghan, J.P., and Miceli, R.C. (1995). Enhanced expression of peripheral benzodiazepine receptors in trimethyltin-exposed rat brain: a biomarker of neurotoxicity. Neurotoxicology *16*, 441–450.

Gulyás, B., Pavlova, E., Kása, P., Gulya, K., Bakota, L., Várszegi, S., Keller, E., Horváth, M.C., Nag, S., Hermecz, I., et al. (2011). Activated MAO-B in the brain of alzheimer patients, demonstrated by [11C]-l-deprenyl using whole hemisphere autoradiography. Neurochem. Int. *58*, 60–68.

Guyon, A., and Nahon, J.-L. (2007). Multiple actions of the chemokine stromal cell-derived factor-1alpha on neuronal activity. J. Mol. Endocrinol. *38*, 365–376.

Haber, R., Bessette, D., Hulihan-Giblin, B., Durcan, M.J., and Goldman, D. (1993). Identification of Tryptophan 2,3-Dioxygenase RNA in Rodent Brain. J. Neurochem. *60*, 1159–1162.

Hadjilambreva, G., Mix, E., Rolfs, A., Müller, J., and Strauss, U. (2005). Neuromodulation by a Cytokine: Interferon-β Differentially Augments Neocortical Neuronal Activity and Excitability. J. Neurophysiol. *93*, 843–852.

Hait, N.C., Allegood, J., Maceyka, M., Strub, G.M., Harikumar, K.B., Singh, S.K., Luo, C., Marmorstein, R., Kordula, T., Milstien, S., et al. (2009). Regulation of Histone Acetylation in the Nucleus by Sphingosine-1-Phosphate. Science *325*, 1254–1257.

Hait, N.C., Wise, L.E., Allegood, J.C., O'Brien, M., Avni, D., Reeves, T.M., Knapp, P.E., Lu, J., Luo, C., Miles, M.F., et al. (2014). Active, phosphorylated fingolimod inhibits histone deacetylases and facilitates fear extinction memory. Nat. Neurosci. *17*, 971–980.

Hait, N.C., Avni, D., Yamada, A., Nagahashi, M., Aoyagi, T., Aoki, H., Dumur, C.I., Zelenko, Z., Gallagher, E.J., Leroith, D., et al. (2015). The phosphorylated prodrug FTY720 is a histone deacetylase inhibitor that reactivates ERα expression and enhances hormonal therapy for breast cancer. Oncogenesis *4*, e156.

Hanisch, U.-K., and Kettenmann, H. (2007). Microglia: active sensor and versatile effector cells in the normal and pathologic brain. Nat. Neurosci. *10*, 1387–1394.

Harhausen, D., Sudmann, V., Khojasteh, U., Muller, J., Zille, M., Graham, K., Thiele, A., Dyrks, T., Dirnagl, U., and Wunder, A. (2013). Specific imaging of inflammation with the 18 kDa translocator protein ligand DPA-714 in animal models of epilepsy and stroke. PLoS One *8*, e69529.

Hashiba, N., Nagayama, S., Araya, S.-I., Inada, H., Sonobe, Y., Suzumura, A., and Matsui, M. (2011). Phenytoin at optimum doses ameliorates experimental autoimmune encephalomyelitis via modulation of immunoregulatory cells. J. Neuroimmunol. *233*, 112–119.

Hayakawa, K., Arai, K., and Lo, E.H. (2010). Role of ERK map kinase and CRM1 in IL-1beta-stimulated release of HMGB1 from cortical astrocytes. Glia *58*, 1007–1015.

He, X., Li, Y., Liu, Z., Yue, X., Zhao, P., Hu, J., Wu, G., Mao, B., Sun, D., Zhang, H., et al. (2013). The association between CCL2 polymorphisms and drug-resistant epilepsy in Chinese children. Epileptic Disord. Int. Epilepsy J. Videotape *15*, 272–277.

Healy, L.M., Sheridan, G.K., Pritchard, A.J., Rutkowska, A., Mullershausen, F., and Dev, K.K. (2013). Pathway specific modulation of S1P1 receptor signalling in rat and human astrocytes. Br. J. Pharmacol. *169*, 1114–1129.

Heck, N., Garwood, J., Loeffler, J.-P., Larmet, Y., and Faissner, A. (2004). Differential upregulation of extracellular matrix molecules associated with the appearance of granule cell dispersion and mossy fiber sprouting during epileptogenesis in a murine model of temporal lobe epilepsy. Neuroscience *129*, 309–324.

Heizmann, C.W. (2002). The multifunctional S100 protein family. Methods Mol. Biol. Clifton NJ *172*, 69–80.

Henshall, D.C., and Engel, T. (2015). P2X purinoceptors as a link between hyperexcitability and neuroinflammation in status epilepticus. Epilepsy Behav. *49*, 8–12.

Henshall, D.C., and Kobow, K. (2015). Epigenetics and Epilepsy. Cold Spring Harb. Perspect. Med. *5*.

Henshall, D.C., Hamer, H.M., Pasterkamp, R.J., Goldstein, D.B., Kjems, J., Prehn, J.H.M., Schorge, S., Lamottke, K., and Rosenow, F. (2016). MicroRNAs in epilepsy: pathophysiology and clinical utility. Lancet Neurol. *15*, 1368–1376.

Heo, K., Cho, Y.-J., Cho, K.-J., Kim, H.-W., Kim, H.-J., Shin, H.Y., Lee, B.I., and Kim, G.W. (2006). Minocycline inhibits caspase-dependent and -independent cell death pathways and is neuroprotective against hippocampal damage after treatment with kainic acid in mice. Neurosci. Lett. *398*, 195–200.

Hermonat, P.L., Quirk, J.G., Bishop, B.M., and Han, L. (1997). The packaging capacity of adeno-associated virus (AAV) and the potential for wild-type-plus AAV gene therapy vectors. FEBS Lett. *407*, 78–84.

Herrmann, J.E., Imura, T., Song, B., Qi, J., Ao, Y., Nguyen, T.K., Korsak, R.A., Takeda, K., Akira, S., and Sofroniew, M.V. (2008). STAT3 is a critical regulator of astrogliosis and scar formation after spinal cord injury. J. Neurosci. Off. J. Soc. Neurosci. *28*, 7231–7243.

Hester, M.S., and Danzer, S.C. (2014). Hippocampal Granule cell Pathology in Epilepsy – a Possible Structural Basis for Epileptic Co-Morbidities? Epilepsy Behav. EB *0*, 105–116.

Hewett, S.J., Csernansky, C.A., and Choi, D.W. (1994). Selective potentiation of NMDA-induced neuronal injury following induction of astrocytic iNOS. Neuron *13*, 487–494.

Hirvonen, J., Kreisl, W.C., Fujita, M., Dustin, I., Khan, O., Appel, S., Zhang, Y., Morse, C., Pike, V.W., Innis, R.B., et al. (2012). Increased in vivo expression of an inflammatory marker in temporal lobe epilepsy. J Nucl Med *53*, 234–240.

Hoffmann, F.S., Hofereiter, J., Rübsamen, H., Melms, J., Schwarz, S., Faber, H., Weber, P., Pütz, B., Loleit, V., Weber, F., et al. (2015). Fingolimod induces neuroprotective factors in human astrocytes. J. Neuroinflammation *12*, 184.

Höft, S., Griemsmann, S., Seifert, G., and Steinhäuser, C. (2014). Heterogeneity in expression of functional ionotropic glutamate and GABA receptors in astrocytes across brain regions: insights from the thalamus. Philos. Trans. R. Soc. Lond. B. Biol. Sci. *369*, 20130602.

Holtman, L., van Vliet, E.A., van Schaik, R., Queiroz, C.M., Aronica, E., and Gorter, J.A. (2009). Effects of SC58236, a selective COX-2 inhibitor, on epileptogenesis and spontaneous seizures in a rat model for temporal lobe epilepsy. Epilepsy Res *84*, 56–66.

Holtman, L., van Vliet, E.A., Edelbroek, P.M., Aronica, E., and Gorter, J.A. (2010). Cox-2 inhibition can lead to adverse effects in a rat model for temporal lobe epilepsy. Epilepsy Res *91*, 49–56.

Holtman, L., van Vliet, E.A., Baas, F., Aronica, E., and Gorter, J.A. (2011). Complement protein 6 deficiency in PVG/c rats does not lead to neuroprotection against seizure induced cell death. Neuroscience *188*, 109–116.

Hort, J., Brožek, G., Komárek, V., Langmeier, M., and Mareš, P. (2000). Interstrain differences in cognitive functions in rats in relation to status epilepticus. Behav. Brain Res. *112*, 77–83.

Hosoya, T., Fukumoto, D., Kakiuchi, T., Nishiyama, S., Yamamoto, S., Ohba, H., Tsukada, H., Ueki, T., Sato, K., and Ouchi, Y. (2017). In vivo TSPO and cannabinoid receptor type 2 availability early in post-stroke neuroinflammation in rats: a positron emission tomography study. J. Neuroinflammation *14*.

Hsieh, J., Nakashima, K., Kuwabara, T., Mejia, E., and Gage, F.H. (2004). Histone deacetylase inhibition-mediated neuronal differentiation of multipotent adult neural progenitor cells. Proc. Natl. Acad. Sci. *101*, 16659–16664.

Hu, S., Sheng, W.S., Ehrlich, L.C., Peterson, P.K., and Chao, C.C. (2000). Cytokine effects on glutamate uptake by human astrocytes. Neuroimmunomodulation *7*, 153–159.

Hubbard, J.A., Szu, J.I., Yonan, J.M., and Binder, D.K. (2016). Regulation of astrocyte glutamate transporter-1 (GLT1) and aquaporin-4 (AQP4) expression in a model of epilepsy. Exp. Neurol. *283*, 85–96.

Hurley, S.D., Olschowka, J.A., and O'Banion, M.K. (2002). Cyclooxygenase inhibition as a strategy to ameliorate brain injury. J Neurotrauma *19*, 1–15.

Huwiler, A., and Zangemeister-Wittke, U. (2018). The sphingosine 1-phosphate receptor modulator fingolimod as a therapeutic agent: Recent findings and new perspectives. Pharmacol. Ther. *185*, 34–49.

Ichiyama, T., Okada, K., Lipton, J.M., Matsubara, T., Hayashi, T., and Furukawa, S. (2000). Sodium valproate inhibits production of TNF-alpha and IL-6 and activation of NF-kappaB. Brain Res *857*, 246–251.

Inoue, K. (2006). The function of microglia through purinergic receptors: neuropathic pain and cytokine release. Pharmacol. Ther. *109*, 210–226.

Iori, V., Maroso, M., Rizzi, M., Iyer, A.M., Vertemara, R., Carli, M., Agresti, A., Antonelli, A., Bianchi, M.E., Aronica, E., et al. (2013). Receptor for Advanced Glycation Endproducts is upregulated in temporal lobe epilepsy and contributes to experimental seizures. Neurobiol Dis *58*, 102–114.

Iori, V., Iyer, A.M., Ravizza, T., Beltrame, L., Paracchini, L., Marchini, S., Cerovic, M., Hill, C., Ferrari, M., Zucchetti, M., et al. (2017). Blockade of the IL-1R1/TLR4 pathway mediates disease-modification therapeutic effects in a model of acquired epilepsy. Neurobiol. Dis. *99*, 12–23.

Ito, M., Natsume, A., Takeuchi, H., Shimato, S., Ohno, M., Wakabayashi, T., and Yoshida, J. (2009). Type I interferon inhibits astrocytic gliosis and promotes functional recovery after spinal cord injury by deactivation of the MEK/ERK pathway. J. Neurotrauma *26*, 41–53.

Ivens, S., Kaufer, D., Flores, L.P., Bechmann, I., Zumsteg, D., Tomkins, O., Seiffert, E., Heinemann, U., and Friedman, A. (2007). TGF- receptor-mediated albumin uptake into astrocytes is involved in neocortical epileptogenesis. Brain *130*, 535–547.

Iyer, A., Zurolo, E., Spliet, W.G., van Rijen, P.C., Baayen, J.C., Gorter, J.A., and Aronica, E. (2010). Evaluation of the innate and adaptive immunity in type I and type II focal cortical dysplasias. Epilepsia *51*, 1736–1773.

Iyer, A., Zurolo, E., Prabowo, A., Fluiter, K., Spliet, W.G., van Rijen, P.C., Gorter, J.A., and Aronica, E. (2012). MicroRNA-146a: a key regulator of astrocyte-mediated inflammatory response. PLoS One *7*, e44789.

Jakubs, K., Nanobashvili, A., Bonde, S., Ekdahl, C.T., Kokaia, Z., Kokaia, M., and Lindvall, O. (2006). Environment Matters: Synaptic Properties of Neurons Born in the Epileptic Adult Brain Develop to Reduce Excitability. Neuron *52*, 1047–1059.

Jamali, S., Bartolomei, F., Robaglia-Schlupp, A., Massacrier, A., Peragut, J.-C., Régis, J., Dufour, H., Ravid, R., Roll, P., Pereira, S., et al. (2006). Large-scale expression study of human mesial temporal lobe epilepsy: evidence for dysregulation of the neurotransmission and complement systems in the entorhinal cortex. Brain J. Neurol. *129*, 625–641.

Janaky, R., Ogita, K., Pasqualotto, B.A., Bains, J.S., Oja, S.S., Yoneda, Y., and Shaw, C.A. (1999). Glutathione and signal transduction in the mammalian CNS. J Neurochem *73*, 889–902.

Janssen, S., Schlegel, C., Gudi, V., Prajeeth, C.K., Skripuletz, T., Trebst, C., and Stangel, M. (2015). Effect of FTY720-phosphate on the expression of inflammation-associated molecules in astrocytes in vitro. Mol. Med. Rep. *12*, 6171–6177.

Jefferys, J., Steinhäuser, C., and Bedner, P. (2016). Chemically-induced TLE models: Topical application. J. Neurosci. Methods *260*, 53–61.

Ji, B., Maeda, J., Sawada, M., Ono, M., Okauchi, T., Inaji, M., Zhang, M.-R., Suzuki, K., Ando, K., Staufenbiel, M., et al. (2008). Imaging of Peripheral Benzodiazepine Receptor Expression as Biomarkers of Detrimental versus Beneficial Glial Responses in Mouse Models of Alzheimer's and Other CNS Pathologies. J. Neurosci. *28*, 12255–12267.

Jiang, J., Ganesh, T., Du, Y., Quan, Y., Serrano, G., Qui, M., Speigel, I., Rojas, A., Lelutiu, N., and Dingledine, R. (2012). Small molecule antagonist reveals seizure-induced mediation of neuronal injury by prostaglandin E2 receptor subtype EP2. Proc Natl Acad Sci U A *109*, 3149–3154.

Jiang, J., Quan, Y., Ganesh, T., Pouliot, W.A., Dudek, F.E., and Dingledine, R. (2013). Inhibition of the prostaglandin receptor EP2 following status epilepticus reduces delayed mortality and brain inflammation. Proc Natl Acad Sci U A *110*, 3591–3596.

Jiang, J., Yang, M.S., Quan, Y., Gueorguieva, P., Ganesh, T., and Dingledine, R. (2015). Therapeutic window for cyclooxygenase-2 related anti-inflammatory therapy after status epilepticus. Neurobiol Dis *76*, 126–136.

Jimenez-Mateos, E.M., Engel, T., Merino-Serrais, P., McKiernan, R.C., Tanaka, K., Mouri, G., Sano, T., O'Tuathaigh, C., Waddington, J.L., Prenter, S., et al. (2012). Silencing microRNA-134 produces neuroprotective and prolonged seizure-suppressive effects. Nat Med *18*, 1087–1094.

Jimenez-Pacheco, A., Mesuret, G., Sanz-Rodriguez, A., Tanaka, K., Mooney, C., Conroy, R., Miras-Portugal, M.T., Diaz-Hernandez, M., Henshall, D.C., and Engel, T. (2013). Increased neocortical expression of the P2X7 receptor after status epilepticus and anticonvulsant effect of P2X7 receptor antagonist A-438079. Epilepsia *54*, 1551–1561.

Jimenez-Pacheco, A., Diaz-Hernandez, M., Arribas-Blazquez, M., Sanz-Rodriguez, A., Olivos-Oré, L.A., Artalejo, A.R., Alves, M., Letavic, M., Miras-Portugal, M.T., Conroy, R.M., et al. (2016). Transient P2X7 Receptor Antagonism Produces Lasting Reductions in Spontaneous Seizures and Gliosis in Experimental Temporal Lobe Epilepsy. J Neurosci *36*, 5920–5932.

Johnson, E.W., de, L., Kim, J.H., Sundaresan, S., Spencer, D.D., Mattson, R.H., Zoghbi, S.S., Baldwin, R.M., Hoffer, P.B., Seibyl, J.P., et al. (1992). “Central” and “peripheral” benzodiazepine receptors: Opposite changes in human epileptogenic tissue. Neurology *42*, 811–815.

Jope, R.S., Morrisett, R.A., and Snead, O.C. (1986). Characterization of lithium potentiation of pilocarpine-induced status epilepticus in rats. Exp. Neurol. *91*, 471–480.

Jung, K.H., Chu, K., Lee, S.T., Kim, J., Sinn, D.I., Kim, J.M., Park, D.K., Lee, J.J., Kim, S.U., Kim, M., et al. (2006). Cyclooxygenase-2 inhibitor, celecoxib, inhibits the altered hippocampal neurogenesis with attenuation of spontaneous recurrent seizures following pilocarpine-induced status epilepticus. Neurobiol Dis *23*, 237–246.

Jung, S., Warner, L.N., Pitsch, J., Becker, A.J., and Poolos, N.P. (2011). Rapid Loss of Dendritic HCN Channel Expression in Hippocampal Pyramidal Neurons following Status Epilepticus. J. Neurosci. *31*, 14291–14295.

Jutila, L., Immonen, A., Partanen, K., Partanen, J., Mervaala, E., Ylinen, A., Alafuzoff, I., Paljärvi, L., Karkola, K., Vapalahti, M., et al. (2002). Neurobiology of epileptogenesis in the temporal lobe. Adv. Tech. Stand. Neurosurg. *27*, 5–22.

Jyonouchi, H. (2016). Intractable Epilepsy (IE) and Responses to Anakinra, a Human Recombinant IL-1 Receptor Antagonist (IL-1Ra): Case Reports. J. Clin. Cell. Immunol. *7*, 456–460.

Kagawa, K., Chugani, D.C., Asano, E., Juhász, C., Muzik, O., Shah, A., Shah, J., Sood, S., Kupsky, W.J., Mangner, T.J., et al. (2005). Epilepsy surgery outcome in children with tuberous sclerosis complex evaluated with alpha-[11C]methyl-L-tryptophan positron emission tomography (PET). J. Child Neurol. *20*, 429–438.

Kang, W., and Hébert, J.M. (2011). Signaling pathways in reactive astrocytes, a genetic perspective. Mol. Neurobiol. *43*, 147–154.

Kanner, A.M. (2016). Management of psychiatric and neurological comorbidities in epilepsy. Nat. Rev. Neurol. *12*, 106–116.

Karhunen, H., Nissinen, J., Sivenius, J., Jolkkonen, J., and Pitkänen, A. (2006). A long-term video-EEG and behavioral follow-up after endothelin-1 induced middle cerebral artery occlusion in rats. Epilepsy Res. *72*, 25–38.

Karhunen, H., Bezvenyuk, Z., Nissinen, J., Sivenius, J., Jolkkonen, J., and Pitkänen, A. (2007). Epileptogenesis after cortical photothrombotic brain lesion in rats. Neuroscience *148*, 314–324.

Kawada, N., Moriyama, T., Kitamura, H., Yamamoto, R., Furumatsu, Y., Matsui, I., Takabatake, Y., Nagasawa, Y., Imai, E., Wilcox, C.S., et al. (2012). Towards developing new strategies to reduce the adverse side-effects of nonsteroidal anti-inflammatory drugs. Clin. Exp. Nephrol. *16*, 25–29.

Kawai, T., and Akira, S. (2007). Signaling to NF-kappaB by Toll-like receptors. Trends Mol Med *13*, 460–469.

Kawai, T., and Akira, S. (2010). The role of pattern-recognition receptors in innate immunity: update on Toll-like receptors. Nat. Immunol. *11*, 373–384.

Kaya M, Becker AJ, Gürses C (2012). Blood-brain barrier, epileptogenesis, and treatment strategies in cortical dysplasia. Epilepsia. 53 Suppl 6:31-6.

Keezer, M.R., Sisodiya, S.M., and Sander, J.W. (2016). Comorbidities of epilepsy: current concepts and future perspectives. Lancet Neurol. *15*, 106–115.

Keller, A.F., Gravel, M., and Kriz, J. (2009). Live imaging of amyotrophic lateral sclerosis pathogenesis: disease onset is characterized by marked induction of GFAP in Schwann cells. Glia *57*, 1130–1142.

Kelley, K.A., Ho, L., Winger, D., Freire-Moar, J., Borelli, C.B., Aisen, P.S., and Pasinetti, G.M. (1999). Potentiation of excitotoxicity in transgenic mice overexpressing neuronal cyclooxygenase-2. Am J Pathol *155*, 995–1004.

Kelly, K.M., Kharlamov, A., Hentosz, T.M., Kharlamova, E.A., Williamson, J.M., Bertram, E.H., Kapur, J., and Armstrong, D.M. (2001). Photothrombotic brain infarction results in seizure activity in aging Fischer 344 and Sprague Dawley rats. Epilepsy Res. *47*, 189–203.

Kenney-Jung, D.L., Vezzani, A., Kahoud, R.J., LaFrance-Corey, R.G., Ho, M.L., Muscardin, T.W., Wirrell, E.C., Howe, C.L., and Payne, E.T. (2016). Febrile infection-related epilepsy syndrome treated with anakinra. Ann. Neurol. *80*, 939–945.

Kettenmann, H., Hanisch, U.-K., Noda, M., and Verkhratsky, A. (2011). Physiology of Microglia. Physiol. Rev. *91*, 461–553.

Kharatishvili, I., Nissinen, J.P., McIntosh, T.K., and Pitkanen, A. (2006a). A model of posttraumatic epilepsy induced by lateral fluid-percussion brain injury in rats. Neuroscience *140*, 685–697.

Kharatishvili, I., Nissinen, J.P., McIntosh, T.K., and Pitkänen, A. (2006b). A model of posttraumatic epilepsy induced by lateral fluid-percussion brain injury in rats. Neuroscience *140*, 685–697.

Khorooshi, R., Mørch, M.T., Holm, T.H., Berg, C.T., Dieu, R.T., Dræby, D., Issazadeh-Navikas, S., Weiss, S., Lienenklaus, S., and Owens, T. (2015). Induction of endogenous Type I interferon within the central nervous system plays a protective role in experimental autoimmune encephalomyelitis. Acta Neuropathol. (Berl.) *130*, 107–118.

Kim, H.J., Chung, J.I., Lee, S.H., Jung, Y.S., Moon, C.H., and Baik, E.J. (2008). Involvement of endogenous prostaglandin F2alpha on kainic acid-induced seizure activity through FP receptor: the mechanism of proconvulsant effects of COX-2 inhibitors. Brain Res *1193*, 153–161.

Kirschman, L.T., Borysiewicz, E., Fil, D., and Konat, G.W. (2011). Peripheral immune challenge with dsRNA enhances kainic acid-induced status epilepticus. Metab Brain Dis *26*, 91–93.

Kobow, K., Auvin, S., Jensen, F., Löscher, W., Mody, I., Potschka, H., Prince, D., Sierra, A., Simonato, M., Pitkänen, A., et al. (2012). Finding a better drug for epilepsy: Antiepileptogenesis targets. Epilepsia *53*, 1868–1876.

Kominato, Y., Galson, D., Waterman, W.R., Webb, A.C., and Auron, P.E. (1995). Monocyte expression of the human prointerleukin 1 beta gene (IL1B) is dependent on promoter sequences which bind the hematopoietic transcription factor Spi-1/PU.1. Mol. Cell. Biol. *15*, 58–68.

Kreutzberg, G.W. (1996). Microglia: a sensor for pathological events in the CNS. Trends Neurosci. *19*, 312–318.

Krishnasamy, S., Weng, Y.-C., Thammisetty, S.S., Phaneuf, D., Lalancette-Hebert, M., and Kriz, J. (2017). Molecular imaging of nestin in neuroinflammatory conditions reveals marked signal induction in activated microglia. J. Neuroinflammation *14*, 45.

Kubova, H., Mares, P., Suchomelova, L., Brozek, G., Druga, R., and Pitkanen, A. (2004). Status epilepticus in immature rats leads to behavioural and cognitive impairment and epileptogenesis. Eur J Neurosci *19*, 3255–3265.

Kulbida, R., Wang, Y., Mandelkow, E.-M., Schoch, S., Becker, A.J., and van Loo, K.M.J. (2015). Molecular imaging reveals epileptogenic Ca2+-channel promoter activation in hippocampi of living mice. Brain Struct. Funct. *220*, 3067–3073.

Kulkarni, S.K., and Dhir, A. (2009). Cyclooxygenase in epilepsy: from perception to application. Drugs Today Barc *45*, 135–154.

Kumar, A., Chugani, H.T., Luat, A., Asano, E., and Sood, S. (2008). Epilepsy Surgery in a Case of Encephalitis: Use of 11C-PK11195 Positron Emission Tomography. Pediatr. Neurol. *38*, 439–442.

Kumlien, E., Hilton-Brown, P., Spannare, B., and Gillberg, P.G. (1992). In vitro quantitative autoradiography of [3H]-L-deprenyl and [3H]-PK 11195 binding sites in human epileptic hippocampus. Epilepsia *33*, 610–617.

Kumlien, E., Bergström, M., Lilja, A., Andersson, J., Szekeres, V., Westerberg, C.-E., Westerberg, G., Antoni, G., and Långström, B. (1995). Positron Emission Tomography with [11C]Deuterium-Deprenyl in Temporal Lobe Epilepsy. Epilepsia *36*, 712–721.

Kumlien, E., Nilsson, A., Hagberg, G., Långström, B., and Bergström, M. (2001). PET with 11C-deuterium-deprenyl and 18F-FDG in focal epilepsy. Acta Neurol. Scand. *103*, 360–366.

Kunz, T., and Oliw, E.H. (2001a). The selective cyclooxygenase-2 inhibitor rofecoxib reduces kainate-induced cell death in the rat hippocampus. Eur J Neurosci *13*, 569–575.

Kunz, T., and Oliw, E.H. (2001b). Nimesulide aggravates kainic acid-induced seizures in the rat. Pharmacol Toxicol *88*, 271–276.

Kuo, P., Scofield, B.A., Yu, I., Chang, F., Ganea, D., and Yen, J. (2016). Interferon-β Modulates Inflammatory Response in Cerebral Ischemia. J. Am. Heart Assoc. *5*, e002610.

Kwan, P., Arzimanoglou, A., Berg, A.T., Brodie, M.J., Hauser, W.A., Mathern, G., Moshé, S.L., Perucca, E., Wiebe, S., and French, J. (2010). Definition of drug resistant epilepsy: Consensus proposal by the ad hoc Task Force of the ILAE Commission on Therapeutic Strategies. Epilepsia *51*, 1069–1077.

Kwan, P., Schachter, S.C., and Brodie, M.J. (2011). Drug-resistant epilepsy. N Engl J Med *365*, 919–926.

Kwon, Y.S., Pineda, E., Auvin, S., Shin, D., Mazarati, A., and Sankar, R. (2013). Neuroprotective and antiepileptogenic effects of combination of anti-inflammatory drugs in the immature brain. J. Neuroinflammation *10*, 30.

Lafon, M., Mégret, F., Meuth, S.G., Simon, O., Velandia Romero, M.L., Lafage, M., Chen, L., Alexopoulou, L., Flavell, R.A., Prehaud, C., et al. (2008). Detrimental contribution of the immuno-inhibitor B7-H1 to rabies virus encephalitis. J. Immunol. Baltim. Md 1950 *180*, 7506–7515.

Lagarde, S., Villeneuve, N., Trébuchon, A., Kaphan, E., Lepine, A., McGonigal, A., Roubertie, A., Barthez, M.A., Trommsdorff, V., LeFranc, J., et al. (2016). Anti-tumor necrosis factor alpha therapy (adalimumab) in Rasmussen's encephalitis. An open pilot study. Epilepsia *57*, 956–966.

Lalancette-Hébert, M., Phaneuf, D., Soucy, G., Weng, Y.C., and Kriz, J. (2009). Live imaging of Toll-like receptor 2 response in cerebral ischaemia reveals a role of olfactory bulb microglia as modulators of inflammation. Brain J. Neurol. *132*, 940–954.

Lalancette-Hébert, M., Faustino, J., Thammisetty, S.S., Chip, S., Vexler, Z.S., and Kriz, J. (2017). Live imaging of the innate immune response in neonates reveals differential TLR2 dependent activation patterns in sterile inflammation and infection. Brain. Behav. Immun. *65*, 312–327.

Lance, E.I., Sreenivasan, A.K., Zabel, T.A., Kossoff, E.H., and Comi, A.M. (2013). Aspirin use in Sturge-Weber syndrome: side effects and clinical outcomes. J. Child Neurol. *28*, 213–218.

Lavisse, S., Guillermier, M., Hérard, A.-S., Petit, F., Delahaye, M., Camp, N.V., Haim, L.B., Lebon, V., Remy, P., Dollé, F., et al. (2012). Reactive Astrocytes Overexpress TSPO and Are Detected by TSPO Positron Emission Tomography Imaging. J. Neurosci. *32*, 10809–10818.

Lawlor, P.A., Bland, R.J., Mouravlev, A., Young, D., and During, M.J. (2009). Efficient Gene Delivery and Selective Transduction of Glial Cells in the Mammalian Brain by AAV Serotypes Isolated From Nonhuman Primates. Mol. Ther. J. Am. Soc. Gene Ther. *17*, 1692–1702.

Lee, B., Dziema, H., Lee, K.H., Choi, Y.S., and Obrietan, K. (2007). CRE-mediated transcription and COX-2 expression in the pilocarpine model of status epilepticus. Neurobiol Dis *25*, 80–91.

Lee, D.-H., Seubert, S., Huhn, K., Brecht, L., Rötger, C., Waschbisch, A., Schlachetzki, J., Klausmeyer, A., Melms, A., Wiese, S., et al. (2017). Fingolimod effects in neuroinflammation: Regulation of astroglial glutamate transporters? PloS One *12*, e0171552.

Lee, E.M., Park, G.Y., Im, K.C., Kim, S.T., Woo, C.-W., Chung, J.H., Kim, K.S., Kim, J.S., Shon, Y.-M., Kim, Y.I., et al. (2012). Changes in glucose metabolism and metabolites during the epileptogenic process in the lithium-pilocarpine model of epilepsy. Epilepsia *53*, 860–869.

Lee, Y., Su, M., Messing, A., and Brenner, M. (2006). Astrocyte heterogeneity revealed by expression of a GFAP-LacZ transgene. Glia *53*, 677–687.

Lee, Y., Messing, A., Su, M., and Brenner, M. (2008). GFAP promoter elements required for region-specific and astrocyte-specific expression. Glia *56*, 481–493.

de Leeuw, B., Su, M., ter Horst, M., Iwata, S., Rodijk, M., Hoeben, R.C., Messing, A., Smitt, P.S., and Brenner, M. (2006). Increased glia-specific transgene expression with glial fibrillary acidic protein promoters containing multiple enhancer elements. J. Neurosci. Res. *83*, 744–753.

Lehtimaki, K.A., Peltola, J., Koskikallio, E., Keranen, T., and Honkaniemi, J. (2003). Expression of cytokines and cytokine receptors in the rat brain after kainic acid-induced seizures. Brain Res Mol Brain Res *110*, 253–260.

Lehtimaki, K.A., Keranen, T., Huhtala, H., Hurme, M., Ollikainen, J., Honkaniemi, J., Palmio, J., and Peltola, J. (2004). Regulation of IL-6 system in cerebrospinal fluid and serum compartments by seizures: the effect of seizure type and duration. J Neuroimmunol *152*, 121–125.

Li, K., Nicaise, C., Sannie, D., Hala, T.J., Javed, E., Parker, J.L., Putatunda, R., Regan, K.A., Suain, V., Brion, J.-P., et al. (2014). Overexpression of the astrocyte glutamate transporter GLT1 exacerbates phrenic motor neuron degeneration, diaphragm compromise, and forelimb motor dysfunction following cervical contusion spinal cord injury. J. Neurosci. Off. J. Soc. Neurosci. *34*, 7622–7638.

Li, L., Fei, Z., Ren, J., Sun, R., Liu, Z., Sheng, Z., Wang, L., Sun, X., Yu, J., Wang, Z., et al. (2008). Functional imaging of interleukin 1 beta expression in inflammatory process using bioluminescence imaging in transgenic mice. BMC Immunol. *9*, 49.

Li, Y., Korgaonkar, A.A., Swietek, B., Wang, J., Elgammal, F.S., Elkabes, S., and Santhakumar, V. (2015a). Toll-like receptor 4 enhancement of non-NMDA synaptic currents increases dentate excitability after brain injury. Neurobiol. Dis. *74*, 240–253.

Li, Y., Xu, X.-L., Zhao, D., Pan, L.-N., Huang, C.-W., Guo, L.-J., Lu, Q., and Wang, J. (2015b). TLR3 ligand Poly IC Attenuates Reactive Astrogliosis and Improves Recovery of Rats after Focal Cerebral Ischemia. CNS Neurosci. Ther. *21*, 905–913.

Libbey, J.E., and Fujinami, R.S. (2011). Neurotropic viral infections leading to epilepsy: focus on Theiler's murine encephalomyelitis virus. Future Virol. *6*, 1339–1350.

Libbey, J.E., Kirkman, N.J., Wilcox, K.S., White, H.S., and Fujinami, R.S. (2010). Role for complement in the development of seizures following acute viral infection. J Virol *84*, 6452–6460.

Librizzi, L., Noè, F., Vezzani, A., Curtis, M. de, and Ravizza, T. (2012). Seizure-induced brain-borne inflammation sustains seizure recurrence and blood–brain barrier damage. Ann. Neurol. *72*, 82–90.

Liddelow, S.A., Guttenplan, K.A., Clarke, L.E., Bennett, F.C., Bohlen, C.J., Schirmer, L., Bennett, M.L., Münch, A.E., Chung, W.-S., Peterson, T.C., et al. (2017). Neurotoxic reactive astrocytes are induced by activated microglia. Nature *541*, 481–487.

Liu, T., and Ji, R.-R. (2014). Toll-Like Receptors and Itch. In Itch: Mechanisms and Treatment, E. Carstens, and T. Akiyama, eds. (Boca Raton (FL): CRC Press/Taylor & Francis), p.

Liu, G., Gu, B., He, X.-P., Joshi, R.B., Wackerle, H.D., Rodriguiz, R.M., Wetsel, W.C., and McNamara, J.O. (2013). Transient Inhibition of TrkB Kinase Following Status Epilepticus Prevents Development of Temporal Lobe Epilepsy. Neuron *79*, 31–38.

Liu, H., Xin, L., Chan, B.P.L., Teoh, R., Tang, B.L., and Tan, Y.H. (2002). Interferon-beta administration confers a beneficial outcome in a rabbit model of thromboembolic cerebral ischemia. Neurosci. Lett. *327*, 146–148.

Lopez de Heredia, L., Gengatharan, A., Foster, J., Mather, S., and Magoulas, C. (2011). Bioluminescence imaging of the brain response to acute inflammation in living C/EBP reporter mice. Neurosci. Lett. *497*, 134–138.

Löscher, W., Klitgaard, H., Twyman, R.E., and Schmidt, D. (2013). New avenues for anti-epileptic drug discovery and development. Nat. Rev. Drug Discov. *12*, 757–776.

Lothman, E.W., Bertram, E.H., Bekenstein, J.W., and Perlin, J.B. (1989). Self-sustaining limbic status epilepticus induced by "continuous" hippocampal stimulation: electrographic and behavioral characteristics. Epilepsy Res *3*, 107–119.

Louboutin, J.-P., Chekmasova, A., Marusich, E., Agrawal, L., and Strayer, D.S. (2011). Role of CCR5 and its ligands in the control of vascular inflammation and leukocyte recruitment required for acute excitotoxic seizure induction and neural damage. FASEB J. Off. Publ. Fed. Am. Soc. Exp. Biol. *25*, 737–753.

Luan, G., Gao, Q., Zhai, F., Chen, Y., and Li, T. (2016). Upregulation of HMGB1, toll-like receptor and RAGE in human Rasmussen's encephalitis. Epilepsy Res. *123*, 36–49.

Lundgaard, I., Osório, M.J., Kress, B.T., Sanggaard, S., and Nedergaard, M. (2014). White matter astrocytes in health and disease. Neuroscience *276*, 161–173.

Luo, J., Ho, P.P., Buckwalter, M.S., Hsu, T., Lee, L.Y., Zhang, H., Kim, D.-K., Kim, S.-J., Gambhir, S.S., Steinman, L., et al. (2007). Glia-dependent TGF-β signaling, acting independently of the TH17 pathway, is critical for initiation of murine autoimmune encephalomyelitis. J. Clin. Invest. *117*, 3306–3315.

Luo, J., Ho, P., Steinman, L., and Wyss-Coray, T. (2008). Bioluminescence in vivo imaging of autoimmune encephalomyelitis predicts disease. J. Neuroinflammation *5*, 6.

Luo, J., Nguyen, A., Villeda, S., Zhang, H., Ding, Z., Lindsey, D., Bieri, G., Castellano, J.M., Beaupre, G.S., and Wyss-Coray, T. (2014). Long-term cognitive impairments and pathological alterations in a mouse model of repetitive mild traumatic brain injury. Front. Neurol. *5*, 12.

Ma, L., Cui, X.-L., Wang, Y., Li, X.-W., Yang, F., Wei, D., and Jiang, W. (2012). Aspirin attenuates spontaneous recurrent seizures and inhibits hippocampal neuronal loss, mossy fiber sprouting and aberrant neurogenesis following pilocarpine-induced status epilepticus in rats. Brain Res. *1469*, 103–113.

Machnes, Z.M., Huang, T.C.T., Chang, P.K.Y., Gill, R., Reist, N., Dezsi, G., Ozturk, E., Charron, F., O'Brien, T.J., Jones, N.C., et al. (2013). DNA Methylation Mediates Persistent Epileptiform Activity In Vitro and In Vivo. PLoS ONE *8*.

Madakasira, P.V., Simkins, R., Narayanan, T., Dunigan, K., Poelstra, R.J., and Mantil, J. (2002). Cortical dysplasia localized by [11C]methionine positron emission tomography: Case report. Am. J. Neuroradiol. *23*, 844–846.

Maeda, Y., Oguni, H., Saitou, Y., Mutoh, A., Imai, K., Osawa, M., Fukuyama, Y., Hori, T., Yamane, F., Kubo, O., et al. (2003). Rasmussen Syndrome: Multifocal Spread of Inflammation Suggested from MRI and PET Findings. Epilepsia *44*, 1118–1121.

Maldonado, M., Baybis, M., Newman, D., Kolson, D.L., Chen, W., McKhann, G., Gutmann, D.H., and Crino, P.B. (2003). Expression of ICAM-1, TNF-alpha, NF kappa B, and MAP kinase in tubers of the tuberous sclerosis complex. Neurobiol Dis *14*, 279–290.

Mandala, S., Hajdu, R., Bergstrom, J., Quackenbush, E., Xie, J., Milligan, J., Thornton, R., Shei, G.-J., Card, D., Keohane, C., et al. (2002). Alteration of lymphocyte trafficking by sphingosine-1-phosphate receptor agonists. Science *296*, 346–349.

Marchi, N., Angelov, L., Masaryk, T., Fazio, V., Granata, T., Hernandez, N., Hallene, K., Diglaw, T., Franic, L., Najm, I., et al. (2007). Seizure-promoting effect of blood-brain barrier disruption. Epilepsia *48*, 732–742.

Marchi, N., Tierney, W., Alexopoulos, A.V., Puvenna, V., Granata, T., and Janigro, D. (2011a). The etiological role of blood-brain barrier dysfunction in seizure disorders. Cardiovasc. Psychiatry Neurol. *2011*, 482415.

Marchi, N., Granata, T., Freri, E., Ciusani, E., Ragona, F., Puvenna, V., Teng, Q., Alexopolous, A., and Janigro, D. (2011b). Efficacy of anti-inflammatory therapy in a model of acute seizures and in a population of pediatric drug resistant epileptics. PLoS One *6*, e18200.

Marcon, J., Gagliardi, B., Balosso, S., Maroso, M., Noe, F., Morin, M., Lerner-Natoli, M., Vezzani, A., and Ravizza, T. (2009). Age-dependent vascular changes induced by status epilepticus in rat forebrain: implications for epileptogenesis. Neurobiol Dis *34*, 121–132.

Maroso, M., Balosso, S., Ravizza, T., Liu, J., Aronica, E., Iyer, A.M., Rossetti, C., Molteni, M., Casalgrandi, M., Manfredi, A.A., et al. (2010). Toll-like receptor 4 and high-mobility group box-1 are involved in ictogenesis and can be targeted to reduce seizures. Nat Med *16*, 413–419.

Maroso, M., Balosso, S., Ravizza, T., Liu, J., Bianchi, M.E., and Vezzani, A. (2011a). Interleukin-1 type 1 receptor/Toll-like receptor signalling in epilepsy: the importance of IL-1beta and high-mobility group box 1. J Intern Med *270*, 319–326.

Maroso, M., Balosso, S., Ravizza, T., Iori, V., Wright, C.I., French, J., and Vezzani, A. (2011b). Interleukin-1beta biosynthesis inhibition reduces acute seizures and drug resistant chronic epileptic activity in mice. Neurotherapeutics *8*, 304–315.

Marsh, B., Stevens, S.L., Packard, A.E.B., Gopalan, B., Hunter, B., Leung, P.Y., Harrington, C.A., and Stenzel-Poore, M.P. (2009). Systemic Lipopolysaccharide Protects the Brain from Ischemic Injury by Reprogramming the Response of the Brain to Stroke: A Critical Role for IRF3. J. Neurosci. *29*, 9839–9849.

Martín, A., Boisgard, R., Thézé, B., Van Camp, N., Kuhnast, B., Damont, A., Kassiou, M., Dollé, F., and Tavitian, B. (2010). Evaluation of the PBR/TSPO Radioligand [18F]DPA-714 in a Rat Model of Focal Cerebral Ischemia. J. Cereb. Blood Flow Metab. *30*, 230–241.

Martín, A., Boisgard, R., Kassiou, M., Dollé, F., and Tavitian, B. (2011). Reduced PBR/TSPO expression after minocycline treatment in a rat model of focal cerebral ischemia: a PET study using [(18)F]DPA-714. Mol. Imaging Biol. MIB Off. Publ. Acad. Mol. Imaging *13*, 10–15.

Matsuda, T., Murao, N., Katano, Y., Juliandi, B., Kohyama, J., Akira, S., Kawai, T., and Nakashima, K. (2015). TLR9 signalling in microglia attenuates seizure-induced aberrant neurogenesis in the adult hippocampus. Nat. Commun. *6*, 6514.

Matthias, K., Kirchhoff, F., Seifert, G., Hüttmann, K., Matyash, M., Kettenmann, H., and Steinhäuser, C. (2003). Segregated expression of AMPA-type glutamate receptors and glutamate transporters defines distinct astrocyte populations in the mouse hippocampus. J. Neurosci. Off. J. Soc. Neurosci. *23*, 1750–1758.

Mazarati, A.M., Wasterlain, C.G., Sankar, R., and Shin, D. (1998). Self-sustaining status epilepticus after brief electrical stimulation of the perforant path. Brain Res. *801*, 251–253.

Mazzuferi, M., Kumar, G., van Eyll, J., Danis, B., Foerch, P., and Kaminski, R.M. (2013). Nrf2 defense pathway: Experimental evidence for its protective role in epilepsy. Ann Neurol *74*, 560–568.

Ménager, P., Roux, P., Mégret, F., Bourgeois, J.-P., Sourd, A.-M.L., Danckaert, A., Lafage, M., Préhaud, C., and Lafon, M. (2009). Toll-Like Receptor 3 (TLR3) Plays a Major Role in the Formation of Rabies Virus Negri Bodies. PLOS Pathog. *5*, e1000315.

Michalak, Z., Sano, T., Engel, T., Miller-Delaney, S.F.C., Lerner-Natoli, M., and Henshall, D.C. (2013). Spatio-temporally restricted blood-brain barrier disruption after intra-amygdala kainic acid-induced status epilepticus in mice. Epilepsy Res. *103*, 167–179.

Michalovicz, L.T., and Konat, G.W. (2014). Peripherally restricted acute phase response to a viral mimic alters hippocampal gene expression. Metab Brain Dis *29*, 75–86.

Miron, V.E., Ludwin, S.K., Darlington, P.J., Jarjour, A.A., Soliven, B., Kennedy, T.E., and Antel, J.P. (2010). Fingolimod (FTY720) enhances remyelination following demyelination of organotypic cerebellar slices. Am. J. Pathol. *176*, 2682–2694.

Mizuguchi, M., and Takashima, S. (2001). Neuropathology of tuberous sclerosis. Brain Dev. *23*, 508–515.

Mizuno, S., Takahashi, Y., Kato, Z., Goto, H., Kondo, N., and Hoshi, H. (2000). Magnetic resonance spectroscopy of tubers in patients with tuberous sclerosis. Acta Neurol Scand *102*, 175–178.

Moldovan, R.-P., Teodoro, R., Gao, Y., Deuther-Conrad, W., Kranz, M., Wang, Y., Kuwabara, H., Nakano, M., Valentine, H., Fischer, S., et al. (2016). Development of a High-Affinity PET Radioligand for Imaging Cannabinoid Subtype 2 Receptor. J. Med. Chem. *59*, 7840–7855.

Moldovan, R.-P., Hausmann, K., Deuther-Conrad, W., and Brust, P. (2017). Development of Highly Affine and Selective Fluorinated Cannabinoid Type 2 Receptor Ligands. ACS Med. Chem. Lett. *8*, 566–571.

Morin-Brureau, M., Lebrun, A., Rousset, M.-C., Fagni, L., Bockaert, J., de Bock, F., and Lerner-Natoli, M. (2011). Epileptiform activity induces vascular remodeling and zonula occludens 1 downregulation in organotypic hippocampal cultures: role of VEGF signaling pathways. J. Neurosci. Off. J. Soc. Neurosci. *31*, 10677–10688.

Morrison, R.S., De Vellis, J., Lee, Y.L., Bradshaw, R.A., and Eng, L.F. (1985). Hormones and growth factors induce the synthesis of glial fibrillary acidic protein in rat brain astrocytes. J. Neurosci. Res. *14*, 167–176.

Mouri, G., Jimenez-Mateos, E., Engel, T., Dunleavy, M., Hatazaki, S., Paucard, A., Matsushima, S., Taki, W., and Henshall, D.C. (2008). Unilateral hippocampal CA3-predominant damage and short latency epileptogenesis after intra-amygdala microinjection of kainic acid in mice. Brain Res *1213*, 140–151.

Muller, S., Ronfani, L., and Bianchi, M.E. (2004). Regulated expression and subcellular localization of HMGB1, a chromatin protein with a cytokine function. J Intern Med *255*, 332–343.

Mullershausen, F., Zecri, F., Cetin, C., Billich, A., Guerini, D., and Seuwen, K. (2009). Persistent signaling induced by FTY720-phosphate is mediated by internalized S1P1 receptors. Nat. Chem. Biol. *5*, 428–434.

Nagao, Y., Harada, Y., Mukai, T., Shimizu, S., Okuda, A., Fujimoto, M., Ono, A., Sakagami, Y., and Ohno, Y. (2013). Expressional analysis of the astrocytic Kir4.1 channel in a pilocarpine–induced temporal lobe epilepsy model. Front. Cell. Neurosci. *7*.

Nakamura, Y. (2002). Regulating factors for microglial activation. Biol. Pharm. Bull. *25*, 945–953.

Nakashima, K., and Taga, T. (2002). Mechanisms underlying cytokine-mediated cell-fate regulation in the nervous system. Mol. Neurobiol. *25*, 233–244.

Neels, H.M., Sierens, A.C., Naelaerts, K., Scharpé, S.L., Hatfield, G.M., and Lambert, W.E. (2004). Therapeutic drug monitoring of old and newer anti-epileptic drugs. Clin. Chem. Lab. Med. *42*, 1228–1255.

Nehlig, A. What is animal experimentation telling us about new drug treatments of status epilepticus? Epilepsia *48*, 78–81.

Neuwelt, E.A., Bauer, B., Fahlke, C., Fricker, G., Iadecola, C., Janigro, D., Leybaert, L., Molnár, Z., O'Donnell, M.E., Povlishock, J.T., et al. (2011). Engaging neuroscience to advance translational research in brain barrier biology. Nat. Rev. Neurosci. *12*, 169–182.

Nguyen, D.-L., Wimberley, C., Truillet, C., Jego, B., Caillé, F., Pottier, G., Boisgard, R., Buvat, I., and Bouilleret, V. (2018). Longitudinal positron emission tomography imaging of glial cell activation in a mouse model of mesial temporal lobe epilepsy: Toward identification of optimal treatment windows. Epilepsia *59*, 1234–1244.

Nishimura, T., Imai, H., Minabe, Y., Sawa, A., and Kato, N. (2006). Beneficial effects of FK506 for experimental temporal lobe epilepsy. Neurosci. Res. *56*, 386–390.

Nishimura, Y., Natsume, A., Ito, M., Hara, M., Motomura, K., Fukuyama, R., Sumiyoshi, N., Aoki, I., Saga, T., Lee, H.J., et al. (2013). Interferon-β Delivery via Human Neural Stem Cell Abates Glial Scar Formation in Spinal Cord Injury. Cell Transplant. *22*, 2187–2201.

Nishiyama, H., Knopfel, T., Endo, S., and Itohara, S. (2002). Glial protein S100B modulates long-term neuronal synaptic plasticity. Proc Natl Acad Sci U A *99*, 4037–4042.

Nissinen, J., Halonen, T., Koivisto, E., and Pitkanen, A. (2000). A new model of chronic temporal lobe epilepsy induced by electrical stimulation of the amygdala in rat. Epilepsy Res *38*, 177–205.

Noe, F.M., Polascheck, N., Frigerio, F., Bankstahl, M., Ravizza, T., Marchini, S., Beltrame, L., Banderó, C.R., Löscher, W., and Vezzani, A. (2013). Pharmacological blockade of IL-1β/IL-1 receptor type 1 axis during epileptogenesis provides neuroprotection in two rat models of temporal lobe epilepsy. Neurobiol. Dis. *59*, 183–193.

Nowak, M., Strzelczyk, A., Reif, P.S., Schrolemmer, K., Bauer, S., Norwood, B.A., Oertel, W.H., Rosenow, F., Strik, H., and Hamer, H.M. (2012). Minocycline as potent anticonvulsivant i a patient with astrocytoma and drug resistant epilepsy. Seizure *21*, 227–228.

Ntziachristos, V. (2006). Fluorescence molecular imaging. Annu. Rev. Biomed. Eng. *8*, 1–33.

Obenaus, A. (2013). Neuroimaging biomarkers for epilepsy: Advances and relevance to glial cells. Neurochem. Int. *63*, 712–718.

Okun, E., Griffioen, K., Barak, B., Roberts, N.J., Castro, K., Pita, M.A., Cheng, A., Mughal, M.R., Wan, R., Ashery, U., et al. (2010). Toll-like receptor 3 inhibits memory retention and constrains adult hippocampal neurogenesis. Proc Natl Acad Sci U A *107*, 15625–15630.

Oliveira, M.S., Furian, A.F., Royes, L.F., Fighera, M.R., Fiorenza, N.G., Castelli, M., Machado, P., Bohrer, D., Veiga, M., Ferreira, J., et al. (2008). Cyclooxygenase-2/PGE2 pathway facilitates pentylenetetrazol-induced seizures. Epilepsy Res *79*, 14–21.

Olsen, M.L., Khakh, B.S., Skatchkov, S.N., Zhou, M., Lee, C.J., and Rouach, N. (2015). New Insights on Astrocyte Ion Channels: Critical for Homeostasis and Neuron-Glia Signaling. J. Neurosci. Off. J. Soc. Neurosci. *35*, 13827–13835.

Olson, J.K., and Miller, S.D. (2004). Microglia initiate central nervous system innate and adaptive immune responses through multiple TLRs. J. Immunol. Baltim. Md 1950 *173*, 3916–3924.

Omran, A., Peng, J., Zhang, C., Xiang, Q.L., Xue, J., Gan, N., Kong, H., and Yin, F. (2012). Interleukin-1beta and microRNA-146a in an immature rat model and children with mesial temporal lobe epilepsy. Epilepsia *53*, 1215–1224.

O'Neill, L.A. (2008). "Fine tuning" TLR signaling. Nat Immunol *9*, 459–461.

O'Neill, L.A., and Bowie, A.G. (2007). The family of five: TIR-domain-containing adaptors in Toll-like receptor signalling. Nat Rev Immunol *7*, 353–364.

O'Neill, L.A., and Dinarello, C.A. (2000). The IL-1 receptor/toll-like receptor superfamily: crucial receptors for inflammation and host defense. Immunol. Today *21*, 206–209.

Oo, M.L., Thangada, S., Wu, M.-T., Liu, C.H., Macdonald, T.L., Lynch, K.R., Lin, C.-Y., and Hla, T. (2007). Immunosuppressive and anti-angiogenic sphingosine 1-phosphate receptor-1 agonists induce ubiquitinylation and proteasomal degradation of the receptor. J. Biol. Chem. *282*, 9082–9089.

Ortinski, P.I., Dong, J., Mungenast, A., Yue, C., Takano, H., Watson, D.J., Haydon, P.G., and Coulter, D.A. (2010). Selective induction of astrocytic gliosis generates deficits in neuronal inhibition. Nat. Neurosci. *13*, 584–591.

Osinde, M., Mullershausen, F., and Dev, K.K. (2007). Phosphorylated FTY720 stimulates ERK phosphorylation in astrocytes via S1P receptors. Neuropharmacology *52*, 1210–1218.

Ostendorf, A.P., and Wong, M. (2015). mTOR inhibition in epilepsy: rationale and clinical perspectives. CNS Drugs *29*, 91–99.

Pan, G., Chen, Z., Zheng, H., Zhang, Y., Xu, H., Bu, G., Zheng, H., and Li, Y. (2018). Compensatory Mechanisms Modulate the Neuronal Excitability in a Kainic Acid-Induced Epilepsy Mouse Model. Front. Neural Circuits *12*.

Pan, L., Zhu, W., Li, C., Xu, X., Guo, L., and Lu, Q. (2012). Toll-like receptor 3 agonist Poly I:C protects against simulated cerebral ischemia in vitro and in vivo. Acta Pharmacol. Sin. *33*, 1246–1253.

Pan, L., Zhu, W., Li, Y., Xu, X., Guo, L., Lu, Q., and Wang, J. (2014). Astrocytic Toll-Like Receptor 3 Is Associated with Ischemic Preconditioning- Induced Protection against Brain Ischemia in Rodents. PLoS ONE *9*, e99526.

Paolicelli, R.C., Bisht, K., and Tremblay, M.-È. (2014). Fractalkine regulation of microglial physiology and consequences on the brain and behavior. Front. Cell. Neurosci. *8*, 129.

Papadopoulos, V., Baraldi, M., Guilarte, T.R., Knudsen, T.B., Lacapère, J.-J., Lindemann, P., Norenberg, M.D., Nutt, D., Weizman, A., Zhang, M.-R., et al. (2006). Translocator protein (18kDa): new nomenclature for the peripheral-type benzodiazepine receptor based on its structure and molecular function. Trends Pharmacol. Sci. *27*, 402–409.

Pardridge, W.M. (1999). Blood-brain barrier biology and methodology. J. Neurovirol. *5*, 556–569.

Parent, J.M. (2007). Adult neurogenesis in the intact and epileptic dentate gyrus. Prog. Brain Res. *163*, 529–540.

Parent, J.M., Yu, T.W., Leibowitz, R.T., Geschwind, D.H., Sloviter, R.S., and Lowenstein, D.H. (1997). Dentate granule cell neurogenesis is increased by seizures and contributes to aberrant network reorganization in the adult rat hippocampus. J. Neurosci. Off. J. Soc. Neurosci. *17*, 3727–3738.

Parvathenani, L.K., Tertyshnikova, S., Greco, C.R., Roberts, S.B., Robertson, B., and Posmantur, R. (2003). P2X7 mediates superoxide production in primary microglia and is up-regulated in a transgenic mouse model of Alzheimer's disease. J. Biol. Chem. *278*, 13309–13317.

Pascente, R., Frigerio, F., Rizzi, M., Porcu, L., Boido, M., Davids, J., Zaben, M., Tolomeo, D., Filibian, M., Gray, W.P., et al. (2016). Cognitive deficits and brain myo-Inositol are early biomarkers of epileptogenesis in a rat model of epilepsy. Neurobiol. Dis. *93*, 146–155.

Patel, A.K., and Hackam, A.S. (2014). A novel protective role for the innate immunity Toll-Like Receptor 3 (TLR3) in the retina via Stat3. Mol. Cell. Neurosci. *63*, 38–48.

Pauletti, A., Terrone, G., Shekh-Ahmad, T., Salamone A, Ravizza, T., Rizzi, M., Pastore, A., Pascente, R., Liang, L.P., Villa, B.R., et al. (2017). Targeting oxidative stress improves disease outcomes in a rat model of acquired epilepsy. Brain *in press*.

Pedrazzi, M., Patrone, M., Passalacqua, M., Ranzato, E., Colamassaro, D., Sparatore, B., Pontremoli, S., and Melloni, E. (2007). Selective proinflammatory activation of astrocytes by high-mobility group box 1 protein signaling. J Immunol *179*, 8525–8532.

Pekny, M., and Nilsson, M. (2005). Astrocyte activation and reactive gliosis. Glia *50*, 427–434.

Pekny, M., and Pekna, M. (2014). Astrocyte reactivity and reactive astrogliosis: costs and benefits. Physiol. Rev. *94*, 1077–1098.

Pernhorst, K., Herms, S., Hoffmann, P., Cichon, S., Schulz, H., Sander, T., Schoch, S., Becker, A.J., and Grote, A. (2013). TLR4, ATF-3 and IL8 inflammation mediator expression correlates with seizure frequency in human epileptic brain tissue. Seizure *22*, 675–678.

Persidsky, Y., Ramirez, S.H., Haorah, J., and Kanmogne, G.D. (2006). Blood-brain barrier: structural components and function under physiologic and pathologic conditions. J. Neuroimmune Pharmacol. Off. J. Soc. NeuroImmune Pharmacol. *1*, 223–236.

Pitkänen, A., and Engel, J. (2014). Past and present definitions of epileptogenesis and its biomarkers. Neurother. J. Am. Soc. Exp. Neurother. *11*, 231–241.

Pitkänen, A., and Kubova, H. (2004). Antiepileptic drugs in neuroprotection. Expert Opin. Pharmacother. *5*, 777–798.

Pitkänen, A., and Lukasiuk, K. (2009). Molecular and cellular basis of epileptogenesis in symptomatic epilepsy. Epilepsy Behav. *14*, 16–25.

Pitkänen, A., and Lukasiuk, K. (2011). Mechanisms of epileptogenesis and potential treatment targets. Lancet Neurol. *10*, 173–186.

Pitkänen, A., and Sutula, T.P. (2002). Is epilepsy a progressive disorder? Prospects for new therapeutic approaches in temporal-lobe epilepsy. Lancet Neurol. *1*, 173–181.

Pitkänen, A., Nehlig, A., Brooks-Kayal, A.R., Dudek, F.E., Friedman, D., Galanopoulou, A.S., Jensen, F.E., Kaminski, R.M., Kapur, J., Klitgaard, H., et al. (2013). Issues related to development of antiepileptogenic therapies. Epilepsia *54 Suppl 4*, 35–43.

Pitkänen, A., Lukasiuk, K., Dudek, F.E., and Staley, K.J. (2015). Epileptogenesis. Cold Spring Harb. Perspect. Med. *5*.

Pitsch, J., Kuehn, J.C., Gnatkovsky, V., Müller, J.A., van Loo, K.M.J., de Curtis, M., Vatter, H., Schoch, S., Elger, C.E., and Becker, A.J. (2018). Anti-epileptogenic and Anti-convulsive Effects of Fingolimod in Experimental Temporal Lobe Epilepsy. Mol. Neurobiol.

Polascheck, N., Bankstahl, M., and Loscher, W. (2010). The COX-2 inhibitor parecoxib is neuroprotective but not antiepileptogenic in the pilocarpine model of temporal lobe epilepsy. Exp Neurol *224*, 219–233.

Portnoy, E., Polyak, B., Inbar, D., Kenan, G., Rai, A., Wehrli, S.L., Roberts, T.P.L., Bishara, A., Mann, A., Shmuel, M., et al. (2016). Tracking inflammation in the epileptic rat brain by bi-functional fluorescent and magnetic nanoparticles. Nanomedicine Nanotechnol. Biol. Med. *12*, 1335–1345.

Pottier, G., Gómez-Vallejo, V., Padro, D., Boisgard, R., Dollé, F., Llop, J., Winkeler, A., and Martín, A. (2017). PET imaging of cannabinoid type 2 receptors with [11C]A-836339 did not evidence changes following neuroinflammation in rats. J. Cereb. Blood Flow Metab. Off. J. Int. Soc. Cereb. Blood Flow Metab. *37*, 1163–1178.

van Praag, H., Schinder, A.F., Christie, B.R., Toni, N., Palmer, T.D., and Gage, F.H. (2002). Functional neurogenesis in the adult hippocampus. Nature *415*, 1030–1034.

Prabowo, A.S., Iyer, A.M., Veersema, T.J., Anink, J.J., Schouten-van Meeteren, A.Y., Spliet, W.G., van Rijen, P.C., Ferrier, C.H., Capper, D., Thom, M., et al. (2013). BRAF V600E mutation is associated with mTOR signaling activation in glioneuronal tumors. Brain Pathol *24*, 52–66.

Préhaud, C., Mégret, F., Lafage, M., and Lafon, M. (2005). Virus infection switches TLR-3-positive human neurons to become strong producers of beta interferon. J. Virol. *79*, 12893–12904.

Price, J.C., Guan, S., Burlingame, A., Prusiner, S.B., and Ghaemmaghami, S. (2010). Analysis of proteome dynamics in the mouse brain. Proc. Natl. Acad. Sci. *107*, 14508–14513.

Priya, R., Patro, I.K., and Parida, M.M. (2014). TLR3 mediated innate immune response in mice brain following infection with Chikungunya virus. Virus Res. *189*, 194–205.

Quinn, S.R., and O'Neill, L.A. (2011). A trio of microRNAs that control Toll-like receptor signalling. Int Immunol *23*, 421–425.

Raabe, A., Schmitz, A.K., Pernhorst, K., Grote, A., von der Brelie, C., Urbach, H., Friedman, A., Becker, A.J., Elger, C.E., and Niehusmann, P. (2012). Cliniconeuropathologic correlations show astroglial albumin storage as a common factor in epileptogenic vascular lesions. Epilepsia *53*, 539–548.

Radu, B.M., Epureanu, F.B., Radu, M., Fabene, P.F., and Bertini, G. (2017). Nonsteroidal anti-inflammatory drugs in clinical and experimental epilepsy. Epilepsy Res. *131*, 15–27.

Rakhade, S.N., and Jensen, F.E. (2009). Epileptogenesis in the immature brain: emerging mechanisms. Nat. Rev. Neurol. *5*, 380.

Ralay Ranaivo, H., and Wainwright, M.S. (2010). Albumin activates astrocytes and microglia through mitogen-activated protein kinase pathways. Brain Res. *1313*, 222–231.

Ralay Ranaivo, H., Patel, F., and Wainwright, M.S. (2010). Albumin activates the canonical TGF receptor-smad signaling pathway but this is not required for activation of astrocytes. Exp. Neurol. *226*, 310–319.

Ransohoff, R.M., and Perry, V.H. (2009). Microglial Physiology: Unique Stimuli, Specialized Responses. Annu. Rev. Immunol. *27*, 119–145.

Rappold, P.M., Lynd-Balta, E., and Joseph, S.A. (2006). P2X7 receptor immunoreactive profile confined to resting and activated microglia in the epileptic brain. Brain Res. *1089*, 171–178.

Ravizza, T., and Vezzani, A. (2006). Status epilepticus induces time-dependent neuronal and astrocytic expression of interleukin-1 receptor type I in the rat limbic system. Neuroscience *137*, 301–308.

Ravizza, T., Moneta, D., Bottazzi, B., Peri, G., Garlanda, C., Hirsch, E., Richards, G.., Mantovani, A., and Vezzani, A. (2001). Dynamic induction of the long pentraxin PTX3 in the CNS after limbic seizures: evidence for a protective role in seizure-induced neurodegeneration. Neuroscience *105*, 43–53.

Ravizza, T., Boer, K., Redeker, S., Spliet, W.G., van Rijen, P.C., Troost, D., Vezzani, A., and Aronica, E. (2006a). The IL-1beta system in epilepsy-associated malformations of cortical development. Neurobiol Dis *24*, 128–143.

Ravizza, T., Lucas, S.M., Balosso, S., Bernardino, L., Ku, G., Noe, F., Malva, J., Randle, J.C., Allan, S., and Vezzani, A. (2006b). Inactivation of caspase-1 in rodent brain: a novel anticonvulsive strategy. Epilepsia *47*, 1160–1168.

Ravizza, T., Gagliardi, B., Noe, F., Boer, K., Aronica, E., and Vezzani, A. (2008a). Innate and adaptive immunity during epileptogenesis and spontaneous seizures: evidence from experimental models and human temporal lobe epilepsy. Neurobiol Dis *29*, 142–160.

Ravizza, T., Noe, F., Zardoni, D., Vaghi, V., Sifringer, M., and Vezzani, A. (2008b). Interleukin Converting Enzyme inhibition impairs kindling epileptogenesis in rats by blocking astrocytic IL-1beta production. Neurobiol Dis *31*, 327–333.

Reinert, L.S., Harder, L., Holm, C.K., Iversen, M.B., Horan, K.A., Dagnæs-Hansen, F., Ulhøi, B.P., Holm, T.H., Mogensen, T.H., Owens, T., et al. (2012). TLR3 deficiency renders astrocytes permissive to herpes simplex virus infection and facilitates establishment of CNS infection in mice. J. Clin. Invest. *122*, 1368–1376.

Reschke, C.R., Silva, L.F.A., Norwood, B.A., Senthilkumar, K., Morris, G., Sanz-Rodriguez, A., Conroy, R.M., Costard, L., Neubert, V., Bauer, S., et al. (2017). Potent Anti-seizure Effects of Locked Nucleic Acid Antagomirs Targeting miR-134 in Multiple Mouse and Rat Models of Epilepsy. Mol. Ther. - Nucleic Acids *6*, 45–56.

Riban, V., Bouilleret, V., Pham-Le, B.T., Fritschy, J.M., Marescaux, C., and Depaulis, A. (2002). Evolution of hippocampal epileptic activity during the development of hippocampal sclerosis in a mouse model of temporal lobe epilepsy. Neuroscience *112*, 101–111.

Rigau, V., Morin, M., Rousset, M.C., de Bock, F., Lebrun, A., Coubes, P., Picot, M.C., Baldy-Moulinier, M., Bockaert, J., Crespel, A., et al. (2007). Angiogenesis is associated with blood-brain barrier permeability in temporal lobe epilepsy. Brain *130*, 1942–1956.

Robel, S., and Sontheimer, H. (2016). Glia as drivers of abnormal neuronal activity. Nat. Neurosci. *19*, 28–33.

Robel, S., Buckingham, S.C., Boni, J.L., Campbell, S.L., Danbolt, N.C., Riedemann, T., Sutor, B., and Sontheimer, H. (2015). Reactive Astrogliosis Causes the Development of Spontaneous Seizures. J. Neurosci. *35*, 3330–3345.

Roch, C., Leroy, C., Nehlig, A., and Namer, I.J. (2002). Magnetic resonance imaging in the study of the lithium-pilocarpine model of temporal lobe epilepsy in adult rats. Epilepsia *43*, 325–335.

Rodgers, K.M., Hutchinson, M.R., Northcutt, A., Maier, S.F., Watkins, L.R., and Barth, D.S. (2009). The cortical innate immune response increases local neuronal excitability leading to seizures. Brain *132*, 2478–2486.

Rodríguez-Arellano, J.J., Parpura, V., Zorec, R., and Verkhratsky, A. (2016). Astrocytes in physiological aging and Alzheimer's disease. Neuroscience *323*, 170–182.

Roncon, P., Soukupovà, M., Binaschi, A., Falcicchia, C., Zucchini, S., Ferracin, M., Langley, S.R., Petretto, E., Johnson, M.R., Marucci, G., et al. (2015). MicroRNA profiles in hippocampal granule cells and plasma of rats with pilocarpine-induced epilepsy--comparison with human epileptic samples. Sci. Rep. *5*, 14143.

Roseti, C., Fucile, S., Lauro, C., Martinello, K., Bertollini, C., Esposito, V., Mascia, A., Catalano, M., Aronica, E., Limatola, C., et al. (2013). Fractalkine/CX3CL1 modulates GABAA currents in human temporal lobe epilepsy. Epilepsia *54*, 1834–1844.

Roseti, C., van Vliet, E.A., Cifelli, P., Ruffolo, G., Baayen, J.C., Di Castro, M.A., Bertollini, C., Limatola, C., Aronica, E., Vezzani, A., et al. (2015). GABA currents are decreased by IL-1beta in epileptogenic tissue of patients with temporal lobe epilepsy: implications for ictogenesis. Neurobiol Dis *82*, 311–320.

Rostène, W., Kitabgi, P., and Parsadaniantz, S.M. (2007). Chemokines: a new class of neuromodulator? Nat. Rev. Neurosci. *8*, 895–903.

Rothermundt, M., Peters, M., Prehn, J.H.M., and Arolt, V. (2003). S100B in brain damage and neurodegeneration. Microsc. Res. Tech. *60*, 614–632.

Rothhammer, V., Mascanfroni, I.D., Bunse, L., Takenaka, M.C., Kenison, J.E., Mayo, L., Chao, C.-C., Patel, B., Yan, R., Blain, M., et al. (2016). Type I interferons and microbial metabolites of tryptophan modulate astrocyte activity and central nervous system inflammation via the aryl hydrocarbon receptor. Nat. Med. *22*, 586–597.

Rothhammer, V., Kenison, J.E., Tjon, E., Takenaka, M.C., de Lima, K.A., Borucki, D.M., Chao, C.-C., Wilz, A., Blain, M., Healy, L., et al. (2017). Sphingosine 1-phosphate receptor modulation suppresses pathogenic astrocyte activation and chronic progressive CNS inflammation. Proc. Natl. Acad. Sci. U. S. A. *114*, 2012–2017.

Rubí, S., Costes, N., Heckemann, R.A., Bouvard, S., Hammers, A., Martí Fuster, B., Ostrowsky, K., Montavont, A., Jung, J., Setoain, X., et al. (2013). Positron emission tomography with α-[11C]methyl-L-tryptophan in tuberous sclerosis complex-related epilepsy. Epilepsia *54*, 2143–2150.

Rupprecht, R., Papadopoulos, V., Rammes, G., Baghai, T.C., Fan, J., Akula, N., Groyer, G., Adams, D., and Schumacher, M. (2010). Translocator protein (18 kDa) (TSPO) as a therapeutic target for neurological and psychiatric disorders. Nat. Rev. Drug Discov. *9*, 971–988.

Russmann, V., Brendel, M., Mille, E., Helm-Vicidomini, A., Beck, R., Günther, L., Lindner, S., Rominger, A., Keck, M., Salvamoser, J.D., et al. (2017). Identification of brain regions predicting epileptogenesis by serial [18F]GE-180 positron emission tomography imaging of neuroinflammation in a rat model of temporal lobe epilepsy. NeuroImage Clin. *15*, 35–44.

Ryu, J.K., and McLarnon, J.G. (2009). A leaky blood-brain barrier, fibrinogen infiltration and microglial reactivity in inflamed Alzheimer's disease brain. J. Cell. Mol. Med. *13*, 2911–2925.

Sakatani, S., Seto-Ohshima, A., Shinohara, Y., Yamamoto, Y., Yamamoto, H., Itohara, S., and Hirase, H. (2008). Neural-activity-dependent release of S100B from astrocytes enhances kainate-induced gamma oscillations in vivo. J Neurosci *28*, 10928–10936.

Santillo, A.F., Gambini, J.P., Lannfelt, L., Långström, B., Ulla-Marja, L., Kilander, L., and Engler, H. (2011). In vivo imaging of astrocytosis in Alzheimer's disease: an 11C-L-deuteriodeprenyl and PIB PET study. Eur. J. Nucl. Med. Mol. Imaging *38*, 2202–2208.

Sasaki, M., Kuwabara, Y., Yoshida, T., Fukumura, T., Morioka, T., Nishio, S., Fukui, M., and Masuda, K. (1998). Carbon-11-methionine PET in focal cortical dysplasia: A comparison with fluorine-18-FDG PET and technetium-99m-ECD SPECT. J. Nucl. Med. *39*, 974–977.

Sato, K., Ishikawa, K., Ui, M., and Okajima, F. (1999). Sphingosine 1-phosphate induces expression of early growth response-1 and fibroblast growth factor-2 through mechanism involving extracellular signal-regulated kinase in astroglial cells. Brain Res. Mol. Brain Res. *74*, 182–189.

Saura, J., Luque, J.M., Cesura, A.M., Prada, M.D., Chan-Palay, V., Huber, G., Löffler, J., and Richards, J.G. (1994). Increased monoamine oxidase b activity in plaque-associated astrocytes of Alzheimer brains revealed by quantitative enzyme radioautography. Neuroscience *62*, 15–30.

Sauvageau, A., Desjardins, P., Lozeva, V., Rose, C., Hazell, A.S., Bouthillier, A., and Butterworth, R.F. (2002). Increased Expression of "Peripheral-Type" Benzodiazepine Receptors in Human Temporal Lobe Epilepsy: Implications for PET Imaging of Hippocampal Sclerosis. Metab. Brain Dis. *17*, 3–11.

Sauvageot, C.M., and Stiles, C.D. (2002). Molecular mechanisms controlling cortical gliogenesis. Curr. Opin. Neurobiol. *12*, 244–249.

Sayyah, M., Javad-Pour, M., and Ghazi-Khansari, M. (2003). The bacterial endotoxin lipopolysaccharide enhances seizure susceptibility in mice: involvement of proinflammatory factors: nitric oxide and prostaglandins. Neuroscience *122*, 1073–1080.

Scharfman, H.E., Goodman, J.H., and Sollas, A.L. (2000). Granule-like neurons at the hilar/CA3 border after status epilepticus and their synchrony with area CA3 pyramidal cells: functional implications of seizure-induced neurogenesis. J. Neurosci. Off. J. Soc. Neurosci. *20*, 6144–6158.

Schitine, C., Nogaroli, L., Costa, M.R., and Hedin-Pereira, C. (2015). Astrocyte heterogeneity in the brain: from development to disease. Front. Cell. Neurosci. *9*.

Scumpia, P.O., Kelly, K.M., Reeves, W.H., and Stevens, B.R. (2005). Double-stranded RNA signals antiviral and inflammatory programs and dysfunctional glutamate transport in TLR3-expressing astrocytes. Glia *52*, 153–162.

Seifert, G., Carmignoto, G., and Steinhäuser, C. (2010). Astrocyte dysfunction in epilepsy. Brain Res. Rev. *63*, 212–221.

Seiffert, E., Dreier, J.P., Ivens, S., Bechmann, I., Tomkins, O., Heinemann, U., and Friedman, A. (2004). Lasting blood-brain barrier disruption induces epileptic focus in the rat somatosensory cortex. J Neurosci *24*, 7829–7836.

Semple, B.D., O'Brien, T.J., Gimlin, K., Wright, D.K., Kim, S.E., Casillas-Espinosa, P.M., Webster, K.M., Petrou, S., and Noble-Haeusslein, L.J. (2017). Interleukin-1 Receptor in Seizure Susceptibility after Traumatic Injury to the Pediatric Brain. J. Neurosci. Off. J. Soc. Neurosci. *37*, 7864–7877.

Shirakawa, F., Saito, K., Bonagura, C.A., Galson, D.L., Fenton, M.J., Webb, A.C., and Auron, P.E. (1993). The human prointerleukin 1 beta gene requires DNA sequences both proximal and distal to the transcription start site for tissue-specific induction. Mol. Cell. Biol. *13*, 1332–1344.

Shlosberg, D., Benifla, M., Kaufer, D., and Friedman, A. (2010). Blood-brain barrier breakdown as a therapeutic target in traumatic brain injury. Nat. Rev. Neurol. *6*, 393–403.

Silver, J., and Miller, J.H. (2004). Regeneration beyond the glial scar. Nat. Rev. Neurosci. *5*, 146–156.

Sloviter, R.S., Zappone, C.A., Harvey, B.D., and Frotscher, M. (2006). Kainic acid-induced recurrent mossy fiber innervation of dentate gyrus GABAergic interneurons. J. Comp. Neurol. *494*, 944–960.

Sofroniew, M.V. (2014). Astrogliosis. Cold Spring Harb. Perspect. Biol. *7*, a020420.

Sofroniew, M.V. (2015). Astrocyte barriers to neurotoxic inflammation. Nat. Rev. Neurosci. *16*, 249–263.

Sofroniew, M.V., and Vinters, H.V. (2010). Astrocytes: biology and pathology. Acta Neuropathol. (Berl.) *119*, 7–35.

Soliven, B., Miron, V., and Chun, J. (2011). The neurobiology of sphingosine 1-phosphate signaling and sphingosine 1-phosphate receptor modulators. Neurology *76*, S9-14.

Sotgiu, S., Murrighile M. R, and Constantin G (2010). Treatment of refractory epilepsy with natalizumab in a apatient with multiple sclerosis. Case report. BMC Neurol. *10*, 84.

Spampinato, S.F., Obermeier, B., Cotleur, A., Love, A., Takeshita, Y., Sano, Y., Kanda, T., and Ransohoff, R.M. (2015). Sphingosine 1 Phosphate at the Blood Brain Barrier: Can the Modulation of S1P Receptor 1 Influence the Response of Endothelial Cells and Astrocytes to Inflammatory Stimuli? PloS One *10*, e0133392.

Spiegel, S., and Milstien, S. (2011). The outs and the ins of sphingosine-1-phosphate in immunity. Nat. Rev. Immunol. *11*, 403–415.

Stafstrom, C.E., Thompson, J.L., and Holmes, G.L. (1992). Kainic acid seizures in the developing brain: status epilepticus and spontaneous recurrent seizures. Brain Res Dev Brain Res *65*, 227–236.

Steinhäuser, C., and Seifert, G. (2012). Astrocyte dysfunction in epilepsy. In Jasper's Basic Mechanisms of the Epilepsies, J.L. Noebels, M. Avoli, M.A. Rogawski, R.W. Olsen, and A.V. Delgado-Escueta, eds. (Bethesda (MD): National Center for Biotechnology Information (US)), p.

Stella, N. (2009). Endocannabinoid signaling in microglial cells. Neuropharmacology *56 Suppl 1*, 244–253.

Stellwagen, D., Beattie, E.C., Seo, J.Y., and Malenka, R.C. (2005). Differential regulation of AMPA receptor and GABA receptor trafficking by tumor necrosis factor-alpha. J Neurosci *25*, 3219–3228.

Stoll, G., and Bendszus, M. (2009). Imaging of inflammation in the peripheral and central nervous system by magnetic resonance imaging. Neuroscience *158*, 1151–1160.

Stoll, G., Jander, S., and Schroeter, M. (2000). Cytokines in CNS disorders: neurotoxicity versus neuroprotection. J. Neural Transm. Suppl. *59*, 81–89.

Su, H., Sochivko, D., Becker, A., Chen, J., Jiang, Y., Yaari, Y., and Beck, H. (2002). Upregulation of a T-type Ca2+ channel causes a long-lasting modification of neuronal firing mode after status epilepticus. J. Neurosci. Off. J. Soc. Neurosci. *22*, 3645–3655.

Sweatt, J.D. (2013). The emerging field of neuroepigenetics. Neuron *80*, 624–632.

Taga, T., and Fukuda, S. (2005). Role of IL-6 in the neural stem cell differentiation. Clin. Rev. Allergy Immunol. *28*, 249–256.

Taganov, K.D., Boldin, M.P., Chang, K.J., and Baltimore, D. (2006). NF-kappaB-dependent induction of microRNA miR-146, an inhibitor targeted to signaling proteins of innate immune responses. Proc Natl Acad Sci U A *103*, 12481–12486.

Takeda, K., and Akira, S. (2004). TLR signaling pathways. Semin. Immunol. *16*, 3–9.

Takemiya, T., Suzuki, K., Sugiura, H., Yasuda, S., Yamagata, K., Kawakami, Y., and Maru, E. (2003). Inducible brain COX-2 facilitates the recurrence of hippocampal seizures in mouse rapid kindling. Prostaglandins Lipid Mediat *71*, 205–216.

Takenouchi, T., Fujita, M., Sugama, S., Kitani, H., and Hashimoto, M. (2009). The role of the P2X7 receptor signaling pathway for the release of autolysosomes in microglial cells. Autophagy *5*, 723–724.

Tarassishin, L., Loudig, O., Bauman, A., Shafit-Zagardo, B., Suh, H.-S., and Lee, S.C. (2011a). Interferon regulatory factor 3 inhibits astrocyte inflammatory gene expression through suppression of the proinflammatory miR-155 and miR-155*. Glia *59*, 1911–1922.

Tarassishin, L., Suh, H.-S., and Lee, S.C. (2011b). Interferon regulatory factor 3 plays an anti-inflammatory role in microglia by activating the PI3K/Akt pathway. J. Neuroinflammation *8*, 187.

Taylor, M.W., and Feng, G. (1991). Relationship between interferon-γ, indoleamine 2,3-dioxygenase, and tryptophan catabolism. FASEB J. *5*, 2516–2522.

Taylor, D.L., Jones, F., Kubota, E.S.F.C.S., and Pocock, J.M. (2005). Stimulation of microglial metabotropic glutamate receptor mGlu2 triggers tumor necrosis factor alpha-induced neurotoxicity in concert with microglial-derived Fas ligand. J. Neurosci. Off. J. Soc. Neurosci. *25*, 2952–2964.

Tchekalarova, J.D., Ivanova, N.M., Pechlivanova, D.M., Atanasova, D., Lazarov, N., Kortenska, L., Mitreva, R., Lozanov, V., and Stoynev, A. (2014). Antiepileptogenic and neuroprotective effects of losartan in kainate model of temporal lobe epilepsy. Pharmacol. Biochem. Behav. *127*, 27–36.

Tchekalarova, J.D., Ivanova, N., Atanasova, D., Pechlivanova, D.M., Lazarov, N., Kortenska, L., Mitreva, R., Lozanov, V., and Stoynev, A. (2016). Long-Term Treatment with Losartan Attenuates Seizure Activity and Neuronal Damage Without Affecting Behavioral Changes in a Model of Co-morbid Hypertension and Epilepsy. Cell. Mol. Neurobiol. *36*, 927–941.

Territo, P.R., Meyer, J.A., Peters, J.S., Riley, A.A., McCarthy, B.P., Gao, M., Wang, M., Green, M.A., Zheng, Q.-H., and Hutchins, G.D. (2017). Characterization of 11C-GSK1482160 for Targeting the P2X7 Receptor as a Biomarker for Neuroinflammation. J. Nucl. Med. Off. Publ. Soc. Nucl. Med. *58*, 458–465.

Terrone, G., Pauletti, A., Salamone, A., Rizzi, M., Villa, B.R., Porcu, L., Sheehan, M.J., Guilmette, E., Butler, C.R., Piro, J.R., et al. (2018). Inhibition of monoacylglycerol lipase terminates diazepam-

resistant status epilepticus in mice and its effects are potentiated by a ketogenic diet. Epilepsia *59*, 79–91.

Toda, Y., Tsukada, J., Misago, M., Kominato, Y., Auron, P.E., and Tanaka, Y. (2002). Autocrine induction of the human pro-IL-1beta gene promoter by IL-1beta in monocytes. J. Immunol. Baltim. Md 1950 *168*, 1984–1991.

Tolón, R.M., Núñez, E., Pazos, M.R., Benito, C., Castillo, A.I., Martínez-Orgado, J.A., and Romero, J. (2009). The activation of cannabinoid CB2 receptors stimulates in situ and in vitro beta-amyloid removal by human macrophages. Brain Res. *1283*, 148–154.

Tomkins, O., Kaufer, D., Korn, A., Shelef, I., Golan, H., Reichenthal, E., Soreq, H., and Friedman, A. (2001). Frequent blood-brain barrier disruption in the human cerebral cortex. Cell Mol Neurobiol *21*, 675–691.

Tomkins, O., Feintuch, A., Benifla, M., Cohen, A., Friedman, A., and Shelef, I. (2011). Blood-brain barrier breakdown following traumatic brain injury: a possible role in posttraumatic epilepsy. Cardiovasc. Psychiatry Neurol. *2011*, 765923.

Toni, N., Laplagne, D.A., Zhao, C., Lombardi, G., Ribak, C.E., Gage, F.H., and Schinder, A.F. (2008). Neurons born in the adult dentate gyrus form functional synapses with target cells. Nat. Neurosci. *11*, 901–907.

Trinka, E., Cock, H., Hesdorffer, D., Rossetti, A.O., Scheffer, I.E., Shinnar, S., Shorvon, S., and Lowenstein, D.H. (2015). A definition and classification of status epilepticus--Report of the ILAE Task Force on Classification of Status Epilepticus. Epilepsia *56*, 1515–1523.

Troy, T., Jekic-McMullen, D., Sambucetti, L., and Rice, B. (2004). Quantitative comparison of the sensitivity of detection of fluorescent and bioluminescent reporters in animal models. Mol. Imaging *3*, 9–23.

Tu, B., and Bazan, N.G. (2003). Hippocampal kindling epileptogenesis upregulates neuronal cyclooxygenase-2 expression in neocortex. Exp Neurol *179*, 167–175.

Turkdogan-Sozuer, D., Ozek, M.M., Sav, A., Dincer, A., and Pamir, M.N. (2000). Serial MRI and MRS studies with unusual findings in Rasmussen's encephalitis. Eur Radiol *10*, 962–966.

Turrin, N.P., and Rivest, S. (2004). Innate immune reaction in response to seizures: implications for the neuropathology associated with epilepsy. Neurobiol Dis *16*, 321–334.

Turski, W.A., Cavalheiro, E.A., Schwarz, M., Czuczwar, S.J., Kleinrok, Z., and Turski, L. (1983). Limbic seizures produced by pilocarpine in rats: behavioural, electroencephalographic and neuropathological study. Behav Brain Res *9*, 315–335.

Udani, V., Pujar, S., Munot, P., Maheshwari, S., and Mehta, N. (2007). Natural history and magnetic resonance imaging follow-up in 9 Sturge-Weber Syndrome patients and clinical correlation. J. Child Neurol. *22*, 479–483.

Ueda, Y., Doi, T., Tokumaru, J., Yokoyama, H., Nakajima, A., Mitsuyama, Y., Ohya-Nishiguchi, H., Kamada, H., and Willmore, L.J. (2001). Collapse of extracellular glutamate regulation during epileptogenesis: down-regulation and functional failure of glutamate transporter function in rats with chronic seizures induced by kainic acid. J. Neurochem. *76*, 892–900.

Ulmann, L., Levavasseur, F., Avignone, E., Peyroutou, R., Hirbec, H., Audinat, E., and Rassendren, F. (2013). Involvement of P2X4 receptors in hippocampal microglial activation after status epilepticus. Glia *61*, 1306–1319.

van Rossum, D., and Hanisch, U.-K. (2004). Microglia. Metab. Brain Dis. *19*, 393–411.

van Scheppingen, J., Iyer, A.M., Prabowo, A.S., Muhlebner, A., Anink, J.J., Scholl, T., Feucht, M., Jansen, F.E., Spliet, W.G., Krsek, P., et al. (2016). Expression of microRNAs miR21, miR146a, and miR155 in tuberous sclerosis complex cortical tubers and their regulation in human astrocytes and SEGA-derived cell cultures. Glia *64*, 1066–1082.

van Stuijvenberg, M., Derksen-Lubsen, G., Steyerberg, E.W., Habbema, J.D., and Moll, H.A. (1998). Randomized, controlled trial of ibuprofen syrup administered during febrile illnesses to prevent febrile seizure recurrences. Pediatrics *102*, E51.

Varella, P.P.V., Santiago, J.F.C., Carrete, H., Higa, E.M.S., Yacubian, E.M.T., Centeno, R.S., Caboclo, L.O.S.F., Castro Neto, E.F. de, Canzian, M., Amado, D., et al. (2011). Relationship between fluid-attenuated inversion-recovery (FLAIR) signal intensity and inflammatory mediator's levels in the hippocampus of patients with temporal lobe epilepsy and mesial temporal sclerosis. Arq. Neuropsiquiatr. *69*, 91–99.

Vargas-Sánchez, K., Mogilevskaya, M., Rodríguez-Pérez, J., Rubiano, M.G., Javela, J.J., and González-Reyes, R.E. (2018). Astroglial role in the pathophysiology of status epilepticus: an overview. Oncotarget *9*, 26954–26976.

Varvel, N.H., Neher, J.J., Bosch, A., Wang, W., Ransohoff, R.M., Miller, R.J., and Dingledine, R. (2016). Infiltrating monocytes promote brain inflammation and exacerbate neuronal damage after status epilepticus. Proc. Natl. Acad. Sci. *113*, E5665–E5674.

Veldhuis, W.B., Derksen, J.W., Floris, S., Van Der Meide, P.H., De Vries, H.E., Schepers, J., Vos, I.M.P., Dijkstra, C.D., Kappelle, L.J., Nicolay, K., et al. (2003). Interferon-beta blocks infiltration of inflammatory cells and reduces infarct volume after ischemic stroke in the rat. J. Cereb. Blood Flow Metab. Off. J. Int. Soc. Cereb. Blood Flow Metab. *23*, 1029–1039.

Verkhratsky, A., Rodríguez, J.J., and Parpura, V. (2013). Astroglia in neurological diseases. Future Neurol. *8*, 149–158.

Verma, R., and Bharti, K. (2017). Toll like receptor 3 and viral infections of nervous system. J. Neurol. Sci. *372*, 40–48.

Vezzani, A., and Friedman, A. (2011). Brain inflammation as a biomarker in epilepsy. Biomark Med *5*, 607–614.

Vezzani, A., and Granata, T. (2005). Brain inflammation in epilepsy: experimental and clinical evidence. Epilepsia *46*, 1724–1743.

Vezzani, A., Conti, M., De Luigi, A., Ravizza, T., Moneta, D., Marchesi, F., and De Simoni, M.G. (1999). Interleukin-1beta immunoreactivity and microglia are enhanced in the rat hippocampus by focal kainate application: functional evidence for enhancement of electrographic seizures. J Neurosci *19*, 5054–5065.

Vezzani, A., Moneta, D., Conti, M., Richichi, C., Ravizza, T., De Luigi, A., De Simoni, M.G., Sperk, G., Andell-Jonsson, S., Lundkvist, J., et al. (2000). Powerful anticonvulsant action of IL-1 receptor

antagonist on intracerebral injection and astrocytic overexpression in mice. Proc Natl Acad Sci U A *97*, 11534–11539.

Vezzani, A., Balosso, S., and Ravizza, T. (2008). The role of cytokines in the pathophysiology of epilepsy. Brain. Behav. Immun. *22*, 797–803.

Vezzani, A., Balosso, S., Maroso, M., Zardoni, D., Noe, F., and Ravizza, T. (2010). ICE/caspase 1 inhibitors and IL-1beta receptor antagonists as potential therapeutics in epilepsy. Curr Opin Investig Drugs *11*, 43–50.

Vezzani, A., French, J., Bartfai, T., and Baram, T.Z. (2011a). The role of inflammation in epilepsy. Nat. Rev. Neurol. *7*, 31–40.

Vezzani, A., Maroso, M., Balosso, S., Sanchez, M.A., and Bartfai, T. (2011b). IL-1 receptor/Toll-like receptor signaling in infection, inflammation, stress and neurodegeneration couples hyperexcitability and seizures. Brain Behav Immun *25*, 1281–1289.

Vezzani, A., Bartfai, T., Bianchi, M., Rossetti, C., and French, J. (2011c). Therapeutic potential of new antiinflammatory drugs. Epilepsia *52*, 67–69.

Vezzani, A., Lang, B., and Aronica, E. (2015). Immunity and Inflammation in Epilepsy. Cold Spring Harb. Perspect. Med. *6*, a022699.

Vezzani, A., Fujinami, R.S., White, H.S., Preux, P.-M., Blümcke, I., Sander, J.W., and Löscher, W. (2016). Infections, inflammation and epilepsy. Acta Neuropathol. (Berl.) *131*, 211–234.

Villapol, S., Balarezo, M.G., Affram, K., Saavedra, J.M., and Symes, A.J. (2015). Neurorestoration after traumatic brain injury through angiotensin II receptor blockage. Brain J. Neurol. *138*, 3299–3315.

Viviani, B., Bartesaghi, S., Gardoni, F., Vezzani, A., Behrens, M.M., Bartfai, T., Binaglia, M., Corsini, E., Di Luca, M., Galli, C.L., et al. (2003). Interleukin-1beta enhances NMDA receptor-mediated intracellular calcium increase through activation of the Src family of kinases. J Neurosci *23*, 8692–8700.

Viviani, B., Gardoni, F., and Marinovich, M. (2007). Cytokines and neuronal ion channels in health and disease. Int. Rev. Neurobiol. *82*, 247–263.

van Vliet, E.A., da Costa Araújo, S., Redeker, S., van Schaik, R., Aronica, E., and Gorter, J.A. (2007). Blood-brain barrier leakage may lead to progression of temporal lobe epilepsy. Brain J. Neurol. *130*, 521–534.

van Vliet, E.A., Zibell, G., Pekcec, A., Schlichtiger, J., Edelbroek, P.M., Holtman, L., Aronica, E., Gorter, J.A., and Potschka, H. (2010). COX-2 inhibition controls P-glycoprotein expression and promotes brain delivery of phenytoin in chronic epileptic rats. Neuropharmacology *58*, 404–412.

van Vliet, E.A., Otte, W.M., Gorter, J.A., Dijkhuizen, R.M., and Wadman, W.J. (2014). Longitudinal assessment of blood-brain barrier leakage during epileptogenesis in rats. A quantitative MRI study. Neurobiol. Dis. *63*, 74–84.

van Vliet, E.A., Aronica, E., and Gorter, J.A. (2015). Blood-brain barrier dysfunction, seizures and epilepsy. Semin Cell Dev Biol *38*, 26–34.

van Vliet, E.A., Otte, W.M., Wadman, W.J., Aronica, E., Kooij, G., de Vries, H.E., Dijkhuizen, R.M., and Gorter, J.A. (2016). Blood-brain barrier leakage after status epilepticus in rapamycin-treated rats II: Potential mechanisms. Epilepsia *57*, 70–78.

van Vliet, E.A., Aronica, E., Vezzani, A., and Ravizza, T. (2018). Review: Neuroinflammatory pathways as treatment targets and biomarker candidates in epilepsy: emerging evidence from preclinical and clinical studies. Neuropathol. Appl. Neurobiol. *44*, 91–111.

Walker (2017). Molecular isoforms of HMGB1 are novel mechanistic biomarkers for epilepsy. J. Clin. Invest. in press.

Walker, L., and Sills, G.J. (2012). Inflammation and Epilepsy: The Foundations for a New Therapeutic Approach in Epilepsy? Epilepsy Curr. *12*, 8–12.

Wang, P.-F., Fang, H., Chen, J., Lin, S., Liu, Y., Xiong, X.-Y., Wang, Y.-C., Xiong, R.-P., lv, F.-L., Wang, J., et al. (2014). Polyinosinic-Polycytidylic Acid Has Therapeutic Effects against Cerebral Ischemia/Reperfusion Injury through the Downregulation of TLR4 Signaling via TLR3. J. Immunol. *192*, 4783–4794.

Wang, T., Town, T., Alexopoulou, L., Anderson, J.F., Fikrig, E., and Flavell, R.A. (2004). Toll-like receptor 3 mediates West Nile virus entry into the brain causing lethal encephalitis. Nat. Med. *10*, 1366–1373.

Wang, X., Wang, Y., Liu, D., Wang, P., Fan, D., Guan, Y., Li, T., Luan, G., and An, J. (2017). Elevated expression of EBV and TLRs in the brain is associated with Rasmussen's encephalitis. Virol. Sin. *32*, 423–430.

Wang, X., Yin, F., Li, L., Kong, H., You, B., Zhang, W., Chen, S., and Peng, J. (2018). Intracerebroventricular injection of miR-146a relieves seizures in an immature rat model of lithium-pilocarpine induced status epilepticus. Epilepsy Res. *139*, 14–19.

Weinberg, M.S., Blake, B.L., and McCown, T.J. (2013). Opposing actions of hippocampus TNFalpha receptors on limbic seizure susceptibility. Exp Neurol *247*, 429–437.

Weis, S., Haug, H., and Budka, H. (1996). Vascular changes in the cerebral cortex in HIV-1 infection: I. A morphometric investigation by light and electron microscopy. Clin. Neuropathol. *15*, 361–366.

Weissberg, I., Wood, L., Kamintsky, L., Vazquez, O., Milikovsky, D.Z., Alexander, A., Oppenheim, H., Ardizzone, C., Becker, A., Frigerio, F., et al. (2015). Albumin induces excitatory synaptogenesis through astrocytic TGF-β/ALK5 signaling in a model of acquired epilepsy following blood-brain barrier dysfunction. Neurobiol. Dis. *78*, 115–125.

Welsh, D.K., and Kay, S.A. (2005). Bioluminescence imaging in living organisms. Curr. Opin. Biotechnol. *16*, 73–78.

Wetherington, J., Serrano, G., and Dingledine, R. (2008). Astrocytes in the Epileptic Brain. Neuron *58*, 168–178.

Williams-Karnesky, R.L., Sandau, U.S., Lusardi, T.A., Lytle, N.K., Farrell, J.M., Pritchard, E.M., Kaplan, D.L., and Boison, D. (2013). Epigenetic changes induced by adenosine augmentation therapy prevent epileptogenesis. J. Clin. Invest. *123*, 3552–3563.

Wolburg, H., Wolburg-Buchholz, K., Kraus, J., Rascher-Eggstein, G., Liebner, S., Hamm, S., Duffner, F., Grote, E.-H., Risau, W., and Engelhardt, B. (2003). Localization of claudin-3 in tight junctions of

the blood-brain barrier is selectively lost during experimental autoimmune encephalomyelitis and human glioblastoma multiforme. Acta Neuropathol. (Berl.) *105*, 586–592.

Wolf, Y., Yona, S., Kim, K.-W., and Jung, S. (2013). Microglia, seen from the CX3CR1 angle. Front. Cell. Neurosci. *7*, 26.

Wong, M. (2008). Mechanisms of epileptogenesis in tuberous sclerosis complex and related malformations of cortical development with abnormal glioneuronal proliferation. Epilepsia *49*, 8–21.

Wu, C., Leong, S.Y., Moore, C.S., Cui, Q.L., Gris, P., Bernier, L.-P., Johnson, T.A., Séguéla, P., Kennedy, T.E., Bar-Or, A., et al. (2013). Dual effects of daily FTY720 on human astrocytes in vitro: relevance for neuroinflammation. J. Neuroinflammation *10*.

Wu, Y., Wang, X., Mo, X., Xi, Z., Xiao, F., Li, J., Zhu, X., Luan, G., Wang, Y., Li, Y., et al. (2008). Expression of monocyte chemoattractant protein-1 in brain tissue of patients with intractable epilepsy. Clin Neuropathol *27*, 55–63.

Wyatt-Johnson, S.K., Herr, S.A., and Brewster, A.L. (2017). Status Epilepticus Triggers Time-Dependent Alterations in Microglia Abundance and Morphological Phenotypes in the Hippocampus. Front. Neurol. *8*.

Xiong, Z.Q., Qian, W., Suzuki, K., and McNamara, J.O. (2003). Formation of complement membrane attack complex in mammalian cerebral cortex evokes seizures and neurodegeneration. J Neurosci *23*, 955–960.

Xu, L., Hao, Y., Wu, X., Yu, P., Zhu, G., and Hong, Z. (2013). Tenidap, an agonist of the inwardly rectifying K+ channel Kir2.3, delays the onset of cortical epileptiform activity in a model of chronic temporal lobe epilepsy. Neurol. Res. *35*, 561–567.

Yamagata, K., Andreasson, K.I., Kaufmann, W.E., Barnes, C.A., and Worley, P.F. (1993). Expression of a mitogen-inducible cyclooxygenase in brain neurons: regulation by synaptic activity and glucocorticoids. Neuron *11*, 371–386.

Yamamoto, M., Sato, S., Hemmi, H., Uematsu, S., Hoshino, K., Kaisho, T., Takeuchi, O., Takeda, K., and Akira, S. (2003). TRAM is specifically involved in the Toll-like receptor 4-mediated MyD88-independent signaling pathway. Nat. Immunol. *4*, 1144–1150.

Yamazaki, F., Kuroiwa, T., Takikawa, O., and Kido, R. (1985). Human indolylamine 2,3-dioxygenase. Its tissue distribution, and characterization of the placental enzyme. Biochem. J. *230*, 635–638.

Yang, F., Liu, Z.-R., Chen, J., Zhang, S.-J., Quan, Q.-Y., Huang, Y.-G., and Jiang, W. (2010). Roles of astrocytes and microglia in seizure-induced aberrant neurogenesis in the hippocampus of adult rats. J. Neurosci. Res. *88*, 519–529.

Yang, Y., Ge, W., Chen, Y., Zhang, Z., Shen, W., Wu, C., Poo, M., and Duan, S. (2003). Contribution of astrocytes to hippocampal long-term potentiation through release of d-serine. Proc. Natl. Acad. Sci. *100*, 15194–15199.

Yankam Njiwa, J., Costes, N., Bouillot, C., Bouvard, S., Fieux, S., Becker, G., Levigoureux, E., Kocevar, G., Stamile, C., Langlois, J.B., et al. (2017). Quantitative longitudinal imaging of activated microglia as a marker of inflammation in the pilocarpine rat model of epilepsy using [11C]-(R)-PK11195 PET and MRI. J. Cereb. Blood Flow Metab. Off. J. Int. Soc. Cereb. Blood Flow Metab. *37*, 1251–1263.

Ye, Z.C., and Sontheimer, H. (1996). Cytokine modulation of glial glutamate uptake: a possible involvement of nitric oxide. Neuroreport *7*, 2181–2185.

Yeh, H.J., He, Y.Y., Xu, J., Hsu, C.Y., and Deuel, T.F. (1998). Upregulation of pleiotrophin gene expression in developing microvasculature, macrophages, and astrocytes after acute ischemic brain injury. J. Neurosci. Off. J. Soc. Neurosci. *18*, 3699–3707.

Yeo, S., Bandyopadhyay, S., Messing, A., and Brenner, M. (2013). Transgenic Analysis of GFAP Promoter Elements. Glia *61*, 1488–1499.

Yilmaz, I., Adiguzel, E., Akdogan, I., Kaya, E., and Hatip-Al-Khatib, I. (2006). Effects of second generation tetracyclines on penicillin-epilepsy-induced hippocampal neuronal loss and motor incoordination in rats. Life Sci. *79*, 784–790.

Yu, J.X., Bradt, B.M., and Cooper, N.R. (2002). Constitutive expression of proinflammatory complement components by subsets of neurons in the central nervous system. J. Neuroimmunol. *123*, 91–101.

Zamanian, J.L., Xu, L., Foo, L.C., Nouri, N., Zhou, L., Giffard, R.G., and Barres, B.A. (2012). Genomic analysis of reactive astrogliosis. J. Neurosci. Off. J. Soc. Neurosci. *32*, 6391–6410.

Zeng, L.-H., Rensing, N.R., and Wong, M. (2009). The mammalian target of rapamycin signaling pathway mediates epileptogenesis in a model of temporal lobe epilepsy. J. Neurosci. Off. J. Soc. Neurosci. *29*, 6964–6972.

Zhang, L., Guo, Y., Hu, H., Wang, J., Liu, Z., and Gao, F. (2015a). FDG-PET and NeuN-GFAP immunohistochemistry of hippocampus at different phases of the pilocarpine model of temporal lobe epilepsy. Int. J. Med. Sci. *12*, 288–294.

Zhang, X., Ha, T., Lu, C., Lam, F., Liu, L., Schweitzer, J., Kalbfleisch, J., Kao, R.L., Williams, D.L., and Li, C. (2015b). Poly (I:C) therapy decreases cerebral ischaemia/reperfusion injury via TLR3-mediated prevention of Fas/FADD interaction. J. Cell. Mol. Med. *19*, 555–565.

Zhang, Z., Liu, Q., Liu, M., Wang, H., Dong, Y., Ji, T., Liu, X., Jiang, Y., Cai, L., and Wu, Y. (2018). Upregulation of HMGB1-TLR4 inflammatory pathway in focal cortical dysplasia type II. J. Neuroinflammation *15*, 27.

Zhao, J., Wang, Y., Xu, C., Liu, K., Wang, Y., Chen, L., Wu, X., Gao, F., Guo, Y., Zhu, J., et al. (2017). Therapeutic potential of an anti-high mobility group box-1 monoclonal antibody in epilepsy. Brain. Behav. Immun. *64*, 308–319.

Zhou, Q., Dalgard, C.L., Wynder, C., and Doughty, M.L. (2011). Histone deacetylase inhibitors SAHA and sodium butyrate block G1-to-S cell cycle progression in neurosphere formation by adult subventricular cells. BMC Neurosci. *12*, 50.

Zhu, L., Ramboz, S., Hewitt, D., Boring, L., Grass, D.S., and Purchio, A.F. (2004). Non-invasive imaging of GFAP expression after neuronal damage in mice. Neurosci. Lett. *367*, 210–212.

Zimmer, E.R., Parent, M.J., Souza, D.G., Leuzy, A., Lecrux, C., Kim, H.-I., Gauthier, S., Pellerin, L., Hamel, E., and Rosa-Neto, P. (2017). [18F]FDG PET signal is driven by astroglial glutamate transport. Nat. Neurosci. *20*, 393–395.

Zolotukhin, S., Potter, M., Zolotukhin, I., Sakai, Y., Loiler, S., Fraites, T.J., Chiodo, V.A., Phillipsberg, T., Muzyczka, N., Hauswirth, W.W., et al. (2002). Production and purification of serotype 1, 2, and 5 recombinant adeno-associated viral vectors. Methods San Diego Calif *28*, 158–167.

Zurolo, E., Iyer, A.M., Spliet, W.G.M., Van Rijen, P.C., Troost, D., Gorter, J.A., and Aronica, E. (2010). CB1 and CB2 cannabinoid receptor expression during development and in epileptogenic developmental pathologies. Neuroscience *170*, 28–41.

Zurolo, E., Iyer, A., Maroso, M., Carbonell, C., Anink, J.J., Ravizza, T., Fluiter, K., Spliet, G.W.M., van Rijen, P.C., Vezzani, A., et al. (2011). Activation of TLR, RAGE and HMGB1 signaling in malformations of cortical development. Brain *134*, 1015–1032.

Zurolo, E., de Groot, M., Iyer, A., Anink, J., van Vliet, E.A., Heimans, J.J., Reijneveld, J.C., Gorter, J.A., and Aronica, E. (2012). Regulation of Kir4.1 expression in astrocytes and astrocytic tumors: a role for interleukin-1 β. J. Neuroinflammation *9*, 280.

Blood–brain barrier, epileptogenesis, and treatment strategies in cortical dysplasia - Kaya - 2012 - Epilepsia - Wiley Online Library.